



# **Microbial dynamics at chemical interfaces within an organic contaminant plume in groundwater**

**Juan F. Mujica-Alarcon**

In partial fulfilment for the degree of

**Doctor of Philosophy**

Department of Civil and Structural Engineering  
University of Sheffield

November 2017



## **Abstract**

In aquifers polluted with organic compounds, the aqueous phase contaminant plume spreads through the aquifer. Nevertheless, natural attenuation processes at the subsurface can slow the spreading of these plumes and therefore mediate the extent of contamination. One of the natural attenuation processes is biodegradation, which is carried out by indigenous microbial communities. This process is able to degrade contaminant molecules, reducing their concentration in the aquifer. The chemical interfaces present within the organic contaminant plumes are known as plume fringes and at these locations, biodegradation is naturally enhanced by different physical and chemical processes. Previous studies of plume fringes have focused on the biodegradation potential of the planktonic microbial community, yet the role of the biofilm community attached to the sediments are not well understood although likely to be of great relevance. Moreover, these fringes are under the influence of different physical processes, causing the chemical environments at these locations to change relatively rapidly compared to the plume core conditions. The response of biofilms and planktonic communities to alterations in their chemical environment, located at these chemical interfaces have not been explored.

This thesis investigates the dynamic responses of microbial communities, both planktonic and attached, to different chemical environments that develop in the chemical interfaces of polluted aquifers. To assess this, different laboratory-based microcosm experiments were carried out using groundwater from a site polluted with phenolic compounds. At this site, field experiments were also developed. The temporal framework of the experiments installed on site in 2014 was extended up to two years. Different chemical analyses were carried out and molecular biology tools were utilised to characterise and assess the microbial communities.

The results show that time-scales of microbial attachment in plumes are a stable feature at laboratory and field scales. During the temporal evolution of the experiment it was observed

that the attached and planktonic community structures differ over time at chemical interfaces. These differences are sustained when changes in the chemical environment are introduced. The study of the biofilm in these experiments allowed to demonstrate the capacity of this community to be resilient towards changes in their chemical environment. Once established, the community structure of the biofilm remained stable under different environmental chemical changes that are found at the chemical interfaces of polluted aquifers, such as plume advance, plume refreshing and source term variation.

This study also considered the variations in chemical interface scenarios introduced by an engineered intervention, such as Pump and Treat (PAT). Using the same study site, where the contaminated aquifer was intervened with a PAT in order to treat the phenolic plume, annual surveys were made for a three-year period to understand the effect of this technology on the planktonic microbial community. With the use of isotope analyses it was possible to demonstrate that the microbial communities remain active after cessation of engineered intervention. The analysis of the microbial community among the different geochemical variables demonstrated that they were under the influence of different gradients of concentration of phenolic compounds. Moreover, the presence of some microbial groups, such as methanogens, could be associated to isotope signatures related to this type of metabolism.

This research provides broader insight into the knowledge about the microbial dynamics taking place during biofilm development at chemical interfaces of a polluted aquifer. The robustness of the biofilm community in these environments signals that their influence should be considered in bioremediation applications for the remediation of organic-contaminant plumes.



## Acknowledgements

There are many people that have helped and supported me during my life and especially during the last years. I would like to extend my wholehearted thanks to:

My supervisor Team: Professor Steven Thornton and Dr. Stephen Rolfe, both made a constant contribution to my work, always gave me excellent professional advice and were willing to cooperate. Also to Michael Cook and Professor Simon Bottrell (both from University of Leeds) for their contribution with the isotopic data and assistance during fieldwork.

To the all the people working in the GPRG, special thanks to Dr. Richard Gill, Dr. Gabriella Kakony, Dr. Elisa Clagnan, Dr. Henry Nicholls and Andrew Fairburn. Also, I would like to recognise the special contribution to the people in the lab C45 in APS, Mrs. Nichola White, Dr. Alexander McFarlane and Dr. Anne Cotton. Also, I would like to show my gratitude to the examiners Dr. Virginia Stovin (University of Sheffield) and Dr. Terry McGenity (University of Essex) for the feedback given during the VIVA.

I want to dedicate this work especially to my mother Talia, and my sisters Paulina and Carolina, and to my father Francisco. Also, to all My Family. I need to be grateful as well to all my dearest friends around the world who have become my family living overseas.

# Table of contents

Abstract.....	i
Acknowledgements.....	iii
Table of contents.....	iv
List of figures.....	vii
List of tables.....	xviii
Abbreviations.....	xix
<b>Chapter 1: Introduction.....</b>	<b>1</b>
1.1 Groundwater pollution.....	2
1.2 Phenolic contamination.....	3
1.3 Monitored Natural Attenuation (MNA) of Plumes.....	5
1.4 Biodegradation of pollutants.....	5
1.5 Microbial ecology of aquifers.....	7
1.6 Biofilm formation.....	10
1.7 Biodegradation of phenolic compounds at the study site.....	11
1.8 Groundwater plume development.....	12
1.9 Redox zonation and plume fringe concept in plumes.....	14
1.10 Chemical interfaces in groundwater pollutant plumes.....	16
1.11 Research Aim and Objectives.....	23
1.12 Thesis structure and author contributions.....	25
<b>Chapter 2: Microbial dynamics and biofilm community structure in chemical interfaces.....</b>	<b>27</b>
2.1 Introduction.....	28
2.2 Methodology.....	30
2.3 Results.....	38
2.4 Discussion.....	55
Do the microcosms replicate the environment at 30 mbgl?.....	55
Does the lower plume fringe environment reflect the environmental variability?.....	55
Is there any signal of Terminal Electron Acceptor Processes (TEAPs) at both systems?.....	56
What is the timescale of attachment in microbial communities in/from chemical interfaces?.....	57
How does the planktonic community differ from the biofilm?.....	58

How do the biofilm and the planktonic communities vary over time?.....	58
2.5 Conclusions.....	61
<b>Chapter 3: Biofilm community in chemical interfaces and their responses to changes in their chemical environment.....</b>	<b>62</b>
3.1 Introduction.....	63
3.2 Methodology.....	68
3.3 Results.....	72
3.4 Discussion.....	117
Do the microcosm treatments recreate the different chemical environments? .....	117
Does the biodegradation observed in the microcosms relate with the presence of OTUs which might be the responsible for it? .....	118
Do the biofilm microbial communities developed in these treatments reflect the geochemical environment evolution? .....	120
Do the changes of environments reflect different Terminal Electro Acceptor Processes (TEAPs) that could take places in dynamic chemical interfaces of polluted aquifers? .....	122
How do the planktonic and attached communities respond to changes in their chemical environment? .....	123
How is the biofilm development driven by chemical interfaces in polluted aquifers? .....	124
3.5 Conclusions.....	125
<b>Chapter 4: Microbial community responses to chemical interfaces induced by Pump and Treat in a phenolic-contaminated aquifer.....</b>	<b>126</b>
4.1 Introduction.....	127
4.2 Methodology.....	130
4.3 Results.....	135
4.4 Discussion.....	152
How does the switching-off of PAT affect the temporal and spatial distribution of pollutants? .....	152
Does the enhancement of biodegradation persist over time? .....	153
What is the influence of an active PAT on the microbial communities? .....	154
How do the microbial communities respond to the cease of PAT operations? .....	154
What chemical gradients explain the variation of the system? .....	156
4.5 Conclusion.....	157

<b>Chapter 5: Conclusions</b> .....	158
Time-scales of microbial attachment in plumes are a stable feature at laboratory and field scales.....	159
Attached and planktonic communities structures differ over time at chemical interfaces.....	160
Biofilm communities are more resilient to changes in their chemical environmental.....	161
Biofilm development is driven by the hydrogeochemical environment.....	161
Microbial communities remain active after cessation of engineered intervention measures.....	162
Different gradients of concentration influence the planktonic bacterial community.....	163
Plume fringe concept as a basis to explain the microbial dynamics at chemical interfaces.....	163
Future work.....	164
<b>References</b> .....	166
<b>Appendix</b> .....	186

## List of figures

**Figure 1.1.** Conceptualization of plume development in groundwater (a) plume zonation and (b) plume fringe concept. (page 18)

**Figure 1.2** (a) Schematic representation of mixing processes which occur in the upper and lower fringe of an organic contaminant plume; (b) Variation in phenol concentration over time due to mixing processes in the lower fringe of a plume, located 30 meters below ground level (mbgl). (page 19)

**Figure 1.3.** Depth profiles of Total Phenolic Content (TPC) and nitrate concentration obtained from a multi-level sampler (MLS) installed in the aquifer at the study site. Note the plume fringe is the chemical interface separating the background groundwater from the plume core. Data of the plume was after 174 days of monitoring. (page 20)

**Figure 1.4** (a) Schematic representation of location (in circle) where the plume front has advanced; (b) Expected change in phenol concentration after advance of the plume front at this location, as described by Elliot *et al.* (2010). (page 21)

**Figure 1.5** (a) Total Phenolic Content (TPC) variation due to operation of a PAT system at the study site (undisclosed location). Note 2009 is pre-implementation of the PAT system, 2011 active PAT and in 2012 the PAT was switched-off, data from Thornton *et al.* (2014) (b) Schematic representation of chemical interfaces induced within the core of an organic contaminant plume due to the operation of a PAT system. (page 22)

**Figure 1.6.** Schematic representation of the thesis structure. Note RO, research objective; RQ, research questions. (page 23)

**Figure 2.1.** Depth profile of total phenolic content (TPC) at BH-59. Note 2009 pre-implementation of PAT system, 2011 active PAT and 2012 PAT was switched-off. The chemical interface at 30 meters below ground level (mbgl) maintains its position over time. (page 29)

**Figure 2.2** Example of a microcosm after the setting-up process in anaerobic conditions. (page 31)

**Figure 2.3** (a) Arrangement of bags filled with sand in the metallic cage. (b) Schematic representation of the final position of the cage 30 mbgl in the open screen of BH-59. (page 32)

**Figure 2.4.** Anaerobic extraction in the field. (a) BH-59 covered with a glove bag and hose introduction, (b) initial steps of purging of the head space (c) nitrogen supply for purging and (d) final recovery of sand bag from the screen of BH-59. (page 33)

**Figure 2.5.** Monitoring of different chemical species and cell counts in microcosms inoculated with groundwater from 30 mbgl of BH-59. Error bars represent the standard deviation of replicates (n=3) Legend in the bottom left corner applies to all graphs except to the cell densities in *graph i*, for which is associated to the legend in the bottom right corner of the figure. (page 40)

**Figure 2.6.** Concentration change of phenolic within 60 minutes of sampling of groundwater from 30 mbgl at BH-59. For other chemical species please see the Appendix 6.1. (page 41)

**Figure 2.7** Monitoring of different chemical species and cell counts of groundwater and sandbag extracted from BH-59 at 30 mbgl, associated to the *in situ* experiment of this chapter. Legend in the bottom left corner applies to all graphs except to the cell densities in *graph i*), for which belongs with the legend in the bottom right corner of the figure. (page 42)

**Figure 2.8.** Visualization of microbial cells by SYTO® 9 staining on sand grains at different intervals of incubation in the microcosms and field. 20X of magnification. The white bar represents 20 µm. (page 44)

**Figure 2.9.** NMDS of microbial communities in the (a) microcosms and (b) field samples. These biplots were constructed using Bray-Curtis dissimilarity matrix on the abundances of the T-RFLP fragments from 16S rRNA genes extracted from the planktonic (P) and attached (A) communities in two different systems. (Note time is shown in weeks). (page 46)

**Figure 2.10.** High throughput sequencing of 16S rRNA genes at class level in planktonic and attached communities harvested from microcosm and field samples at different time intervals after inoculation. (Note time is shown in weeks). (page 47)

**Figure 2.11.** Unifrac weighted NMDS of all planktonic and attached communities harvested from microcosm and field samples at different time intervals after inoculation. This analysis considers the abundances of different groups and their phylogenetic relationships to each other. The effects of time was not taken into account. (page 48)

**Figure 2.12.** Unifrac weighted NMDS of all planktonic and attached communities harvested from microcosm and field samples at different time intervals after inoculation. This analysis considers the abundances of different groups, their phylogenetic relationships and the effect of time (Note time is shown in weeks). (page 49)

**Figure 2.13.** Unifrac unweighted NMDS of all planktonic and attached communities harvested from microcosm and field samples at different time intervals following inoculation. This analysis considers the presence/absence of different groups, their phylogenetic relationships to each other and the effect of time. (Please note time is shown in weeks). (page 50)

**Figure 2.14.** Richness of OTUs in planktonic and attached communities harvested from the microcosms and the field at different time intervals upon inoculation. (Note time is shown in weeks). (page 52)

**Figure 2.15.** Evenness in planktonic and attached communities harvested from the microcosms and the field at different time intervals upon inoculation. (Note time is shown in weeks). (page 52)

**Figure 2.16.** Microbial identification at genus level of different microorganisms harvested at different time intervals after the inoculation in the microcosm experiment. Multiple genus appears repeated as the taxa assignment is able to distinguish different variants under this taxonomic level (Note time is shown in weeks). (page 54)

**Figure 3.1.** Mixing processes in the upper and lower plume fringes. (a) Schematic representation of the locations and (b) nitrate fluctuations registered in the lower plume fringe (BH-59, 30 mbgl) of a phenolic plume. (page 65)

**Figure 3.2.** Plume advance, from low to medium phenol concentrations. (a) In grey locations exposed to plume advance 1 (adv\_1); (b) Expected increase of pollutant content at these locations. (page 66)

**Figure 3.3.** Plume advance, from medium to high phenol concentrations (a) In grey locations exposed to plume advance 2 (adv\_2); (b) Expected increase of pollutant content at these locations. (page 66)

**Figure 3.4.** Plume refreshing, from medium to low phenol concentrations (a) Diving of the plume into the aquifer from t=1 to t=2, in grey the locations exposed to plume refreshing process. (b) Expected reduction of pollutant content at these locations. (page 66)

**Figure 3.5.** Source term variation, from high to medium phenol concentrations (a) Source term variation in the aquifer from t=1 to t=2, in grey the locations exposed to source term process. (b) Expected decrease of pollutant content at these locations. (page 67)

**Figure 3.6.** Construction of microcosms to recreate the low, medium and high phenolic environments. Field groundwater samples were introduced into microcosms and incubated for 101 or 195 days. For a subset of microcosms, the aqueous phase was decanted after 3 months, filtered to remove planktonic cells, and then re-introduced into the microcosm. Attached (A) and planktonic (P) phases were sampled. For 11 mbgl microcosms only, nitrate was re-added at intervals to maintain  $\text{NO}_3^-$  concentrations at  $30 \text{ mg L}^{-1}$ . (page 69)

**Figure 3.7.** Construction of microcosms to recreate plume advance scenarios. Microcosms were established for 101 days with groundwater from low, medium and high phenolic content. To simulate the transition from low to medium phenol (adv\_1), the aqueous phase from a medium phenolic microcosm was added to the attached phase of low phenolic microcosm with and without filtering. Equivalent transfers using the planktonic phase from microcosms with high phenolic and the attached phase from microcosm with medium phenolic content were used to simulate the transition from medium to high phenol (adv\_2). (page 70)

**Figure 3.8.** Construction of microcosms to recreate plume the plume refreshing (PR) and source term (ST) scenarios. microcosms were established for 101 days with groundwater from low, medium and high phenolic environment. To simulate the transition from medium to low phenol, the aqueous phase from a low phenolic microcosm was added to the attached phase of a medium phenolic microcosm with and without filtering. Equivalent transfers using the planktonic phase from medium phenolic and the attached phase from high phenolic microcosm, simulated the transition from high to medium phenol. (page 71)

**Figure 3.9.** Monitoring of different chemical species in microcosms inoculated with groundwater from 11 mbgl. Error bars represent the standard deviation of replicates (n=3). Legend in the middle applies for all graphs except for the cell densities in h. (page 74)

**Figure 3.10.** Unifrac weighted Principal coordinate analysis of attached and planktonic communities harvested from microcosms inoculated with groundwater from a low phenolic environment. Note 1 and 2, attached communities after 101 and 195 days of incubation in a microcosm. 3, attached community formed after the removal of the planktonic community. 6, planktonic community from 11 mbgl (inoculum); 4 and 5, planktonic communities after 101 and 195 days of incubation respectively. (page 76)

**Figure 3.11.** Deseq analysis between planktonic samples in the low phenolic environment inoculum and the planktonic community after 101 days of incubation (\*). OTUs showing statistical differences in the relative abundances between these communities are shown. Note, the relative abundance was normalised to 10,000 counts and (\*) indicates groups which exhibited the larger changes in the relative abundances between these communities. (page 77)

**Figure 3.12.** Deseq analysis between attached communities from low phenolic microcosms after 101 and 195 days of incubation (\*). OTUs showing statistical differences in the relative abundances between these communities are shown. Note, the relative abundance was normalised to 10,000 counts and (\*) indicates groups which exhibited the larger changes in the relative abundances between these communities. (page 78)

**Figure 3.13.** Deseq analysis between attached communities from low phenolic microcosms after 195 days of incubation (\*). OTUs showing statistical differences in the relative abundances between these communities are shown. Note, the relative abundance was normalised to 10,000 counts and (\*) indicates groups which exhibited the larger changes in the relative abundances between these communities. (page 79)

**Figure 3.14.** Monitoring of different chemical species in microcosms inoculated with groundwater from 14 mbgl. Error bars represent the standard deviation of replicates (n=3). Legend from lower left corner applies for all graphs except for the cell densities in i. (page 81)

**Figure 3.15.** Unifrac weighted Principal coordinate analysis of attached and planktonic communities harvested from microcosms inoculated with groundwater from a medium phenolic environment. Note 1 and 2, attached communities after 101 and 195 days of incubation in a microcosm. 3, attached community formed after the removal of the planktonic community. 6, planktonic community from 11 mbgl (inoculum); 4 and 5, planktonic communities after 101 and 195 days of incubation respectively. (page 82)

**Figure 3.16.** Deseq analysis between planktonic samples in the medium phenolic environment inoculum and the planktonic community after 101 days of incubation (\*). OTUs showing statistical differences in the relative abundances between these communities are shown. Note, the relative abundance was normalised to 10,000 counts and (\*) indicates groups which exhibited the larger changes in the relative abundances between these communities. (page 84)

**Figure 3.17.** Deseq analysis between attached communities from medium phenolic microcosms after 101 and 195 days of incubation (\*). OTUs showing statistical differences in the relative abundances between these communities are shown. Note, the relative abundance was normalised to 10,000 counts and (\*) indicates groups which exhibited the larger changes in the relative abundances between these communities. (page 85)

**Figure 3.18.** Monitoring of different chemical species in microcosms inoculated with groundwater from 21mbgl. Error bars represent the standard deviation of replicates (n=3). Legend from lower left corner applies for all graphs except for the cell densities in i. (page 86)

**Figure 3.19.** Unifrac weighted Principal coordinate analysis of attached and planktonic communities harvested from microcosms inoculated with groundwater from a high phenolic



environment. Note 1 and 2, attached communities after 101 and 195 days of incubation in a microcosm. 3, attached community formed after the removal of the planktonic community. 6, planktonic community from 11 mbgl (inoculum); 4 and 5, planktonic communities after 101 and 195 days of incubation respectively. (page 88)

**Figure 3.20.** Deseq analysis between planktonic samples in the high phenolic environment inoculum and the planktonic community after 101 days of incubation (\*). OTUs showing statistical differences in the relative abundances between these communities are shown. Note, the relative abundance was normalised to 10,000 counts and (\*) indicates groups which exhibited the larger changes in the relatives abundances between these communities. (page 89)

**Figure 3.21.** Deseq analysis between attached communities from high phenolic microcosms after 101 and 195 days of incubation (\*). OTUs showing statistical differences in the relative abundances between these communities are shown. Note, the relative abundance was normalised to 10,000 counts and (\*) indicates groups which exhibited the larger changes in the relatives abundances between these communities. (page 90)

**Figure 3.22.** Monitoring of different chemical species in microcosms recreating the adv\_1. Legend from lower left corner applies for all graphs except for the cell densities in i. Note, adv\_1 was constructed with sediments from low phenolic microcosms and the supernatant of the medium phenolic microcosms. adv\_1 filtered, planktonic community was removed before putting these phases together. Residual pore water was contained in the sediments after the removal of the supernatant. Expected conc. mixing was the predicted concentration as a result of the mixing between the new supernatant (medium phenolic) and the residual pore water (low phenolic). (page 92)

**Figure 3.23.** Unifrac weighted Principal coordinate analysis of attached and planktonic communities harvested from microcosms recreating the adv\_1. Note, 1 and 2 attached communities after 101 and 195 days of incubation in a microcosm inoculated with groundwater from a low phenolic environment. 3, attached community after 195 days which experimented the change from a low to a medium phenolic environment. 4, planktonic community after 195 days of incubation in low phenolic microcosms. 5, planktonic communities after 195 days of incubation in a microcosm inoculated with medium phenolic contents. 6, planktonic community after plume advance 1. (page 93)

**Figure 3.24.** Unifrac weighted Principal coordinate analysis of planktonic communities related to plume advance 1 treatment. Note 1 and 2, planktonic communities after 101 and 195 days of incubation in a microcosm inoculated with groundwater from a low phenolic environment. 3 and 4, planktonic communities after 101 and 195 days of incubation in a microcosm inoculated with groundwater from a medium phenolic environment. 5, planktonic community after adv\_1. 6, synthetic planktonic community. (page 94)

**Figure 3.25.** Deseq analysis between biofilms related to plume advance 1 treatment (\*). OTUs showing statistical differences in the relative abundances between these communities are shown. Note, the relative abundance was normalised to 10,000 counts and (\*) indicates groups which exhibited the larger changes in the relatives abundances between these communities. (page 95)

**Figure 3.26.** Deseq analysis between biofilms related to plume advance 1 treatment considering the effect of the geochemical environment, through the removal of the planktonic community (\*). OTUs showing statistical differences in the relative abundances between these communities are shown. Note, the relative abundance was normalised to 10,000 counts. (page 96)

**Figure 3.27.** Monitoring of different chemical species in microcosms recreating the adv\_2. Legend from lower left corner applies for all graphs except for the cell densities in i. Note, adv\_2 was constructed with sediments from medium phenolic microcosms and the supernatant of the high phenolic microcosms. adv\_2 filtered, planktonic community was removed before putting these phases together. Residual pore water was contained in the sediments after the removal of the supernatant. Expected conc. mixing was the predicted concentration as a result of the mixing between the new supernatant (high phenolic) and the residual pore water (medium phenolic). (page 98)

**Figure 3.28.** Unifrac weighted Principal coordinate analysis of attached and planktonic communities harvested from microcosms recreating the adv\_2. Note, 1 and 2 attached communities after 101 and 195 days of incubation in a microcosm inoculated with groundwater from a medium phenolic environment. 3, attached community after 195 days which experimented the change from a medium to a high phenolic environment. 4, planktonic community after 195 days of incubation in medium phenolic microcosms. 5, planktonic communities after 195 days of incubation in a microcosm inoculated with high phenolic content. 6, planktonic community after plume advance 2. (page 99)

**Figure 3.29.** Unifrac weighted Principal coordinate analysis of planktonic communities related to plume advance 2 treatment. Note 1 and 2, planktonic communities after 101 and 195 days of incubation in a microcosm inoculated with groundwater from a medium phenolic environment. 3 and 4, planktonic communities after 101 and 195 days of incubation in a microcosm inoculated with groundwater from a high phenolic environment. 5, planktonic community after adv\_2. 6, synthetic planktonic community. (page 100)

**Figure 3.30.** Deseq analysis between biofilms related to plume advance 2 treatment (\*). OTUs showing statistical differences in the relative abundances between these communities are shown. Note, the relative abundance was normalised to 10,000 counts and (\*) indicates groups which exhibited the larger changes in the relatives abundances between these communities. (page 101)

**Figure 3.31.** Deseq analysis between biofilms related to plume advance 2 treatment considering the effect of the geochemical environment, through the removal of the planktonic community (\*). OTUs showing statistical differences in the relative abundances between these communities are shown. Note, the relative abundance was normalised to 10,000 counts. (page 102)

**Figure 3.32.** Monitoring of different chemical species in microcosms recreating the plume refreshing. Legend from the middle applies for all graphs except for the cell densities in h. Note, plume refreshing was constructed with sediments from medium phenolic microcosms and the supernatant of the low phenolic microcosms. Plume refreshing filtered, planktonic

community was removed before putting these phases together. Residual pore water, was contained in the sediments after the removal of the supernatant. Expected conc. mixing, was the predicted concentration as a result of the mixing between the new supernatant (low phenolic) and the residual pore water (medium phenolic). (page 105)

**Figure 3.33.** Unifrac weighted Principal coordinate analysis of attached and planktonic communities harvested from microcosms recreating plume refreshing. Note, 1 and 2 attached communities after 101 and 195 days of incubation in a microcosm inoculated with groundwater from a medium phenolic environment. 3, attached community after 195 days which experimented the change from a medium to a low phenolic environment. 4, planktonic community after 195 days of incubation in low phenolic microcosms. 5, planktonic communities after 195 days of incubation in a microcosm inoculated with medium phenolic content. 6, planktonic community after plume refreshing. (page 106)

**Figure 3.34.** Unifrac weighted Principal coordinate analysis of planktonic communities related to plume refreshing treatments. Note 1 and 2, planktonic communities after 101 and 195 days of incubation in a microcosm inoculated with groundwater from a low phenolic environment. 3 and 4, planktonic communities after 101 and 195 days of incubation in a microcosm inoculated with groundwater from a medium phenolic environment. 5, planktonic community after plume refreshing. 6, synthetic planktonic community. (page 107)

**Figure 3.35.** Deseq analysis between biofilms related to plume refreshing treatment (\*). OTUs showing statistical differences in the relative abundances between these communities are shown. Note, the relative abundance was normalised to 10,000 counts and (\*) indicates groups which exhibited the larger changes in the relatives abundances between these communities. (page 108)

**Figure 3.36.** Deseq analysis between biofilms related to plume refreshing treatment considering the effect of the geochemical environment, through the removal of the planktonic community (\*). OTUs showing statistical differences in the relative abundances between these communities are shown. Note, the relative abundance was normalised to 10,000 counts. (page 109)

**Figure 3.37.** Monitoring of different chemical species in microcosms recreating the source term variation (stv). Legend from lower left corner applies for all graphs except for the cell densities in i. Note, stv was constructed with sediments from high phenolic microcosms and the supernatant of the medium phenolic microcosms. STV filtered, planktonic community was removed before putting these phases together. Residual pore water was contained in the sediments after the removal of the supernatant. Expected conc. mixing was the predicted concentration as a result of the mixing between the new supernatant (medium phenolic) and the residual pore water (high phenolic). (page 111)

**Figure 3.38.** Unifrac weighted Principal coordinate analysis of attached and planktonic communities harvested from microcosms recreating the source term variation, stv. Note, 1 and 2 attached communities after 101 and 195 days of incubation in a microcosm inoculated with groundwater from a high phenolic environment. 3, attached community after 195 days which experimented the change from a high to a medium phenolic environment. 4, planktonic community after 195 days of incubation in medium phenolic microcosms. 5, planktonic

communities after 195 days of incubation in a microcosm inoculated with high phenolic content. 6, planktonic community after stv. (page 112)

**Figure 3.39.** Unifrac weighted Principal coordinate analysis of planktonic communities related to source term variation treatment. Note 1 and 2, planktonic communities after 101 and 195 days of incubation in a microcosm inoculated with groundwater from a medium phenolic environment. 3 and 4, planktonic communities after 101 and 195 days of incubation in a microcosm inoculated with groundwater from a high phenolic environment. 5, planktonic community after adv\_2. 6, synthetic planktonic community. (page 113)

**Figure 3.40.** Deseq analysis between biofilms related to source term variation treatment (\*). OTUs showing statistical differences in the relative abundances between these communities are shown. Note, the relative abundance was normalised to 10,000 counts and (\*) indicates groups which exhibited the larger changes in the relative abundances between these communities. (page 114)

**Figure 3.41.** Deseq analysis between biofilms related to source term variation treatments considering the effect of the geochemical environment, through the removal of the planktonic community (\*). OTUs showing statistical differences in the relative abundances between these communities are shown. Note, the relative abundance was normalised to 10,000 counts. (page 115)

**Figure 4.1.** Plan view of the study site showing location of boreholes (BH) 59 and 60, and extraction wells P1 and P2 used for the operation of the PAT system. The dashed line shows the approximate location of plume boundaries (modified from Thornton *et al.*, 2014). (page 128)

**Figure 4.2.** Gas sampling system used for gas sampling in the field. Groundwater port was connected to an inverted collection bottle. The gate valve was closed and nitrogen was injected into the bottle through the septum of a rubber bung stopper. Then, the gate valve was opened to allow a constant flow of  $\sim 100 \text{ ml min}^{-1}$  into the collection bottle for approximately 30 minutes. After this time, two aliquots of 10 ml of gas were recovered and injected into septum-sealed vials, previously filled with nitrogen. (page 131)

**Figure 4.3.** Depth profiles of TPC in (a) BH-59, close to this BH a PAT was switched-off on 2011 and (b) BH-60, location under the influence of a PAT close to the location (n=1). The water table was located at 5 mbgl approximately. (page 135)

**Figure 4.4.** Depth profiles of different electron acceptors in groundwater at BH59 (left) and BH-60 (right). The water table was located at 5 mbgl approximately (n=1). Manganese and iron were not measured in 2011. (page 138)

**Figure 4.5.** Depth profiles of different compounds (concentration and isotopic composition) in groundwater at BH-59 (left) and BH-60 (right). The water table was located at 5 mbgl approximately (n=1). Potentially dominant processes at specific depth are shown. Methane was not measured in 2011. (page 140)

**Figure 4.6.** Depth profiles of acetate concentration and cell densities in groundwater at BH-59 (left) and BH-60 (right). The water table was located at 5 mbgl approximately (n=1). Acetate and cells counts were not measured in 2011. (page 141)

**Figure 4.7.** Relative abundances of different microbial groups at Phylum level at BH-59 (left) and BH-60 (right) over a three year period (2014, 2015 and 2016). (page 142)

**Figure 4.8** Relative abundances of Proteobacteria Phylum at Class level at BH-59 and BH-60 over a three year period (2014, 2015 and 2016). (page 143)

**Figure 4.9.** Community structure metrics of richness, inverse Simpson and Shannon indexes at BH59 and BH-60 over a three year period (2014, 2015 and 2016). (page 144)

**Figure 4.10.** Unifrac weighted PCoA on the community structures in groundwater at two boreholes in a site polluted with phenolic compounds. (page 145)

**Figure 4.11.** Unifrac weighted PCoA on the community structures in groundwater at BH-59 (left) and BH-60 (right) of a site polluted with phenolic compounds. (page 146)

**Figure 4.12.** Canonical Analysis of Principal Coordinates of steady-state data obtained at BH-59 (left) and BH-60 (right) over a 3 years period (2014, 2015 and 2016). (page 147)

**Figure 4.13.** Correlations between chemical measurements (complete observations only). Coloured squares show significant positive (blue) or negative (red) correlations. BH-59 (left) and BH-60 (right). (page 148)

**Figure 4.14.** Constrained ordination based on the chemical gradients of samples at BH-59 over time. Overlying are the chemical gradients of the most relevant compounds explaining the variation of the system. (page 149)

**Figure 4.15.** Constrained ordination based on the chemical gradients of samples at BH-60 over time. Overlying are the chemical gradients of the most relevant compounds explaining the variation of the system. (page 150)

**Figure 4.16.** NMDS of the overlaid ordinations based on OTUs abundances and different chemical species at (a) BH-59 and (b) BH-60. (page 151)

**Figure 6.1.** Concentration change of chemical species within 60 minutes of sampling of groundwater from 30 mbgl at BH-59. (page 187)

**Figure 6.2** Metabolites detection in the microcosm. (a) 4-hydroxybenzoic acid, (b) 4-hydroxy-3-methyl benzoic acid. Results were the average of 3 independent microcosms +/- standard deviation sampled destructively at each time point. (page 188)

**Figure 6.3.** DNA extraction of groundwater from the study site using two different method of mechanic lysis. (1) Vortex Mobio adapter and (2) mixer M: Ladder IV (page 189)

**Figure 6.4.** PCR Amplification of 16S rRNA gene of DNA from the study site using different method of lysis. Amplification was made using 63F and 806R primers labelled with FAM (blue), HEX (red) or both. M: Ladder IV, (1) Vortex Mobio adapter, (2) mixer (-) Negative control. (page 189)

**Figure 6.5.** PCR Amplification of 16S rRNA gene of groundwater harvested from microcosm at different intervals after the inoculation. Amplification was made using 63F and 806R primers

labelled with FAM (blue), HEX (red) or both. M: Ladder IV (+) Positive control (-) Negative control. (page 190)

**Figure 6.6.** t-RFLP peaks of FAM labelled amplicons of 16S rRNA gene. These peaks were obtained after digestion with different restriction enzymes (a) AluI and (b) CfoI. The samples were harvested from the supernatant of microcosms at different intervals: 7 (blue), 23 (red), 47 (black) and 104 (green) days after the inoculation. (page 192)

**Figure 6.7.** PCR Amplification of 16S rRNA gene of sediments harvested from microcosm at different intervals after the inoculation. Amplification was made using FAM labelled 341F and 805R primers M: Ladder IV (+) Positive control (-) Negative control. (page 193)

**Figure 6.8.** PCR Amplification of 16S rRNA gene of sediments harvested from microcosm at different intervals after the inoculation. The amount of DNA was doubled. Amplification was made using FAM labelled 341F and 805R primers M: Ladder IV (+) Positive control (-) Negative control. (page 194)

**Figure 6.9.** PCR Amplification of 16S rRNA gene of sediments harvested from microcosm and field at different intervals after the inoculation. DNA template was a result of DNA concentration of 6 aliquots. Amplification was made using FAM labelled 341F and 805R primers M: Ladder IV (+) Positive control (-) Negative control. (page 194)

**Figure 6.10.** PCR Amplification of 16S rRNA gene of groundwater harvested from microcosm and field at different intervals after the inoculation. Amplification was made using FAM labelled 341F and 805R primers M: Ladder IV (+) Positive control (-) Negative control. (page 195)

**Figure 6.11.** Additive Main Effects and Multiplicative Interaction (AMMI) of planktonic and attached communities in the microcosms. The data considered was (a) binary data, (b) peak height and (c) peak area. E1 to E6 represents planktonic community (green oval) and E7 to E12 attached community (brown oval) at different intervals. (page 198)

**Figure 6.12.** Additive Main Effects and Multiplicative Interaction (AMMI) of planktonic and attached communities in the field. The data considered was (a) binary data, (b) peak height and (c) peak area. E1 to E7 represents planktonic community (green oval) and E8 to E13 attached community (brown oval) at different intervals. (page 199)

**Figure 6.13.** Additive Main Effects and Multiplicative Interaction (AMMI) of planktonic and attached communities in microcosm and the field. The data considered was (a) binary data, (b) peak height and (c) peak area. E1 to E6 represents planktonic microcosm community, E7 to E12 sediment microcosm community, E13 to E19 field planktonic community and E20 to E25 attached field community at different intervals. (page 200)

**Figure 6.14.** PCR Amplification of 16S rRNA gene of supernatant and sediments harvested from microcosm at different intervals after the inoculation. The amplification was made using Illumina 341 and 805 primers and two different polymerases. M: Ladder IV (1-2) sediments, (3-4) planktonic, (+) Positive control and (-) Negative control. (page 201)

**Figure 6.15.** PCR Amplification of 16S rRNA gene to DNA extracted from sediments to demonstrate the presence of soluble inhibitors. The amplification was made using Illumina 341

and 805 primers. (M) Ladder IV, (1 and 4) positive controls, (2 and 5) half of the input template of the positive controls, (3, 6 and 7) mix of sediment samples and positive controls, (+) Positive control and (-) Negative control. (page 202)

**Figure 6.16.** PCR Amplification of 16S rRNA gene of DNA extracted from sediments and treated with dialysis. The amplification was made using Illumina 341 and 805 primers. (M) Ladder IV, sediments after (1) 7, (2) 23, (3) 47, (4) 104, (5) 174 and (6) 400 days after the inoculation. (page 203)

**Figure 6.17.** PCR Amplification of 16S rRNA gene of DNA extracted from sediments and treated with drop-dialysis. The amplification was made using Illumina 341 and 805 primers. (M) Ladder IV, sediments after (1 and 8) 7, (2 and 9) 23, (3 and 10) 47, (4 and 11) 104, (5 and 12) 174 and (6, 7, 13 and 14) 400 days after the inoculation. (page 204)

**Figure 6.18.** PCR Amplification of 16S rRNA gene of DNA extracted from sediments and treated (a) microcon according to manufacture instructions and (b) extra desalting steps. The amplification was made using Illumina 341 and 805 primers. (M) Ladder IV, (1-3) Sediments after 780 days of inoculation, (4) sediments final volume reaction of 50 ul. Note arrow indicates approximately 600 bp. (page 205)

**Figure 6.19.** PCR Amplification of 16S rRNA gene of DNA extracted from sediments and treated with microcon plus extra desalting steps. (a) The amplification was made using Illumina 341 and 805 primers. (M) Ladder IV, sediments after (1) 7, (2) 23, (3) 47, (4) 104, (5) 174, (6) 400 and (7) 780 days the inoculation. (b) previous samples treated with AM pure beads. (page 206)

**Figure 6.20.** PCR Amplification of 16S rRNA gene of sediments harvested from microcosm at different intervals after the inoculation. DNA was treated with microcon to eliminate soluble inhibitors. Amplification was made using FAM labelled 341F and 805R primers M: Ladder IV (+) Positive control (-) Negative control. (page 207)

**Figure 6.21.** PCR Amplification of 16S rRNA gene of sediments harvested from field at different intervals after the inoculation. DNA was treated with microcon to eliminate soluble inhibitors. Amplification was made using FAM labelled 341F and 805R primers M: Ladder IV (+) Positive control (-) Negative control. (page 208)

**Figure 6.22.** PCR Amplification of 16S rRNA gene of supernatant harvested from microcosm at different intervals after the inoculation. Amplification was made using FAM labelled 341F and 805R primers M: Ladder IV (+) Positive control (-) Negative control. (page 209)

**Figure 6.23.** PCR Amplification of 16S rRNA gene of groundwater harvested from field at different intervals after the inoculation. Amplification was made using FAM labelled 341F and 805R primers M: Ladder IV (+) Positive control (-) Negative control. Note Screening represents samples previous to the beginning of the experiment. (page 209)

**Figure 6.24.** Depth profiles of sulfide in groundwater at BH59 (left) and BH-60 (right). The water table was located at 5 mbgl approximately (n=1). (page 210)

## List of tables

**Table 1.1.** Locations of different potential sources and types of contaminants in groundwater. (Unesco, 2002) (**page 2**)

**Table 2.1** Redox half reaction of biodegradation of phenolic compound extracted from Thornton *et al.* 2001b (**page 37**)

**Table 2.2.** Likelihood ratio test for 16S rRNA sequences from communities (attached and planktonic) obtained from different experimental settings (microcosms and field). (**page 53**)

**Table 2.3.** ANOVA analysis on the richness and evenness parameters of communities (attached and planktonic) obtained from different experimental settings (microcosms and field). (**page 53**)

**Table 2.4.** Tukey significance comparisons of richness and evenness parameters of communities (attached and planktonic) obtained from different experimental settings (microcosms and field). (**page 53**)

**Table 3.1** Tabulated key findings for Chapter 4. (**page 116**)

**Table 4.1.** Depth selection for sequencing of field samples harvested during surveys in 2014, 2015 and 2016. (**page 131**)

**Table 6.1** Percent of variation in T-RFLP data set from analysis of variance. Three type of data was considered in every comparison. (**page 197**)



## **Abbreviations**

AMO, anaerobic methane oxidation  
BH, borehole  
bp, base pair  
BSR, bacterial sulphate reduction  
CAP, Canonical Analysis of Principal Coordinates  
CSM, conceptual site model  
DNAPL, dense non-aqueous phase liquid  
EAs, electron acceptors  
EDs, electron donors  
mbgl, meters below ground level  
MLS, multi-level samples  
MNA, monitored natural attenuation  
NA, natural attenuation  
NMDS, Nonmetric Multidimensional Scaling  
OTU, Operational taxa unit  
PAT, Pump and treat  
PCoA, Principal Coordinates analysis  
PCR, polymerase chain reaction  
rRNA, ribosomal ribonucleic acid  
TDIC, total dissolved inorganic carbon  
TPC, total phenolic compounds  
T-RFLP, terminal restriction fragment length polymorphism

**Note that during the thesis the biofilm community will be also referred as attached community**

# **Chapter 1**

---

## **Introduction**

---

## 1.1 Groundwater pollution

Groundwater represents 30% of the total freshwater available (Shiklomanov, 1992). In some arid and semi-arid areas, populations rely almost entirely on groundwater. Estimations indicate that groundwater is the freshwater source for a large part of the world population, with ~2 billion people depending on this asset (Kemper, 2004). Considering that the majority of freshwater is located in ice caps and snow, and the small amount available in the surface has been frequently polluted due to increasing populations and industrial activities, groundwater has become an extremely important resource (Fitts, 2002; Delleur, 2006). In this context, contamination of groundwater has gained attention because it threatens the environment and human health (Delleur, 2007; Schwarzenbach *et al.*, 2010; Allouche *et al.*, 2017).

There are many sources and activities that can result in groundwater contamination. For instance, the leaking of stored fertilizers used in agriculture, or from underground tanks in airports or petrol stations, plus leaking from industrial activities such as mining or chemical manufacturer plants which rely in underground pipelines networks, or filtrations from underground septic systems used in residential areas (EPA, 1991; EPA, 1993). The release of contaminants from these sources and activities have the potential to contaminate groundwater and are widely spread in all countries. **Table 1.1** shows different types of sources and examples of groundwater pollutants.

**Table 1.1.** Locations of different potential sources and types of contaminants in groundwater (Unesco, 2002).

Location	potential sources			
	Municipal	Industrial	Agricultural	Domestic
Close to surface	de-icing storages	surface chemical storage	facilities	homes
	municipal waste	mine drainage	land spreading animal waste	
Underground	landfills	pipelines	underground storage	septic systems
		underground storage tanks		
Occurrence	High	High	High	High
Type of contaminants	Inorganic	Volatile organic hydrocarbons (VOCs)	pesticides-fertilizers	Emerging organic compounds (EOCs)
Examples	arsenic	petroleum hydrocarbons	endosulfan	erythromycin
	lead	PAHs	atrazine	17R-ethinylestradiol
	sulphate	MTBE	nitrate	nitroglycerin
	ammonium	BTEX	phosphate	monensin
	copper	phenolic compounds	potassium	sulfamethazine

These different activities and sources of contamination supply the groundwater with different types of inorganic and organic contaminants, which alter the natural groundwater quality. For example, inorganic contaminants include chloride, sulphate, nitrate, carbonate, sodium, potassium, manganese and magnesium, and heavy metals such as lead, zinc, cadmium, mercury or chromium (Ribera, 2001). Organic contaminants are grouped in three main categories, volatile organic compounds (VOCs), pesticides and emerging organic compounds (EOCs) (Wang *et al.* 2013). In the VOC category there are a large number of compounds such as BTEXs (benzene, toluene, ethyl benzenes and xylenes) and chlorinated solvents (Zhang *et al.*, 1998; Madsen, 2008). Examples of pesticides include endosulfan and atrazine (Arias-Estévez *et al.*, 2008). Detected EOCs such as nitroglycerin and 17 $\beta$ -ethinylestradiol erythromycin from the pharmaceutical industry have been reported, along with veterinary medicines for instance, monensin, sulfamethazine and tylosin (Lapworth *et al.*, 2012).

Around 50,000 groundwater polluted sites have been reported in the UK, compared to 400,000 sites in the US (National Research Council, 1997; Lerner *et al.*, 2000). The number of polluted sites in other countries is not better, for example, in China, 90% of the aquifers have been reported as contaminated (Qiu, 2010). In many other developing countries, the extent of groundwater pollution is still uncertain due to the lack of research (Lewis *et al.*, 1982).

For the purposes of this thesis, the focus has been placed in organic compounds which came from D-NAPLs (dense non-aqueous phase liquids) sources, for example coal tar and creosote (Keuper *et al.*, 2003; Rivett *et al.*, 2014). Emphasis has been placed on phenolic compounds derived from D-NAPLs released from a coal tar distillery industry, which was the source of contamination in the study site

## **1.2 Phenolic contamination**

Phenolic compounds are a wide range of organic substances characterised by a phenyl ring (C<sub>6</sub>H<sub>5</sub>) joined to a hydroxyl group (-OH). Varying types of phenolic compounds are created when different functional groups attach to the aromatic ring. For instance, methylphenols (-CH<sub>3</sub>), chlorophenols (-Cl), nitrophenols (-NO<sub>2</sub>), alkylphenols (-R) and aminophenols (-NH<sub>2</sub>). These phenolic compounds are highly soluble in water, which is a relevant property when these substances reach groundwater and form aqueous phase plumes in aquifers (NPA, 2017; EBI, 2017).

Phenolic compounds have both natural and anthropogenic origins. These organic compounds can be found naturally occurring in plants or during the decomposition of plant biomass (Proestos and Komaitis, 2013). Nevertheless, most of the phenolic compounds impacting on

the groundwater quality of different aquifers originate from industrial activities such as pharmaceutical, petro-chemical, plastic and tinctoral industries. (PDB, 2017; William *et al.*, 2017).

The effects of phenolic contaminations on human health are quite severe. Dermal exposure or ingestion of these compounds could cause necrosis, damage to the eyes, liver, kidney or even death (Michałowicz and Duda, 2017). In this sense, phenolic contamination represents a high risk to humans (EPA, 2002). The high solubility of these compounds in water make them quite likely to reach different receptors, plus their severe effects on human health raise the risk levels (EEA, 2008).

Despite the harmful effects of phenolic compounds on human health they are still widely produced. For example, the global phenol production in 2010 was estimated around 8.5 million metric tons (CPCB, 2016).

In the past, phenol was produced during the distillation of coal-tar or during the coal-gas production (Thornton *et al.*, 2001b). In the UK, these industries produced large quantities of D-NAPL compounds, which were released through the leaking of underground tanks towards the aquifers (Environment Agency, 2003). These D-NAPLs contained a wide variety of phenolic compounds such as phenols, different type of cresols, BTEX or polyaromatic hydrocarbons (PAHs). Once released to the environment this immiscible mixture of compounds migrates to deeper levels.

The main feature of D-NAPL compounds is that they are denser than water and, due to this property they sink in groundwater. Once DNAPLs contamination reach the water table, the different chemicals form aqueous phase plumes, which are difficult to contain and remediate (Environment Agency, 2003; Thornton *et al.*, 2017).

There are a wide range of different engineered interventions used to remediate groundwater plumes, such as air sparging and pump and treat. These techniques have been effectively used in the treatment of organic plumes. Air sparging injects air into the plume to favour the volatilization of the pollutants, whereas PAT removes pollutants from the aquifers to be treated *ex-situ*. Nevertheless, these techniques are usually limited by the type of aquifer material, for example in silt and clay sediments, where these are not very effective due to the low permeability of these materials (Khan *et al.*, 2015). Considering the physical heterogeneity of the subsurface has become critical for the remediation of plumes, which could be very difficult.

### **1.3 Monitored Natural Attenuation (MNA) of Plumes**

The application of remediation technologies is often challenging due to the nature and extent of plumes, such as depth, and has therefore focused the attention of Natural Attenuation (NA) processes in the aquifer. NA is understood as different physical, chemical and biological natural processes taking place underground, and contributing to the reduction of toxicity, pollutant concentration or pollutant mass removal. “The processes of NA are dispersion, dilution, sorption, volatilisation, and chemical or biological stabilisation, transformation or destruction” (Wilson *et al.*, 2004; Wilson *et al.*, 2008; Jorgensen *et al.*, 2010).

In this sense, the monitoring of the NA processes, is referred as Monitored Natural Attenuation (MNA), has emerged as a risk-based strategy for the remediation and management of a contaminant aqueous phase plume, to protect the environment and human health (Khan and Husain, 2001; Blum *et al.*, 2011). The use of MNA as a management tool requires a good understating of these processes, consideration of the remedial targets and the timescale of the natural process to remove or reduce a certain amount of contaminant (Chapelle *et al.*, 2003; Rugner *et al.*, 2006). Therefore, several factors must be considered to demonstrate the presence of NA processes, such as the hydrogeology of the aquifer, laboratory studies, an adequate monitoring network, long-term sampling and good spatial resolution. This information should be integrated to create conceptual site models (CSM) able to predict the fate and transport of pollutants (Azadpour-Keeley *et al.*, 2001).

MNA requires long term monitoring to ensure that predictions made were achieved and to refine the CSM if necessary. This strategy is not a “do nothing” approach and has proved to be effective in the management of contaminant aqueous phase plume, and in successfully guiding the implementation of engineered interventions such as PAT (Rivett and Thornton, 2008; Thornton *et al.* 2017).

### **1.4 Biodegradation of pollutants**

Biodegradation is the only process able to permanently reduce the pollutant concentrations. This process is catalysed by different organisms (plant, fungi, bacteria and archaea) which use different pollutants as a source of carbon, breaking them down into smaller molecules (Alexander, 2004). In this sense, this biological process is a cost-effective and environment-friendly method to reduce the concentration of pollutants *ex* or *in situ* (Xiaoying *et al.*, 2011).

The breaking-down of pollutants uses different metabolic pathways of these organisms. In the case of aromatic hydrocarbons, there are upper pathways which destabilise the benzene ring (e.g. aerobic biodegradation of phenol through meta- and ortho-cleavage of the aromatic ring),

followed by a set of lower pathways, which finishes in the breaking-down of the aromatic compound into metabolites (e.g. succinyl-CoA and acetyl-CoA), which can then be used in different metabolic pathways (e.g. citric acid cycle) to finally be assimilated as biomass (Fritsche and Hofrichter, 2008; Fuchs *et al.*, 2011; Ladino-Orjuela *et al.*, 2016).

There are several environmental and biological factors influencing the biodegradation of pollutants. For example, pH affects the biosorption process of the pollutant; the presence of different electron acceptors (EA), such as oxygen, nitrate, iron, manganese or sulphate determines which metabolic pathways might become active in the presence of different contaminants; temperature influences the rate of the biodegradation and the solubility of pollutants; the amount of nutrients (phosphate, nitrogen) limits the growth achievable by the microbial community (Das and Chandran, 2011; Joutey *et al.*, 2013). In aquifers, the porosity in the unsaturated and saturated zone affects the flow and therefore pollutant migration, which impacts in the EA and electron donor (ED) availability for the microbes (EPA, 1998). On the other hand, there are biological factors such as the number of bacteria able to metabolize the pollutants and their activity state; threshold of toxicity influencing the activity state of the community, the microbial diversity, metabolic multi-species networks, and microbial interactions such as competition or cooperation between members of the microbial community (Madhavi, 2012; Sihag *et al.*, 2014; Srivastava *et al.*, 2014).

The ability of indigenous microbial communities to respond to contaminants has been widely described, and subject of study in microbes from pristine aquifers exposed to different pollutants (Aelion *et al.*, 1987). In polluted aquifers, the biodegradation of different organic pollutants has been proved in sediments collected from aquifers contaminated with Poly-aromatic hydrocarbons (PAH), and the ability of microbes to respond to naphthalene and phenanthrene, was demonstrated (Konopka and Turco, 1991; Madsen *et al.*, 1991). Other organic compounds, such as benzene and toluene were shown to be biodegradable by the autochthonous microbial community extracted from the aquifer material of a polluted aquifer; in the same manner halogenated aliphatic hydrocarbons have also shown to be degraded by aquifer microbes (Alvarez *et al.*, 1991; Chaudhry and Chapalamadugu, 1991).

The biodegradation of different organic compounds has been registered under different environmental conditions. For instance, in sediments from a jet-fuel polluted aquifer with PAHs, the ability of microbes to biodegrade under aerobic conditions, and accompanied by nitrate reduction was demonstrated with the addition of <sup>14</sup>C labelled organic pollutants. Similar pollutant mass removal of PAHs was observed during the first order decay degradation reactions in *in situ* microcosm (ISM) and laboratory batch microcosm (LBM) under aerobic

conditions (Aelion *et al.*, 1991; Hutchins *et al.*, 1991; MacIntyre *et al.*, 1993; Nielsen *et al.*, 1996). BTEX compounds and MTBE biodegradation under aerobic and nitrate reducing conditions have also been reported in aquifer columns and in a gasoline-polluted aquifer (Anid *et al.*, 1997; Borden *et al.*, 1997). On the other hand, biodegradation of organic compounds, such as toluene and xylenes from gasoline-polluted sediment sand has also been registered under sulphate reducing conditions (Edwards *et al.*, 1992). The biodegradation of other BTEX compounds, such as benzene, has also been studied in sediments from a petroleum-polluted aquifer under iron reducing conditions, which had the ability of removing contaminant inputs by the activity of *Geobacter spp.* (Edwards and Grbic-Galic, 1992; Rooney-Varga *et al.*, 1999). Chlorinated hydrocarbons could be broken-down under anaerobic and aerobic conditions, through their use as EA, ED or via co-metabolism (Suarez and Rifai, 1999).

Considering the relevance of the biodegradation processes in the removal of contaminants more detail in the microbial ecology of aquifers is presented below.

### **1.5 Microbial ecology of aquifers**

The presence of microbial populations in the subsurface has been described in the different environments located through the unsaturated and saturated areas of pristine and contaminated aquifers (Chapelle, 2001). In these locations, groundwater chemistry and various physical, hydrogeological properties of the aquifer material create diverse micro-environments, which serve as “niches”, used by different types of microorganism groups (Finlay *et al.*, 1997).

According to the British Geological Survey (BGS), these different chemical, physical and hydrogeological characteristics make possible the identification of three principal aquifers in the UK: Cretaceous chalk, Triassic sandstone and Jurassic limestone aquifers (Allen *et al.*, 1997).

The different features of these aquifers impact on the distribution of the microorganisms in these environments. For example, the high porosity but low pore space (<1.5  $\mu\text{m}$ ) of the chalk aquifers affect the distribution of different groups (Johnson *et al.*, 2000). In this type of aquifer, it has been suggested that the small pore size may prevent bacteria entering to these locations, driving them to the aquifer fissures (West and Chilton, 1997; Goody *et al.*, 2001). Similarly, the throats of limestone matrix, estimated between 0.1 - 0.3  $\mu\text{m}$ , has been pointed as the limiting factor preventing the settlement of bacteria into these locations, which would explain their distribution as confined into the aquifer fractures (Bottrell *et al.*, 2000). In the case of sandstone aquifers, the pore-sizes are bigger (1 – 90  $\mu\text{m}$ ), thus bacteria are likely to



spread and colonise the pore space of unconsolidated sandstone aquifers (Bloomfield *et al.*, 2001).

In the various aquifers there is also a strong influence of recharge events and temperature on the microbial composition (O'Dwyer *et al.*, 2014; De Giglio *et al.*, 2016). For instance, heavy rainfall can influence the inputs of nutrients and contaminants to the aquifer from industrial or agricultural activities developed over the aquifer (Böhlke, 2002). Importantly, temperature is one of the key limiting factors affecting growth, metabolic and survival rates of bacterial communities in aquifer sediments (Price and Sowers, 2004).

In summary, different aquifer types impact on the composition and activity of bacterial groups, which in turn have a critical role in the diverse geochemical reactions influencing the groundwater quality and the fate and transport of different solutes (Flynn *et al.*, 2013).

Bacterial communities can be distinguished based on their metabolic functions, such as aerobic respiration, along with anaerobic respiration processes such as nitrate, manganese, iron, sulphate reduction and fermentation (Lerner *et al.*, 2000; Thornton *et al.*, 2001a; Delleur, 2006). These types of microbial groups will also be affected by contamination inputs, which have been described as a driver in the change of community structures in organic-contaminated aquifers, and also in experiments using sediments from chalk and sandstone aquifer material which have become able to biodegrade organic-pesticides after the initial exposure (Shi *et al.*, 1999; Johnson *et al.*, 2000)

There are different bacterial groups which have been identified in contaminated aquifers and/or studies using aquifer material from different aquifers, these groups have shown changes in the microbial composition after contaminant-inputs have been applied (Gregory *et al.*, 2014). For instance, microcosms constructed with groundwater and sandstone material, after a BTEX input, the community switched the dominance of Proteobacteria to Actinobacteria (Fahy *et al.*, 2005; Fahy *et al.*, 2008). In aerobic microcosms, using sandstone aquifer material and after the application of benzene, the community was dominated by *Polaromonas*, *Acidovorax* and *Pseudomonas* (Aburto *et al.*, 2009). In similar microcosms, spiked with benzene the community changed from the dominance of *Rhodospirillum rubrum* to be dominated by *Hydrogenophaga* spp. and *Rhodococcus* (Fahy *et al.*, 2006). In microcosm experiments using permo-triassic sandstone material and phenolic-contaminated groundwater, it was possible to establish the sulphate reducer, nitrate reduction and methanogenesis activity and the identification of *Azoarcus* and *Acidovorax* in microcosms constructed with groundwater containing nitrate (Pickup *et al.*, 2001; Rizoulis *et al.*, 2013). In the case of limestone and chalk aquifers, the potential of microorganisms to degrade an

organic herbicide was explored through different microcosms experiments, and in the latter aquifer it was possible to establish their potential for the biodegradation of these compounds and a shift in the community composition which became dominated by *Pseudomonas* after the application of isoproturon (Johnson *et al.*, 2000; Johnson *et al.*, 2004). Shifts in the sediment microbial composition has also been documented with the addition of acetate, which augmented the abundance of *Geobacter* (Castelle *et al.*, 2013).

The different groups mentioned are part of the microbial community, but within this group it is possible to distinguish the planktonic and attached communities, the former likely to be associated to the mobile or free-living members of the community, whereas the latter are able to grow in surfaces and form biofilms (Costerton *et al.*, 1999; Crump *et al.*, 1999; Yoshida-Takashima *et al.*, 2011).

There are several studies in aquifers which have explored the differences between the attached and planktonic microbial communities. For instance, in sandy aquifers dominated by porous groundwater flow and contaminated with chlorophenols and D-NAPL-associated compounds, differences between archaeal communities located in groundwater and cores was determined and presented in terms of abundances of methanogens, which were found to be more predominant in the groundwater (Godsy *et al.*, 1992). Similarly, a preference of archaeal members for the planktonic community has been described in pristine aquifers, and another difference between these two communities was detected in terms of the abundances of iron reducers, which were preferentially attached to the sediments (Flynn *et al.*, 2013; Gregory *et al.*, 2014). In shallow contaminated and pristine aquifers, the use of *in situ* microcosms with natural substrates allowed the identification of higher microbial abundances located in the biofilm, while also informing about a ratio between these two communities relating to the contamination state of the aquifers (Griebler *et al.*, 2002). In fractured quartz aquifers, the majority of microbial biomass has been located in the planktonic phase (Lehman *et al.*, 2001a). In microcosm studies simulating fractures of basalt aquifers, differences in the composition of these communities has been established with members of *Enterococcus sp.*, *Bacillus psychrophilus* and *Pseudomonas stutzeri* only identified in groundwater, there were also differences in the relative abundances and activity between these two communities (Lehman *et al.*, 2001b). The shift in composition of these communities is not exclusive for groundwater contaminated environments and has also been described in sand polluted with polyaromatic hydrocarbons (PAHs) (Folwell *et al.*, 2016).

The ability of the microbial community to attach to natural surfaces and function in contaminated environments has been exploited in the use of biofilm reactors for wastewater

treatment and the production of fermentation products in the industry (Nicoletta *et al.*, 2000a). There are different types of biofilm bioreactors, such as the expanded granular sludge blanket (EGSB), biofilm airlift suspension (BAS) and biofilm fluidized bed (BFB), where these reactors can be supplied with different carbon sources, electron acceptors (EAs) and nutrients to produce the desired products (Nicoletta *et al.*, 2000b). It is also possible to control different conditions which enhance the metabolism of the biofilm, such as temperature, pH and the concentration of different substrates (Qureshi *et al.*, 2005). Nevertheless, in the wastewater treatment biofilm bioreactors, the effect of the reactor design on the composition of the biofilm communities treating similar material has been determined, and in some arrangements the community was dominated by different ammonia oxidising bacteria (Rowan *et al.*, 2003).

Given the differences between planktonic and attached communities observed in aquifers, and the ability of the biofilm to be used in different industrial applications, its role in the biodegradation potential of contaminated aquifers is likely to be important. Therefore, the biofilm formation process is detailed below.

### **1.6 Biofilm formation**

Biofilms have been defined as microbial groups able to attach to different substrates (O'Toole *et al.*, 2000). This community can be composed of multi-species of microorganisms which aggregates together or could be developed as a single-species biofilm, as has been described for *Bacillus spp.* and *Pseudomonas spp.* (Lindsay *et al.*, 2002; Rickard *et al.*, 2003; Steinberger and Holden, 2005). Biofilm formation is a complex process which contains several stages. Firstly, primary colonizers adhere to substrates during the early stages. This is followed by a more intense adhesion onto the surface when different extracellular polymeric substances (EPS) are produced, supporting the binding, adhesion and cohesion of cells (O'Toole and Kolter, 1998; Wingender *et al.*, 1999). Finally, the early attachers facilitate the attachment of secondary colonizers by co-adhesion, which results in the aggregation and formation of cells in micro-colonies, which can create a multi-species biofilm (Rickard *et al.*, 2003; Hall-Stoodley *et al.*, 2004). These stages have been proposed during the biofilm development of *Pseudomonas aeruginosa* (Sauer *et al.*, 2002; Stoodley *et al.*, 2002). The biofilm from the formation to the maturation stages can have different architectures. Some will have arrangements with microbial cells with an EPS around them, or forming channels where water and nutrients flow (Danese *et al.*, 2000). Usually biofilms are mushroom-shaped or have a flat structure (Hall-Stoodley *et al.*, 2004).

The extended presence of biofilms in different types of environments, such as hot springs, groundwater sediments and artificial surfaces relates to the advantages associated living

within them (Watnick and Kolter, 2000; Hall-Stoodley *et al.*, 2004). For instance, the ability to resist environmental disturbances, such as changes in temperature and pH, can be tolerated more successfully when microbes are associated in environments which have heterogeneity and may be protected with EPS (Jefferson, 2004; Stewart and Franklin, 2008). Also, in biofilms the proximity between their members can favour the transfers of advantageous genetic material which may confer resistance to antibiotics (Watnick and Kolter, 2000). Within biofilms higher transfers of plasmids and conjugation processes has been reported (Angles *et al.*, 1993; Hausner and Wuertz, 1999). Another advantage conferred by biofilms could be in environments where electron acceptor molecules are limited, and therefore the recycling of EAs become critical. This recycling can be mediated by outer membrane proteins of members of the biofilm, as has been suggested in biofilms formed by *Shewanella oneidensis* (Hernandez and Newman, 2001).

For the purposes of this thesis, the focus has been in the biodegradation of phenolic related compounds in a contaminated aquifer located in the UK.

### **1.7 Biodegradation of phenolic compounds at the study site**

In a permo-triassic sandstone unconfined aquifer, a phenolic plume was produced due to the former coal-tar distillery activity developed on the site (Thornton *et al.*, 2001a; Thornton *et al.*, 2001b). Two multi-level samplers (MLS), called BH-59 and BH-60 were installed on the site to study this phenolic plume. The compounds registered in this plume were phenol, *m,p,o*-cresol and different type of xylenols. This plume extends for 500 meters towards a public water supply, which reinforces the groundwater flow in this aquifer. The observed high pollutant concentrations and plume dynamics predicted that natural attenuation processes would not be able to cope with the level of contaminants, and the plume would grow under those conditions. Reactive transport modelling, considering pollutant concentrations and the abundance of different EA supported the ineffectiveness of natural attenuation as the sole remediation process to contain the plume in this aquifer (Lerner *et al.*, 2000; Meyer *et al.*, 2001).

The biodegradation of the different pollutants contained in the plume, take place following different routes, and is strongly dependant on the availability of different EAs and influenced by the inhibitory effects exerted by high pollutant concentrations. For example, bacterial nitrate reduction (BNR) activity is naturally contained within the plume fringes and this biodegradation is sustained over time by the transverse mixing between low concentration of pollutant fringes and background groundwater. These conditions favour high numbers and activity of the microbial community, where nitrate is rapidly used in these fringes and is

depleted to the core of the plume (Pickup *et al.*, 2001; Spence *et al.*, 2001a; Thornton *et al.*, 2001a; Thornton *et al.*, 2001b).

The pollutants of this plume are able to be biodegraded at deeper levels through the activity of bacterial sulphate reduction (BSR), evidence of this activity was the enrichment of the  $^{34}\text{SO}_4^{2-}$  and the depletion on  $^{34}\text{S}^{2-}$  sulphide. Nevertheless, the activity of BSR was inhibited due to pollutant concentration above 2000 mg/l (Spence *et al.*, 2001). Complementary to this, the presence of methane in the locations where BSR was absent, was accompanied by an enrichment of  $^{13}\text{C-CO}_2$  and depletion of  $^{13}\text{C-CH}_4$ , which suggested methanogenesis at these locations by microbes able to cope with high pollutant concentrations. Also, the high concentration of manganese and iron in groundwater suggested the presence of reductive dissolution from the iron and manganese oxide coatings of the aquifer material (Thornton *et al.*, 2001a; Thornton *et al.*, 2001b; Baker *et al.*, 2012).

The biodegradation observed in the site relates to different processes during the plume formation.

## 1.8 Groundwater plume development

Plume development due to pollution by D-NAPL is dependent on the composition of the source area as well as the different physical, chemical and biological processes during the plume formation.

As D-NAPL is released into the unsaturated zone, the advancement will be mostly influenced by gravity, forming residual D-NAPL in the unsaturated zone during the migration to deeper levels, due capillary forces from the interfaces formed between the D-NAPL, air and water. D-NAPL will migrate until it reaches the water table, and given that it is denser than water, it will sink to depths below the water table (Delleur, 2006; Bear and Cheng, 2010). Once this migration process starts below the water table, groundwater will pass through this immiscible mixture dissolving the chemicals, creating aqueous phase plumes (Environment Agency, 2003).

The **chemical composition** of the source zone will directly influence the plume composition as the D-NAPL starts dissolving into the groundwater (Rivett *et al.*, 2001). The varying **solubility** of the different chemicals in the D-NAPL is regulated by Raoult's law, where the effective aqueous solubility of the chemical compound in the D-NAPL is dependent on the mole fraction in the D-NAPL and the aqueous solubility of the pure phase compound (Fraser *et al.*, 2008; Apello and Rolle., 2010). This will determine the variation on the effective solubility of each chemical, as more soluble components dissolve first, changing the mole fractions of the D-NAPL (Rivett *et al.*, 2014). Another effect on chemical variation is the **source history**, taking

into account that a number of different industrial activities may contribute to the contamination with different groups of chemicals and pollutants (Thornton *et al.*, 2001a; Thornton *et al.*, 2001b).

The fundamental **physical processes**, which facilitate the spreading of the chemical plume through the aquifer, are **advection** and **hydrodynamic dispersion** (Hiscock, 2005; Bear and Cheng, 2010). The advective velocity is calculated using Darcy's law. The pore water velocity is the average linear velocity considering the porosity of the aquifer material (Edmunds and Shand, 2008). The advective velocity is important in the transport of non-reactive dissolved contaminants. Physical dispersion occurs due to mechanical mixing and molecular diffusion. In general, the longitudinal dispersion is higher than the transversal dispersion (Morris and Novak, 1989; Hiscock, 2005). The mechanical mixing is due to variations in the velocities at the pore space and to dispersion by tortuosity, whereas molecular diffusion is due to chemical concentration gradients (Schwartz, 1977; Gillham *et al.*, 1984). As a consequence of the advection and hydrodynamic dispersion processes the pollutants concentrations are diluted.

A **chemical-physical process** in the development of aqueous phase plumes is **sorption**. During this process the dissolved reactive contaminants will be retained due to chemical interaction with functional groups of the aquifer material (Weber *et al.*, 1992). Therefore, their spreading velocity through the aquifer will be lower than the groundwater velocity. As a result of the interaction between the functional groups and the reactive pollutant, the dissolved concentration of the pollutant will decrease without changing the total mass of pollutant. The retardation factor can be estimated with the average groundwater velocity and the average linear velocity of the reactive contaminant pollutant (Mackay *et al.*, 1986; Hiscock, 2005).

As mentioned earlier, an important **biological process** in the plume development is **biodegradation**. Biodegradation of chemicals results in the destruction of pollutants generally to less harmful species and is an important process of pollutant mass removal from contaminated aquifers (Wilson *et al.*, 2004; Rees *et al.*, 2007; Rivett and Thornton, 2008). The biodegradation of pollutants is driven by microbial communities, which are able to respire organic molecules using different electron acceptors (i.e. archaea, bacteria and eukarya) (Rizoulis *et al.*, 2013). The effect of biodegradation in the plume results in shrinking, steady-state or expansion depending on the bioremediation potential of the microbial community (Thornton *et al.*, 2001b).

## 1.9 Redox zonation and plume fringe concept in plumes

As part of the study of plume development through MNA in the last decades, different conceptualization of the plume compartmentalizations have been developed, such as the redox zone and plume fringe concepts.

The hydrogeological properties of the aquifer, the chemistry of the source area and the spatial and temporal variability within the plume create different redox zones which are distributed with reduced zones close to the source area and more oxidized environments to the front and outskirts of the plume (Christensen *et al.*, 2000). The different redox environments will be from methanogenic zones near the source area, followed by sulphate reduction to the core of the plume, iron manganese reduction surrounding the core to nitrate and aerobic respiration at the edges of the plume (Bjerg *et al.*, 2011; Thornton *et al.*, 2001). Signs of these redox zones are the reduction of electron acceptors for the oxidation of molecules, and the production of methane, sulfide, iron(II), manganese(II), nitrite, which are signs of the reduction of CO<sub>2</sub>, sulphate, iron(III), manganese(IV) and nitrate respectively (Bjerg *et al.*, 1995; Lerner *et al.*, 2000; Thornton *et al.*, 2001a).

The electron succession predicted to occur in the aqueous phase plumes is related to the Gibbs free energy of the process associated to the oxidation of the electron donor (organic molecule) and passing from the most energetic electron acceptor to the lowest. In these terms the predicted succession is O<sub>2</sub> > nitrate > manganese (IV) > iron (III) > sulphate > CO<sub>2</sub>, and it is associated to terminal electron acceptor processes (TEAP) (Thornton *et al.*, 2001b; McMahon and Chapelle, 2008).

Redox zonation has been described for several aqueous phase plumes on different sites. For instance, a leachate plume derived from old landfill in Vejen, Denmark with methanogenic activity and sulphate, iron, manganese and nitrate reduction and aerobic activity from the source area to the front of the plume (Lyngkilde and Christensen, 1992). Another example of evolution from aerobic degradation at the top fringe, followed by manganese and iron reduction to methanogenic activity has also been described in a plume of BTEX (benzene, toluene, ethylbenzene, and xylenes) from a crude oil spill in Minnesota, USA (Cozarelli *et al.*, 2001). Similar spatial electronic acceptor successions have been described in a plume formed by phenols, cresols and xylenols derived from a coal tar distillery in Wolverhampton UK (Thornton *et al.*, 2001b; Lerner *et al.* 2000). There is evidence that biodegradation of the pollutant organic carbon in this aquifer occurs by different processes: aerobic respiration, NO<sub>3</sub>-reduction, Mn(IV)/Fe(III)- reduction, SO<sub>4</sub><sup>2-</sup>reduction, methanogenesis and fermentation, with the following production of some metabolites and reduced species (Thornton *et al.*, 2001a).

Those processes seem to develop redox zones and produce methane and carbon dioxide, but biodegradation of the pollutants is slow for the high phenol concentration at the core of the plume (Williams *et al.*, 2001). Other plumes exhibit different arrangements of the redox zonation, for example with iron reduction at the core of the plume and denitrification at the top fringe, and absence of sulphate reduction and methanogenesis have been described in Banisveld, The Netherlands (Van Breukelen *et al.*, 2003).

Nevertheless, the concept of redox zonation has been revisited recently because some argued that it would not be possible to replenish the aqueous EA used at the source area to downstream zones. In this sense, the only possible processes to the core of the plume would be given by insoluble iron and manganese (manganese and iron reduction) and methanogenesis; while nitrate and sulphate reduction would be able to take place only in the plume fringes due to mixing of small pollutant concentration with background groundwater. Therefore, the redox zonation pattern will not develop as expected (Meckenstock *et al.*, 2015).

In the plume fringe concept, most of the biodegradation occurs in this location, whereas to the source area and plume core there are inhibition effects, exerted by the high amounts of pollutant concentrations (Thornton *et al.*, 2001a; Bahr *et al.*, 2015). In these fringes different microbial processes would be able to happen simultaneously, limited by the availability of different EAs, instead of their thermodynamics properties (Meckenstock *et al.*, 2015).

The importance of these plume fringes in polluted environments is related to the high biodegradation capacity observed on these locations, due to high numbers and activity of microorganisms (Pickup *et al.*, 2001; Tuxen *et al.*, 2006), derived from the chemical conditions in these areas, with constant supply of EA and ED in concentrations favouring biodegradation and pollutant mass removal (Wilson *et al.*, 2004; Rees *et al.*, 2007).

It should be noted that despite the model of plume zonation, the plume fringes arise as a highly important location for biodegradation and different areas are able to be distinguished in plumes. Different models have predicted the presence of micro niches in groundwater systems, influenced by the geochemistry and hydrogeology features of each aquifer (Jakobsen, 2007).



## 1.10 Chemical interfaces in groundwater pollutant plumes

A major difficulty in ensuring groundwater quality is its susceptibility to pollution given the potentially high residence time in the subsurface. The travel time from recharge to discharge points could be years, decades to centuries (UNEP, 2003; Appelo and Postma, 2004). Therefore, pollutants may remain in groundwater for a long time.

A wide range of organic and inorganic pollutants can occur in contaminated aquifers from different industrial activities (Madsen, 2008). The most common organic pollutants in groundwater are fuel related hydrocarbons such as BTEX (benzene, toluene, ethylbenzene and xylenes), PAHs (polycyclic aromatic hydrocarbons) and fuel additives (e.g. MTBE, methyl tert-butyl ether) and industrial chemicals for example chlorinated solvents and coal tar by-products (Lerner & Harris, 2009; Megharaj *et al.*, 2011; Wang *et al.*, 2013)

Organic pollutants form aqueous phase plumes in groundwater which are dispersed through the aquifer by groundwater flow. Different physical, chemical and biological processes influence their development and in turn the fate of compounds contained within them (Environment Agency, 2003; Environment Agency, 2014). Biodegradation of organic compounds in groundwater typically changes the geochemical environment of the aquifer and is an important influence on the natural attenuation of specific organic chemicals (Lyngkilde & Christensen, 1992a; Frohlich *et al.*, 1994; Spence *et al.*, 2001; Thornton *et al.* 2001a; Spence *et al.*, 2005; Baker *et al.* 2012). Different hydrogeochemical and redox zones can be distinguished within an organic plume as a result of this biodegradation (Lyngkilde & Christensen, 1992b). These zones are conventionally defined spatially by a relative dominance of methanogenic conditions near the source area, with successively less reducing conditions characterised by consumption of sulphate, iron oxides, manganese oxides, nitrate and respiration of oxygen in the aquifer, further along the plume flow path (**Figure 1.1.a**). As a general feature, organic plumes develop with a high concentration of pollutants close to the source area and to the core of the plume, and lower concentrations to the periphery of the plume (Christensen *et al.*, 2000; Lerner *et al.*, 2000). Plume development and the spatial-temporal distribution of redox zones and biodegradation processes within them reflect a balance between the flux of biodegradable compounds released from the source area and the bioavailability of oxidants supporting specific biodegradation in the plume. In general, the bioavailability of dissolved oxidants (oxygen, nitrate, sulphate) is controlled by hydrodynamic dispersion in groundwater. This property is typically very small in most aquifers. The bioavailability of iron and manganese metals oxides in aquifers is typically determined by the form and type of oxide fraction present on the aquifer material (Lerner *et al.*, 2000).

The conventional understanding of the spatial-temporal development of organic contaminant plumes, as depicted in **Figure 1.1.b**, has now been superseded by one which recognises two distinct zones of biodegradation activity, based on evidence from numerous field studies (Lerner *et al.*, 2000; Thornton *et al.*, 2001b; Tuxen *et al.*, 2006; Baker *et al.* 2012; Bahr *et al.*, 2015; Meckenstock *et al.*, 2015). In this conceptual model, the plume consists of a relatively narrow zone (usually <1m in thickness), termed the *plume fringe*, located at the periphery of a plume, which envelopes a much larger anaerobic plume core. Biodegradation and the distribution of microbial communities is typically enhanced at the plume fringe, due to the supply of energetically favourable electron acceptors (oxygen and nitrate) from the background groundwater (Lerner *et al.*, 2000; Thornton *et al.*, 2001a; Tuxen *et al.*, 2006). Conversely, the plume core is characterised by biodegradation rates which are typically lower than those at the plume fringe, due to oxidant mass transfer limitations and other factors (e.g. metal oxidant properties, as iron and manganese oxides, and contaminant concentration effects) which may inhibit reaction rates (Spence *et al.*, 2001; Thornton *et al.*, 2014). The plume fringe represents a chemical interface, which separates the core of the plume from the background groundwater and also more oxidizing redox conditions from the reduced environment found within the plume core (Lerner *et al.*, 2000; Thornton *et al.*, 2001a; Thornton *et al.*, 2001b, Williams *et al.*, 2001). In this context, these chemical interfaces develop by physical and biological processes, separating two regions in terms of pollutants and redox environment (Bjerg *et al.*, 1995; Van Breukelen & Griffioen, 2004).

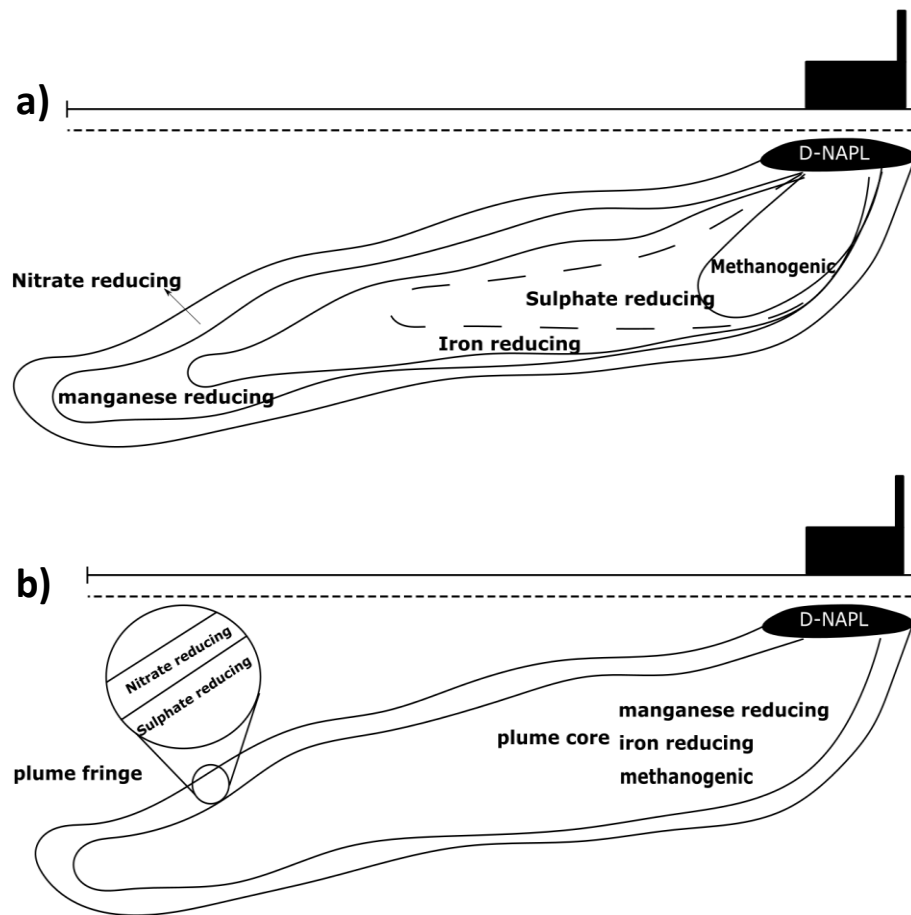


**Figure 1.1.** Conceptualization of plume development in groundwater (a) plume zonation and (b) plume fringe concept.

The importance of these chemical interfaces in organic contaminant plumes is related to the high biodegradation capacity observed at these locations, due to high numbers and activity of microorganisms (Pickup *et al.*, 2001; Tuxen *et al.*, 2006), derived from the chemical conditions in these areas, with constant supply of electron acceptors (EA) and electron donors (ED) in concentrations favouring biodegradation and pollutant mass removal (Wilson *et al.*, 2004; Rees *et al.*, 2007).

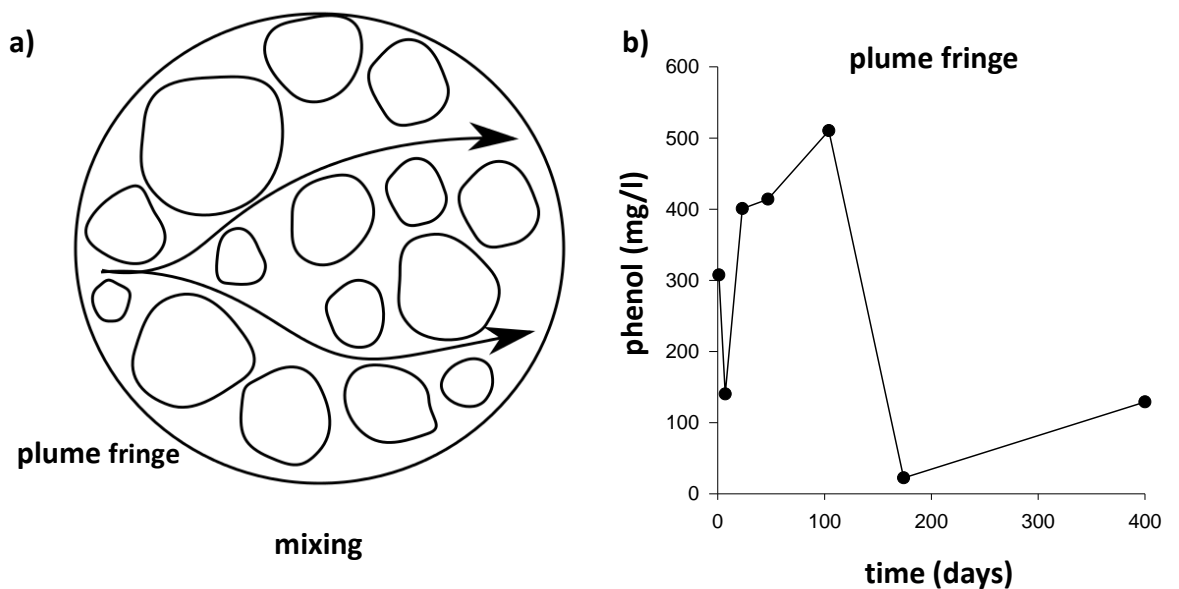


**Figure 1.2** (a) Schematic representation of mixing processes which occur in the upper and lower fringe of an organic contaminant plume; (b) Variation in phenol concentration over time due to mixing processes in the lower fringe of a plume, located 30 meters below ground level (mbgl).

The development of these chemical interfaces in plumes is influenced by different physical processes which make them changeable environments in terms of their hydro-chemical composition. For example, transverse hydrodynamic dispersion due to mechanical mixing and molecular diffusion, that occurs as the plume migrates through the aquifer, controls the flux of dissolved electron acceptors supplied from the background groundwater to the upper and lower plume fringe, (Wilson *et al.*, 2004; Thornton & Rivett, 2008). **Figure 1.2** illustrates the origin and relative scale of influence of the process which contributes hydrodynamic dispersion in an aquifer. In this regard, the concentrations of organic compounds and different electron acceptors mixed within the plume fringe are likely to fluctuate over time due to changes in the contaminant flux from the plume source and background groundwater composition. Therefore, the plume fringe can be considered to have a steady-state position with respect to the development and geometry of the plume, but the respective concentrations of solutes which create the interface will be subject to natural fluctuations.

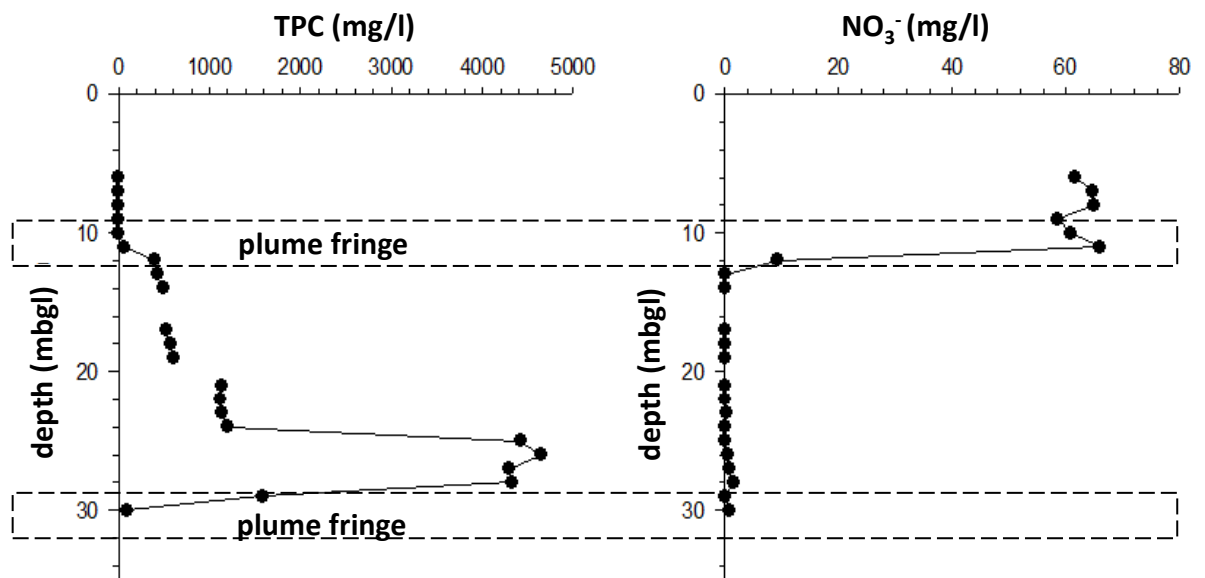


**Figure 1.3.** Depth profiles of Total Phenolic Content (TPC) and nitrate concentration obtained from a multi-level sampler (MLS) installed in the aquifer at the study site. Note the plume fringe is the chemical interface separating the background groundwater from the plume core. Data of the plume was after 174 days of monitoring.

Conversely, the chemical interface at the front (or leading edge) of a plume develops in response to longitudinal hydrodynamic dispersion that occurs by advection of the plume (Breu *et al.*, 2008; Hiscock, 2005). In this respect, the hydrochemical conditions at the interface develop as contaminated groundwater in the plume core advances into the uncontaminated aquifer downstream. This results in a chemical interface characterised by increases in contaminant concentrations over time (for a fixed spatial location), which eventually stabilise as concentrations approach those found in the plume core. Therefore, the chemical interface at the plume front becomes a more stable chemical environment over time.

The chemical interfaces described in **Figure 1.2**, **1.3** and **1.4** are located at the fringe of a contaminant plume and occur naturally in response to the development of the plume in the aquifer. However, in some situations chemical interfaces resembling the plume fringe can be induced within the plume core by engineered remediation measures, such as pump and treat (PAT) systems.

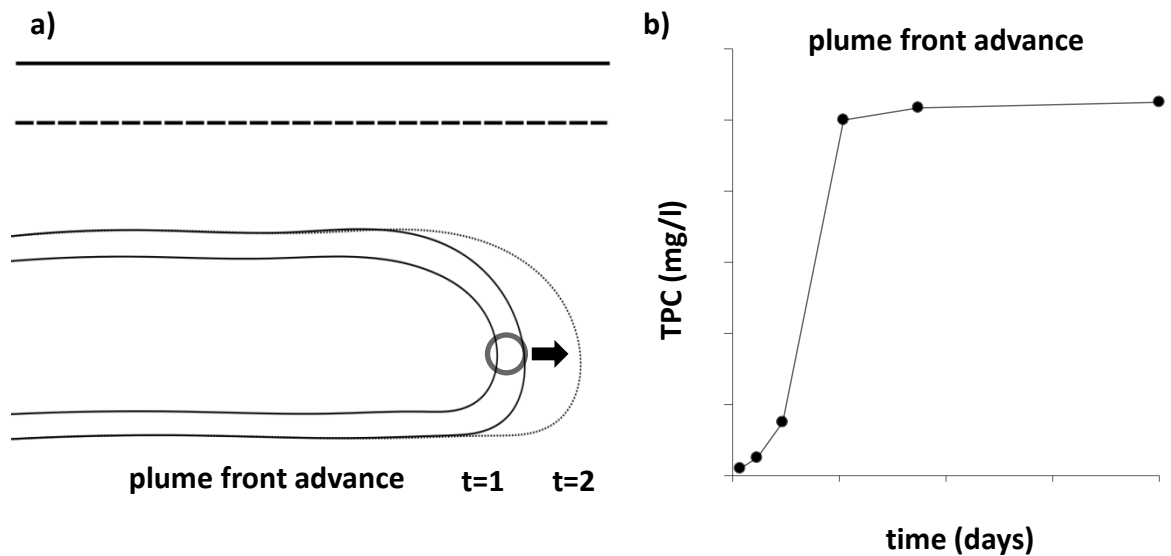


**Figure 1.4** (a) Schematic representation of location (in circle) where the plume front has advanced; (b) Expected change in phenol concentration after advance of the plume front at this location, as described by Elliot *et al.* (2010).

PAT systems are typically used for hydraulic containment of a plume, to restrict further contaminant migration, or to extract contaminated groundwater for *ex situ* treatment (Keelay, 1989; Palmer *et al.*, 1992). The hydraulic manipulation of the plume and aquifer flow field created by the operation of a PAT system can result in development of chemical interfaces between the plume and background groundwater. This feature arises from physical heterogeneity in the aquifer, which creates variability in the spatial distribution of aquifer hydraulic conductivity (ie. permeability). Under a constant pumping rate, groundwater is extracted preferentially along more permeable zones, drawing the background groundwater laterally into the plume to create a series of chemical interfaces, analogous to a plume fringe, but with the overall appearance of "fingers" of mixed contaminated and uncontaminated groundwater in vertical profile (Thornton *et al.*, 2014). **Figure 1.5** illustrates this scenario in schematic form and compared with vertical profiles of total phenolic compounds (TPC) from 2009 to 2012 obtained from an MLS at the study site under natural conditions (2009) and following the initiation of (2011) and stop of a PAT system (2012)

Moreover, after these types of interventions are stopped, the previously induced chemical interfaces are likely to change their location due to the response of the system and the influence of source term variations (Thornton *et al.*, 2014). In **Figure 1.5** in the year 2012, the PAT system was switched off, 2 years after TPC values increase due source term variation, an indication of the movement of the previously induced chemical interface at the core of the plume.

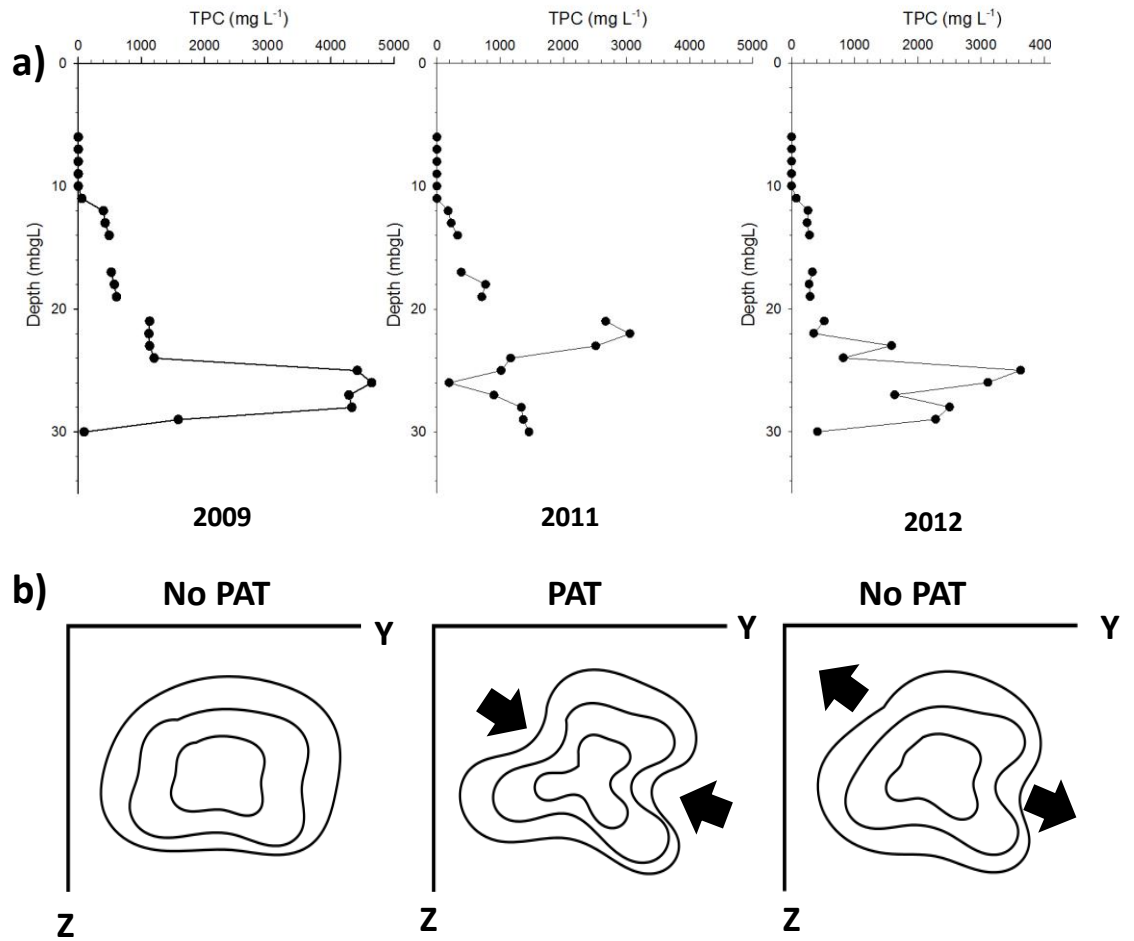


**Figure 1.5** (a) Total Phenolic Content (TPC) variation due to operation of a PAT system at the study site (undisclosed location). Note 2009 is pre-implementation of the PAT system, 2011 active PAT and in 2012 the PAT was switched-off, data from Thornton *et al.* (2014) (b) Schematic representation of chemical interfaces induced within the core of an organic contaminant plume due to the operation of a PAT system.

The interactions between microbial communities responsible for the relatively high biodegradation potential observed at the fringe and similar chemical interfaces in plumes remain poorly understood. In general, the research on this subject has focused on the planktonic microbial community, the mobile phase, and usually assuming similarity with the biofilm, the attached phase.

Considering other aquatic systems such as oceans and rivers, studies have shown differences in activity and phylogeny between these two phases (DeLong *et al.*, 1993; Crump *et al.*, 1999; Folwell *et al.*, 2016). Recent research in aquifer settings has highlighted the need to study both the attached and planktonic communities and to establish the functional relationships

between these two phases to relate microbial community structure and interactions to biodegradation potential (Rizoulis *et al.* 2013).

However, little is known about the response of microbial communities to the chemical conditions found at such interfaces, or how the community response varies with time as conditions evolve. Studies have shown the existence of steep gradients in organic pollutants and electron acceptors at the plume fringe (Lerner *et al.*, 2000; Thornton *et al.*, 2001; Tuxen *et al.*, 2006). It is expected that this will create conditions in which the relative dominance of specific populations varies spatially and temporally within the microbial community. Key influences will be the availability of electron acceptors and substrates, as well as specific interactions due to contaminant-specific properties (e.g. competition and toxicity effects). In turn, this is likely to influence microbial attachment, the succession of microorganisms that develop in biofilms and interactions between planktonic and attached communities. Moreover, the differences, stability and dynamics between the planktonic and attached phases of the microbial community are not well understood.

This is expected to define the potential for contaminant biodegradation within a plume, given that biodegradation of specific organic chemicals may be mediated by microbial populations with a restricted functional and metabolic capability, linked to a defined pathway.

### 1.11 Research Aim and Objectives

The aim of this Ph.D. was to investigate the responses of microbial communities to different chemical environments that develop in polluted aquifers. The thesis considers three research objectives with associated sets of research questions. **Figure 1.6** illustrates the thesis structure.

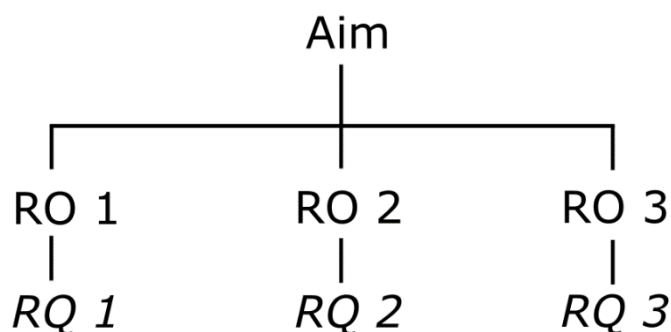


**Figure 1.6.** Schematic representation of the thesis structure. Note RO, research objective; RQ, research questions.



**Research objective 1:** To determine microbial dynamics of communities located at chemical interfaces within an organic contaminant plume in groundwater.

In the literature, different microbial dynamics that take place at these locations have not been explored. For example, the time-scales of attachment of the microbial community have not been determined. Also, the temporal evolution of the planktonic and biofilm communities during biofilm development remains unclear. The following questions guided the research.

***Research questions 1 (RQ-1)***

- What is the timescale of attachment in microbial communities of chemical interfaces?
- How do the biofilm and the planktonic communities vary over time?
- How does the planktonic community differ from the biofilm community?

**Research objective 2:** To evaluate the response of biofilm communities to changes in their chemical environment at laboratory scale.

The technical difficulty to access the biofilm community (attached) in polluted aquifers has made that their role during the biodegradation of pollutants remains unclear. Moreover, there are chemical modifications at chemical interfaces of groundwater plumes. The responses of the biofilm to alterations of their chemical environment have not been determined. The following questions arose.

***Research questions 2 (RQ-2)***

- What is the effect of changing the chemical environment on the biofilm communities at chemical interfaces?
- What drives community development in biofilms at chemical interfaces?

**Research objective 3:** To evaluate the effect of induced chemical interfaces scenarios by Pump and Treat (PAT), on the planktonic community

The responses of the microbial community to a PAT system have not been explored. It is not clear if communities shift and how these potential changes modify the activity of the entire community. Using a site intervened with PAT, the following questions emerged.

***Research question 3 (RQ-3)***

- How will different PAT regimes influence the structure and activity of the microbial community?
- Does the enhancing of biodegradation persist over time?

- How do the microbial communities respond to a cease of operation of PAT?

### **1.12 Thesis structure and author contributions**

The thesis was structured according to the research objectives. Author contributions are from the primary author J.F. Mujica and the Supervisory Team S.F. Thornton and S.A. Rolfe. All from the University of Sheffield.

### **Chapter 2. Microbial dynamics and biofilm community structure in chemical interfaces**

This chapter addresses the first research questions (**RQ-1**) related to the timescales of attachment, and the differences and stability between the planktonic and attached communities. The systems used in the field and lab are explained among the hypothesis. The geochemistry methodology and data includes phenolic, metabolites, metals, major ions, and gases for the two years of monitoring. The microbiology methodology and data includes preliminary tests, cell counting, terminal restriction length polymorphism (t-RFLP), sequencing library preparation and bioinformatics. Selection of restriction enzymes for t-RFLP and troubleshooting guide for the amplification of contaminated sediments are included. The discussion was based on the microbial responses during biofilm development. This work has been presented as platform presentations in two conferences. The Fourth International Symposium on Bioremediation and Sustainable Environmental Technologies held in Miami, USA May 22-25<sup>th</sup> 2017 and in the Sustainable Use and Management of Soil, Sediment and Water Resources 14th International Conference held in Lyon, France 26-30<sup>th</sup>, June 2017.

### **Chapter 3. Biofilm community in chemical interfaces and their responses to changes in their chemical environment**

This chapter focuses on the effects of environmental changes in the biofilms located at the chemical interfaces of polluted aquifers, to address different research questions (**RQ-2**). Justifications on the chosen depths to recreate different environments of the plume are presented. The settling times of the attached communities come from the findings of Chapter 3 and were used to change the experimental conditions. Emphasis on the experimental design which has recreated different scenarios, such as mixing in upper plume fringe, plume advance, source term variation and plume refreshing situations, using a large set of microcosms. The geochemistry methodology and bioinformatics analysis of data were similar to Chapter 3. Discussion was based on the microbial responses to environmental changes and their relation with plume development.

#### **Chapter 4. Microbial community responses to chemical interfaces induced by Pump and Treat in a phenolic-contaminated aquifer**

This chapter explores the effects on the microbial community when a polluted aquifer is intervened with PAT. The operation of one of the PAT stopped its operation and how the system responded to the cease of operations is unclear. The effects on the mass of pollutant and microbiology were studied using similar techniques to Chapter 2 and 3. Annual surveys using high-resolution multi-Level Samplers (MLS) next to the pumping borehole were made before and after the change of the pumping regime for a period of 3 years. Samples were also collected next to a pumping borehole, to compare the effect of a continuous operation. The discussion was based on the geochemical effect of different PAT regimes and its effect on the microbial community. Chemical gradients explaining the variation in microbial communities were also considered.

#### **Chapter 5. Conclusion**

This chapter gathers all the relevant results and findings. It shows how these findings represent an advance in the understanding of biofilm in changeable environments of polluted aquifers. It suggests future lines of research and what could be improved.

# Chapter 2

---

*Microbial dynamics and biofilm community structure in  
chemical interfaces*

---

## 2.1 Introduction

In aquifers polluted with organic compounds, biodegradation by autochthonous microbial communities contributes to the breakdown of contaminants, generally, to less harmful species. This is an important biological process critical for contaminant mass removal and the remediation of these environments (Lerner *et al.*, 2000; Pickup *et al.*, 2001; Thornton *et al.*, 2001a, Wilson *et al.*, 2004; Rizoulis *et al.*, 2013). These processes contribute to Natural Attenuation (NA) that have an important role in the remediation of plumes (Lerner *et al.*, 2000; Thornton *et al.*, 2001a).

In polluted aquifers, the chemical interfaces formed at plume fringes are areas identified for high biodegradation rates (Pickup *et al.*, 2001; Thornton *et al.*, 2001b; Tuxen *et al.*, 2006). While most studies have focused on the biodegradation potential of the planktonic microbial community within the plume fringes, the role of the biofilm community attached to the sediments is not understood and likely to be important.

Biofilms are composed of species able to adhere to surfaces (O'Toole *et al.*, 2000; Madsen *et al.*, 2012). Attachment is a complex process: The attachment of primary colonizers to new substrates facilitates the attachment of secondary colonizers by co-adhesion, which results in a multi-species biofilm, such as in human tooth plaque (Rickard *et al.*, 2003). The complexity of the biofilm system has been shown through other systems, such as the human colon, where interactions and competition within the microbial community have been observed after a change in diet (Flint *et al.*, 2007). Other microbial features have also been described in the attached phase, such as richness of fluctuation in the formation of biofilms (Santegoeds *et al.*, 1998; Jackson, 2003).

Previous studies using microcosms and groundwater from polluted sites have shown an increase in the complexity of the microbial community and in the biodegradation of organic compounds in sediments inoculated with a microbial community from a contaminated aquifer (Elliott *et al.*, 2009). Moreover, culture-independent techniques have established differences between the planktonic and attached phases, with the attached phase being more diverse (Rizoulis *et al.*, 2013). However, these studies were made at single time points and the development of community structures over time has not been investigated in the chemical interfaces of polluted aquifers.

In this study, the chemical interface of a plume located at 30 mbgl at BH-59, was used to study the biofilm formation. This depth was selected as it represents a transition zone, a chemical interface between the plume core and background groundwater. Despite chemical variability

over time, due to source term variation and engineered interventions, this lower plume fringe has maintained its position. **Figure 2.1** shows the depth profile of total phenolic compounds (TPC) within the plume over different surveys between 2009 and 2016.

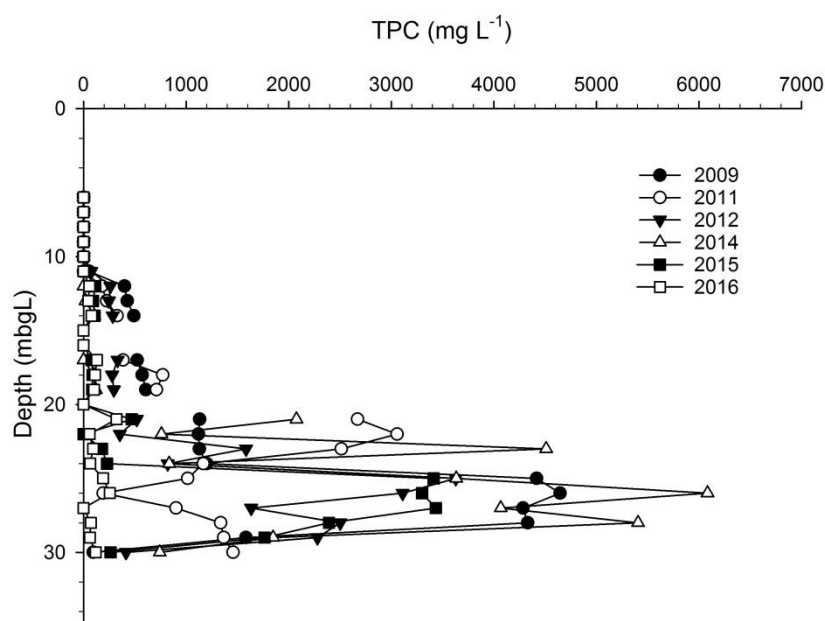


**Figure 2.1.** Depth profile of total phenolic content (TPC) at BH-59. Note 2009 pre-implementation of PAT system, 2011 active PAT and 2012 PAT was switched-off. The chemical interface at 30 meters below ground level (mbgl) maintains its position over time.

### Research questions

The research questions considered for this chapter are the following:

- What is the timescale of attachment in microbial communities in/from chemical interfaces?
- How do the biofilm and the planktonic communities vary over time?
- How does the planktonic community differ from the biofilm?

### Research aim

The aim of this chapter was to examine biofilm formation from early attachment events in sediments through to the development of a mature biofilm. This is then compared to the structure of the planktonic microbial community. The biofilm formation was assessed in laboratory microcosms containing substratum with similar mineralogy to the aquifer material, and an inoculum of groundwater from 30 meters below ground level (mbgl) collected from the

study site polluted with phenolic compounds. *In situ* biofilm formation was studied using sand bags placed in the screen of a Multi-Level Sampler (MLS) located at the same site.

### **Research Hypothesis**

The following hypotheses were tested:

1. Early attachment events will promote an increase the bacterial diversity in the biofilm when sediments are inoculated with polluted groundwater. The alternative hypothesis considered is that there is proliferation or preferential attachments of some bacterial groups and the diversity of the biofilm will not increase from the initial attachment period.
2. The planktonic and biofilm communities will differ from each other over the period of the study.
3. The structure of the biofilm community, as well as the planktonic community will differ and evolve over the period of the study.

### **Research Objectives**

The following objectives were followed:

1. To determine the time-scales of biofilm attachment at laboratory and field scale
2. To evaluate the differences between planktonic and attached microbial communities structures during biofilm development over time at laboratory and field scale
3. To determine the variability within each of the microbial communities over time during biofilm development at lab and field scale

## **2.2 Methodology**

### ***Substrate preparation***

Permo-Triassic red sandstone with similar mineralogy of the original aquifer material (Harrison *et al.*, 2001) was obtained from Penkrige Pottal Pool (Hanson Aggregates, Penkrige, UK). The sandstone was smashed and sieved using 150 and 300  $\mu\text{m}$  sieves (Endecotts Ltd, London, UK). This fraction demonstrated to be representative of the aquifer material (Baker, 2011). The sand grains were sterilized by autoclaving at 121°C for 20 min.

### ***Microcosm system and inoculum***

The microcosms were assembled under aseptic and anaerobic conditions using an anaerobic chamber (PlasLabs 815-Glove Box, PlasLabs Inc, USA) reflecting the field environment. Each microcosm consisted of 125 ml Wheaton glass serum bottles previously cleaned by a series of washes using Decon 90® and 0.1 M HNO<sub>3</sub>. The bottles were sterilized by autoclaving at 121°C for 20 min. 20 l of groundwater from a plume previously characterized (Pickup *et al.*, 2001; Thornton *et al.*, 2001b; Williams *et al.*, 2001) and containing a mixture of phenols, cresols and xylenols was collected from 30 mbgl of borehole 59 of the study site, using a peristaltic pump into sterile, N<sub>2</sub>-filled containers (Elliot *et al.*, 2009). Each microcosm was filled with 100 g of sterilized sand grains described above and with 100 ml of the collected groundwater. Microcosms were capped with a butyl rubber stopper secured by an aluminium crimp (Fisherbrand, UK). Abiotic controls were made adding sodium azide (NaN<sub>3</sub>) at a final concentration of 2 g/l. The microcosms were incubated at 10°C and in dark conditions. **Figure 2.2** shows a picture of a microcosm after the construction process.



**Figure 2.2** Example of a microcosm after the setting-up process in anaerobic conditions.

### ***Incubation in situ***

Bags were constructed using sterile nylon mesh of 100 µm pore diameter (Plastok, Ltd., Birkenhead, UK) and filled with 75 g of sand grains. The sandbags were put into a metallic cage of 50 cm length and 4 cm diameter. The cage filled with sandbags was enveloped with aluminium foil. On May 29<sup>th</sup> 2014, the cage was placed at the screen of borehole 59 in the



polluted aquifer of the study site, close to Wolverhampton, UK, at 30 mbgl, where the lower fringe of the plume is located. Figure 2.3 shows a picture of the cage and its position at BH-59.

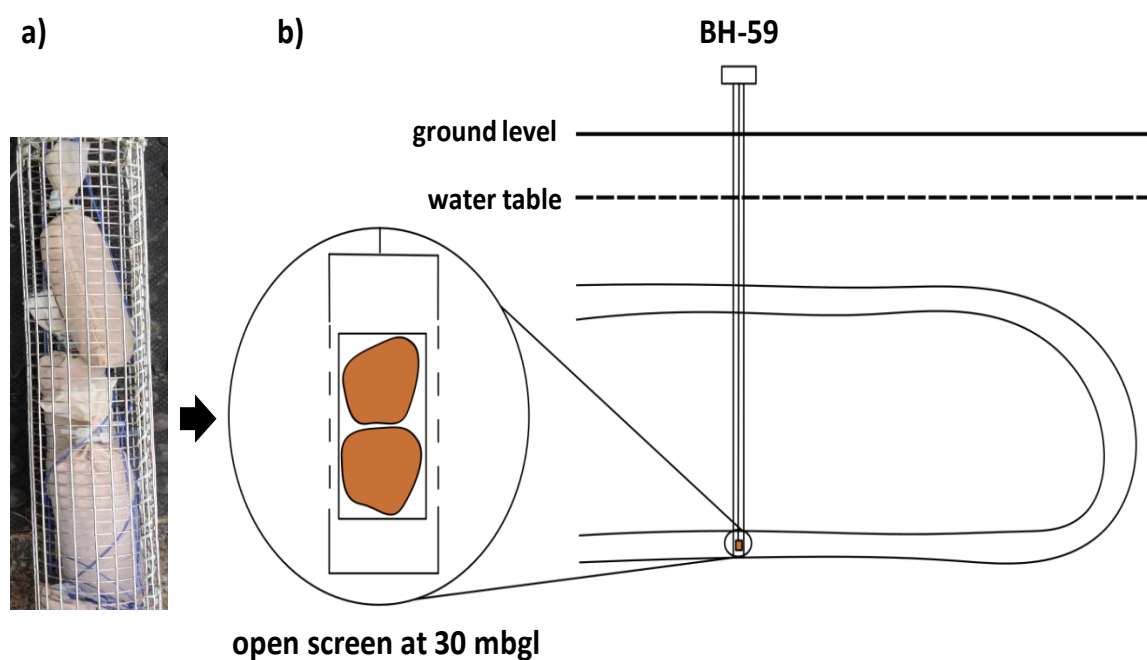


**Figure 2.3** (a) Arrangement of bags filled with sand in the metallic cage. (b) Schematic representation of the final position of the cage 30 mbgl in the open screen of BH-59.

### ***Microcosm sampling***

Triplicate microcosms were sampled destructively at 7, 23, 47, 104, 174, 400 and 800 days after inoculation. Triplicate abiotic controls were also sampled. The supernatant was removed with a pipette. Thirty ml of supernatant was filtered through sterilized 0.22  $\mu\text{m}$  filters (Whatman<sup>®</sup> polycarbonate membrane, 25 mm diameter), and stored at  $-80^{\circ}\text{C}$  prior to DNA extraction. Five ml of the supernatant was fixed with 4 % (v/v) formaldehyde and stored at  $4^{\circ}\text{C}$  for cell counts. The remaining supernatant was filtered with nylon 0.22  $\mu\text{m}$  filter (Fisher Brand, UK) and stored at  $4^{\circ}\text{C}$  for chemical analysis. For metals analysis two aliquots were fixed using  $\text{HNO}_3$  final concentration of either 1 or 10 %. The sediments were collected and homogenized using a sterile spatula. The homogenized sediments were separated into two groups, one stored at  $-80^{\circ}\text{C}$  for DNA extraction and the remaining sand was fixed with formaldehyde 4 % and stored at  $4^{\circ}\text{C}$  for cell counts. This sampling procedure was repeated for each microcosm.

### Field sampling

For sand bag collection, BH-59 was covered with a glove bag and a hose was introduced into the borehole to purge the head space with nitrogen, both below and above the water table, to provide anaerobic conditions. The cage was brought to the bag-covered borehole entrance and one sand bag was extracted and put in a container previously filled with nitrogen. The sampling intervals in the field were similar to the one applied in the microcosm sampling. **Figure 2.4** shows the anaerobic extraction performed in the field. Groundwater of 30 mbgl depth was extracted for hydrochemistry and microbiological analysis. Samples were taken after 1, 30 and 60 minutes after the purging of the borehole. The samples were collected and processed as described in the microcosm sampling section.



**Figure 2.4.** Anaerobic extraction in the field. (a) BH-59 covered with a glove bag and hose introduction, (b) initial steps of purging of the head space (c) nitrogen supply for purging and (d) final recovery of sand bag from the screen of BH-59.

### **Cell counts**

Groundwater and supernatant from the microcosms samples were filtered through black 0.22 µm filters (Whatman® polycarbonate membranes, 25 mm diameter). Sediments were placed on a Cover Well™ Imaging Chamber volume of 300 µl and 0.9 mm depth (Science services, UK). Grains were washed with a filtered solution of 0.15 M NaCl. Samples were stained with 200 µl of SYTO® 9 (Green Fluorescent Nucleic Acid Stain; Dilution 1:800) for 15 minutes. At least 10 randomly distributed fields of view were visualized using a RT-KE Slider 7.4 digital camera (Diagnostic Instruments) and epifluorescence microscope (BX50, Olympus Optical Co., London, UK) using excitation at 470 nm wavelength and emission at 510 nm (Thermo Scientific, UK). Fluorescent microbial cells were counted using Image Pro Plus version 4.5 (MediaCybernetics, UK) (Rizoulis *et al.*, 2013). The detection limit was 1 cell per field of view. For the grains analysis z-stacks were collected under both bright field and fluorescent light. To calculate cell numbers in the attached community, the average grain size diameter was measured (215.6 µm) and the volume of 1 grain was estimated using  $V_{\text{grain}} = 1.3 \cdot \pi \cdot r^3$ , where r is the radius. The volume was used to estimate the number of grains contained in 1 ml, considering a porosity of 26% (Lerner *et al.*, 2000; Baker, 2011). Using the average number of bacteria attached to 1 grain and considering only one side of the grain could be analysed (Gough and Stahl, 2003), the cell densities of the biofilm was calculated per 1 ml of saturated sand. Additionally, to calculate the number of bacteria per surface area the formula  $\text{Surface}_{\text{grain}} = \pi \cdot r^2$ , was used to calculate the number of bacteria per cm<sup>2</sup>.

### **DNA extraction**

DNA from the planktonic community was extracted using the UltraClean® Microbial DNA Isolation kit (Mobio, 2014). The polycarbonate membrane used to collect the planktonic community was placed into the microbeads tube and then processed according manufacturer's instructions. DNA from the attached community was extracted using the PowerSoil® DNA Isolation Kit (Mobio, 2014). DNA from sediments was concentrated using the DNA obtained from 6 independent extractions per each sample, plus 1200 µl of pure ethanol and a final concentration of 11 mM of sodium chloride. The total volume was centrifuged at 10,000 g for 5 minutes, followed by speed vacuum until dryness and resuspended in 50 µl of PCR water.

### **Community profiling terminal- Restriction length Polymorphism (t-RFLP)**

Communities were profiled using T-RFLP of 16S rRNA gene fragments. PCR amplification of 16SRNA genes was performed using two primer pairs: FAM63F (5`-GCCTAACACATGCAAGTC-3`) HEX806R (5`-GGACTACCAGGGTATCTAAT-3`) and FAM341F (5`-CCTACGGGNGGCWGCAG-3`)

HEX805R (5`-GACTACHVGGGTATCTAATCC-3`) (McBain *et al.*, 2003; Yu & Morrison, 2004; Klindworth *et al.*, 2012). The primers were labelled at the 5` end with the phosphoramidite dyes 6-FAM and HEX (Applied Biosystems) respectively (Osborn *et al.*, 2000). The PCR conditions were 95 °C for 5 minutes, 30 cycles of 95°C 60 s, 55°C 60 s, and 72°C for 60 s and then a final step of 72°C for 7 min. PCR products were purified using the QIAquick PCR Purification Kit according to the manufacturer's instructions. Five µl of the PCR purified products were digested using CfoI and AluI (Promega, UK), for 3 hours at 37°C (Felske & Osborn, 2005). The digested products were desalted using 5 µl of the digested product, glycogen 20 mg ml<sup>-1</sup>, 3 M sodium acetate pH5.2 (1/10 total volume) and ethanol 70% (2.5 total volume). After desalting the samples were analysed by capillary electrophoresis in a 3730 DNA analyser (Thermo Scientific, UK) with a ROX internal size standard (Applied Biosystems, UK). T-RFLP peaks were analysed using Peak Scanner software, version 2.1. (Applied Biosystems, UK). Peaks were aligned using T-align web tool (Smith *et al.*, 2005). Aligned peaks were analysed with two methods; Additive Main Effects and Multiplicative Interaction (AMMI) model available from T-REX software (T-RFLP analysis EXpedited) (Culman *et al.*, 2008) and Non-metric Multidimensional Scaling (NMDS) using the phyloseq package (McMurdie & Holmes 2013) in R (R Development Core Team, 2011).

### **16S rRNA gene fragment library preparation**

Thirty µl of DNA from sediments was cleaned by dilution using a Microcon device, DNA Fast Flow PCR Grade with Ultracel membrane and 470 µl of PCR water, according to the troubleshooting guide of the manufacturer's instructions (Merck, 2013). Three aliquots from each sample were amplified in separate PCR reactions using the primer pair Illumina-341F (5`-TCGTCGGCAGCGTCAGATGTGTATAAGAGACAGCCTACGGGNGGCWGCAG -3`) and Illumina-805R (5`-GTCTCGTGGGCTCGGAGATGTGTATAAGAGACAGGACTACHVGGGTATCTAATCC -3`) (Klindworth *et al.*, 2012). The PCR conditions were 95 °C for 5 minutes, 30 cycles of 95°C 40 s, 55°C for 60 s, and 72°C for 60 s and then a final step of 72°C for 7 min. 2.0 % agarose gels were used to visualize the amplicons. Amplification conditions were chosen to produce bands of low-mid intensity (Ihmark *et al.*, 2012). If high band intensities were obtained, input DNA samples were diluted until the desired intensity was obtained. The PCR products from each amplification were pooled and purified using AMPure XP PCR purification beads in ratio of 1:0.95 (sample:beads) according to the manufacturer instructions (Beckman Coulter). 5 µl of purified amplicons were indexed using Illumina Nextera® XT DNA Library Preparation Kit (Illumina, 2016). The Index-PCR conditions were 95 °C for 3 minutes, 12 cycles of 95°C 30 s, 55°C 30 s, and 72°C for 30 s and then a final step of 72°C for 5 min. The AMPure purification step was repeated. Quantification of the final Indexed samples was made using Quant-iT™

PicoGreen™ dsDNA Assay Kit (Thermo Scientific, UK). The final pooling of the library required samples at a final concentration of 16 ng/μl, dilution of the samples was performed as required. Samples were sequenced by synthesis using the illumina<sup>R</sup> high-throughput sequencing technology at the Earlham Institute.

### **Bioinformatics**

Demultiplexed 16S rRNA sequences were provided by The Earlham Institute as forward (R1) and reverse (R2) reads in FASTQ format. For quality checks Usearch 8.1 (Edgar, 2010) was used. For data processing QIIME (Caporaso *et al.*, 2010) was used. Sequences with greater than 1 in 1000 errors and short reads below 350 bp were removed. The forward and reverse reads were merged and converted to FASTA format. The primer sequences (17 bp from 5' and 21 bp from 3' ends respectively) were removed. Chimeras were identified and removed using *de novo* abundances and comparing with the RDP gold data base (Wang *et al.*, 2007). A biom table was generated using Greengenes data base (McDonald *et al.*, 2012; DeSantis *et al.*, 2006) at 97% similarity. The Biom table was input into phyloseq package (McMurdie & Holmes 2013), in R (R Development Core Team, 2011). In R rarefaction was applied to all the samples to obtain similar sequencing depths (2e+05 counts). Unifrac weighted and unweighted analyses were done using NMDS (Lozupone *et al.*, 2011).

### **Chemical analysis**

Chemical analysis followed Thornton *et al.* (2001a) and Thornton *et al.* (2014). Phenol, *o*-cresol, *m/p*-cresol and xylenols (2,3-xyleneol, 2,4/2,5-xyleneol, 2,6-xyleneol, 3,5-xyleneol, 3,6-xyleneol) were analysed by high-performance liquid chromatography (HPLC). The stationary phase was a Hypersil C18 column, 250 mm length, 4.6 mm diameter and 5 μm particle size (Thermo Scientific, UK). The mobile phase was composed of 20% pure acetonitrile HPLC grade (Merck, UK) and 80% of a 1% (v/v) acetic acid solution. The instrument used was a Perkin-Elmer Series 200 (Perkin Elmer, UK) system with an UV/VIS detector calibrated with standards and analytical quality controls. The method detection limit and precision was 1 mg l<sup>-1</sup> and ± 5%, respectively. One ml of sample was put in 2 ml glass vials (Restek, UK) and 100 μl of sample was taken and injected into the instrument. Major ions (including acetate, NO<sub>3</sub><sup>-</sup>, NO<sub>2</sub><sup>-</sup> and SO<sub>4</sub><sup>2-</sup>) were determined by ion chromatography using a Dionex 3000 (Thermo Scientific, UK) system with a detection limit of 1 mg l<sup>-1</sup> and precision of ± 3%. Samples were diluted 10 times and put in 2 ml glass vials. Metals concentrations were determined by inductively coupled plasma spectrophotometry using Perkin Elmer Elan DRC II ICP mass spectrophotometer with a detection limit of 0.001 mg l<sup>-1</sup> and precision of ± 2%. Samples were serially diluted to 10, 20, 50

and 100 times and acidified at 1% using nitric acid trace metal grade (Fisher Chemical, UK). For the mass spectrometry analysis, different fractions of the HPLC eluent were collected in 2 ml glass vials previously filled with nitrogen. The samples were manually injected into a QStar Elite (ABI Sciex) mass spectrometer with an ion spray injector. Samples were run in negative mode, the ion spray voltage was of -38000 V and the source temperature was 100°C.

### Mass balances

Mass balances were calculated to estimate the biodegradation of phenolic compounds using different electron acceptors. For these calculations, redox semi-reactions described in Thornton *et al.* (2001b) were used to equilibrate the different biodegradation processes. These reactions are depicted in Table 2.1.

### Statistical analysis

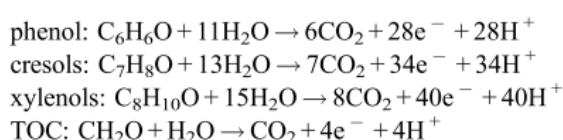
One-way and two-way ANOVAs were made to evaluate changes in the geochemistry of different treatments. The Post-hoc test used was Tukey's or Dunnet's test using GraphPad Prism version 7.00 for Windows, GraphPad Software, La Jolla California USA, www.graphpad.com.

**Table 2.1** Redox half reaction of biodegradation of phenolic compound extracted from Thornton *et al.* (2001b)

---

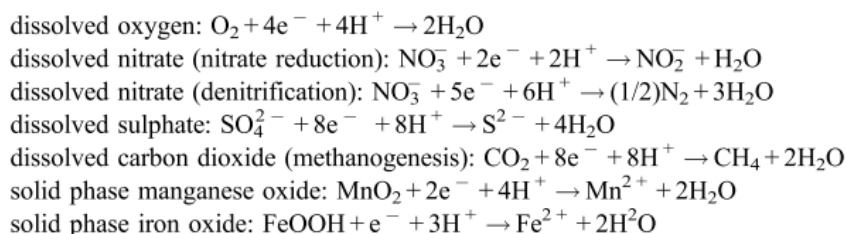
#### Electron donating reactions

*Oxidation of organic fractions*



#### Electron accepting reactions

*Reduction of aqueous and mineral oxidants*



## 2.3 Results

Sand bags, containing sterile substrate, were introduced into the open screen of Borehole 59 at 30 mbgl. Laboratory microcosms were established using the same sand and inoculated with groundwater from 30 mbgl. Sand bags from the field and laboratory microcosms were sacrificed at intervals for analysis of attached and planktonic microbial communities and geochemistry.

**Figure 2.5** shows the groundwater chemistry of the microcosms. The starting groundwater contained  $\sim 220 \text{ mg L}^{-1}$  phenol,  $\sim 100 \text{ mg L}^{-1}$  cresols (*m,p* and *o*) and  $50 \text{ mg L}^{-1}$  xylenols. The concentrations of *m,p* and *o*-cresols and xylenols did not show statistically significant differences during the 780 day duration of the experiment, nor did live microcosms differ systematically from the azide-treated controls. Nevertheless, two-way ANOVA indicated differences on phenol concentration over time (phenol:  $F_{(6,24)}: 3.47, p < 0.05$ ), but the post-hoc Tukey's test did not find significant differences across multiple comparisons. Although the bulk concentrations of these phenolic compounds did not change upon incubation, smaller amounts of metabolites ( $\sim 0.1 \text{ mg L}^{-1}$ ) appeared after 47 days of incubation and remained largely stable over the remaining duration of the experiment (**Appendix 6.2**). The soluble iron (principally  $\text{Fe}^{2+}$ ) concentrations fell significantly (iron:  $F_{(6,24)}: 43.5, p < 0.05$ ) from a starting concentration of  $1.5 \text{ mg L}^{-1}$  to  $0.5 \text{ mg L}^{-1}$  by the first sampling point, 23 days after inoculation and then remained constant (supported by Tukey's test). Iron concentrations in the abiotic control also fell but much more slowly, taking 400-780 days to reach the same concentrations. The two-way ANOVA indicated statistical differences (treatment:  $F_{(1,4)}: 187.4 < 0.05$ ) in iron concentrations between live microcosm and abiotic controls. The Tukey's test indicated that the differences were located within 23 and 174 days of the experiment. In both live and control microcosms, Mn increased significantly (manganese:  $F_{(6,24)}: 190.5, p < 0.05$ ) from an initial concentration of  $1 \text{ mg L}^{-1}$  to  $3 \text{ mg L}^{-1}$  over the first 200 days. The Tukey's test indicated the differences between manganese values within the 23 days of experiment and concentrations reaching  $\sim 3 \text{ mg L}^{-1}$ . Nitrate was consumed rapidly in live microcosms falling significantly (nitrate:  $F_{(6,14)}: 92.37, p < 0.05$ ) from an initial concentration of  $30 \text{ mg L}^{-1}$  to  $> 5 \text{ mg L}^{-1}$  within 50 days. The Tukey's test indicated statistical differences between nitrate content over the first 23 days and the values registered from 47 days of the experiment onwards. (No comparable measurements were made in the abiotic controls as azide interferes with measurement of nitrate). In contrast, sulphate concentrations remained stable throughout at  $\sim 23 \text{ mg L}^{-1}$ . Statistical differences for sulphate were not found.

Cell numbers of field inoculum were  $\sim 10^7$  cell ml<sup>-1</sup>. In the microcosms, the planktonic community decreased after 47 of the experiment. From 47 to 100 days of the experiment, cell numbers rose and became stable ( $10^7$  cell ml<sup>-1</sup>) for the remaining period of monitoring. In the biofilm, the cell numbers increased over the first 47 and became stable 100 days after the inoculation with approximately  $\sim 10^6$  cells per ml of saturated sediments. The value of bacteria per unit of surface area during the stable phase in the biofilm was of  $\sim 10^5$  cells cm<sup>-2</sup>.

**Figure 2.8** shows the visualization of microbial cells by SYTO® 9 staining in grains. The microscopic inspection revealed similar trends in the field and microcosms, with a few cells attached to the grains at early stages, increasing in number within 47 days and cell number stability from 100 days. The kinetics of attachment was similar in the two different systems and the biofilm was stable in terms of numbers from 100 days onwards (**Figure 2.5.i** and **2.7.i**).



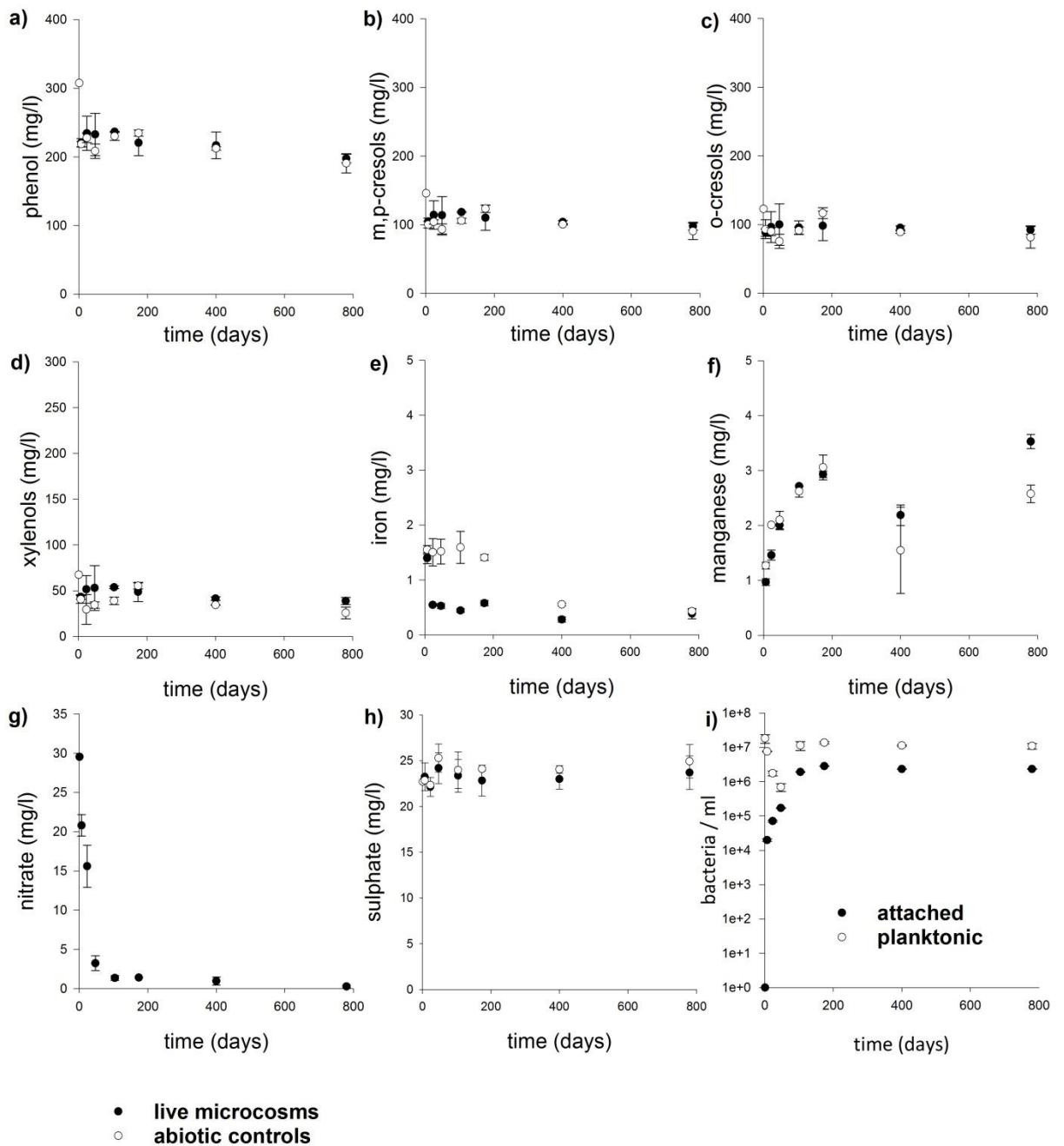


**Figure 2.5.** Monitoring of different chemical species and cell counts in microcosms inoculated with groundwater from 30 mbgl of BH-59. Error bars represent the standard deviation of replicates (n=3) Legend in the bottom left corner applies to all graphs except to the cell densities in *graph i*), for which is associated to the legend in the bottom right corner of the figure.

In the field, after purging the borehole samples were collected after 1, 30 and 60 minutes.

**Figure 2.6** shows the stability in phenolic content was reached after 30 minutes of pumping.

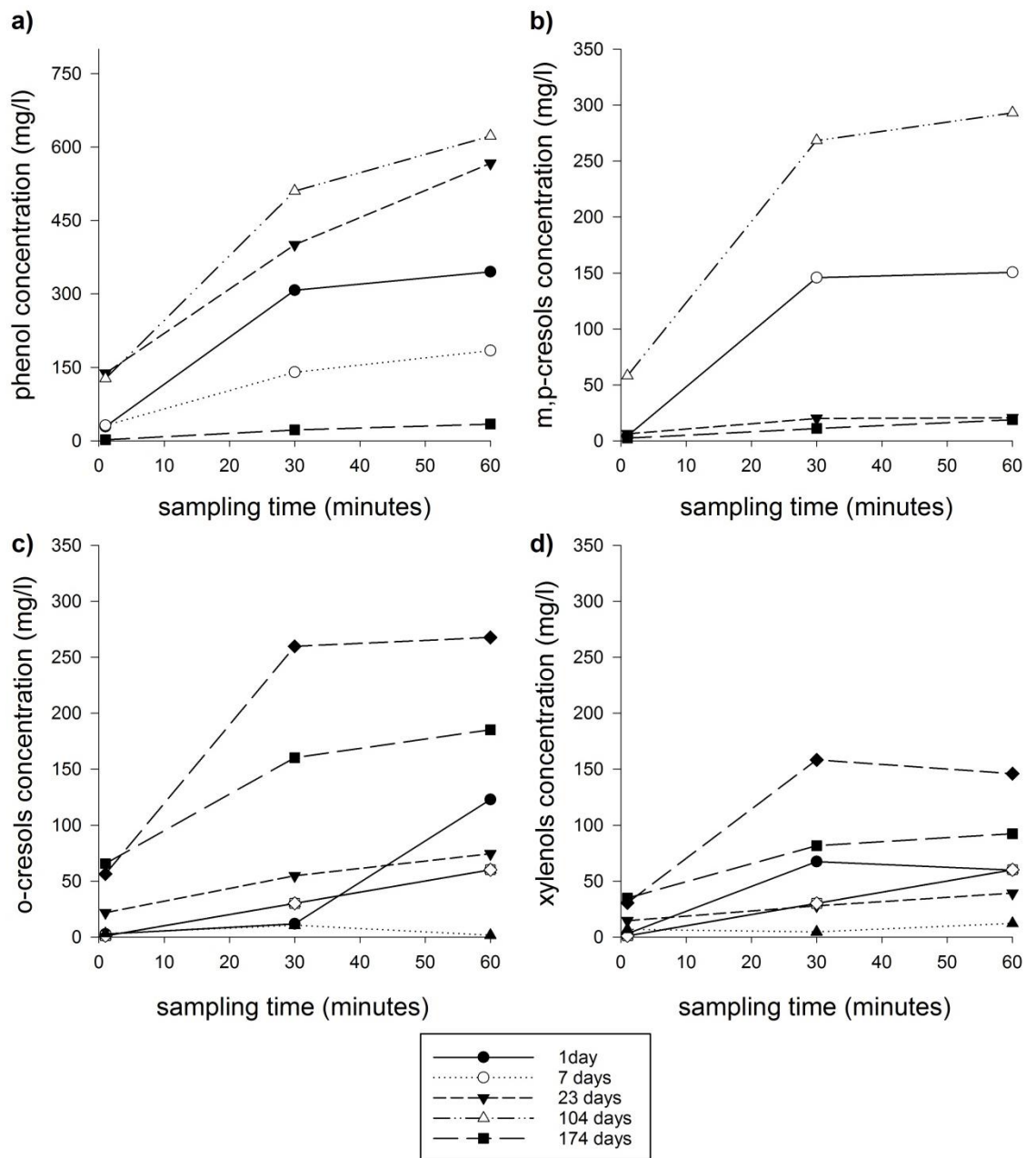


**Figure 2.6.** Concentration change of phenolic within 60 minutes of sampling of groundwater from 30 mbgl at BH-59. For other chemical species please see the Appendix 6.1.

**Figure 2.7** shows the groundwater chemistry of the field. The geochemistry of field samples varied much more than the microcosms. At the start of the experiment, phenolic concentrations were similar to those used to establish the microcosm. (The groundwater samples were measured 30 min after the start of peristaltic pumping, whilst the water used to inoculate microcosms was collected for 2 h to provide a sufficient volume for all samples). Over the duration of the experiment, the phenolic concentration at BH59 30 mbgl varied markedly. Concentrations had fallen by approximately half after 7 days but almost doubled in samples taken at 23-104 days. By 174 days concentrations had fallen again, increased to

starting concentrations at 400 days and were much lower ( $\sim 1.2 \text{ mg L}^{-1}$ ) at the final time point. Similar oscillations were seen in the iron and manganese measurements. Nitrate concentrations showed an opposite trend – they fell from  $30 \text{ mg L}^{-1}$  at the start of the experiment to  $5 \text{ mg L}^{-1}$  at 7 days with concentrations varying between  $\sim 3$  and  $15 \text{ mg L}^{-1}$  throughout the rest of the sampling period. Sulphate concentrations also ranged from 10-30  $\text{mg L}^{-1}$  during this time.

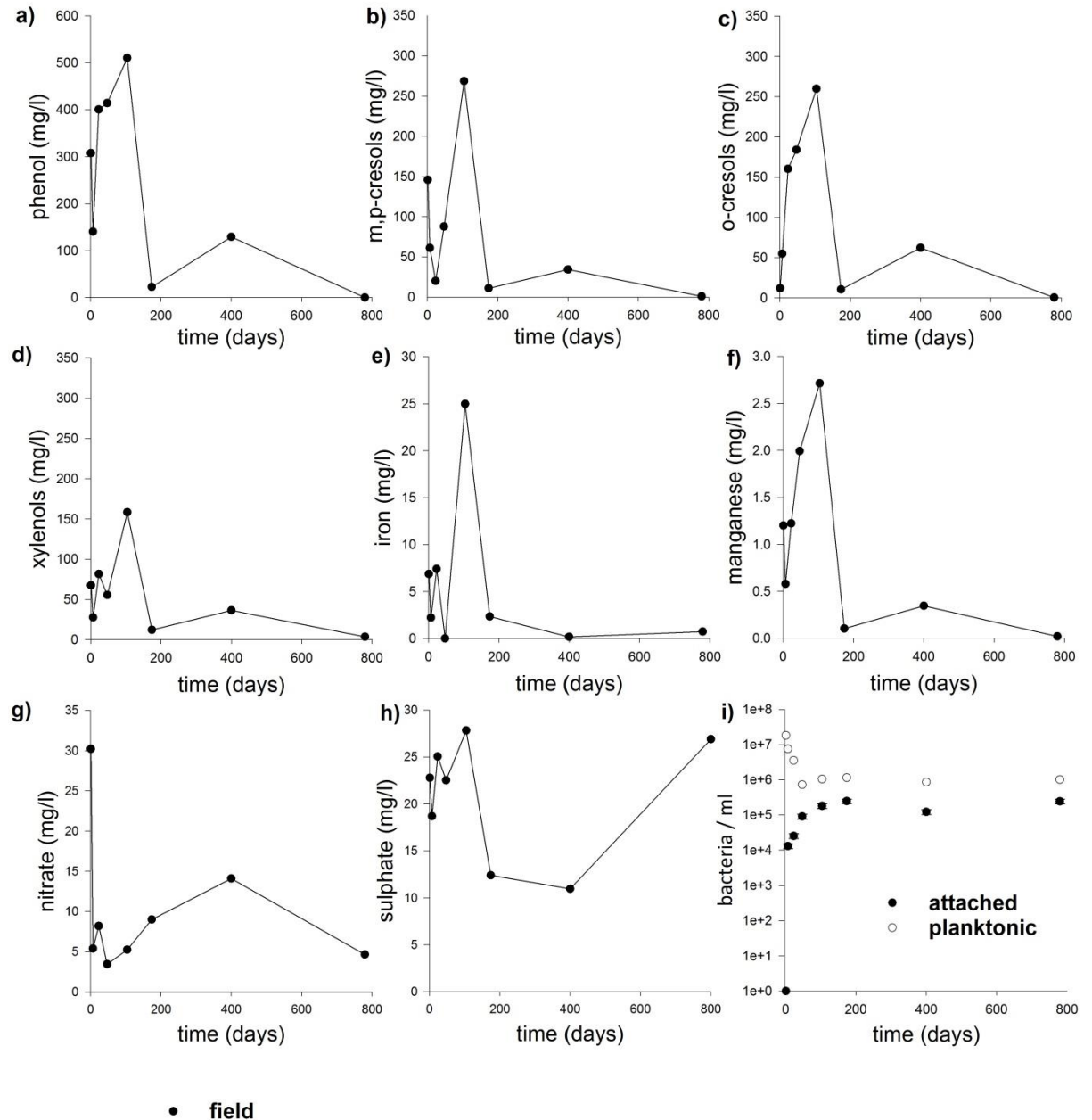


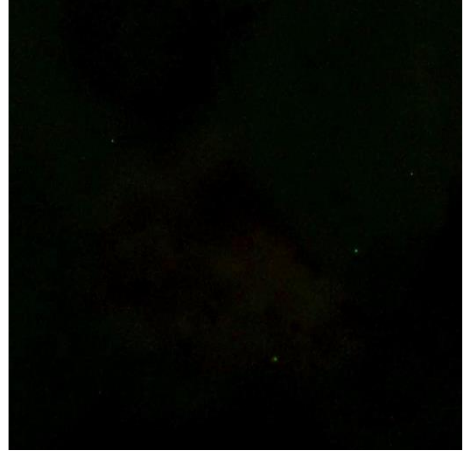
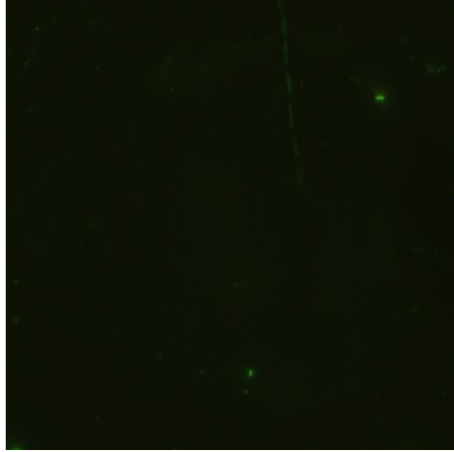
**Figure 2.7** Monitoring of different chemical species and cell counts of groundwater and sandbag extracted from BH-59 at 30 mbgl, associated to the *in situ* experiment of this chapter. Legend in the bottom left corner applies to all graphs except to the cell densities in *graph i*), for which belongs with the legend in the bottom right corner of the figure.

*days*

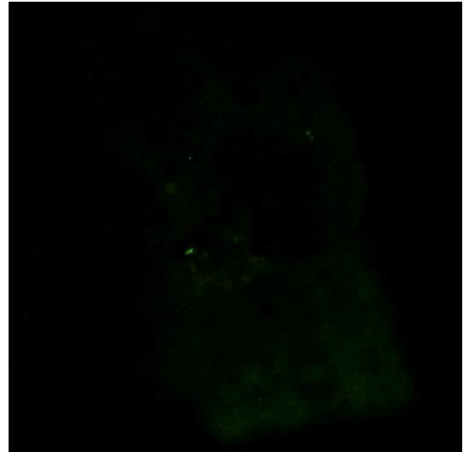
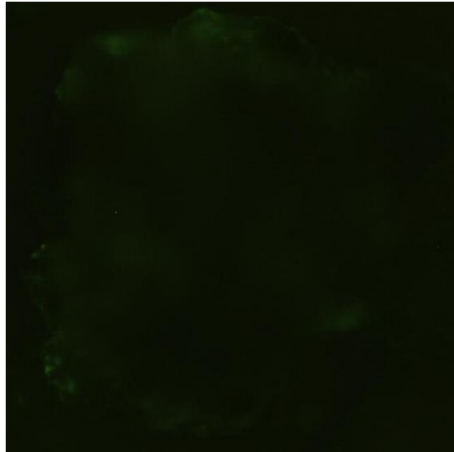
**microcosm**

**field**

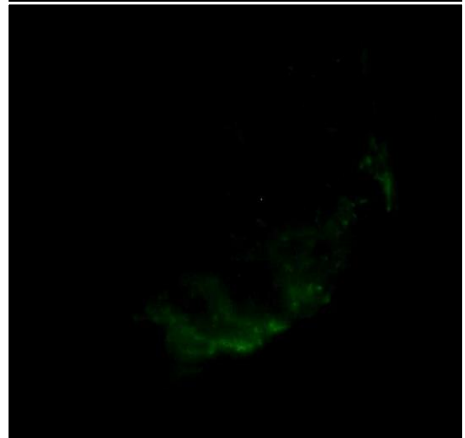
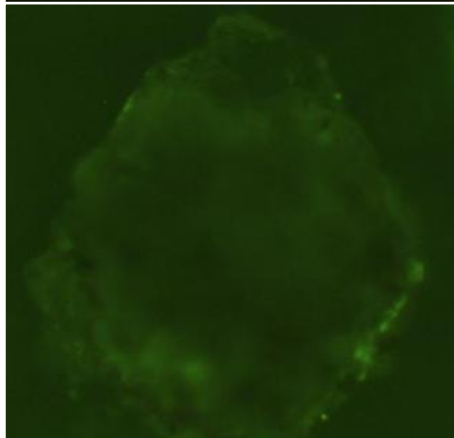
**7**



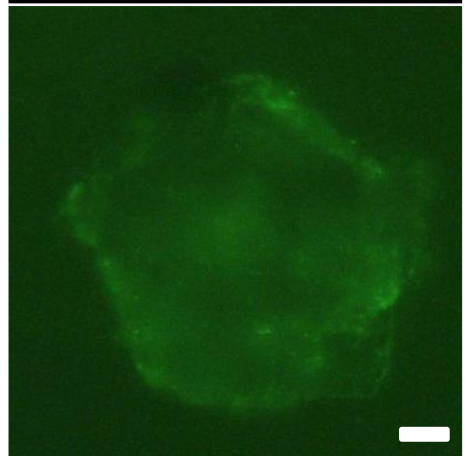
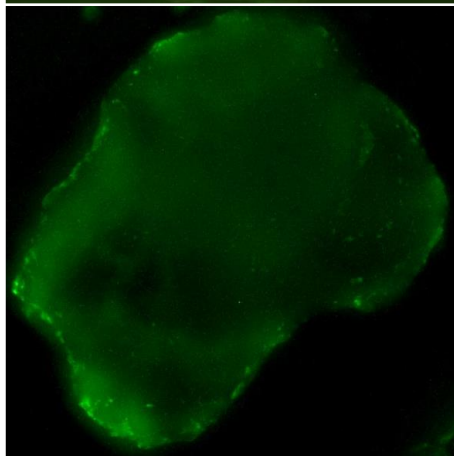
**23**



**47**



**104**



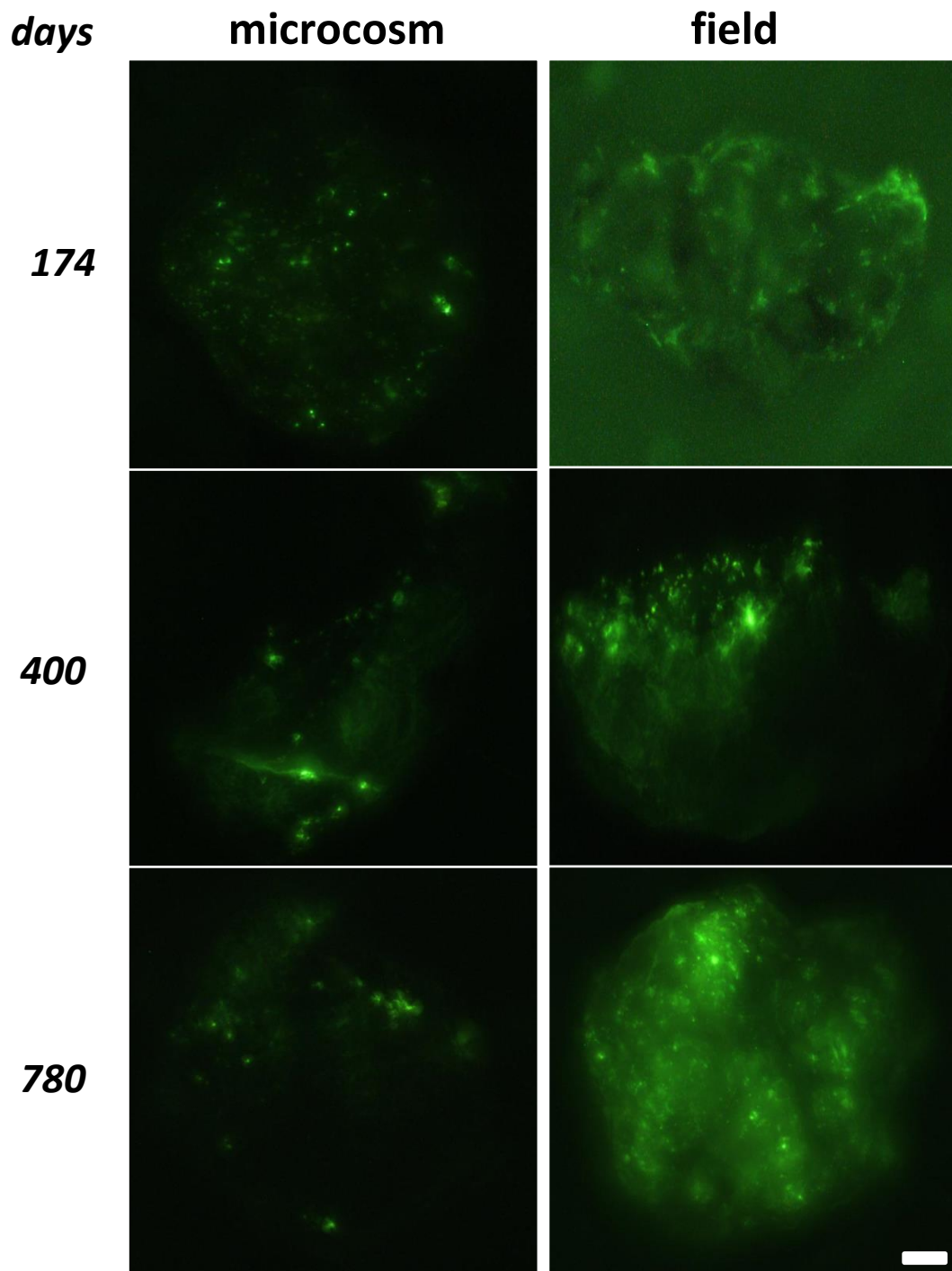


**Figure 2.8.** Visualization of microbial cells by SYTO® 9 staining on sand grains at different intervals of incubation in the microcosms and field. 20X of magnification. The white bar represents 20  $\mu\text{m}$ .

In the field (**Figure 2.7.i**), cell numbers of the planktonic community vary by an order of magnitude  $\sim 10^6$  to  $10^7$  cells  $\text{ml}^{-1}$  during the monitoring period. The biofilm cell numbers analysis revealed a period of rapid attachment, within the 47 days after the sand grains were exposed to the planktonic community of the open screen of BH-59. The cell numbers in the biofilm stabilized over 100 days reaching  $\sim 10^5$  cells  $\text{ml}$  of saturated sediments, and remained stable during the duration the field incubation. The value of bacteria per unit of surface area during the stable phase in the biofilm was of  $\sim 6.8 \times 10^4$  cells  $\text{cm}^{-2}$ .

Determination of the bacterial community profile was made using terminal restriction length polymorphism (t-RFLP).

For details of the molecular biology preparation and preliminary results of t-RFLP see the t-RFLP preparation and preliminary results section in the Appendix (**Figure 6.3 – 6.11**).

The differences between the planktonic and attached communities were explored using a distance-based method, Nonmetric Multidimensional Scaling (NMDS). Note that assignment of T-RFs sizes was improved using the T-align tool. NMDS were performed using a similarity matrix for the T-RFs from microcosm and field samples.

**Figure 2.9** shows an NMDS of the microbial communities in the microcosms (a) and the field (b). The NMDS biplot from samples of microcosms showed a general pattern when the impact of time was not considered. Samples from the attached community located to the left and samples from the planktonic community to the right, in consequence possible differences between these two communities structures.

On the other hand, in the field biplot the attached community locates in the middle upper-right position, whereas samples from the planktonic community to the left.

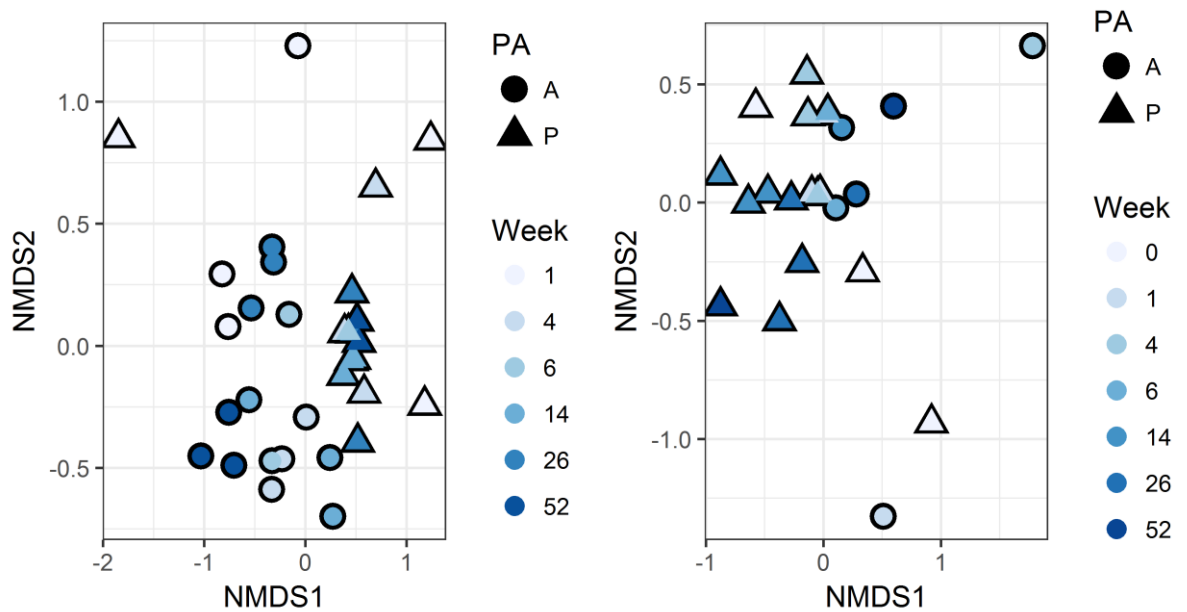


**Figure 2.9.** NMDS of microbial communities in the (a) microcosms and (b) field samples. These biplots were constructed using Bray-Curtis dissimilarity matrix on the abundances of the T-RFLP fragments from 16S rRNA genes extracted from the planktonic (P) and attached (A) communities in two different systems. (Note time is shown in weeks).

In brief, the t-RFLP analysis suggested differences between the planktonic and attached communities in the microcosms and at some extent in these two communities in the field. Nevertheless, the different groups behind the differences and their abundances cannot be determined based on the size of T-RFs. A t-RF does not necessarily imply a specific OTU, as different OTUs could exhibit similar t-RFs. At this stage, the data presented was promising enough to point into the next stage of analysis, high-throughput sequencing.

Previous experience on sediment samples demonstrated the difficulty to amplify these samples from the microcosms and field. The length of the Illumina-Bakt341F and Illumina-Bakt805R primers used in the sequencing library preparation, consist of 50 and 55 bp respectively, they had different sizes for the adaptor regions required for the Illumina sequencing, included in the usual sequences of the 341F and Bakt805R primers. It was necessary to perform PCR trials to establish the best conditions for the amplification. For details of the sequencing library preparation refer to the sequencing library preparation section in the Appendix (**Figure 6.12 – 6.22**).

**Figure 2.10** shows the result of high throughput sequencing of 16S rRNA genes at Phylum level in the planktonic and attached communities. It was possible to confirm that microbial communities from the planktonic and attached communities were quite diverse in both

microcosm and field samples. At this level it was possible to observe that these communities were related to each other, but also some differences were detected. For instance, the difference between planktonic and attached communities was apparent (both microcosms and field samples). Furthermore, the microcosm communities detected were different from field communities. Also, communities changed their composition over time. Therefore, it was necessary to further explore these differences.

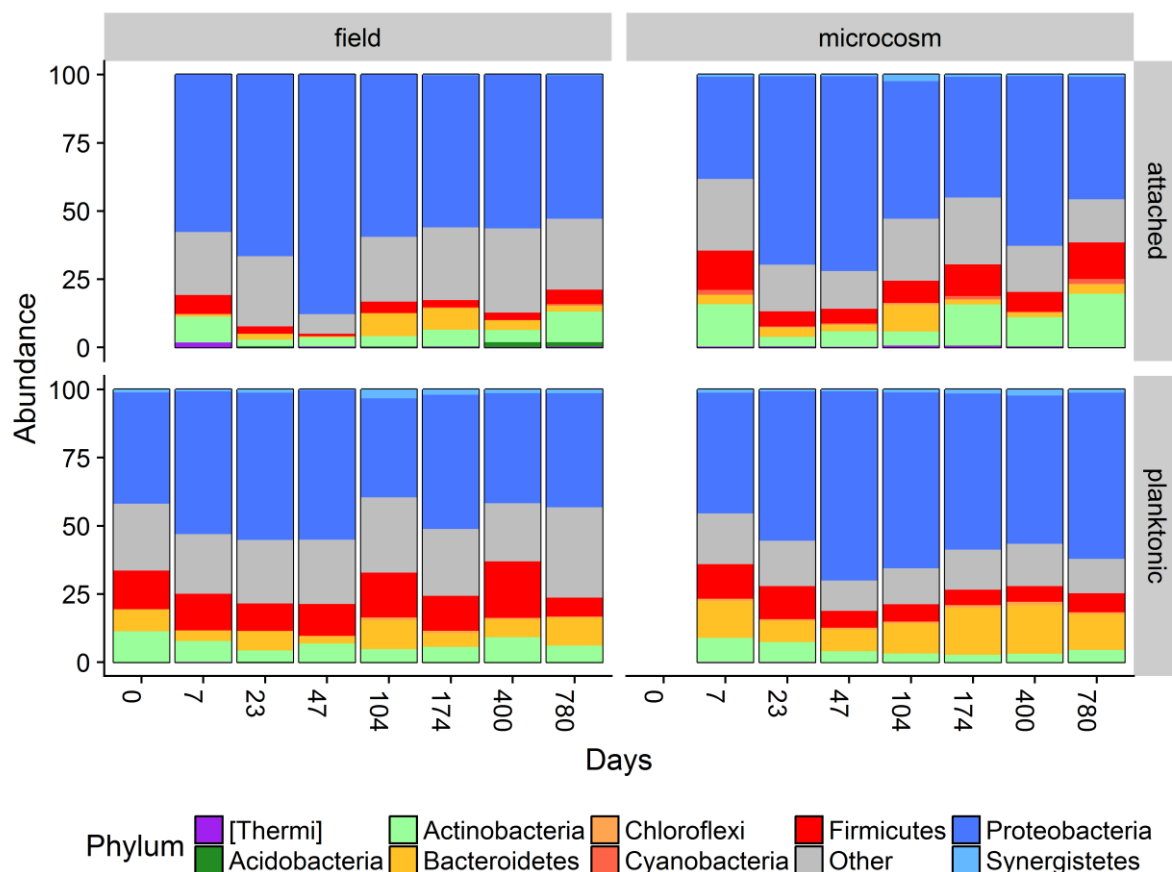


**Figure 2.10.** High throughput sequencing of 16S rRNA genes at Phylum level in planktonic and attached communities harvested from microcosm and field samples at different time intervals after inoculation. (Note time is shown in weeks).

To understand the differences between microbial communities and to consider the relative abundance of the groups, the dataset was analysed with an Unifrac weighted analysis. This analysis considers the phylogenetic relationship between different OTUs and the abundances in the samples (Lozupone *et al.*, 2007). **Figure 2.11** shows a Unifrac weighted NMDS of all planktonic and attached communities. To determine the difference between the planktonic and attached communities the impact of time was not considered. The Unifrac weighted analysis was plotted into an NMDS. Attached communities are grouped to the right of the plot, whereas the planktonic communities cluster to the left. Considering the communities from the different experimental setting, it was possible to observe microcosm communities to the



upper part, whereas field communities to the bottom of the plot. These grouping patterns were an indication of differences between the planktonic and attached communities, and between different experimental settings. The likelihood ratio test supported this finding (p-value <0.05), indicating a significant effect of community, experiment type and an interaction between these two (**Table 2.2**).

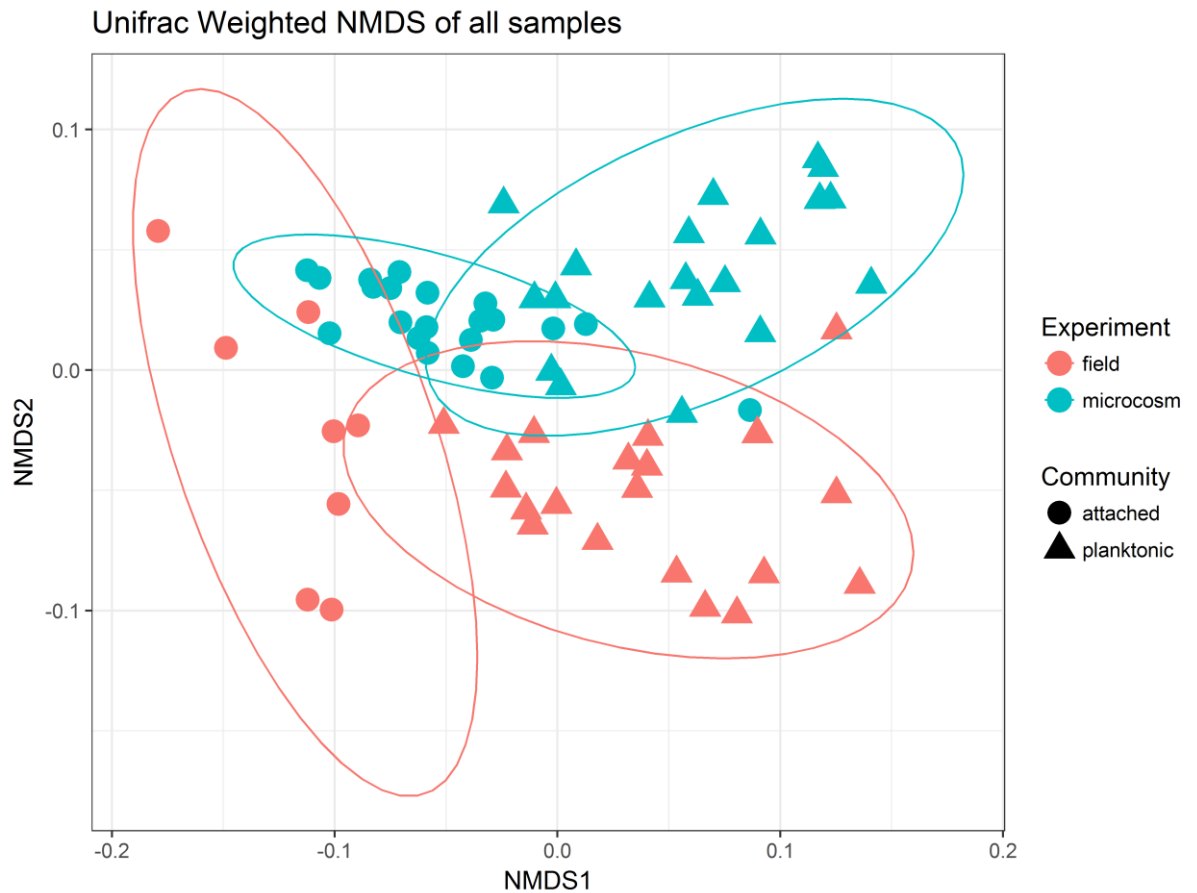


**Figure 2.11.** Unifrac weighted NMDS of all planktonic and attached communities harvested from microcosm and field samples at different time intervals after inoculation. This analysis considers the abundances of different groups and their phylogenetic relationships to each other. The effects of time was not taken into account.

**Figure 2.12** shows the Unifrac weighted analyses now considering the impact of time. Neither the attached nor the planktonic communities from the field and microcosms showed a time trend. The communities did not develop their community structures in a specific direction. This indicates that community structures are dynamic and change over time, considering the phylogenetic relationship and the abundances of different OTUs.

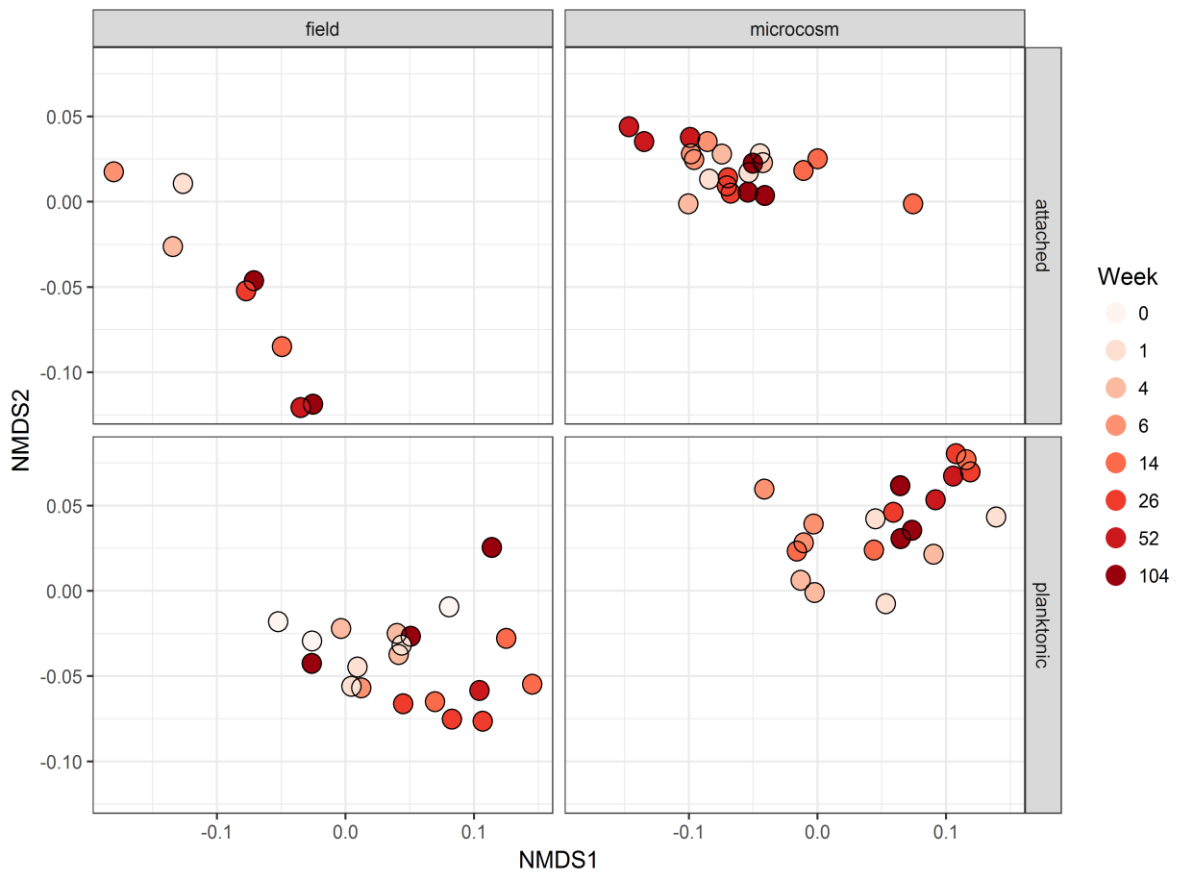


**Figure 2.12.** Unifrac weighted NMDS of all planktonic and attached communities harvested from microcosm and field samples at different time intervals after inoculation. This analysis considers the abundances of different groups, their phylogenetic relationships and the effect of time (Note time is shown in weeks).

The previous two analyses were based on weighted Unifrac analysis. **Figure 2.13** shows an unweighted Unifrac analysis. This was made to understand the similarities between the communities, but just considering the presence/absence of different OTUs, to assess the differences on the community membership across the same data set. The analysis revealed attached communities memberships in the field were not following a clear time trend from early to late stages of the biofilm development; a similar situation to attached communities in the microcosms. On the other hand, the planktonic communities from the field and microcosms, exhibited similar community composition over the period of study. Therefore, the community membership in the planktonic community was more stable over time, whereas the community members in the attached phases were changeable over the experiment.

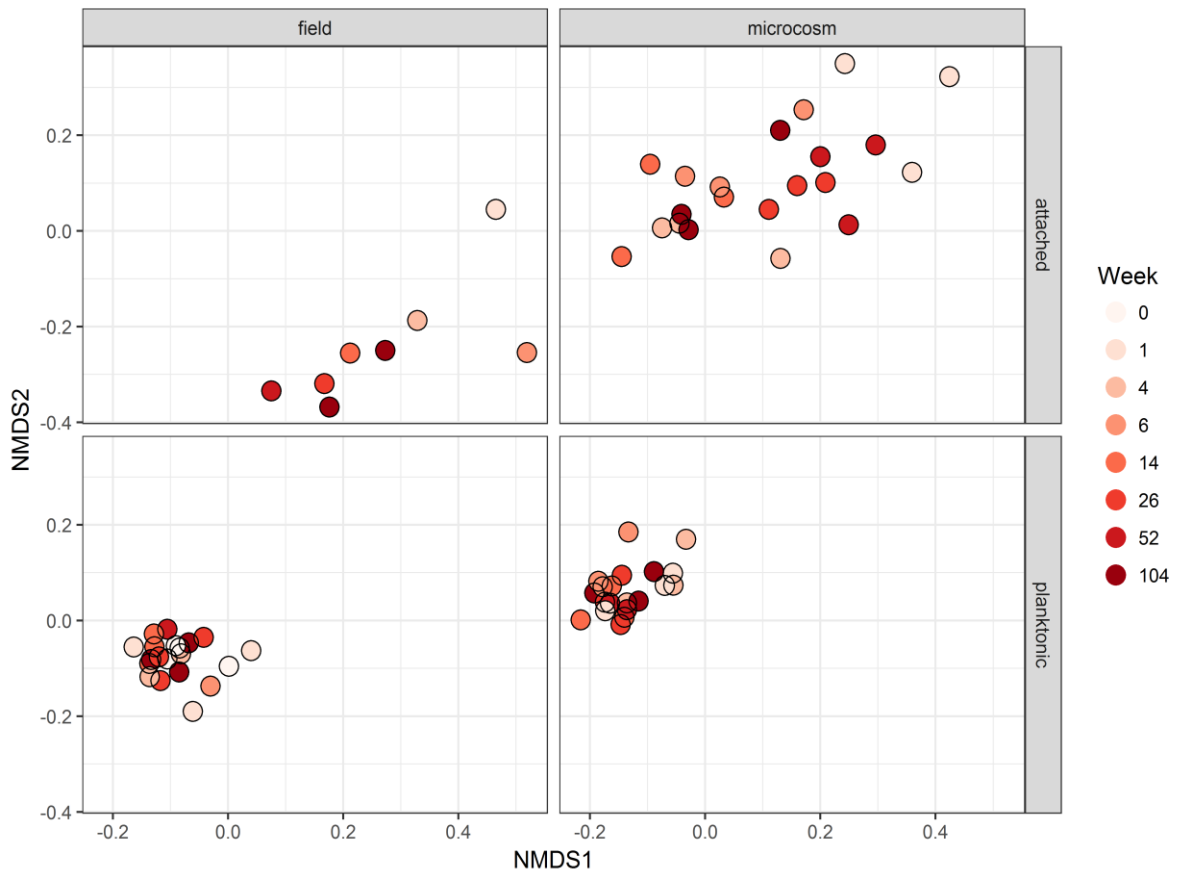


**Figure 2.13.** Unifrac unweighted NMDS of all planktonic and attached communities harvested from microcosm and field samples at different time intervals following inoculation. This analysis considers the presence/absence of different groups, their phylogenetic relationships to each other and the effect of time. (Please note time is shown in weeks).

To identify the differences over time in the community membership of the planktonic and attached communities, a richness analysis was considered. **Figure 2.14** shows the richness on the data set. Richness is an indicator of the number of OTUs in a sample. The richness increased in the attached community of the field. In the microcosms, the richness also increased from early to late stages of the experiment. In the case of the planktonic community in the field and microcosms, richness varied over time. The relatively stable number of OTUs in the planktonic community might be related to the similarities observed in the unweighted Unifrac analysis. ANOVA analysis on the richness revealed no differences between the richness of planktonic and attached communities, whereas the statistical differences were indicated between the experimental settings. The Tukey test confirmed the differences between the field and microcosm experiments. This test also indicated statistical differences on the richness between the communities located in the field (**Table 2.3**).

On the other hand, the differences in similarities observed in the attached communities from the field and microcosms, considering the abundances or presence/absence of different OTUs, are not explained for the increase of richness. Considering the evenness, which is community

diversity corrected for the relative abundance, might help to understand these differences. For instance, in a community, a decrease in evenness reflects some groups becoming more abundant. **Figure 2.15** shows the evenness on the data set. In the attached community from the field and microcosm, evenness measures showed oscillations with initial drops on the evenness, followed by a partial recovery and then another fall in this measure. In the case the planktonic communities in the field evenness is changeable over time, whereas in the microcosm after an initial drop tends to be quite stable. The different dynamics registered in the evenness of different communities and settings suggested that some groups might be preferentially attached or in the planktonic community. ANOVA analysis on the evenness revealed statistical differences between the experimental settings, the communities, and in the interaction between the settings and different communities. The Tukey test confirmed the differences between the microcosms and the field, and the planktonic and attached communities from both settings. This indicates differences between the relative abundance of the dominant groups within these communities (**Table 2.4**).

The sequencing of the 16S rRNA gene on microcosms samples was used to identify different microbial groups at the Genus level. Depending on their abundance in the attached or planktonic community, it was possible to determine if they were preferentially attached or planktonic. The changes in abundance are expressed in log<sub>2</sub> fold changes. Some microbes were preferentially attached, for instance *Sedimentibacter* and *Staphylococcus*. Other microorganisms were preferentially planktonic, such as *Corynebacterium* (**Figure 2.16**).

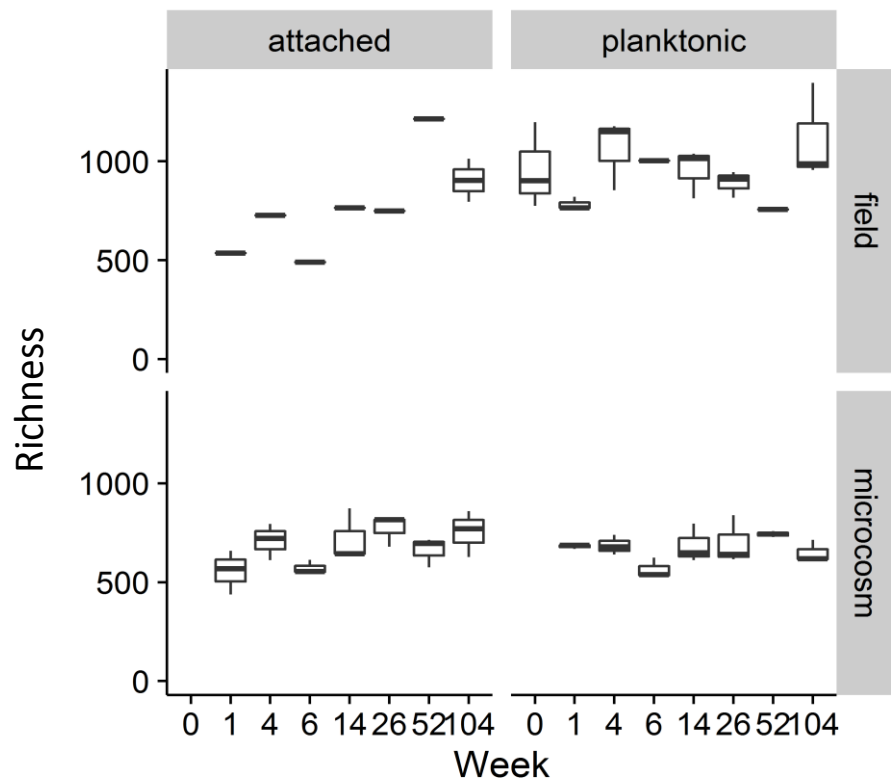


**Figure 2.14.** Richness of OTUs in planktonic and attached communities harvested from the microcosms and the field at different time intervals upon inoculation. (Note time is shown in weeks).

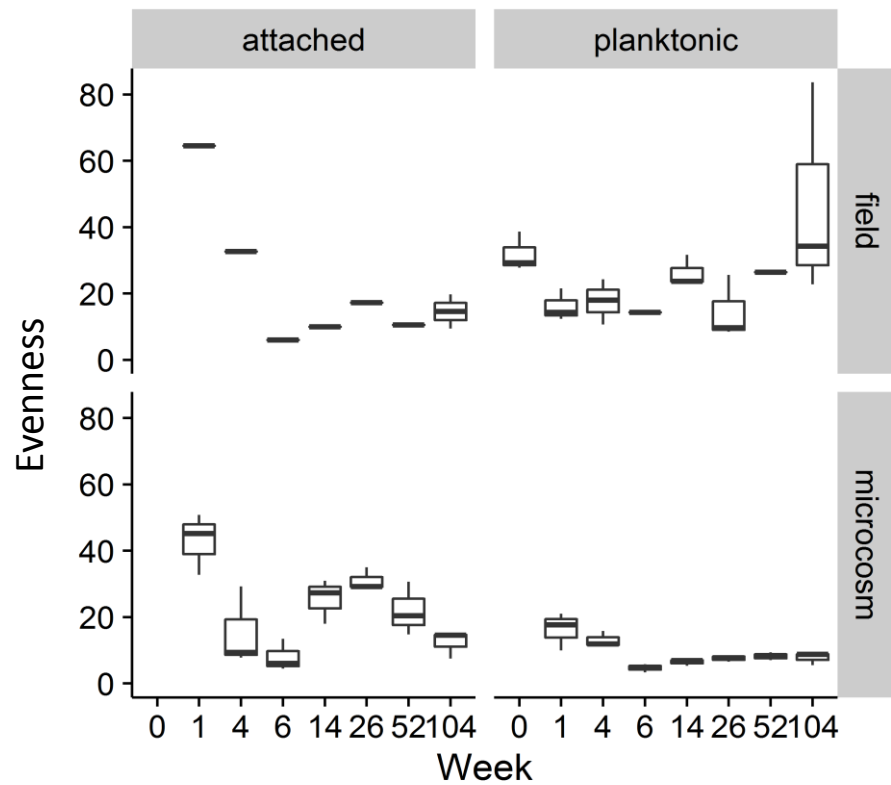


**Figure 2.15.** Evenness in planktonic and attached communities harvested from the microcosms and the field at different time intervals upon inoculation. (Note time is shown in weeks).

**Table 2.2.** Likelihood ratio test for 16S rRNA sequences from communities (attached and planktonic) obtained from different experimental settings (microcosms and field).

Source of Variation	Likelihood ratio	p-value
Intercept	88989	0.001
Community	5445	0.001
Experiment	5820	0.001
Community*Experiment	4783	0.001

**Table 2.3** ANOVA analysis on the richness and evenness parameters of communities (attached and planktonic) obtained from different experimental settings (microcosms and field).

Richness (ANOVA)					
Source of Variation	Df	Sum Sq	Mean Sq	F-value	p-value
Experiment	1	0.248	0.248	41.633	0.0000
Community	1	0.016	0.016	2.742	0.1026
Community*Experiment	1	0.033	0.033	5.543	0.022
Residuals	65	0.387	0.006		
Evenness (ANOVA)					
Source of Variation	Df	Sum Sq	Mean Sq	F-value	p-value
Experiment	1	0.6700	0.6702	10.127	2E-03
Community	1	0.4900	0.4899	7.403	8E-03
Community*Experiment	1	0.8310	0.8313	12.563	7E-03
Residuals	65	4.3010	0.0662		

**Table 2.4.** Tukey significance comparisons of richness and evenness parameters of communities (attached and planktonic) obtained from different experimental settings (microcosms and field).

Richness	
Comparison	p-value
microcosm-field	0.0000
planktonic-attached	0.1115
microcosm (attached-planktonic)	0.9998
field (attached-planktonic)	0.0000
Evenness	
Comparison	p-value
microcosm-field	0.0022
planktonic-attached	0.0101
microcosm (attached-planktonic)	0.0003
field (attached-planktonic)	0.0000

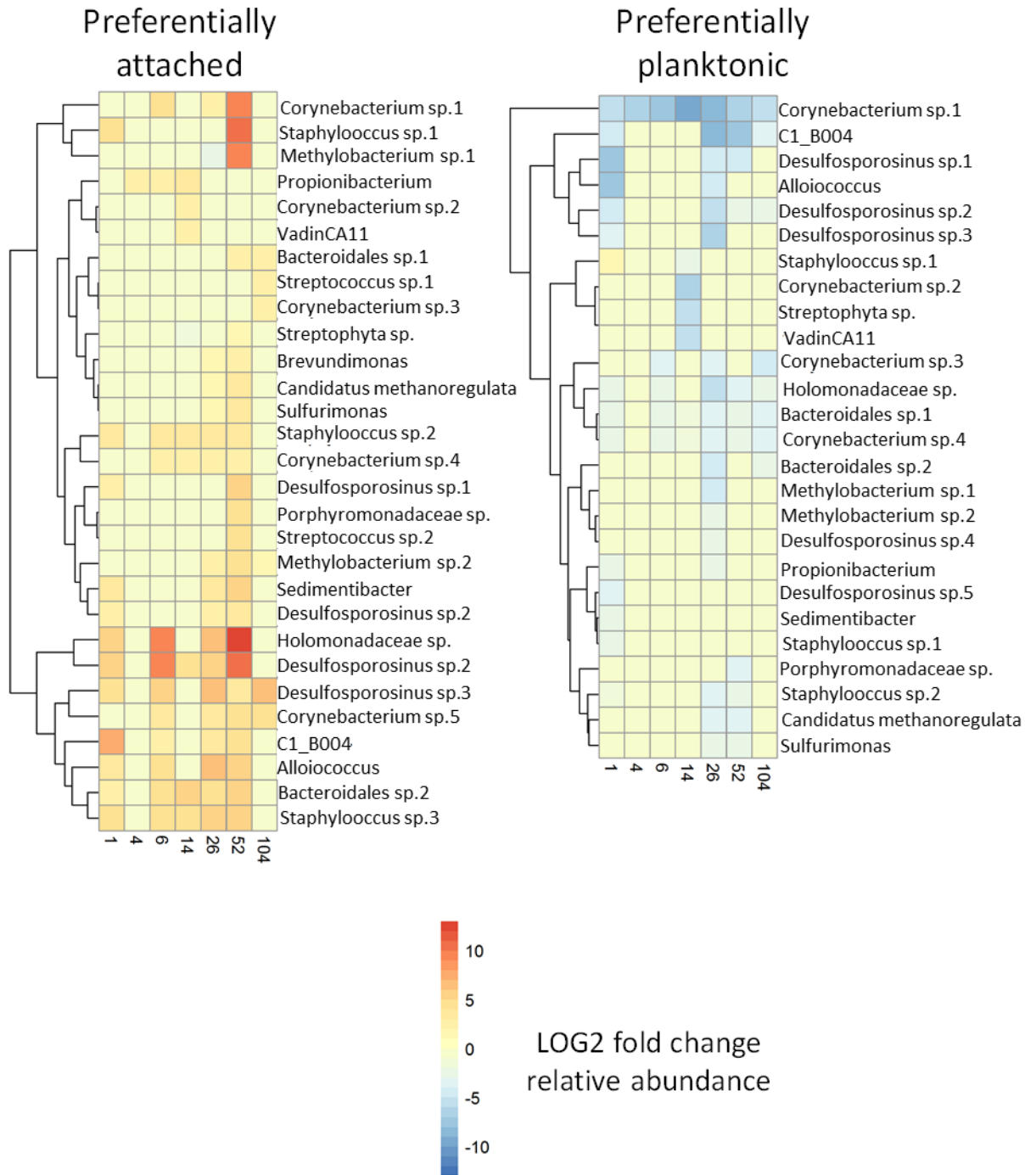


**Figure 2.16.** Microbial identification at Genus level of different microorganisms harvested at different time intervals after the inoculation in the microcosm experiment. Multiple Genera appears repeated as the taxa assignment is able to distinguish different variants under this taxonomic level (Note time is shown in weeks).

## 2.4 Discussion

### ***Do the microcosms replicate the environment at 30 mbgl?***

In the microcosms, there was no significant biodegradation of the phenolic compounds during the experiment. As throughout the whole microcosm experiment, the concentrations of these organic chemicals remained similar to the initial values in the plume fringe at 30 mbgl at the field site. This feature may reflect the adaptation of microorganisms within the inoculum of the experimental/laboratory conditions. This is plausible given biodegradation is active at this chemical interface but not complete and the microbial community has been exposed to this contaminant matrix for a considerable time (Thornton *et al.*, 2001a; Thornton *et al.*, 2001b; Thornton *et al.*, 2014). Therefore, the microcosms replicate the field system and represent a good model to study polluted aquifers, as previously demonstrated (Tuxen *et al.*, 2006; Thornton and Rivett, 2008; Elliott *et al.*, 2010).

The production of 4-hydroxybenzoic acid and 4-hydroxy-3-methyl benzoic acid after 47 days of inoculation (**Appendix 6.2**) indicates that there was some biodegradation of either phenol and *o*-cresol. These parent compounds can be biodegraded through para-carboxylation and the *p*-cresols via oxidation (Bossert and Young, 1986; Bisailon *et al.*, 1991; Boll and Fuchs, 2005). These two organic metabolites were also found in the anode chamber of microbial biofuel cells using groundwater from this field site (Hedbavna *et al.*, 2015). It is likely that this feature records anaerobic biodegradation of these parent compounds in the microcosms but at a rate which could not be detected by measurement of their respective concentrations.

### ***Does the lower plume fringe environment reflect the environmental variability?***

During sampling the water table was constantly located approximately 3.7 meters below ground; hence recharge events did not affect the variability observed at 30 mbgl. At this depth, the concentration of pollutants varied over time. The variation of the contaminant concentration entering to aquifers from point source areas (also referred as source term variation), has been described as one of the most important processes influencing the temporal plume contaminant composition (Thornton *et al.*, 2001a; Thornton *et al.*, 2001b).

This lower plume fringe is a chemical interface with high biodegradation potential, due to high numbers and activity of microorganisms (Pickup *et al.*, 2001; Tuxen *et al.*, 2006). At this location, the constant supply of electron acceptors and electron donors favour the biodegradation and pollutant mass removal (Wilson *et al.*, 2004; Rees *et al.*, 2007). The process behind this balance is the vertical transverse dispersion and could explain the



variability of pollutant content at this chemical interface (Thornton *et al.*, 2001a; Huang *et al.*, 2003).

***Is there any signal of Terminal Electron Acceptor Processes (TEAPs) at both systems?***

Nitrate concentration in the microcosms disappeared almost to depletion levels within 200 days after inoculation. The nitrate is the most energetically favourable electron acceptor for anaerobic biodegradation and is expected to be utilised very quickly in metabolism of the phenolic compounds (Gonzales *et al.*, 2006). This behaviour was similar to that previously observed at the field site, where nitrate supplied to the plume by transverse dispersion is rapidly consumed by anaerobic biodegradation at the plume fringe (Thornton *et al.*, 2001b, Baker *et al.*, 2012; Thornton *et al.*, 2014).

The increasing concentration of dissolved manganese within the microcosms is likely to result from dissolution of manganese oxide coatings in the aquifer material, which is known to be present in these fractions (Lerner *et al.*, 2000; Wu, 2002; Thornton *et al.*, 2001a; Baker, 2011). The difference between live microcosm and abiotic controls at the late stage of the experiments may be related to manganese reducer activity which has been described in contaminant plumes in groundwater (Gounot, 1994; Christensen *et al.*, 2000).

The concentration of total dissolved iron decreased in the live microcosms over 400 days more rapidly than abiotic controls. This feature is attributed to the consumption of oxide fractions in the aquifer material during biodegradation of either the phenolic compounds or uncharacterised organic compounds in the groundwater, as is common in organic contaminant plumes (Lerner *et al.*, 2000; Cozzarelli *et al.*, 2001, Thornton *et al.*, 2001; Bjerg *et al.* 2011) Nevertheless, this data needs to be taken with caution, because it does not discriminate between Fe (III) and Fe (II). Only information on the relative abundance of different oxidation states of iron would give insights about the potential metabolic activity, such as dissimilatory Fe (III) reduction or Fe (II) lithotrophic oxidation (Weber *et al.*, 2006). However, in many cases Fe(III) is a negligible fraction of total Fe under anaerobic conditions at the pH and redox conditions generally found in groundwater (Stumm and Morgan, 1996), and the iron most likely exists predominantly as Fe(II).

The total phenolic content (TPC) in the microcosms was constant across the experiment; the presence of metabolites suggested that some biodegradation pathways may be activated. The total nitrate consumption within the experiment was of 29.2 mg l<sup>-1</sup>, this amount according to the mass balances on the nitrate reduction and denitrification (Table 2.1), could have biodegraded a total of 0.89 and 2.26 mg l<sup>-1</sup> of TPC, respectively. On the other hand, there was

higher manganese content in the live microcosms at the end of the experiment. The amount of manganese was  $0.95 \text{ mg l}^{-1}$  and this quantity would have biodegraded  $0.171 \text{ mg l}^{-1}$  of TPC. Despite the stability of TPC, another parent compound may be biodegraded using these EAs. At this site there were more organic pollutants than phenols, cresols and xylenols. For instance, there were different types of ethyl phenols and wide range of compounds derived from tar neutrals and tar bases, thus these compounds may be the ones biodegraded (Lerner *et al.*, 2000; Williams *et al.*, 2001).

***What is the timescale of attachment in microbial communities in/from chemical interfaces?***

In terms of cell numbers, the initial drop in the numbers of planktonic microorganisms in the microcosms is attributed to the disturbance of the community. Initially, the community was taken from its natural environment; this could have stressed the community due to extraction, transportation and/or inoculation during setting up of the experiment. This is not the typical lag phase behaviour in microbial growth, and a similar decrease in cell numbers at early stages of inoculation has been observed on surfaces made of polyethylene terephthalate (Wang *et al.*, 2015). The subsequent recovery of the planktonic population in the microcosms is related to the stationary phase reached by the planktonic community (Kolter *et al.*, 1993). Furthermore, the planktonic cell numbers in the field also change over time. This variability relates to the community being entrained in the groundwater flow and must be influenced by the vertical transverse dispersion (Thornton *et al.*, 2001a; Huang *et al.*, 2003). This is natural variability in the groundwater system caused by the plume dynamics and transverse dispersion, as opposed to the microcosms which are static in nature with a fixed population sampled at one event.

Conversely, the cell numbers in the biofilm are characterized by a rapid phase of attachment within the first 104 days of inoculation, with subsequent stabilization over time in both systems. These growth dynamics have been described in other biofilm systems developed in different types of surfaces on medical instruments, pipes and other equipment in the oil and food industries respectively (Garett *et al.*, 2008). In this study, the time-scale of attachment seems to be a stable property of the microbial community, independently of the geochemical stability of the environment. The cell numbers calculated per  $\text{cm}^2$  were close to the values detected in surfaces of microcosms constructed with material from basalt aquifers (Lehman *et al.*, 2001). Furthermore, it was possible to observe similar kinetics of attachment in the microcosms and the field system. The visualization of the SYTO-9 stained grains also revealed similarity within the attachment process in both systems. Therefore, the time-scale of biofilm development in this groundwater system, inoculated with a planktonic community from a

chemical interface such as the plume fringe, is ~100 days. Once stabilised, the biofilm formed tends to be stable in terms of numbers.

#### ***How does the planktonic community differ from the biofilm?***

The t-RFLP analysis of the microcosms indicated differences between the planktonic and attached communities with respect to the binary data, peak height and peak area analysis. The values of the interaction were as high as the differences observed in previous studies (44 – 52 %) comparing soil from different environments (Culman *et al.*, 2008), suggesting that the planktonic and attached communities from chemical interfaces in a phenol-contaminated aquifer were different. In the AMMI biplots, from these comparisons, it was possible to observe these differences between the two communities. In the NMDS (Nonmetric Multidimensional Scaling) it was also possible to distinguish the separation between the samples according to the similarities and intensities of their OTUs.

From the t-RFLP analysis, it was also possible to deduce the differences between the attached and planktonic communities in the microcosms and field samples when the presence/absence and abundance of different OTUs were considered. Also, t-RFLP data suggested that community membership in the planktonic community might be more stable than in biofilm communities. This evidence supported the sequencing stage of the analysis.

#### ***How do the biofilm and the planktonic communities vary over time?***

One of the hypotheses for this experiment was that planktonic and biofilm communities will be different from each other over the period of study. The results from Illumina high-throughput sequencing support this hypothesis. The differences came from 3 analyses. Firstly, the likelihood ratio showed there was a significant effect between the communities, experiment and the interaction between these two. This supported the findings made with t-RFLP, that these two communities were different. Secondly, the ANOVA on the evenness showed a significant effect on the communities. These two results imply that the relative abundance distributions between the planktonic and attached communities were different. Finally, the Unifrac weighted analysis helped to visualize these differences. For instance, when the impact of time on the different experimental settings (microcosms and field) was ignored, it was possible to appreciate two different distributions for the attached and planktonic communities. Given that this Unifrac weighted analysis considers the phylogenetic relationship and the relative abundances of the different OTUs (Lozupone *et al.*, 2007), these two communities differed from each other as the experiment progressed.

The measured differences are consistent with another study made in the same environment (30 mbgl). This study also considered both communities, but did not take a more extensive temporal framework for the comparison between the planktonic and attached communities (Rizoulis *et al.*, 2013). The differences between planktonic and attached communities have been observed in different types of aquifers. For instance, in sandy aquifers dominated by porous groundwater flow, the archaeal communities identified in groundwater and core samples presented differences in the methanogen abundances, and the methanogens were more predominant in the groundwater (Godsy *et al.*, 1992). Similarly, a preference of the archaeal community for the planktonic community has been described in pristine aquifers (Flynn *et al.*, 2013; Gregory *et al.*, 2014). In shallow contaminated and pristine aquifers, the higher microbial abundances were located in the biofilm (Griebler *et al.*, 2002). In fractured quartz aquifers, most of the microbial abundance was located in the planktonic phase (Lehman *et al.*, 2001a). In microcosm studies simulating fractures of basalt aquifers, differences in the relative abundances and activity of these two communities have been also detected (Lehman *et al.*, 2001b). Nevertheless, it was possible to identify differences between the communities, yet both communities were related, as the planktonic community being the inoculum of the biofilm.

Another hypothesis was that structures of each community will differ over the period of study. There were two approaches to examine this hypothesis. Considering the impact of time and abundance of different OTUs, and the phylogenetic relationships within each community, it was possible to identify changes in terms of distances of the community structures. Also, in the attached communities there was an initial drop in the evenness, which might be related to some groups becoming more abundant. The following increase in evenness could be reflecting the attachment of new groups into the biofilm. Some studies have suggested similar dynamics of community structure changes across the development of epilithon biofilms (Jackson *et al.*, 2001). On the other hand, in the planktonic communities, the evenness of different groups changed but was influenced by the experimental setting. Therefore, the communities were changing as the experiment progressed.

Conversely, when a Unifrac unweighted analysis was performed to assess the stability of the community membership, it was possible to observe that the presence/absence of groups in the biofilm communities of both settings was quite dynamic. This might be related to the increase of diversity in the biofilm, as more groups are able to attach as the biofilm matures. This has been observed in biofilm development in drinking water distribution systems (Jackson, 2003; Martiny *et al.*, 2003). In contrast, the planktonic community membership was more stable over time, as was earlier suggested by the t-RFLP analysis. This might be related to

a steady-state of the community membership, because this community has been formed with some groups which were preferentially planktonic.

The groups identified in the experiment can be related to groundwater systems and/or their presence explained by their physiological properties. For instance, the presence of different types of *Desulfosporosinus sp.* could be linked to the capacity of this group to live in anoxic areas of hydrocarbon-contaminated aquifers, and use sulphate as electron acceptor during the biodegradation of organic pollutants (Kümmel *et al.*, 2015; Kleinstaubler *et al.*, 2012; Robertson *et al.*, 2000). Other groups, such as *C1\_B004*, are bacteria belonging to the *Chloroflexi* Phylum, and have been found in chemical gradients derived from D-NAPL source areas in coal tar contaminated aquifers (Scherr *et al.*, 2016). Another group detected was *Alloicoccus*, which has been described in contaminated shallow aquifers (Inoue *et al.*, 2015). Despite the link between these groups and their physiological properties in groundwater environments, it is not possible using 16S rRNA gene sequencing technologies to establish their functional state (Langille *et al.*, 2013).

Also, it is important to mention that the appearance of different types of *Staphylococcus* and *Corynebacterium* does not imply contamination in the sequenced samples, as some species within these Genera have been described as part of the skin microbiota (Gao *et al.*, 2007). During the library sample preparation no contamination was introduced into the samples. This was carefully and constantly checked through the negative control in the PCR amplifications (See Appendix for library sequencing library preparation). Moreover, the presence of *Corynebacterium* in both communities at different stages of the experiment could be related to the ability of this Genus of bacteria of using manganese as electron acceptor, as has been suggested in aquifer sediments (Di-Ruggiero and Gounot, 1990; Du *et al.*, 2010). Also, the presence of *Staphylococcus* has been detected in groundwater from contaminated aquifers (Krapac *et al.*, 2002; Ozler and Aydin, 2008; Grisey *et al.*, 2010).

The hypothesis related to early attachment events promoting an increase in the bacterial diversity in the biofilm, when sediments are inoculated with polluted groundwater was partially accepted. The findings suggest that the inoculum contained some microbes that are early attachers, which then proliferate at early stages of the biofilm formation. These early attachers increase their relative abundances. Over time the complexity of attached communities increases due to physical and metabolic interactions becoming established. Similar dynamics in biofilm development have been observed in the formation of the human dental plaque, where after the attachment of primary colonizers, secondary colonizers start to adhere and finally form a multi-species biofilm (Rickard *et al.*, 2003; Tool *et al.*, 2000).

The groundwater flow in this aquifer was reported to be up to 11 meters per year (Lerner *et al.*, 2000; Thornton *et al.*, 2001a). It is estimated that the advancing plume front will pass from an unpolluted phase into plume fringe in less than 100 days. Therefore, the attached community is not likely to be well-adapted during this transition or may be showing adaptations to a variable environment. It is likely that microbes from chemical interface environments may be able to respond to gradients observed, as they do in different systems where their composition and function strongly influenced by environmental factors (Logue *et al.*, 2015).

## **2.5 Conclusions**

This study concluded that there was a period of rapid attachment from the planktonic microbial community to the surface of the sediments. This attachment event was the precursor of the biofilm formation, which needs ~100 days to stabilise in numbers. Similar kinetics was observed in the microcosms and the field samples. Attached communities differ from planktonic communities in cell numbers, community membership and relative abundances. The biofilm community structure is not stable over time.

# Chapter 3

---

*Biofilm community in chemical interfaces and their responses to changes in their chemical environment*

---

### 3.1 Introduction

Chemical interfaces in organic contaminant plumes are important for the high biodegradation observed at these locations, due to high numbers and activity of microorganisms (Pickup *et al.*, 2001; Tuxen *et al.*, 2006); derived from the chemical conditions in these areas, with a constant supply of electron acceptors and electron donors in concentrations favouring biodegradation and pollutant mass removal (Wilson *et al.*, 2004; Rees *et al.*, 2007).

The development of these chemical interfaces in plumes is influenced by different physical processes creating changeable environments in terms of their hydro-chemical composition. For example, transverse hydrodynamic dispersion due to mechanical mixing and molecular diffusion that occurs as the plume migrates through the aquifer, controlling the flux of dissolved electron acceptors supplied from the background groundwater to the upper and lower plume fringe. Also, there are source term variation processes (Lerner *et al.*, 2000; Thornton *et al.*, 2001; Wilson *et al.*, 2004; Thornton & Rivett, 2008). Conversely, the chemical interface at the front (or leading edge) of a plume develops in response to longitudinal hydrodynamic dispersion that occurs by advection of the plume (Breu *et al.*, 2008; Hiscock, 2005). In this respect, the hydro-chemical conditions at the interface develop as contaminated groundwater in the plume core advances into the uncontaminated aquifer downstream. This results in a chemical interface characterised by increases in contaminant concentrations over time (for a fixed spatial location), which eventually stabilise as concentrations approach those found in the plume core. Therefore, at these chemical interfaces the concentrations of organic compounds and different electron acceptors fluctuate over time.

In this context, the presence of biofilms in aquifers has been established in both pristine and contaminated environments, where this microbial community is proposed to offer advantages to its members, through the facilitation of access to nutrients or to different electron acceptors (Williamson *et al.*, 2012). Previous studies have shown differences in community structure and diversity between attached and planktonic communities at one specific depth, without considering temporal effects (Elliot *et al.*, 2010; Rizoulis *et al.*, 2013). The responses of biofilms located in these changeable chemical interface environments have not been explored.

#### Research questions

- What is the effect of changing the chemical environment on the biofilm communities of chemical interfaces?
- What drives community development in biofilms of chemical interfaces?
- Which community is more stable in response to environmental changes?



## Research aim

The aim of this chapter is to examine the responses of biofilms at chemical interfaces to changes in their chemical environment. Laboratory microcosms were established with groundwater inocula from different chemical environments within a phenolic contaminated plume (11, 14 and 21 mbgl) and allowed to establish for 100 days. Environmental changes were then simulated by transferring the planktonic phase (contaminants +/- microbial cells) from one microcosm to another.

## Research Hypothesis

The following hypotheses were tested:

1. The community structure of an established biofilm will change when exposed to a new chemical environment, becoming more similar to the planktonic community of the new environment. Alternatively, the biofilm community is resistant to environmental change and its structure will therefore remain stable.
2. Biofilm community structure is governed by a combination of geochemical conditions and the planktonic microbial community. Alternatively, the biofilm community structure is governed by the chemical environment with little interaction with the planktonic community.
3. Biofilm communities are more stable than the planktonic communities in response to environmental changes.

These hypotheses were tested in a number of scenarios that represent different conditions within the plume.

## Scenarios

### Scenario 1: Low phenolic environment (low)

At the plume fringes, mixing occurs between background groundwater and the plume due to longitudinal dispersion (Elliot *et al.*, 2010). A re-supply of  $\text{NO}_3^-$  as a terminal electron acceptor is expected from agricultural activities from the field above the aquifer, followed by consumption of  $\text{NO}_3^-$  by nitrate reducer activity (Thornton *et al.*, 2001a; Thornton *et al.*, 2001b; Spence *et al.*, 2001). This scenario is shown conceptually in **Figure 3.1a** with variation in  $\text{NO}_3^-$  at the lower plume fringe (BH-59, 30 mbgl) shown in **Figure 3.1b**.

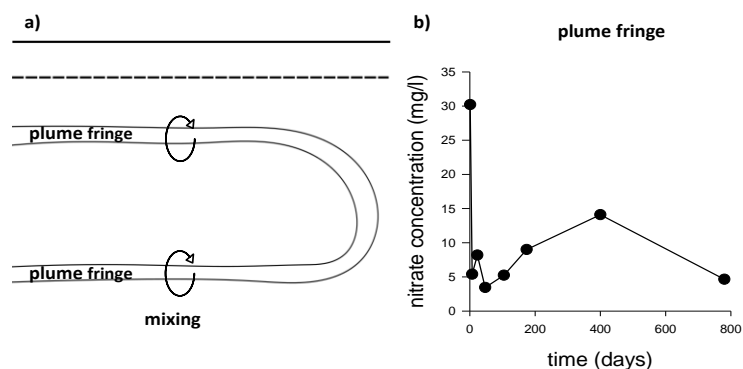


**Figure 3.1.** Mixing processes in the upper and lower plume fringes. (a) Schematic representation of the locations and (b) nitrate fluctuations registered in the lower plume fringe (BH-59, 30 mbgl) of a phenolic plume.

This scenario was reproduced by establishing microcosms with groundwater from BH-59 11 mbgl (Upper plume fringe, low phenolic concentration) and constant anaerobic re-addition of  $\text{NO}_3^-$  to a constant level (**Figure 3.1**).

**Scenario 2: Plume advance (adv\_1 and adv\_2)**

As the plume advances in the aquifer, the aquifer substratum and associated attached microbial communities encounter increasing concentrations of contaminated groundwater and associated planktonic communities. It is not possible to sample these horizontally stratified zones; therefore the vertical gradient provided by BH-59 was used. Samples from 11, 14 and 21 mbgl represented regions of low, moderate and high phenol concentrations, respectively. Two plume advance scenarios were considered: the intrusion of the outskirts of plume core into plume fringe (**Figure 3.2**) and further plume migration where phenolic concentrations rise from medium to high (**Figure 3.3**).

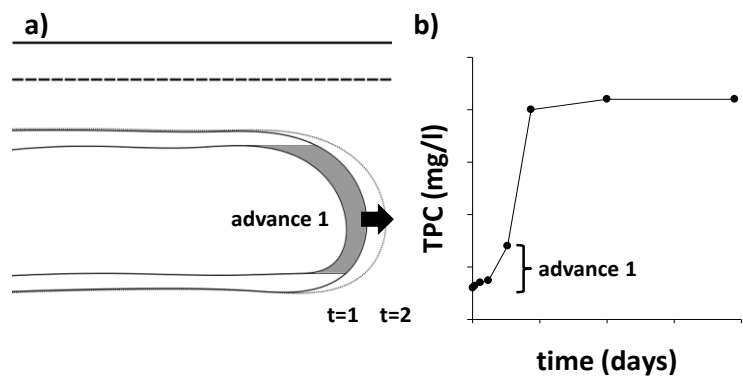


**Figure 3.2.** Plume advance, from low to medium phenol concentrations. (a) In grey locations exposed to plume advance 1 (adv\_1); (b) Expected increase of pollutant content at these locations.

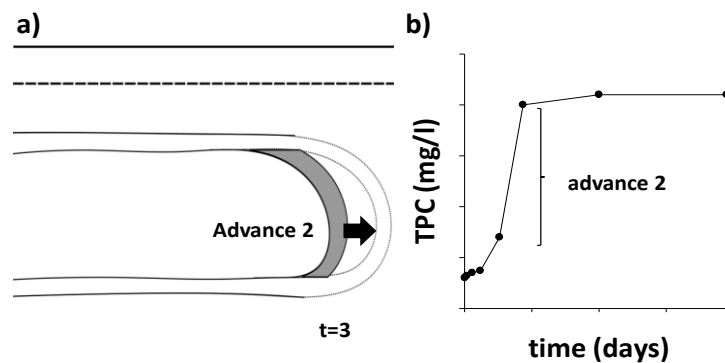


**Figure 3.3.** Plume advance, from medium to high phenol concentrations (a) In grey locations exposed to plume advance 2 (adv\_2); (b) Expected increase of pollutant content at these locations.

**Scenario 3: Plume refreshing (PR)**

**Figure 3.4** shows a plume spreading through an aquifer when it is submerging to deeper levels. This could happen in aquifers where the flow is mostly controlled by pumping boreholes (Lerner *et al.*, 2000). In the locations exposed to refreshing, there will be a change from medium to low pollutant content, and in addition more energetic EA (nitrate) will become available.

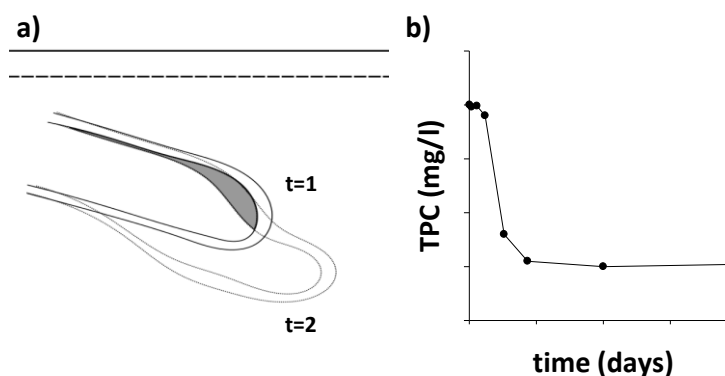


**Figure 3.4.** Plume refreshing, from medium to low phenol concentrations (a) Diving of the plume into the aquifer from  $t=1$  to  $t=2$ , in grey the locations exposed to plume refreshing process. (b) Expected reduction of pollutant content at these locations.

#### Scenario 4: Source term variation (STV)

Pollutant plumes are influenced by source history, with a changeable chemical composition related to different pollutant releases (Thornton *et al.*, 2001b; Rees *et al.*, 2007). Source history could have even more importance in plume composition than biodegradation reactions (Mayer *et al.*, 2001). In industrial sites contaminated with phenolic compounds, several orders of magnitude differences have been observed temporally at the same locations, reflecting the impact of source term fluxes (Watson *et al.*, 2005; Baker *et al.*, 2012). **Figure 3.5** shows one type of source term variation passing from high to medium pollutant content.

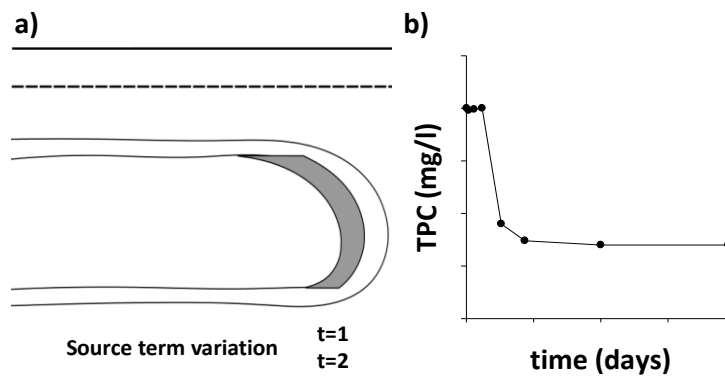


**Figure 3.5.** Source term variation, from high to medium phenol concentrations (a) Source term variation in the aquifer from  $t=1$  to  $t=2$ , in grey the locations exposed to source term process. (b) Expected decrease of pollutant content at these locations.

## 3.2 Methodology

Microbiological and chemical analyses were performed as described in chapter 2.

### ***Substrate preparation***

Sandstone from a quarry near the study site, with similar mineralogy to the aquifer material (Baker, 2011) was ground and sieved to obtain particles between 150 - 300  $\mu\text{m}$ . The sand grains were sterilized by autoclaving at 121 °C for 20 min.

### ***Inoculum and microcosm initial setting***

Groundwater samples from 11, 14 and 30 (mbgl) of a plume (Pickup *et al.*, 2001; Thornton *et al.*, 2001b; Williams *et al.*, 2001) containing a mixture of phenols, cresols and xylenols were collected using a peristaltic pump into sterile, N<sub>2</sub>-filled containers (Elliot *et al.*, 2009). These depths represent low, medium and high contaminant content respectively. The microcosms consisted of 125 ml Wheaton serum bottles cleaned by a series of washes using Decon 90® and 0.1 M HNO<sub>3</sub>. The bottles were sterilized by autoclaving at 121 °C for 20 min and then filled with 100 g of sterilized sieved sand grains. Each microcosm was inoculated with 110 ml of groundwater from a specific depth (11, 14 and 21 mbgl) under aseptic and anaerobic conditions using a Coy vinyl anaerobic chamber (Wolflab, UK). The microcosms were capped with a bromo-butyl rubber stopper with an aluminium crimp (Fisherbrand, UK) and incubated at 10 °C in the dark.

### **Microcosm treatments**

#### **Incubations of groundwater samples**

Microcosms were inoculated with field water from either 11, 14 or 21 mbgl. Destructive samples of attached and planktonic communities (3 replicates of each treatment) were collected after 101 and 195 days of incubation (**Figure 3.6**). For microcosms containing groundwater from a low phenolic environment, nitrate concentrations were measured and when concentrations fell below 25 mg L<sup>-1</sup>, 4g L<sup>-1</sup> NaNO<sub>3</sub> was added to restore the concentration to 30 mg L<sup>-1</sup>. An equivalent set of microcosms were incubated for 3 months and then the planktonic community removed by filtering the aqueous phase three times (0.22  $\mu\text{m}$  Whatman® polycarbonate membranes, 25 mm diameter). The aqueous phase was re-introduced into the microcosm and incubated for a further 3 months before sampling.

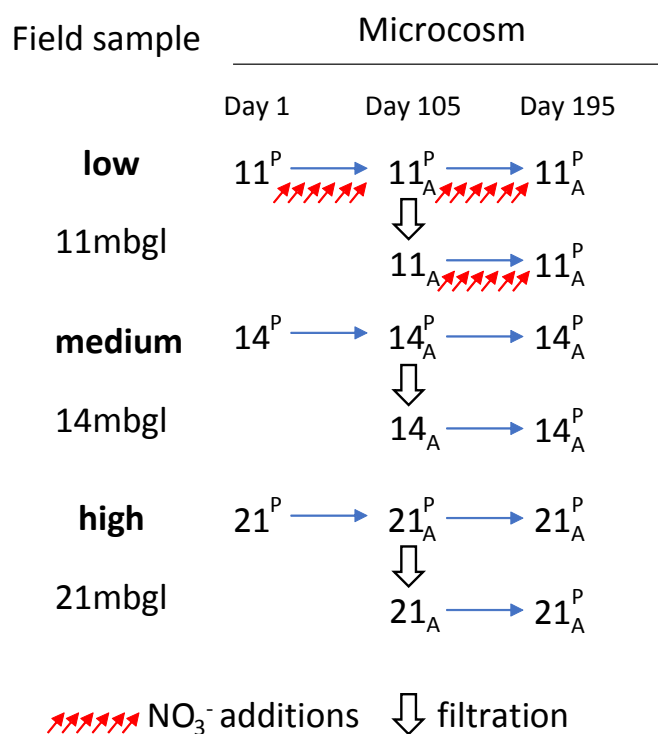


**Figure 3.6.** Construction of microcosms to recreate the low, medium and high phenolic environments. Field groundwater samples were introduced into microcosms and incubated for 101 or 195 days. For a subset of microcosms, the aqueous phase was decanted after 3 months, filtered to remove planktonic cells, and then re-introduced into the microcosm. Attached (A) and planktonic (P) phases were sampled. For 11 mbgl microcosms only, nitrate was re-added at intervals to maintain NO<sub>3</sub><sup>-</sup> concentrations at 30 mg L<sup>-1</sup>.

***Plume advance scenarios.***

To test the plume advance scenarios, microcosms were established with groundwater from low, medium and high phenolic environment for 101 days as described above (including nitrate re-additions for low phenolic microcosms). To examine the plume advance scenario (from low to medium phenolic, adv\_1), the aqueous phase (water + planktonic community) from a medium phenolic microcosm was added to the attached community from a low phenolic microcosm and incubated for a further 94 days. Equivalent microcosms were established where the microbial community was removed from the planktonic phase by filtering. The plume advance scenario (from medium to high phenolic, adv\_2) was examined using the aqueous phase from a high phenolic microcosm (both unfiltered and filtered) with the attached phase from a medium phenolic community (**Figure 3.7**).

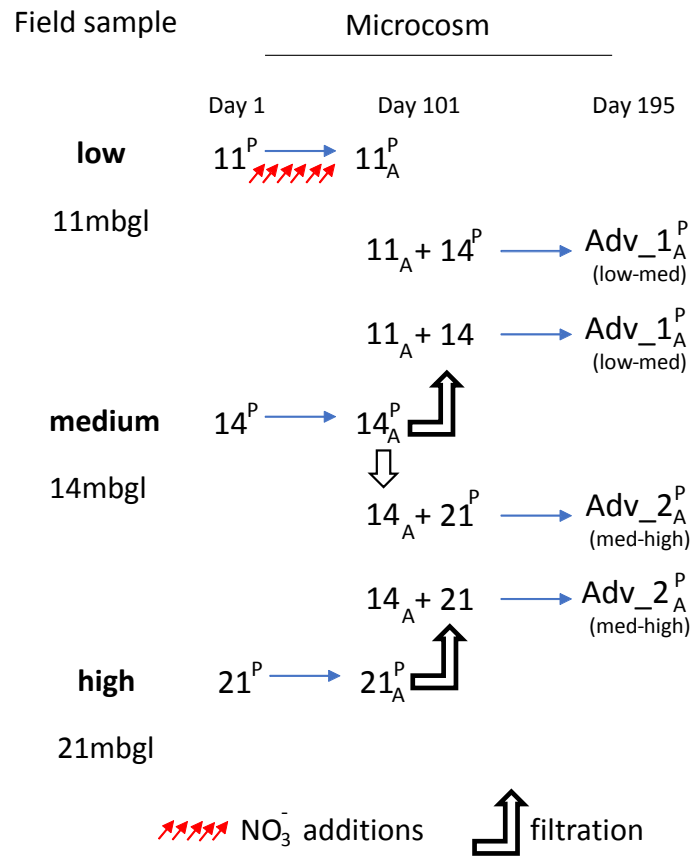


**Figure 3.7.** Construction of microcosms to recreate plume advance scenarios. Microcosms were established for 101 days with groundwater from low, medium and high phenolic content. To simulate the transition from low to medium phenol (adv\_1), the aqueous phase from a medium phenolic microcosm was added to the attached phase of low phenolic microcosm with and without filtering. Equivalent transfers using the planktonic phase from microcosms with high phenolic and the attached phase from microcosm with medium phenolic content were used to simulate the transition from medium to high phenol (adv\_2).

### Plume refreshing and source term scenarios

To test the plume refreshing and source term scenarios, microcosms were established with groundwater from low, medium and high phenolic environment for 101 days as described above (including nitrate re-additions for low phenolic microcosms). To examine the plume refreshing, (from medium to low), the aqueous phase (water + planktonic community) from a medium phenolic microcosm was added to the attached community from a medium phenolic microcosm and incubated for a further 94 days. Equivalent microcosms were established where the microbial community was removed from the planktonic phase by filtering. Nitrate concentrations were measured and when concentrations fell below  $25 \text{ mg L}^{-1}$ ,  $4 \text{ g L}^{-1} \text{ NaNO}_3$  was added to restore the concentration to  $30 \text{ mg L}^{-1}$ .

The source term scenario (from high to medium phenol) was examined using the aqueous phase from a medium phenolic microcosm (both unfiltered and filtered) with the attached phase from a high phenolic community (**Figure 3.8**).

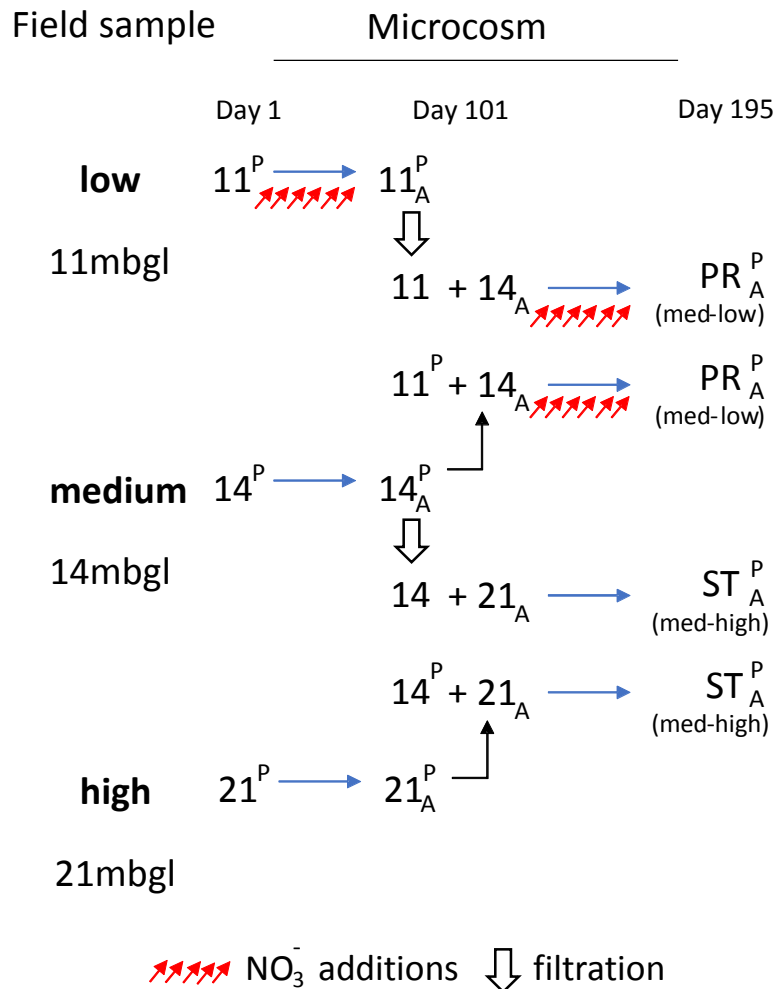


**Figure 3.8.** Construction of microcosms to recreate plume the plume refreshing (PR) and source term (ST) scenarios. microcosms were established for 101 days with groundwater from low, medium and high phenolic environment. To simulate the transition from medium to low phenol, the aqueous phase from a low phenolic microcosm was added to the attached phase of a medium phenolic microcosm with and without filtering. Equivalent transfers using the planktonic phase from medium phenolic and the attached phase from high phenolic microcosm, simulated the transition from high to medium phenol.

#### Residual pore water calculation

When the aqueous phase was removed from a microcosm, residual pore water remained in the sediments that could not to be removed. The amount of residual water calculated as follows; A microcosm bottle containing 100 g sand was weighed before and after addition of 110 ml of water. The phases were mixed and allowed to settle for 10 min. The supernatant



was removed and the bottle weighed again providing the mass of residual pore water. This measurement was made 3 times using different bottles.

### **Planktonic synthetic community**

In the different treatments considering a change of environment, there was residual pore water containing a residual pore water community, which mixed with the new supernatant. To evaluate if the new community was purely a result of mixing these two communities, a synthetic community was modelled using phyloseq package (McMurdie & Holmes 2013) in R (R Development Core Team, 2011). The percentage occupied in the final arrangement and the growth of two planktonic communities independently after 195 days of incubation was considered. For example, to calculate the synthetic planktonic community in the adv\_1 treatment, the planktonic communities of the low and medium phenolic microcosms after 195 days of incubation and the volume of each one in the final arrangement (29 and 81 ml, respectively) was considered.

### **Statistical analysis**

One-way and two-way ANOVAs were made to evaluate changes in the geochemistry of different treatments. The Post-hoc test used was Tukey's or Dunnet's test using GraphPad Prism (version 7.00 for Windows, GraphPad Software, La Jolla California USA, www.graphpad.com).

## **3.3 Results**

### **Low phenolic environment (low).**

The microcosms were inoculated with groundwater from BH59, 11 mbgl (see **Figure 3.6 for details**). **Figure 3.9** shows different parameters measured in the microcosms. The starting groundwater contained  $\sim 0.5 \text{ mg l}^{-1}$  phenol,  $\sim 4 \text{ mg l}^{-1}$  cresols (*m,p* and *o*) and  $6 \text{ mg l}^{-1}$  xylenols. These concentrations decreased during the 195 days duration of the experiment. The decreasing in cresols and xylenols was significant (*m,p*-cresols:  $F_{(1,4)}: 362.5$ ; *o*-cresols:  $F_{(1,4)}: 258$ ; xylenols:  $F_{(1,4)}: 102.3$ ,  $p < 0.05$ , differences were given between day 1, with days 101 and 195 according to Tukey's test). In the microcosm where the planktonic community was removed, a similar trend was observed, but no statistical differences were detected between treatments. Iron concentrations were low  $0.5 \text{ mg l}^{-1}$  and remained stable within the entire duration of the experiment in both treatments (Nevertheless, statistical differences were found over time, *iron*:  $F_{(1,4)}: 69.35$ ,  $p < 0.05$ , but Tukey's test did not find any differences over time or between treatments). Manganese concentration increased significantly from an initial concentration of

0.1 mg l<sup>-1</sup> to 2.5 mg l<sup>-1</sup>, this value remained stable after 200 days of the experiment (manganese: F<sub>(1,4)</sub>: 1222, p<0.05, and the differences were given between equal sampling period than cresols). In the filtered treatment, manganese content kept rising up to 6.7 mg l<sup>-1</sup>, and the *post-hoc* test found statistical differences between treatments (treatment: F<sub>(1,4)</sub>: 2646, p<0.05). Nitrate concentrations increased up to 30 mg l<sup>-1</sup> through spiking with a 4000 mg l<sup>-1</sup> NaNO<sub>3</sub> solution. Nitrate was consumed rapidly within the first 26 days of the experiment up to 3.5 mg l<sup>-1</sup>. After this period and within the 146 days of incubation, nitrate consumption was more gradual (lowest level within this period was 17 mg l<sup>-1</sup>). Finally, in the last 50 days of the experiment, nitrate consumption decreased more rapidly after each spiking, reaching values as low as 2.4 mg l<sup>-1</sup>. In the filtered treatments, nitrate consumption was fast, reaching depletion levels on different measurements. Nitrate consumption was higher in the filtered treatment during the monitoring period. Sulphate concentrations remained stable throughout at ~18 mg l<sup>-1</sup>, without statistical differences associated.

Mass balances were applied to estimate biodegradation processes using redox half reactions described in Thornton *et al.* (2001b). Iron and sulphate were not considered as their concentrations were stable over time.

Total phenolic compounds (TPC) consumed was 10.63 mg l<sup>-1</sup>; and the rise of manganese concentration due to manganese reduction from manganese oxides, within the 100 days of experiments was of 2.45 mg l<sup>-1</sup>. Manganese increasing could allow for a maximum of 0.44 mg l<sup>-1</sup> of TPC to be biodegraded through this mechanism. Even though, taking into account the manganese dissolution in the second half of the experiment in the filtered microcosm, the rise was of 4.16 mg l<sup>-1</sup>, and this amount would have biodegraded only 0.75 mg l<sup>-1</sup>. Therefore, nitrate reduction might be the mechanism behind the biodegradation of TPC in these treatments. The total nitrate consumption within the experiment was of 181.58 mg l<sup>-1</sup>, this amount according to the mass balances on the nitrate reduction and denitrification, could have biodegraded a total of 55.58 and 139.05 mg l<sup>-1</sup> of TPC respectively. Nitrate reduction would explain 100% of the biodegradation of the pollutants analysed, but manganese reduction may be also involved (manganese reduction of manganese oxides from the sediments). Also, other organic compounds could have been biodegraded.

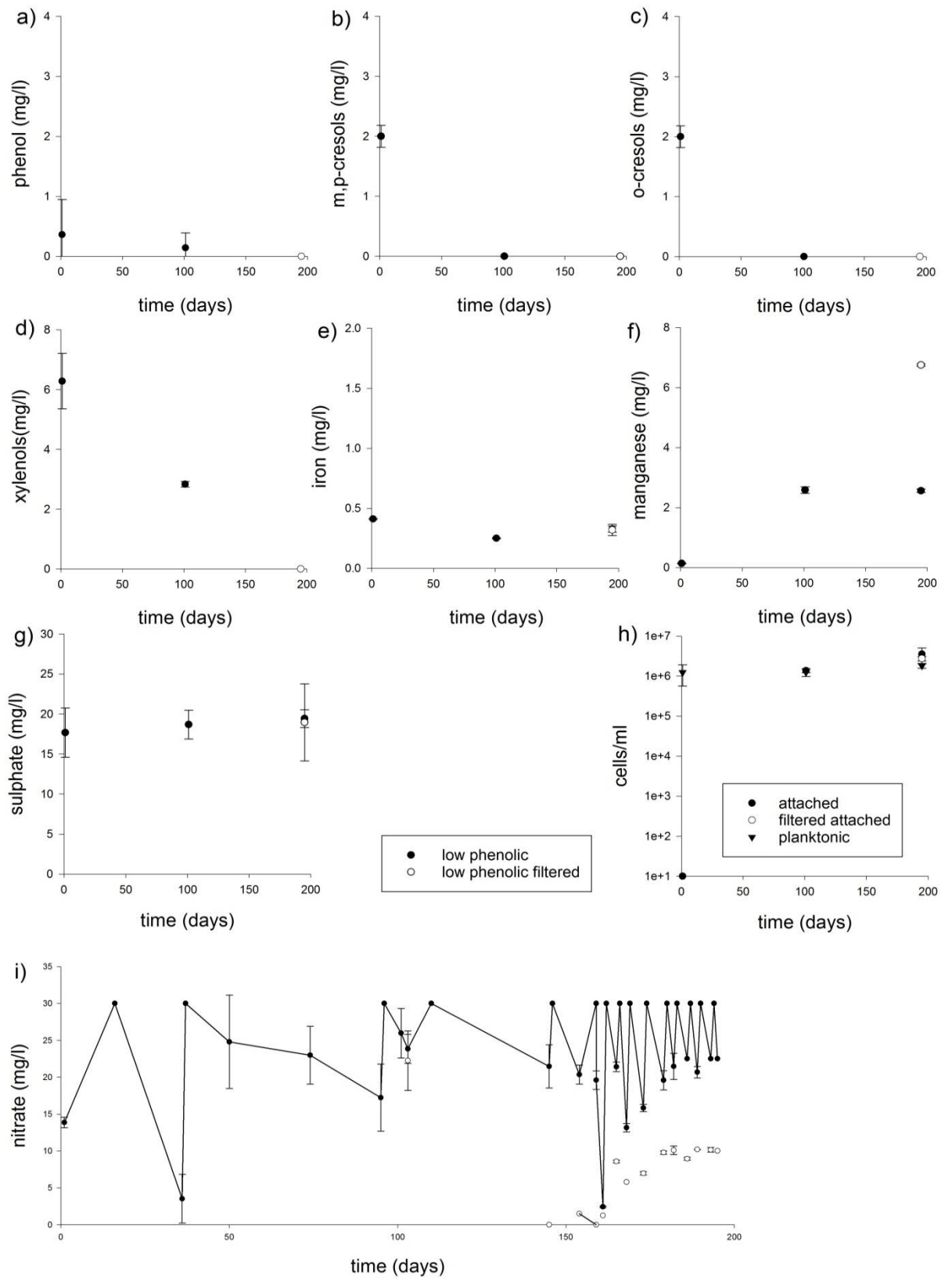


**Figure 3.9.** Monitoring of different chemical species in microcosms inoculated with groundwater from 11 mbgl. Error bars represent the standard deviation of replicates (n=3). Legend in the middle applies for all graphs except for the cell densities in h.

In the field, cell numbers at 11 mbgl were  $\sim 10^6$  cells  $\text{ml}^{-1}$ . These samples were used to inoculate microcosms containing sterile sediments. After 101 and 195 days of incubation in the microcosms the cell densities in the supernatant were similar to the values observed in the field. In the attached phase, the cell numbers reach  $\sim 10^6$  cells per ml of saturated sediments after 101 days of incubation. This value increased slightly after 195 days of total incubation, in both treatments.

To understand the differences between microbial communities, the data set was analysed using a Unifrac Principal Coordinates (PCo) weighted analysis, which considers the relative abundances and phylogenetic relationship between different groups. **Figure 3.10** shows the PCoA weighted analysis. A shift in the community structures was registered, from field samples (inoculum), to the attached and planktonic communities developed after 3 months of incubation in the microcosms. In the microcosms the attached and planktonic communities develop their community structures towards different directions.

The biofilm communities tend to be more dispersed after 101 days of incubation, which is an indication of differences between biofilm communities at this period, but after 94 days these communities were similar (unfiltered and filtered treatments). Planktonic communities tend to be relatively stable under the nitrate spiking regime applied to these treatments, and more distant from the community structures of samples from the field

The large shift of the community structures from samples from the field to lab has been hypothesized to be a response of the microbial community to a new environment (bottle effect). There was a change of conditions from a variable to a more stable environment. Furthermore, not all the microbes are able to be cultivated. Among these factors, another selection pressure was added with the nitrate spiking. It was necessary to explore the possibility if this shift was significant and what groups would be behind the changes. **Figure 3.11** shows a Deseq analysis which contrasted the planktonic samples from the field and microcosm planktonic samples after 101 days of incubation. The contrast indicated a significant change in the relative abundance of the *Myxococcales sp.*, which decreased its relative abundance from the field to and after 3 months of incubation in the lab. Similar significant trends were observed for *Desulfobacteraceae sp.* and *Desulfosporosinus sp.* On the other hand, *Pseudomonadaceae sp.* increased its relative abundance significantly, similar to *Enhydrobacter*. Therefore, the large shift observed in the PCoA is related to significant changes of the relative abundances of the different groups, favoured by the change of conditions.

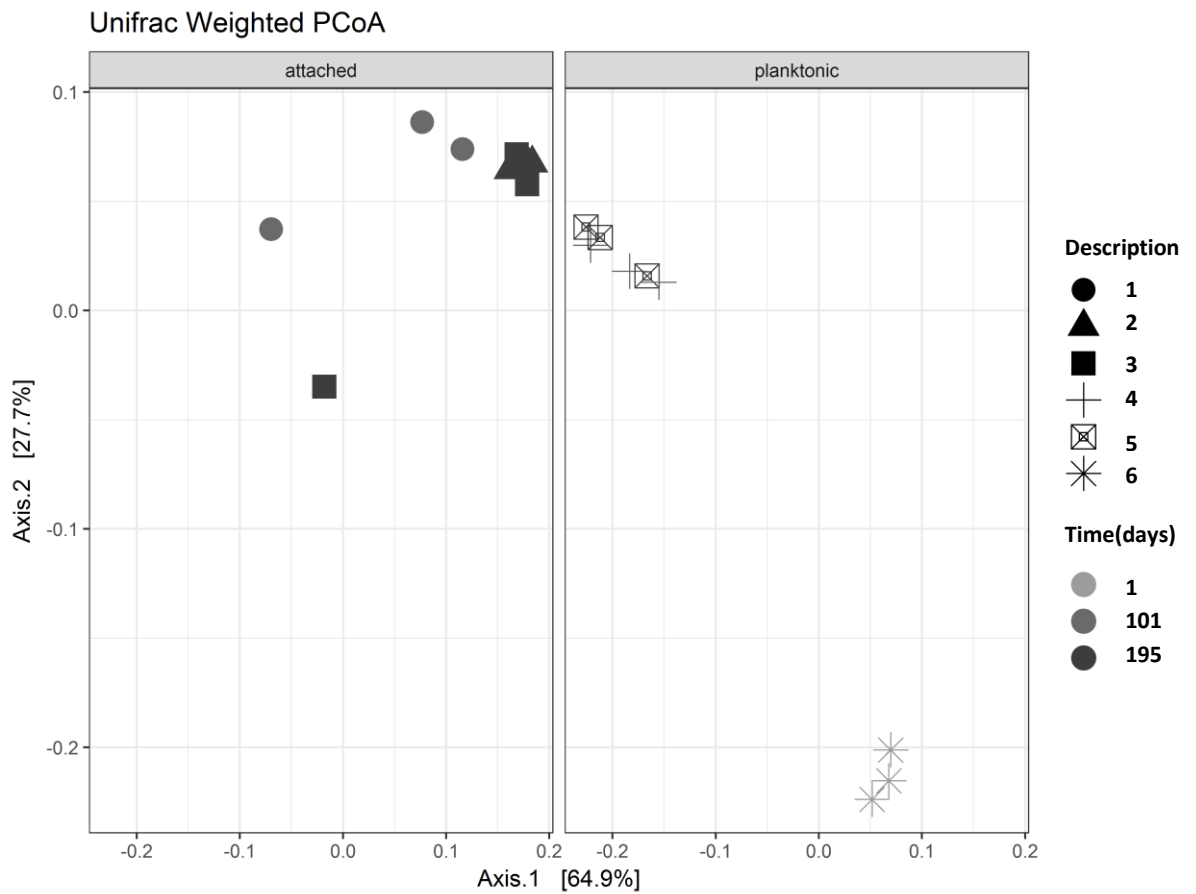


**Figure 3.10.** Unifrac weighted Principal coordinate analysis of attached and planktonic communities harvested from microcosms inoculated with groundwater from a low phenolic environment. Note 1 and 2, attached communities after 101 and 195 days of incubation in a microcosm. 3, attached community formed after the removal of the planktonic community. 6, planktonic community from 11 mbgl (inoculum); 4 and 5, planktonic communities after 101 and 195 days of incubation respectively.

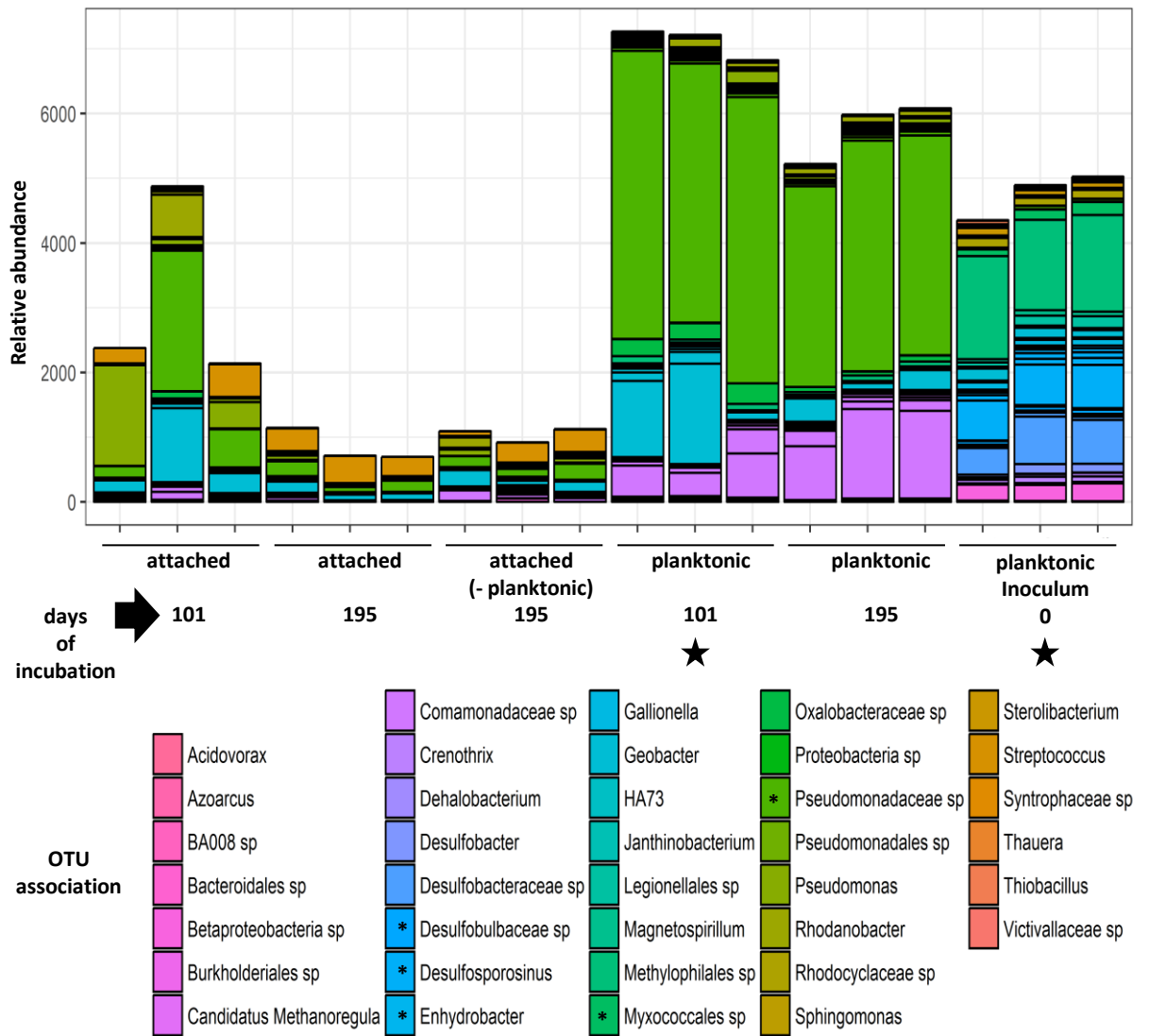


**Figure 3.11.** Deseq analysis between planktonic samples in the low phenolic environment inoculum and the planktonic community after 101 days of incubation (\*). OTUs showing statistical differences in the relative abundances between these communities are shown. Note, the relative abundance was normalised to 10,000 counts and (\*) indicates groups which exhibited the larger changes in the relative abundances between these communities.

The PCoA indicated that community structures of the biofilm samples after 3 months of incubation were more distant from each other and different from community structures of the biofilm after 6 months of incubation. **Figure 3.12** shows a Deseq analysis which contrasted attached communities considering the effect of time. The contrast indicated significant change in the relative abundance of the *Pseudomonadaceae* sp. and *Pseudomonas* which decreased its presence from 3 to 6 months of incubation in the biofilms settled in the microcosm. Similar significant trends were observed for *Geobacter* and *Thermomonas* sp. On the other hand, *Magnetospirillum* sp. increased its relative abundance significantly.

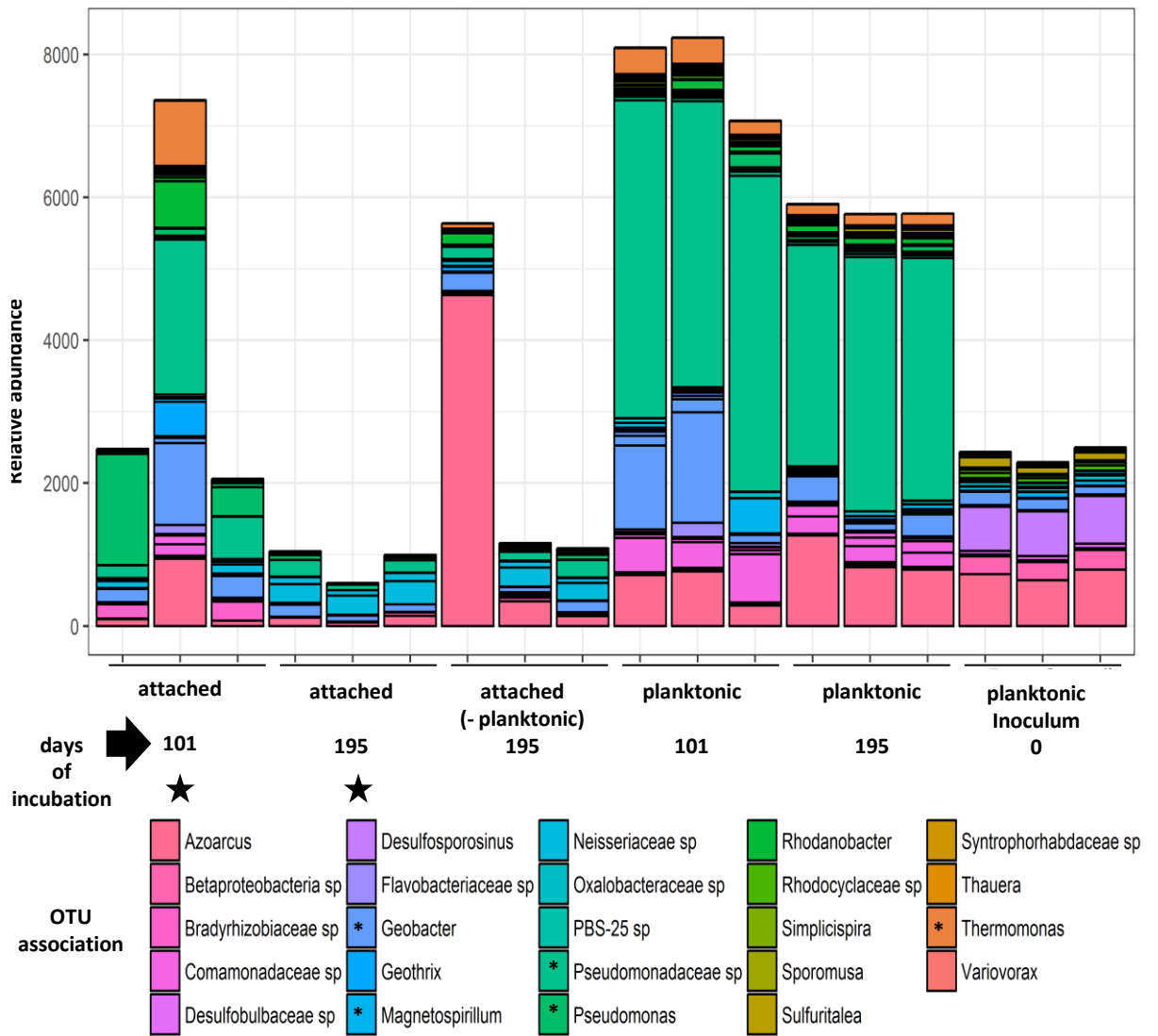


**Figure 3.12.** Deseq analysis between attached communities from low phenolic microcosms after 101 and 195 days of incubation (\*). OTUs showing statistical differences in the relative abundances between these communities are shown. Note, the relative abundance was normalised to 10,000 counts and (\*) indicates groups which exhibited the larger changes in the relative abundances between these communities.

**Figure 3.13** shows a Deseq analysis which contrasted the attached communities after 6 months considering the effect of the geochemical environment. The contrast indicated significant change in the relative abundance of *Pseudomonas* and *Bacteroidales*. Nevertheless, the statistical differences on the relative abundances between these two biofilms represent less than 5%.

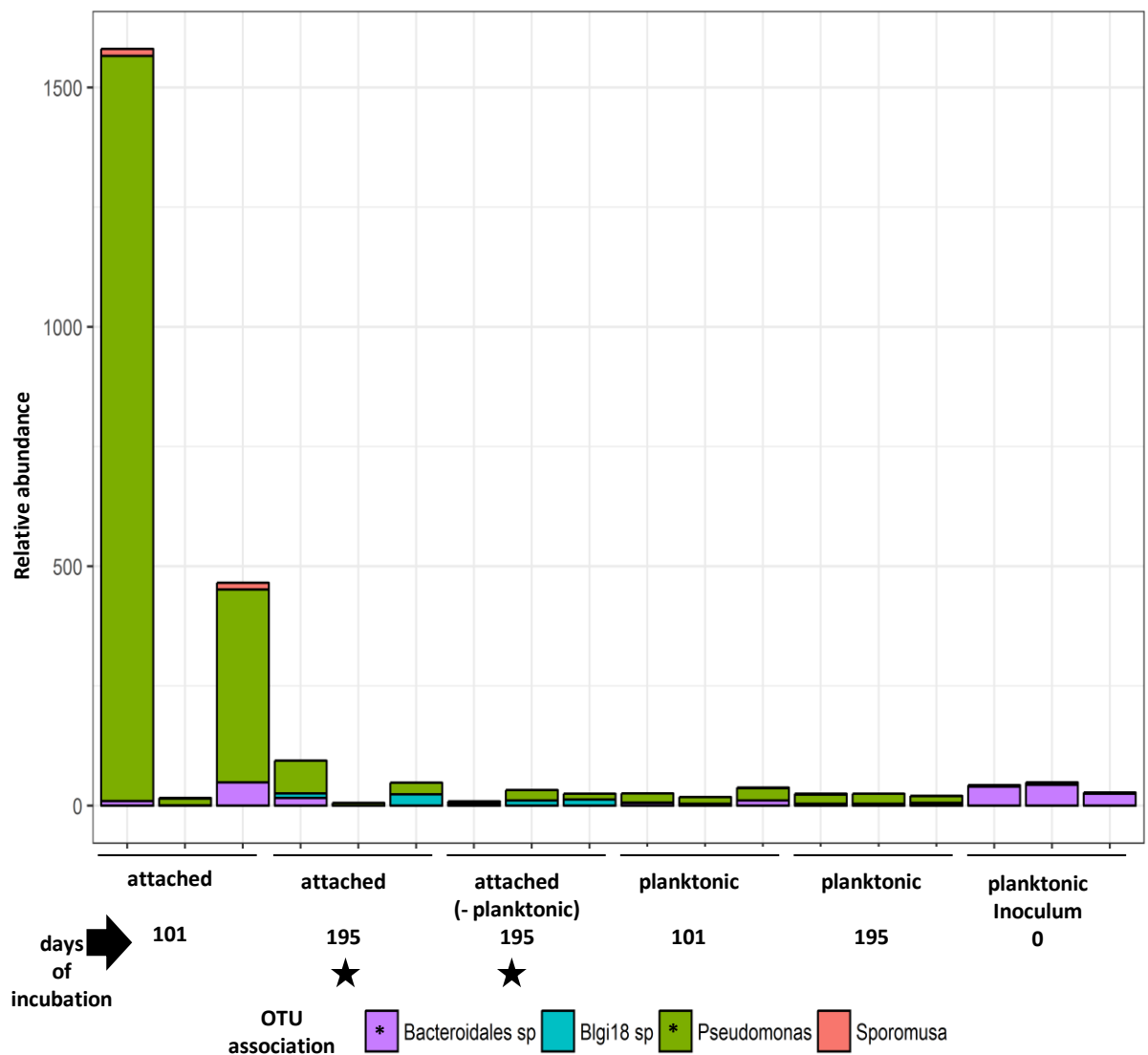


**Figure 3.13.** Deseq analysis between attached communities from low phenolic microcosms after 195 days of incubation (\*). OTUs showing statistical differences in the relative abundances between these communities are shown. Note, the relative abundance was normalised to 10,000 counts and (\*) indicates groups which exhibited the larger changes in the relative abundances between these communities.

**Note, the medium and high phenolic microcosm do not represent changeable scenarios described in the introduction, but will be used to recreate them.**

**Medium phenolic environment (medium).**

The microcosms were inoculated with groundwater from BH59, 14 mbgl (see **Figure 3.6** for details). **Figure 3.14** shows different parameters measured in the microcosm. The starting groundwater contained ~6 mg l<sup>-1</sup> phenol, ~33 mg l<sup>-1</sup> cresols (*mp* and *o*) and 33 mg l<sup>-1</sup> xylenols. These concentrations decreased in both treatments during the 195 day duration of the experiment. The decrease in *m,p*-cresols was significant ( $F_{(1,4)}: 51.16, p < 0.05$ , differences were given between day 1 and 195 according to Tukey's test). No differences were detected



between treatments. Iron concentrations decreased significantly from an initial concentration of  $\sim 4 \text{ mg l}^{-1}$  to  $1 \text{ mg l}^{-1}$  in both treatments (iron:  $F_{(1,4)}$ : 16.46,  $p < 0.05$ , differences were given between day 1, with day 101 and 195 of experiment). No differences were detected between treatments. Manganese concentration increased significantly from an initial concentration of  $1 \text{ mg l}^{-1}$  to  $\sim 14 \text{ mg l}^{-1}$  (manganese:  $F_{(1,4)}$ : 295.7,  $p < 0.05$ , differences were given between all different sampling periods). In filtered treatments manganese content was slightly lower, the *post-hoc* test found statistical differences between treatments after 195 days of experiment (treatments:  $F_{(1,4)}$ : 6.835,  $p < 0.05$ ). Nitrate concentrations were low  $\sim 1 \text{ mg l}^{-1}$  and decreased to  $\sim 0.2 \text{ mg l}^{-1}$ , and no statistical differences were detected. Sulphate concentrations decreased significantly from  $\sim 6 \text{ mg l}^{-1}$  to  $\sim 4 \text{ mg l}^{-1}$  (sulphate:  $F_{(1,4)}$ : 66.85,  $p < 0.05$ , differences were given between day 1 and 101, with day 195). For sulphate and nitrate no differences were observed between treatments.

The mass balances of the different electron acceptors consumed due to biodegradation did not explain the decrease in pollutant concentrations observed in these treatments. The total phenolic compounds (TPC) consumed was  $27.23 \text{ mg l}^{-1}$  and the total nitrate consumption within the experiment was  $0.63 \text{ mg l}^{-1}$ . According to the mass balances for nitrate reduction and denitrification, these processes could have biodegraded a total of  $0.19$  and  $0.49 \text{ mg l}^{-1}$  of TPC respectively. Moreover, the rise in manganese concentration due to manganese reduction from manganese oxides, within the 101 days of experiments was of  $17.4 \text{ mg l}^{-1}$ . According to the mass balance, this increase could allow a maximum of  $3.14 \text{ mg l}^{-1}$  of TPC to be biodegraded through this mechanism. Also, the decrease in sulphate concentration ( $5.85 \text{ mg l}^{-1}$ ) could explain a TPC decrease through biodegradation of  $4.22 \text{ mg l}^{-1}$ . In total, the use of the different electron acceptors could explain only  $8.24 \text{ mg l}^{-1}$  of the total reduction of pollutants, which is a 29.5% of the biodegradation of the pollutants analysed.

In the field, cell numbers at  $14 \text{ mbgl}$  were  $\sim 10^6 \text{ cells ml}^{-1}$ . After 195 days of incubation in the microcosms the cell densities in the supernatant were similar to the values observed in the field. In the attached phase, the cell numbers reach  $\sim 10^6 \text{ cells per ml}$  of saturated sediments after 101 days of incubation. The cell numbers of the attached communities after 195 days of incubation in both treatments were slightly higher than cell densities in the planktonic community.

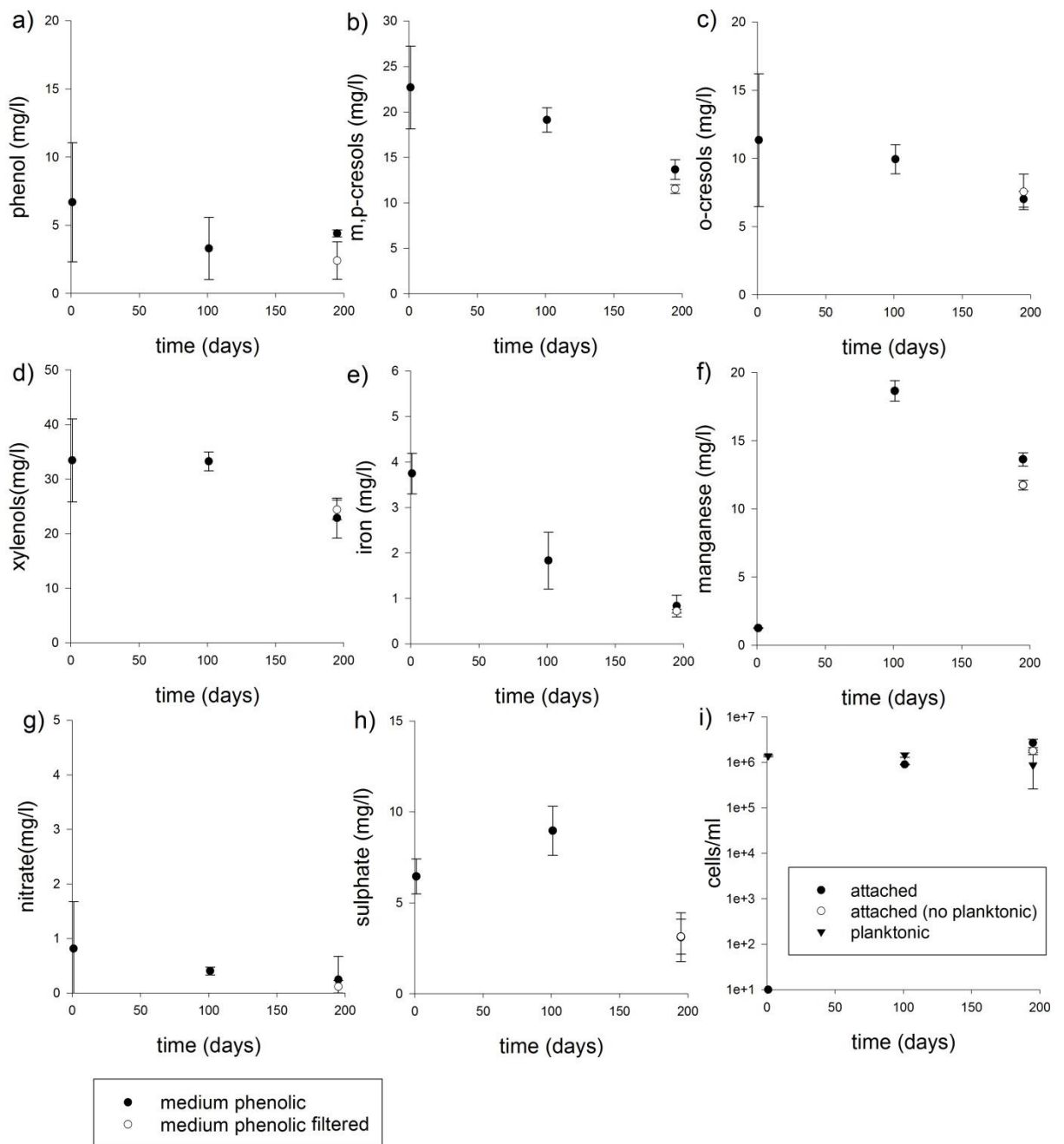


**Figure 3.14.** Monitoring of different chemical species in microcosms inoculated with groundwater from 14 mbgl. Error bars represent the standard deviation of replicates (n=3). Legend from lower left corner applies for all graphs except for the cell densities in i.

**Figure 3.15** shows the PCoA weighted analysis on the microbial community. The PCoA showed a shift in the community structures from field samples (inoculum), to samples from the attached and planktonic communities after 101 days of incubation in the microcosms. In the microcosms the attached and planktonic communities develop their community structures towards different directions (similar trends to microcosm formed with groundwater of 11 mbgl, **Figure 3.10**)

The biofilm communities tend to be more dispersed after 101 days of incubation, but after 195 days of total incubation these communities tend to be relatively similar (unfiltered and filtered treatments). On the other hand, the planktonic community tend to be relatively stable over the monitoring period in the microcosms.

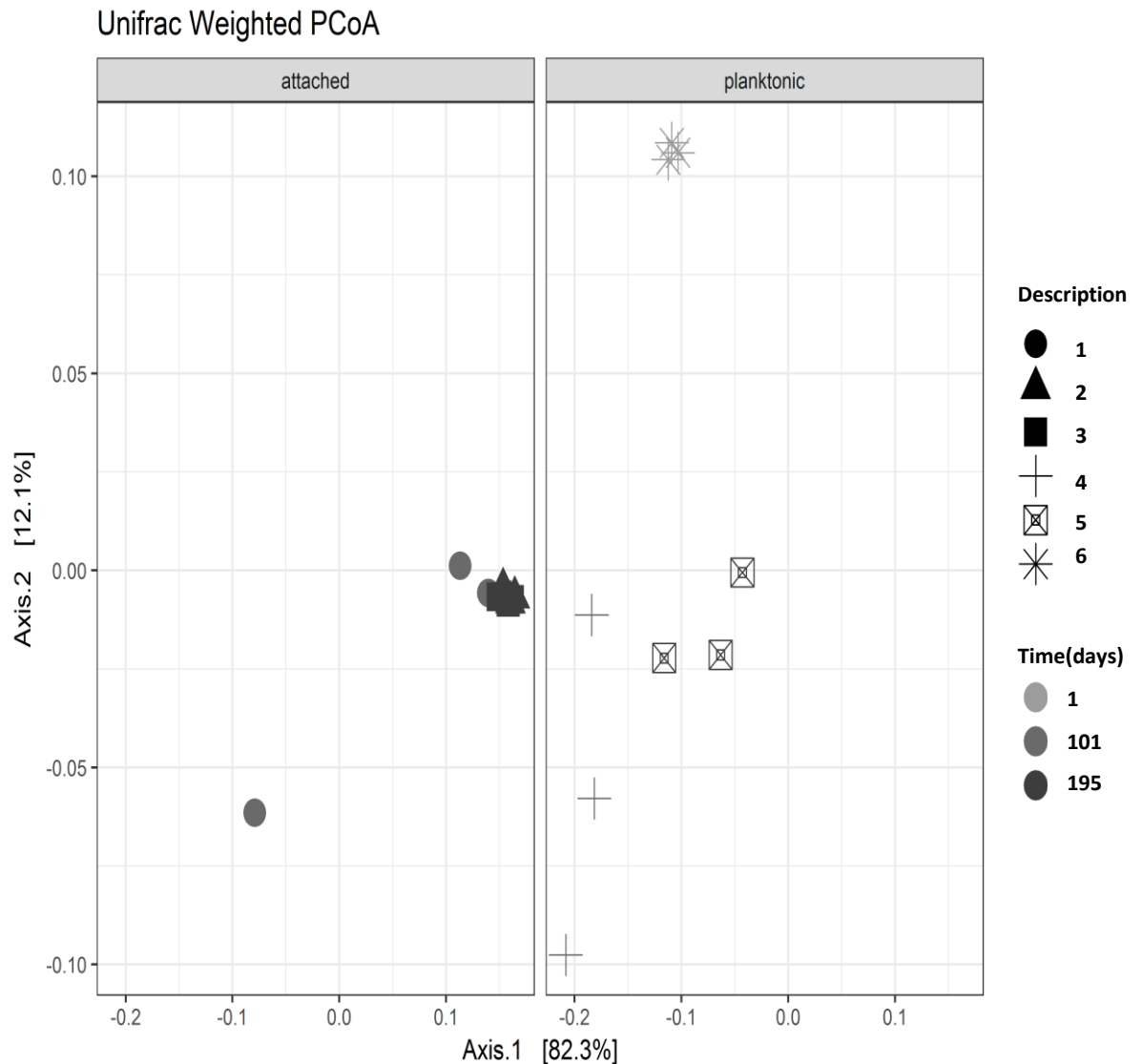


**Figure 3.15.** Unifrac weighted Principal coordinate analysis of attached and planktonic communities harvested from microcosms inoculated with groundwater from a medium phenolic environment. Note 1 and 2, attached communities after 101 and 195 days of incubation in a microcosm. 3, attached community formed after the removal of the planktonic community. 6, planktonic community from 11 mbgl (inoculum); 4 and 5, planktonic communities after 101 and 195 days of incubation respectively.

The large shift of the community structures from samples from the field to the lab has been hypothesized to be a response of the microbial community to a new environment. There was a change of conditions from a variable to a more stable environment. Nevertheless, on these

treatments nitrate was not added and the environment had a medium phenolic content. In this sense, the shift between the field and microcosm planktonic samples after 101 days of incubation could be explained by changes of different OTUs.

**Figure 3.16** shows a Deseq analysis which contrasted planktonic samples from both the field and microcosms after 101 days of incubation. This contrast indicated a significant change in the relative abundance of the *Azoarcus sp.* and *Bacteroidales sp.*, which decreased largely their presence from the field and after 3 months of incubation in the lab. Similar significant trends were observed for *Candidatus methanoregula*, *Desulfobacteraceae sp.*, *Desulfosporosinus sp.* and *Sporomusa*. On the other hand, *Pseudomonadaceae sp.* did not show any significant change, which has previously identified in the low phenolic microcosms. This was an indication that changes in medium phenolic treatment is related to different OTUs, and represents a different environment, both chemically and biologically.

PCoA indicated that community structures of the biofilm after 101 days of incubation were more distant from each other and different from the community structures of the biofilm after 195 days of incubation. **Figure 3.17** shows a Deseq analysis which contrasted the attached communities considering the effect of time. The contrast of these samples indicated significant changes, largely explained by 1 replicate of the biofilm formed after 101 days of incubation, with initially high relative abundances of *Pseudomonas* and *Geobacter*, which then almost disappeared. After 195 days of incubation the relative abundances of *Corynebacterium* and *Staphylococcus* increased significantly in the biofilm.

PCoA showed similarity between the community structures of biofilms settled after 6 months of incubation. In **Figure 3.17** a contrast between the attached communities formed after 195 days, considering the effect of the geochemical environment can be visualised. The contrast of these samples showed similarities between these communities.

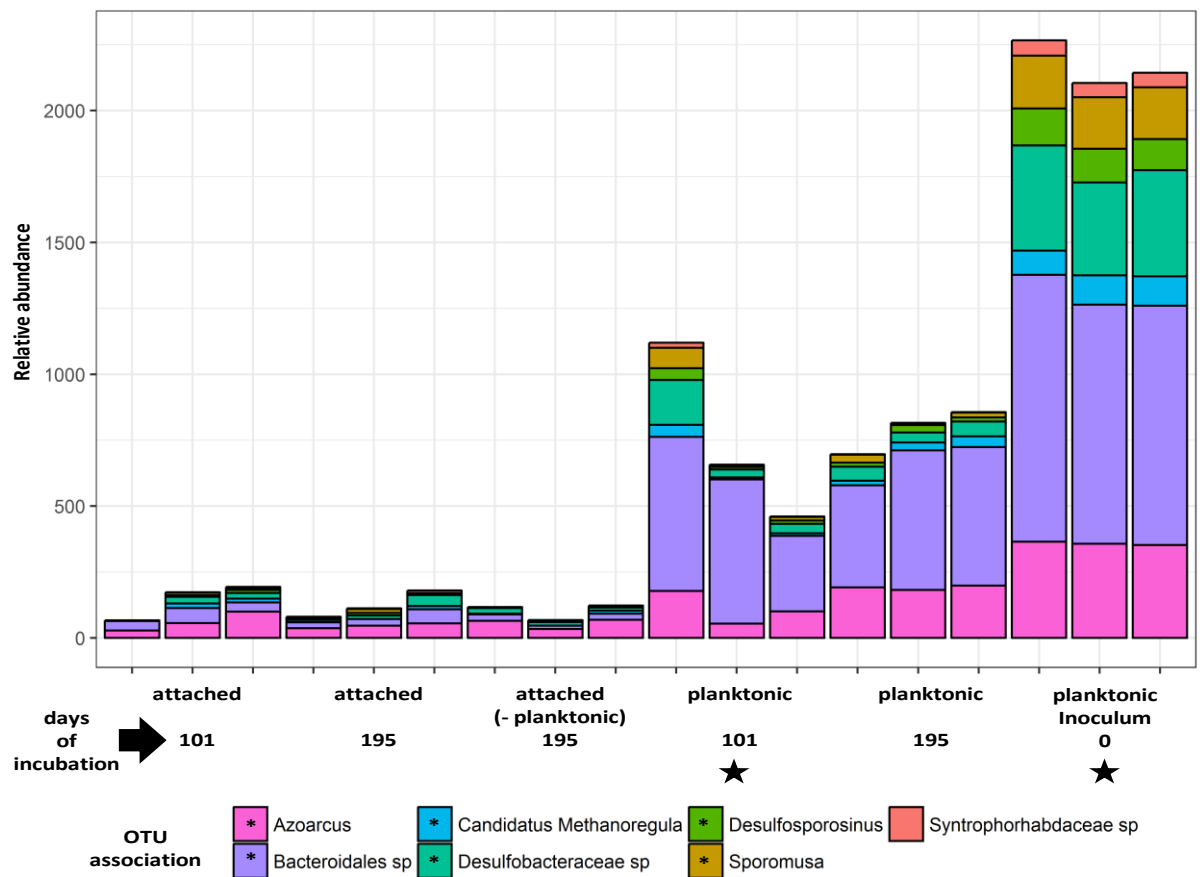


**Figure 3.16.** Deseq analysis between planktonic samples in the medium phenolic environment inoculum and the planktonic community after 101 days of incubation (\*). OTUs showing statistical differences in the relative abundances between these communities are shown. Note, the relative abundance was normalised to 10,000 counts and (\*) indicates groups which exhibited the larger changes in the relative abundances between these communities.

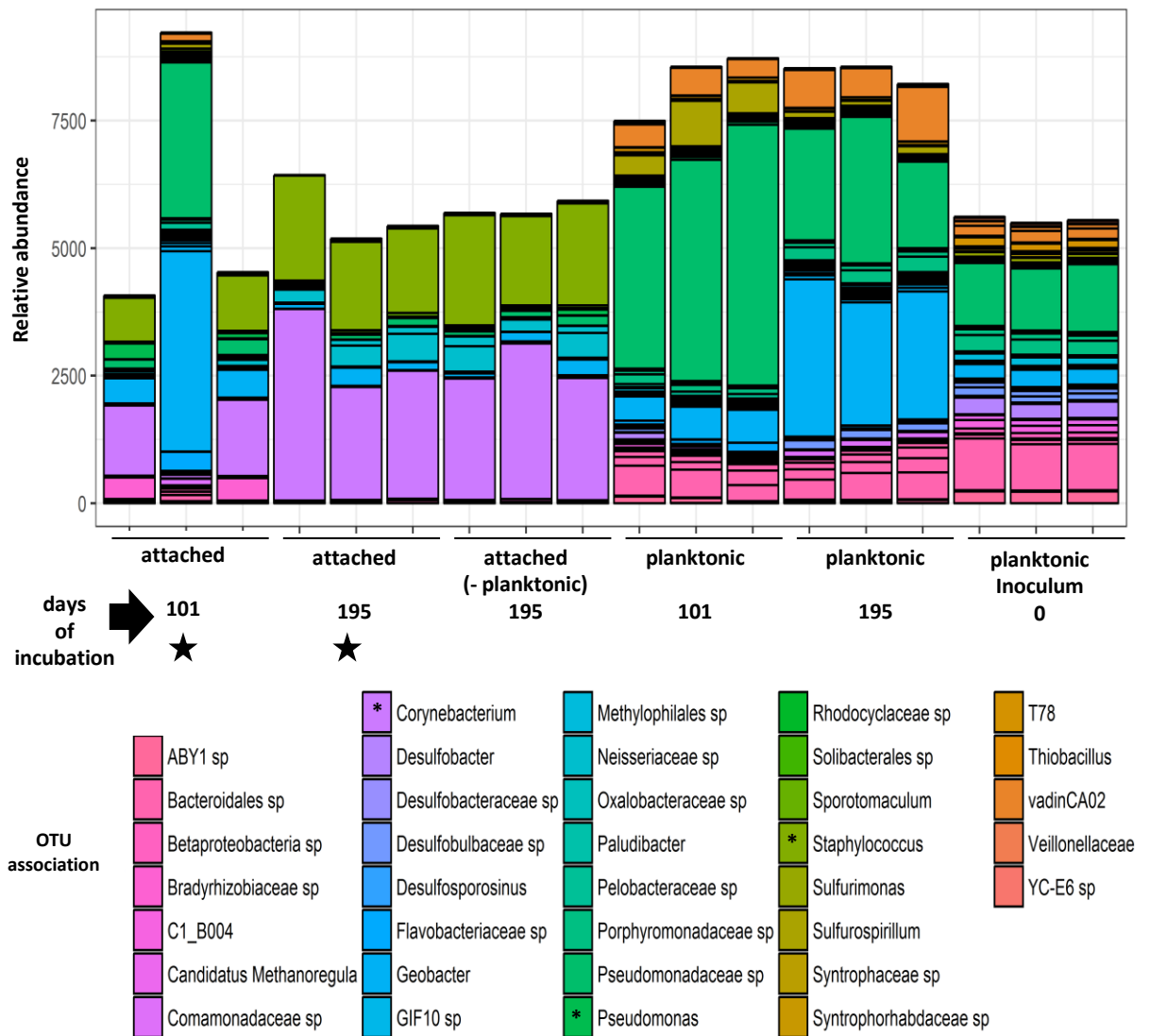


**Figure 3.17.** Deseq analysis between attached communities from medium phenolic microcosms after 101 and 195 days of incubation (\*). OTUs showing statistical differences in the relative abundances between these communities are shown. Note, the relative abundance was normalised to 10,000 counts and (\*) indicates groups which exhibited the larger changes in the relative abundances between these communities.

### High phenolic environment (high).

The microcosms were inoculated with groundwater from BH59, 21 mbgl (see **Figure 3.6** for details). **Figure 4.18** shows different parameters measured in the microcosm. The starting groundwater contained  $\sim 80 \text{ mg l}^{-1}$  phenol,  $\sim 95 \text{ mg l}^{-1}$  cresols (*mp* and *o*) and  $40 \text{ mg l}^{-1}$  xylenols. These concentrations decreased significantly in both treatments during the 195 days duration of the experiment (phenol  $F_{(1,8)}: 22.44$ , *mp*-cresols:  $F_{(1,8)}: 22.44$ , *o*-cresols:  $F_{(1,8)}: 36.02$ , xylenols:  $F_{(1,8)}: 71.68$   $p < 0.05$ , differences for phenol were given between day 101 and 195, whereas for cresols and xylenols, the Tukey's test indicated differences between day 101 with day 1 and 195). Only for xylenols there were significant differences between treatments (treatments:

$F_{(1,8)}$ : 14.18  $p < 0.05$ ). Iron concentrations decreased significantly from an initial concentration of  $\sim 12 \text{ mg l}^{-1}$  to  $1 \text{ mg l}^{-1}$  in both treatments (iron:  $F_{(1,8)}$ : 626.2,  $p < 0.05$ , differences were between day 1, with day 101 and 195). Manganese concentration increased significantly from an initial concentration of  $3 \text{ mg l}^{-1}$  to  $\sim 30 \text{ mg l}^{-1}$  (manganese:  $F_{(1,8)}$ : 75.68,  $p < 0.05$ , differences between all sampling points). Nitrate concentrations were low  $\sim 1 \text{ mg l}^{-1}$  and decreased to  $\sim 0.1 \text{ mg l}^{-1}$ . No statistical differences were detected for nitrate. Sulphate concentrations decreased significantly from  $\sim 6 \text{ mg l}^{-1}$  to  $\sim 4 \text{ mg l}^{-1}$  (sulphate:  $F_{(1,8)}$ : 42.25  $p < 0.05$ , differences were at similar intervals for phenol). For iron, manganese, nitrate and sulphate no differences were detected between treatments.

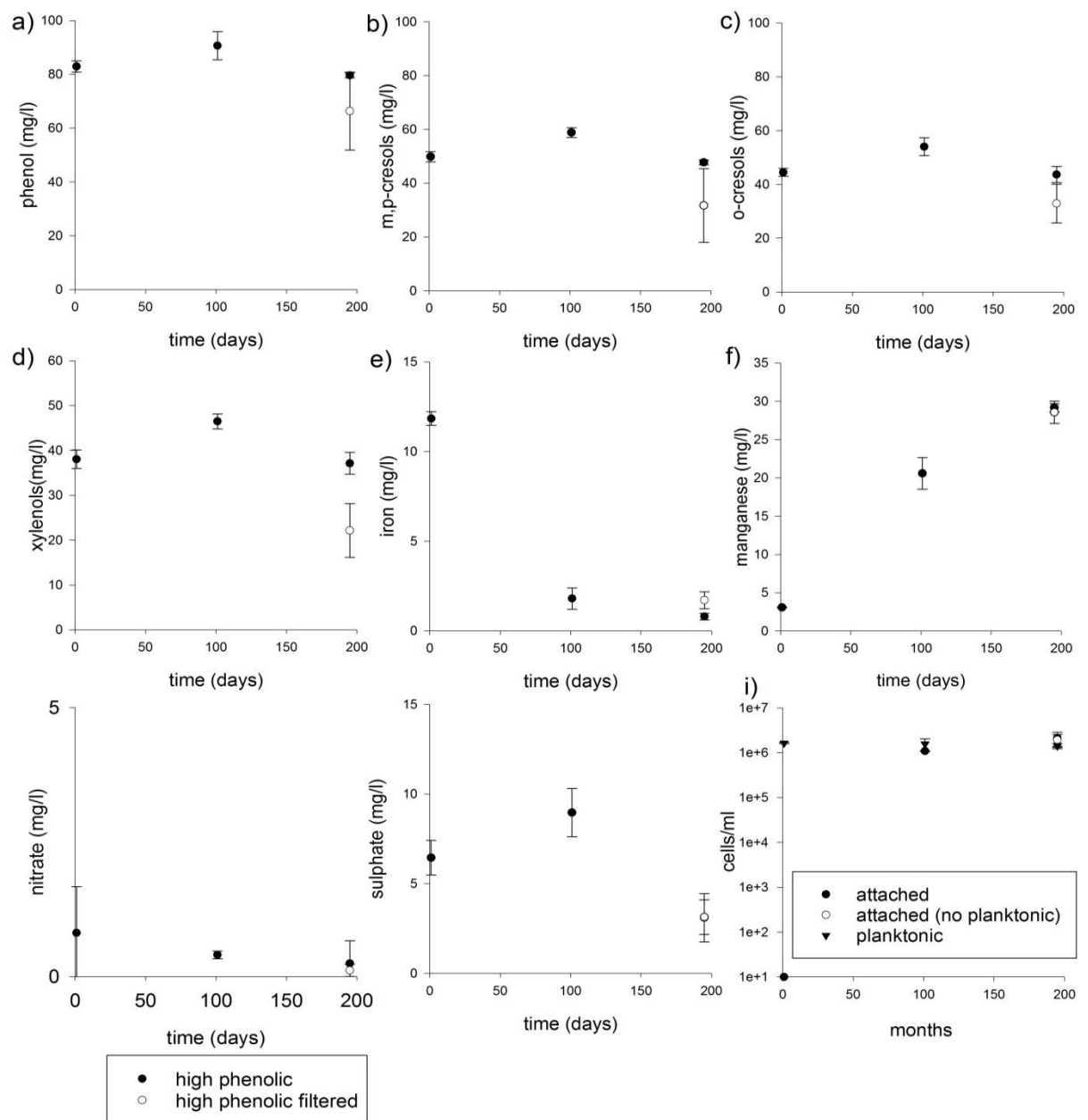


**Figure 3.18.** Monitoring of different chemical species in microcosms inoculated with groundwater from 21mbgl. Error bars represent the standard deviation of replicates (n=3). Legend from lower left corner applies for all graphs except for the cell densities in i.

In the field, cell numbers at 21 mbgl were  $\sim 10^6$  cells  $\text{ml}^{-1}$ . After 195 days of incubation in the microcosms the cell densities in the supernatant were similar to the values observed in the field. In the attached phase, the cell numbers reach  $\sim 10^6$  cells per ml of saturated sediments after 101 days months of incubation. The cell numbers of the attached communities after 195 days of total incubation in both treatments were similar.

The mass balances of the different electron acceptors consumed due to biodegradation, did not explain the decrease in pollutant concentrations observed in these treatments. TPC consumed was of  $34.69 \text{ mg l}^{-1}$  and the total nitrate consumption within the experiment was of  $1.17 \text{ mg l}^{-1}$ , according to the mass balances for nitrate reduction and denitrification, these processes could have biodegraded a total of  $0.36$  and  $0.91 \text{ mg l}^{-1}$  of TPC respectively. Furthermore, the increase on manganese concentration due to manganese reduction from manganese oxides during the experiment was of  $25.79 \text{ mg l}^{-1}$ . This increase could allow a maximum of  $4.65 \text{ mg l}^{-1}$  of TPC biodegraded through this mechanism. Also, the decrease in sulphate concentration was of  $4.43 \text{ mg l}^{-1}$ , could explain a TPC decrease through biodegradation of  $3.19 \text{ mg l}^{-1}$ . In total, the use of the different electron acceptors could explain only  $9.11 \text{ mg l}^{-1}$  of the total reduction of pollutants, which is a 26.3% of the biodegradation of the pollutants analysed.

**Figure 3.19** shows the PCoA weighted analysis on the microbial community. The analysis showed a shift in the community structures from field samples (inoculum), to samples from the attached and planktonic communities after 101 days of incubation in the microcosms. In the microcosms the attached and planktonic communities develop their community structures towards different directions (similar trends in microcosms formed with groundwater from low and medium environments. The biofilm communities tend to be more dispersed after 101 days of incubation, but after 195 of total incubation these communities tend to be relatively similar. On the other hand, the planktonic community structures differ over the monitoring period in the microcosm.

**Figure 3.20** shows Deseq analysis which contrasted the planktonic samples from the field and microcosm planktonic samples after 101 days. The contrast indicated a significant change in the relative abundance of the *Syntrophobacterales* sp. and *Desulfobacteraceae* sp., which decreased largely their presence from the field and after 3 months of incubation in the lab. Similar significant trends were observed for *Candidatus methanoregula* and *Desulfosporosinus* sp. This was an indication that changes in high phenolic treatment is related to different OTUs (compared to the shift in the low and medium phenolic treatments), and represents a different environment both chemically and biologically.



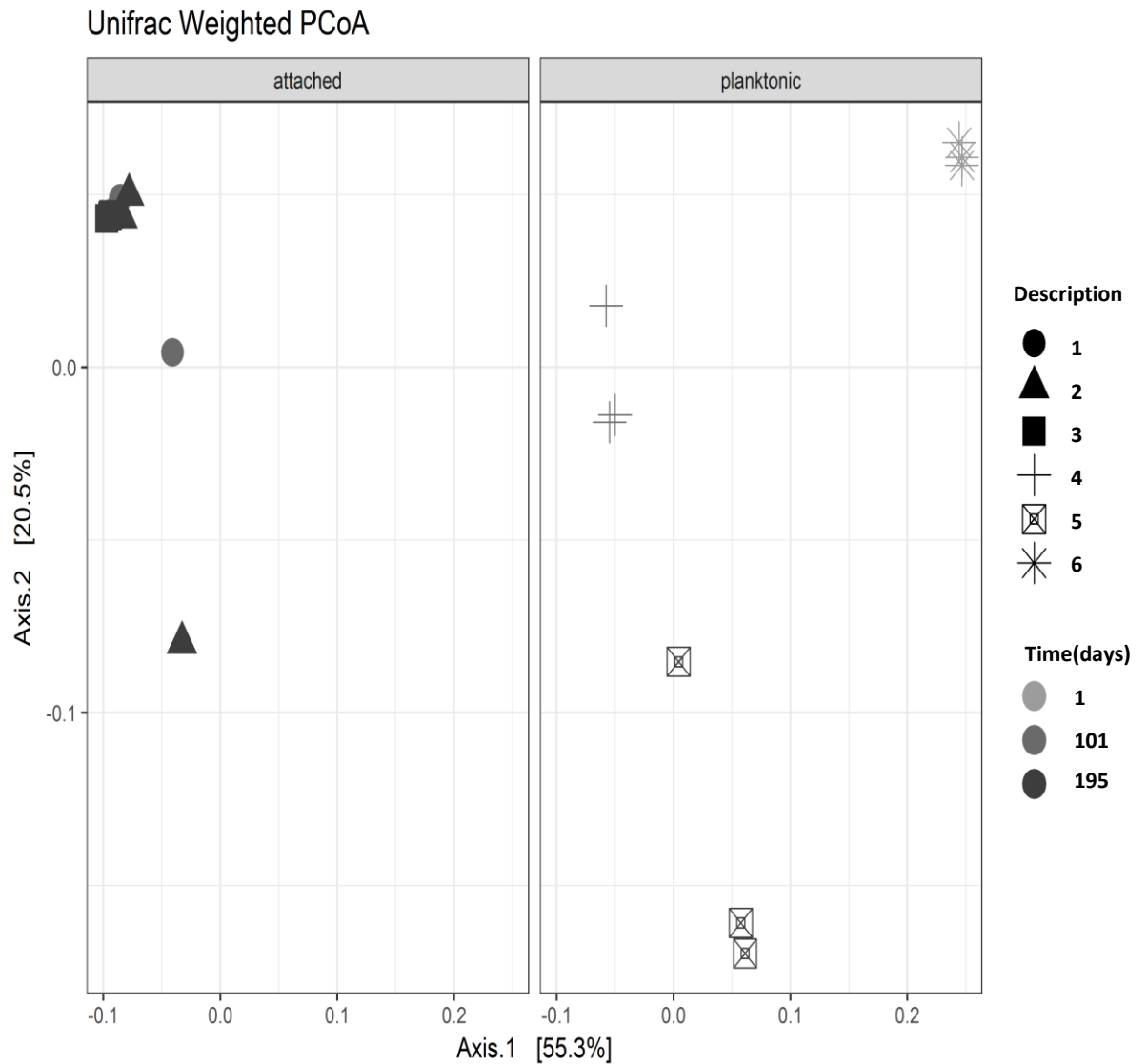


**Figure 3.19.** Unifrac weighted Principal coordinate analysis of attached and planktonic communities harvested from microcosms inoculated with groundwater from a high phenolic environment. Note 1 and 2, attached communities after 101 and 195 days of incubation in a microcosm. 3, attached community formed after the removal of the planktonic community. 6, planktonic community from 11 mbgl (inoculum); 4 and 5, planktonic communities after 101 and 195 days of incubation respectively.

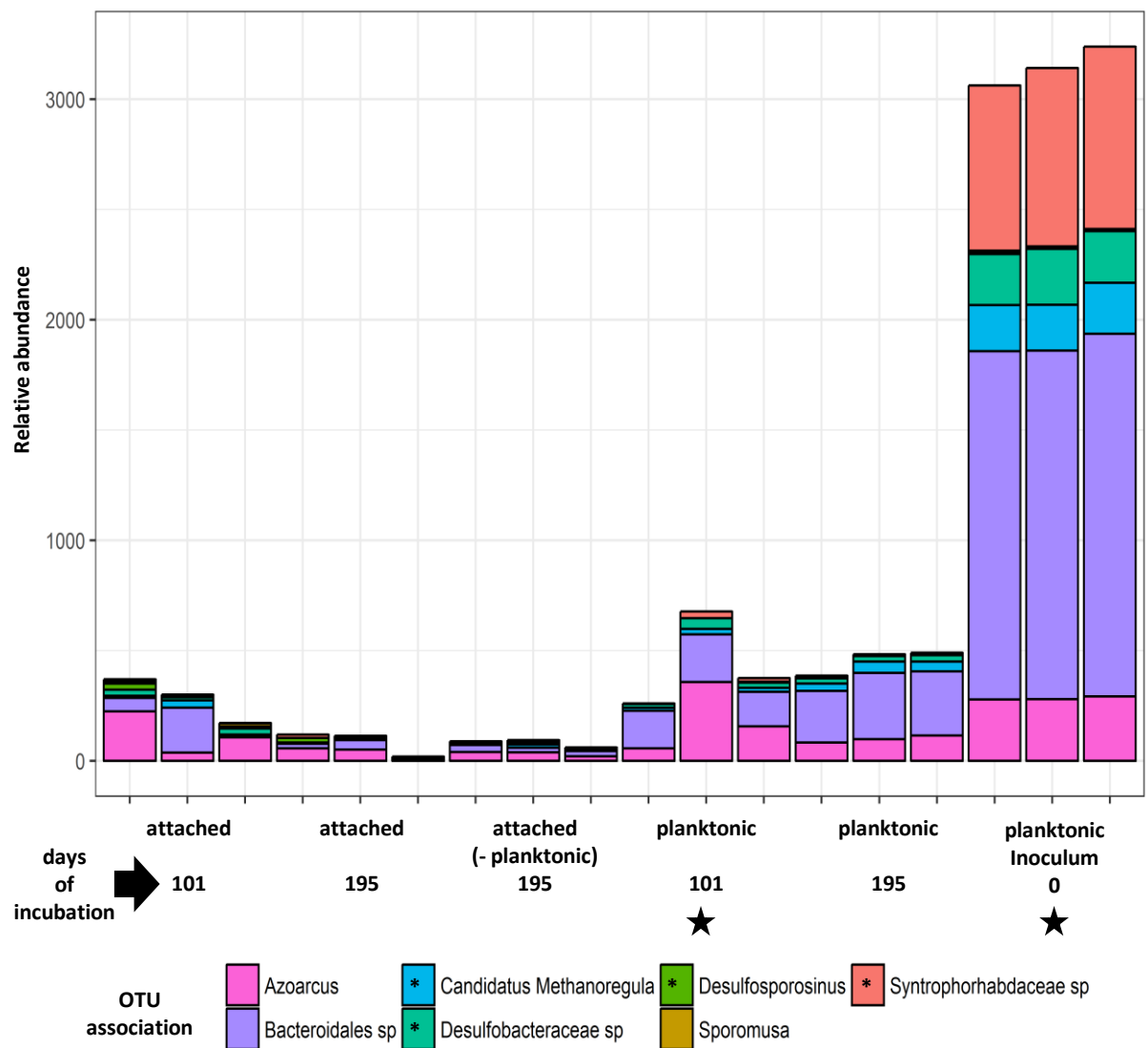


**Figure 3.20.** Deseq analysis between planktonic samples in the high phenolic environment inoculum and the planktonic community after 101 days of incubation (\*). OTUs showing statistical differences in the relative abundances between these communities are shown. Note, the relative abundance was normalised to 10,000 counts and (\*) indicates groups which exhibited the larger changes in the relative abundances between these communities.

PCoA indicated that community structures of the biofilm after 3 months of incubation were more distant from each other and different from the community structures of the biofilm after 6 months of incubation. **Figure 3.21** shows a Deseq analysis which contrasted the attached communities considering the effect of time. The contrast of these samples indicated significant changes, largely explained for 1 replicate of the biofilm after 101 days of incubation, which had high relative abundances of *Pseudomonadaceae* sp. and *Geobacter*, which then almost disappear. After 195 days of total incubation the relative abundance of *Staphylococcus* increased significantly in the biofilm.

PCoA showed similarity between the community structures of biofilms settled after 6 months of incubation. In **Figure 3.21** the contrast between the attached communities formed after 195 days, considering the effect of the geochemical environment can be visualised. The contrast of these samples indicated a significant change in the relative abundances of *Fusobacterium* and *Staphylococcus*; which is explained for the variation in two replicates of the biofilm settled after 195 days of incubation.

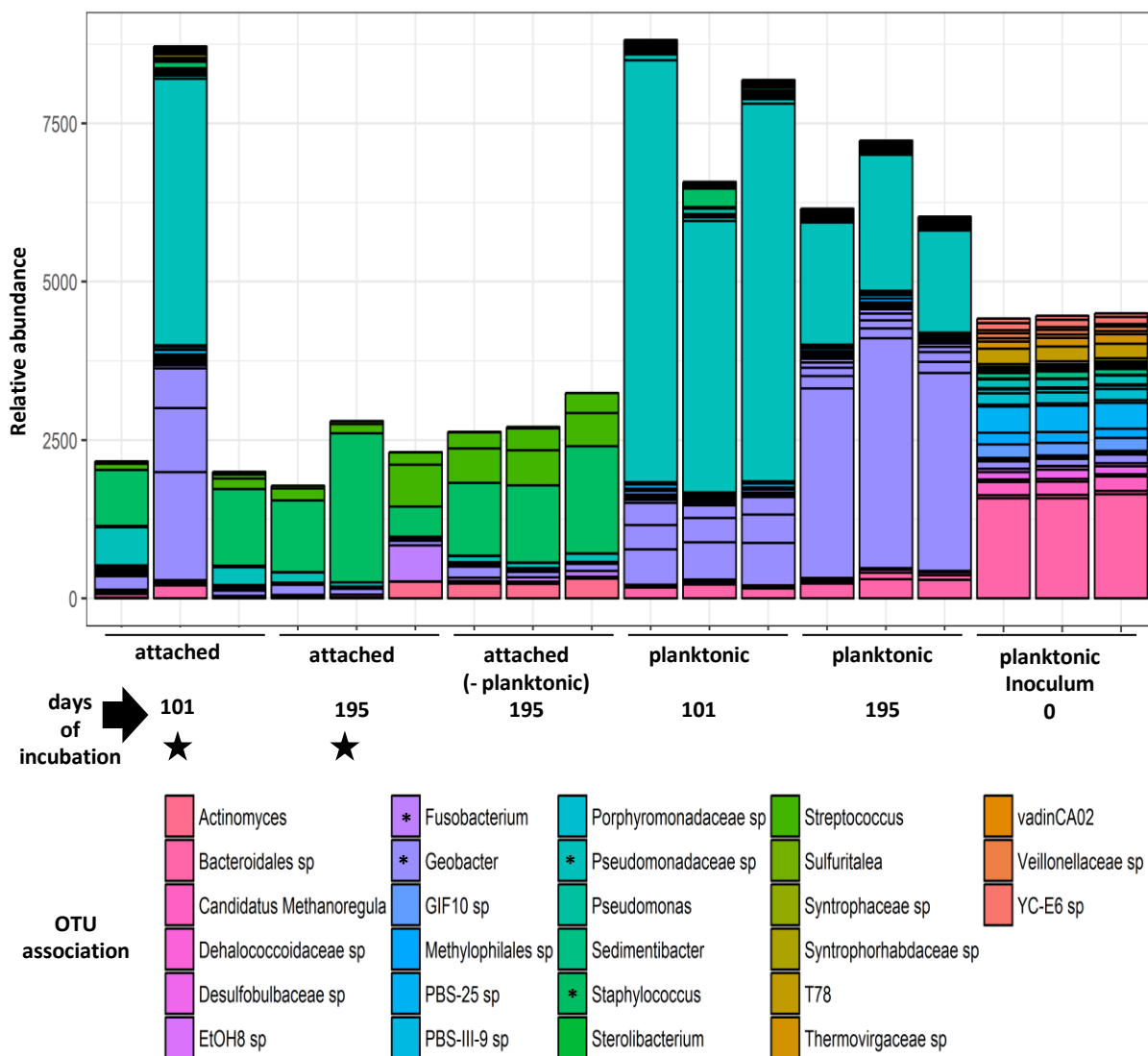


**Figure 3.21.** Deseq analysis between attached communities from high phenolic microcosms after 101 and 195 days of incubation (\*). OTUs showing statistical differences in the relative abundances between these communities are shown. Note, the relative abundance was normalised to 10,000 counts and (\*) indicates groups which exhibited the larger changes in the relative abundances between these communities.

**Plume advance 1 (adv\_1), change from a low to medium phenolic environment, see Figure 3.7 for details.**

The plume advance 1 treatments were constructed using sediments from low phenolic microcosms and the supernatant of the medium phenolic microcosms. Both phases were put together after 101 days of independent incubation. Residual pore water was contained in the sediments after the removal of the supernatant and was geochemically related to the supernatant of the low phenolic treatment. This volume was considered to calculate the expected concentration of different chemical species, as a result of the mixing between the new supernatant (medium phenolic) and the residual pore water (low phenolic). **Figure 3.22** shows different parameters measured in the microcosm recreating this change of condition.

The expected concentration purely by mixing was calculated considering residual pore water (29 ml) plus the supernatant (81 ml). The expected concentrations were  $\sim 5 \text{ mg l}^{-1}$  phenol,  $47 \text{ mg l}^{-1}$  *m,p,o*-cresols and  $\sim 25 \text{ mg l}^{-1}$  *xilenols*. Nevertheless, the real pollutant concentrations were lower in both treatments, except for phenol. No statistical differences were found between the filtered and the unfiltered treatments. The difference between the expected concentration purely by dilution and the observed concentration was related to biodegradation of these compounds.

For the mass balances of the electron acceptors (EA), the differences between the expected and real EA was taken into account. These differences could explain the variation between the expected pollutant concentration and the real phenolic content in these treatments at the end of the experiment.

The total amount of *m,p,o*-cresols and *xilenols* consumed was  $20.72 \text{ mg l}^{-1}$ ; and the reduction of sulphate related to sulphate reduction was  $5.98 \text{ mg l}^{-1}$ , and this amount could have biodegraded  $4.31 \text{ mg l}^{-1}$ . The increasing of iron was  $2.05 \text{ mg l}^{-1}$ , this amount could have biodegraded  $0.18 \text{ mg l}^{-1}$  of TPC. The difference between the expected nitrate content and the real nitrate concentration was  $7.11 \text{ mg l}^{-1}$ , this amount according to the mass balances on the nitrate reduction and denitrification could have biodegraded a total of  $1.43$  and  $3.57 \text{ mg l}^{-1}$  of TPC respectively. No statistical differences between the filtered and the unfiltered treatments recreating the change of environment were found for sulphate, iron and nitrate. In summary, the estimated biodegradation of the TPC was  $9.5 \text{ mg l}^{-1}$ , which is explained in 45.9 % by the changes of the EA concentrations after the plume advance 1.

The cell numbers of the supernatant of the medium phenolic microcosms were  $\sim 10^6 \text{ cells ml}^{-1}$ . After being in contact with sediments from low phenolic microcosms, cell numbers remain

stable after 195 days of total incubation. The cell numbers of the biofilm before the change of conditions reached  $\sim 10^6$  cells per ml of saturated sediments. This value increased slightly after the change of conditions. In the filtered plume advance 1 cell densities remained stable.

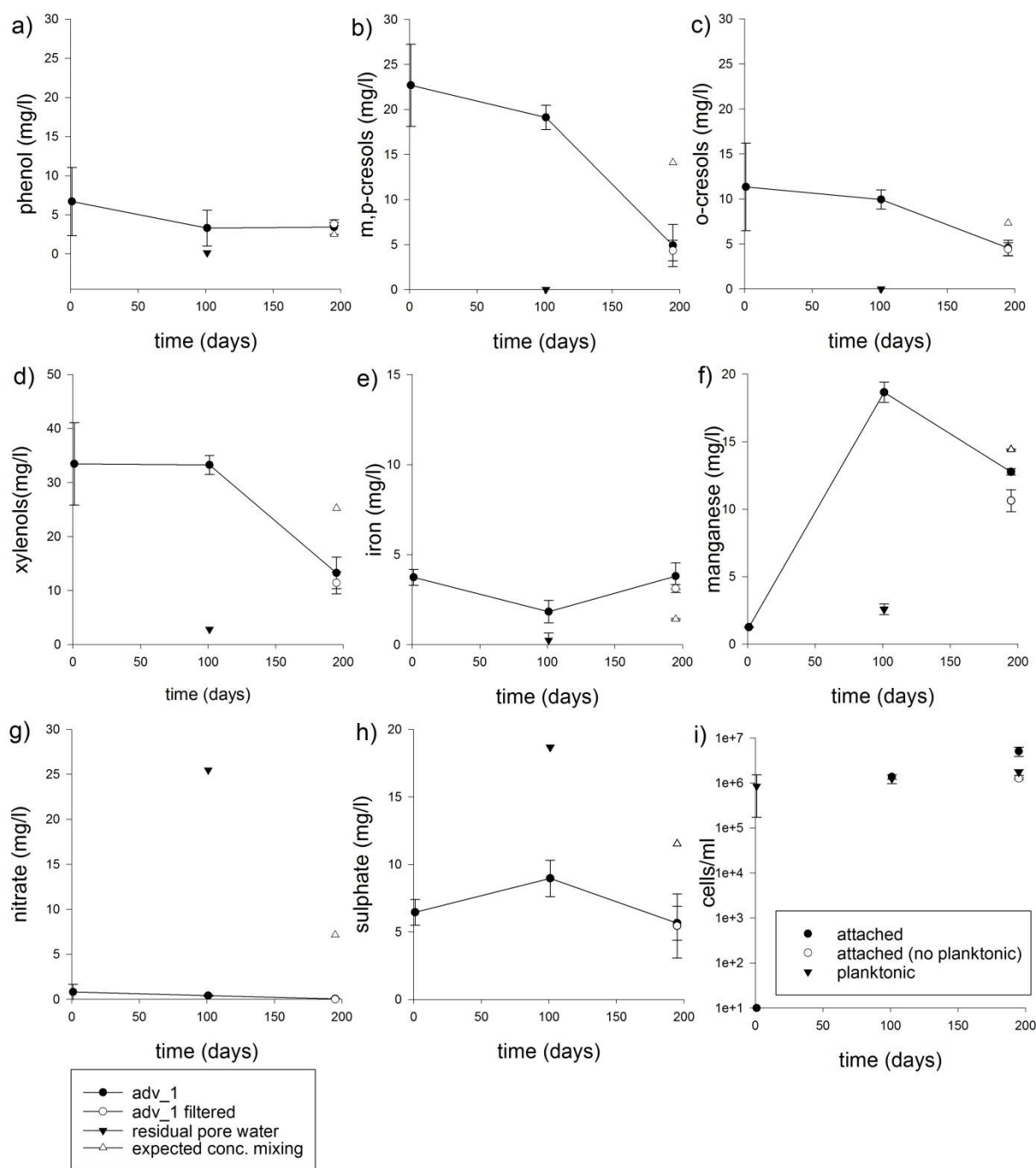


**Figure 3.22.** Monitoring of different chemical species in microcosms recreating the adv\_1. Legend from lower left corner applies for all graphs except for the cell densities in i. Note, adv\_1 was constructed with sediments from low phenolic microcosms and the supernatant of the medium phenolic microcosms. adv\_1 filtered, planktonic community was removed before putting these phases together. Residual pore water was contained in the sediments after the removal of the supernatant. Expected conc. mixing was the predicted concentration as a result of the mixing between the new supernatant (medium phenolic) and the residual pore water (low phenolic).

**Figure 3.23** shows the PCoA weighted analysis on the microbial community. It was possible to observe that the attached communities after the change of conditions (adv\_1) were relatively similar to the biofilm communities without any interventions (attached communities from low phenolic microcosms after 195 days of incubation). The planktonic communities of the adv\_1 treatment, at the end of the experiment shift in the opposite direction of planktonic communities from medium phenolic microcosms, after 195 days of incubation. This direction is towards the planktonic communities found in the low phenolic microcosms after 195 days of incubation

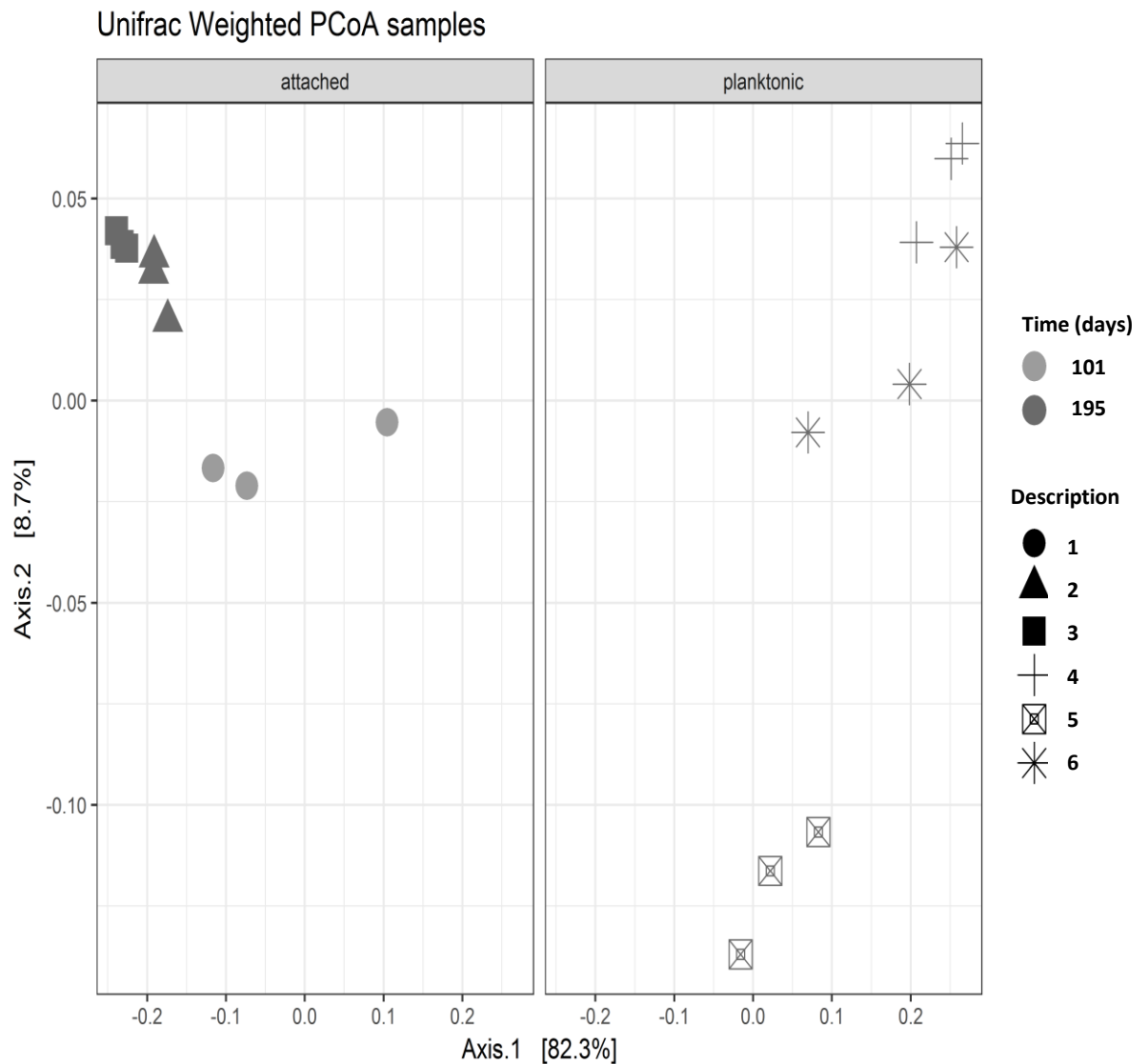


**Figure 3.23.** Unifrac weighted Principal coordinate analysis of attached and planktonic communities harvested from microcosms recreating the adv\_1. Note, 1 and 2 attached communities after 101 and 195 days of incubation in a microcosm inoculated with groundwater from a low phenolic environment. 3, attached community after 195 days which experimented the change from a low to a medium phenolic environment. 4, planktonic community after 195 days of incubation in low phenolic microcosms. 5, planktonic communities after 195 days of incubation in a microcosm inoculated with medium phenolic contents. 6, planktonic community after plume advance 1.

In the sediments prior to the change of conditions, there was residual water which it was not possible to remove and therefore there was a residual planktonic community. The effect on the planktonic adv\_1 community was explored through the simulation of a planktonic synthetic community. The simulated community was calculated considering the planktonic communities of the low and medium phenolic microcosms after 195 days of incubation and the volume of each one in the final arrangement (29 and 81 ml, respectively). **Figure 3.24** shows the Unifrac PCoA weighted of planktonic communities. The synthetic community was between the original communities. The planktonic community resulting after the change of conditions was distant from this zone. Therefore, there was an influence of the biofilm community on the community structure of the planktonic community.

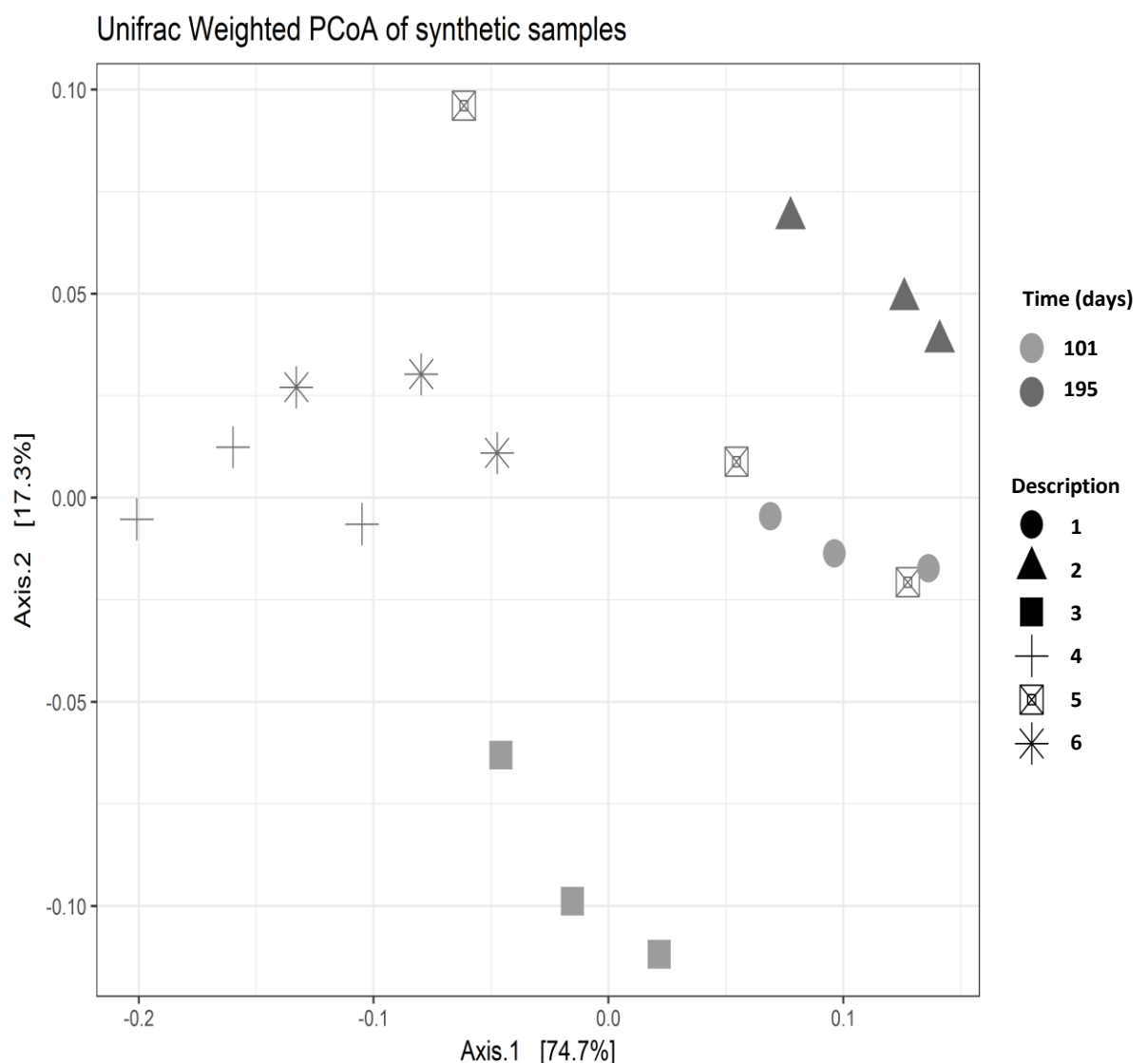


**Figure 3.24.** Unifrac weighted Principal coordinate analysis of planktonic communities related to plume advance 1 treatment. Note 1 and 2, planktonic communities after 101 and 195 days of incubation in a microcosm inoculated with groundwater from a low phenolic environment. 3 and 4, planktonic communities after 101 and 195 days of incubation in a microcosm inoculated with groundwater from a medium phenolic environment. 5, planktonic community after adv\_1. 6, synthetic planktonic community.

PCoA indicated that community structures of samples of the biofilm formed after 195 days of incubation with low phenolic microcosms were close from the biofilm after the change of conditions. **Figure 3.25** shows a Deseq analysis which contrasted these attached communities considering the impact of change of conditions. The contrast of these samples indicated significant differences, but these differences were related to higher relative abundances of different OTUs in the biofilm which experience the change of environment, but these differences represented less than 5% change. Furthermore, there are significant differences related to higher abundances of *Streptophyta* in the biofilm settled after 6 months of incubation, but the large difference is related to 1 replicate.

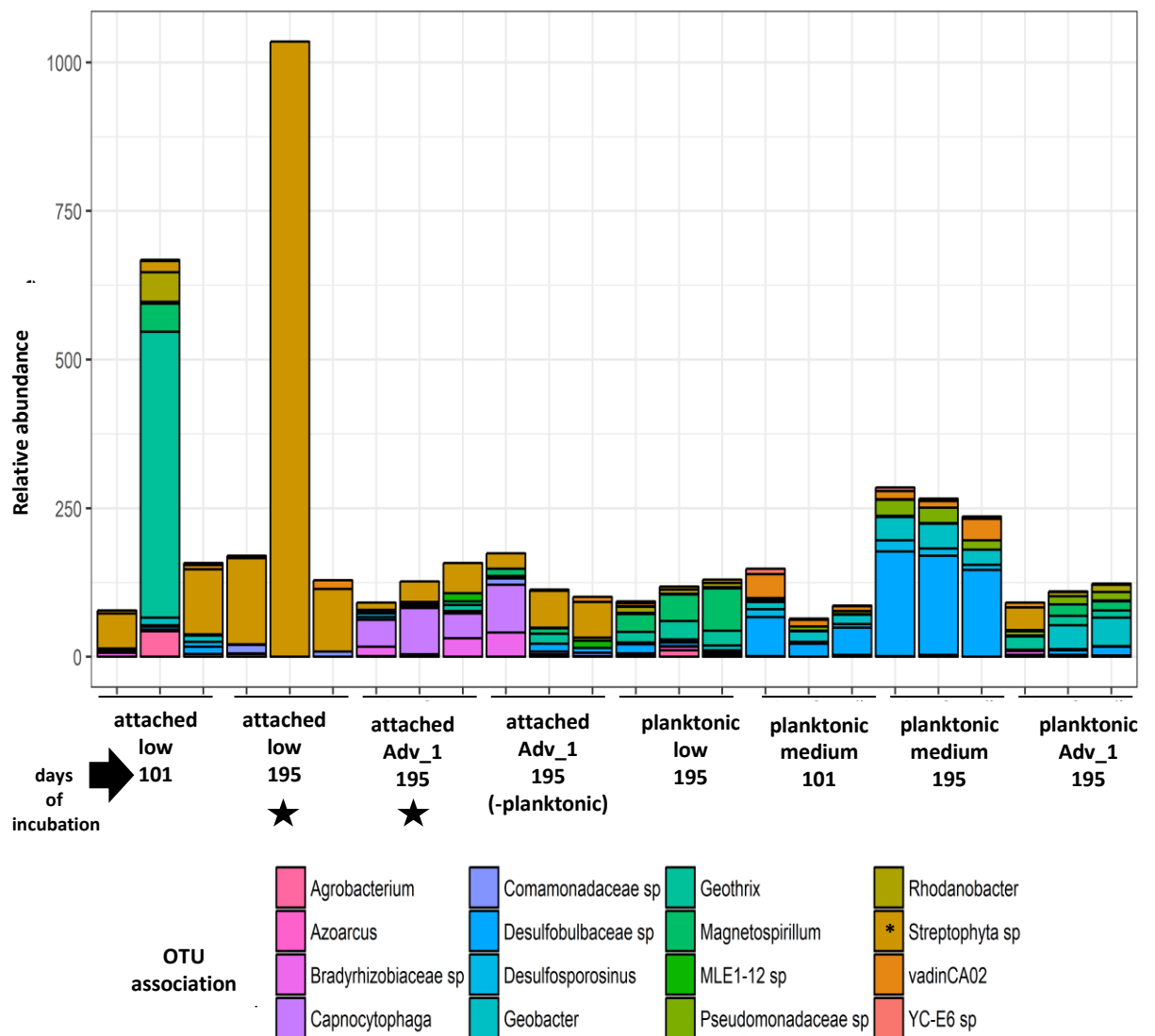


**Figure 3.25.** Deseq analysis between biofilms related to plume advance 1 treatment (\*). OTUs showing statistical differences in the relative abundances between these communities are shown. Note, the relative abundance was normalised to 10,000 counts and (\*) indicates groups which exhibited the larger changes in the relative abundances between these communities.



Figure 3.26 shows a Deseq analysis which contrasted the attached communities formed after the change of conditions considering the effect of the geochemical environment (through the removal of the planktonic community). The contrast of these samples indicated significant change on the relative abundances of different OTUs, but these differences represent less than 1%.

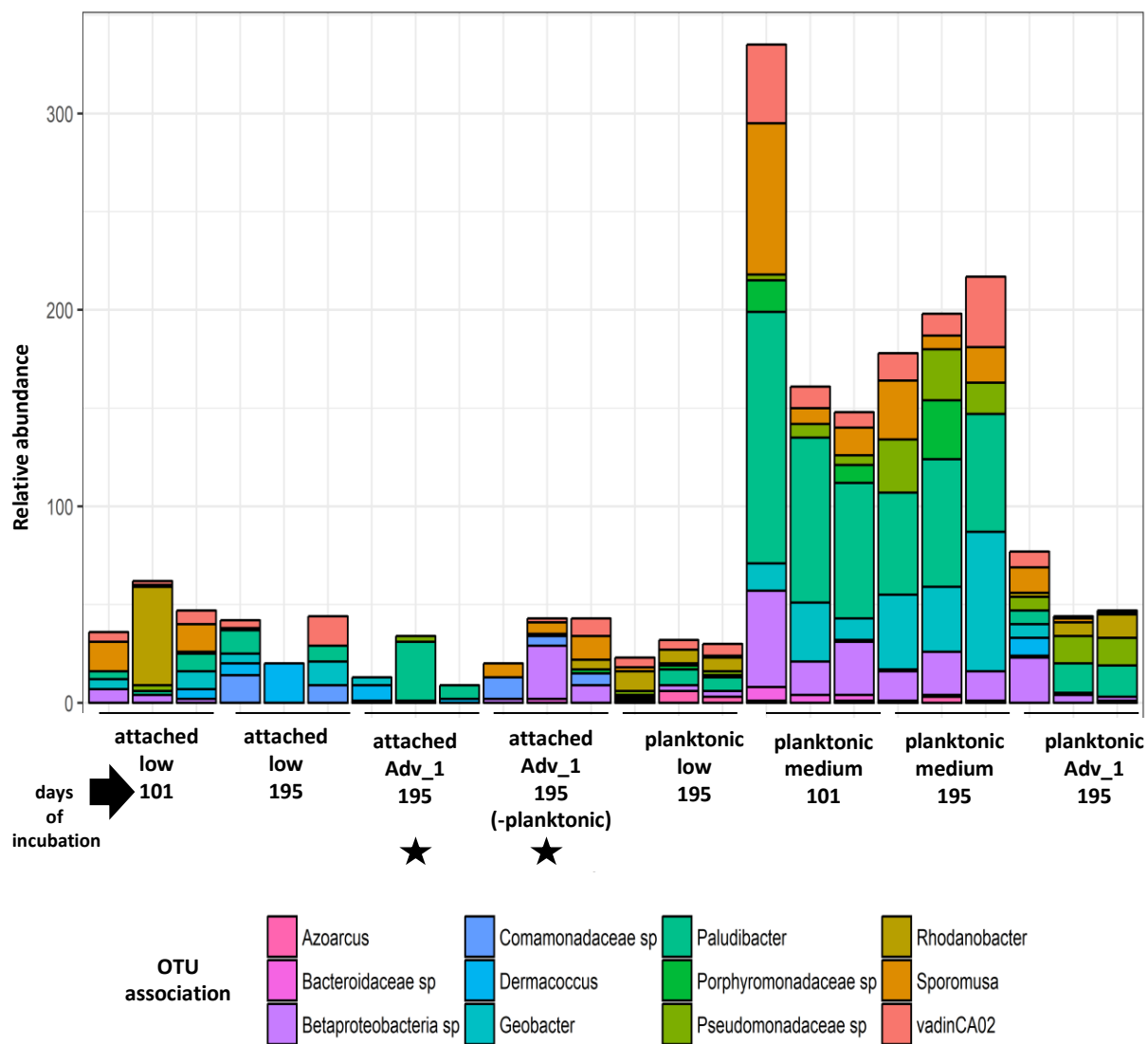


Figure 3.26. Deseq analysis between biofilms related to plume advance 1 treatment considering the effect of the geochemical environment, through the removal of the planktonic community (\*). OTUs showing statistical differences in the relative abundances between these communities are shown. Note, the relative abundance was normalised to 10,000 counts.

**Plume advance 2 (adv\_2), change from a medium to high phenolic environment, see Figure 3.7 for details.**

The plume advance 2 treatments were constructed using sediments from medium phenolic microcosms and the supernatant of the high phenolic microcosms. Both phases were put together after 101 days of independent incubation. Residual pore water was contained in the sediments after the removal of the supernatant and was geochemically related to the supernatant of the medium phenolic treatment. This volume was considered to calculate the expected concentration of different chemical species, as a result of the mixing between the new supernatant (high phenolic) and the residual pore water (medium phenolic). **Figure 4.27** shows different parameters measured in the microcosm recreating this change of condition.

The expected concentration purely by mixing was calculated using residual pore water (29 ml) plus the supernatant (81 ml). The expected concentrations were,  $\sim 70 \text{ mg l}^{-1}$  phenol,  $95 \text{ mg l}^{-1}$  *m,p,o*-cresols and  $\sim 42 \text{ mg l}^{-1}$  xylenols. Nevertheless, actual pollutant concentrations were lower in both treatments. No statistical differences were found between the filtered and the unfiltered treatments.

The total amount of phenol, *m,p,o*-cresols, and xylenols consumed were  $48.60 \text{ mg l}^{-1}$ ; and the reduction on sulphate related to sulphate reduction was of  $14.55 \text{ mg l}^{-1}$ , this amount could have biodegraded  $10.49 \text{ mg l}^{-1}$  phenols. The increasing of iron was  $18.01 \text{ mg l}^{-1}$ . This amount could have biodegraded  $1.70 \text{ mg l}^{-1}$  TPC. The difference between the expected nitrate content and the real nitrate concentration was  $0.3 \text{ mg l}^{-1}$ . This amount according to the mass balances on the nitrate reduction and denitrification could have biodegraded a total of  $0.09$  and  $0.23 \text{ mg l}^{-1}$  of TPC respectively. In summary, the estimated biodegradation of the TPC was  $48.6 \text{ mg l}^{-1}$ , which is explained in 29.5 % by the changes of the EA concentrations after the plume advance 2. No statistical differences between the filtered and the unfiltered treatments recreating the change of environment were found for sulphate and nitrate. Nevertheless, there were statistical differences between treatments for iron. In summary, the estimated biodegradation of the TPC was  $9.5 \text{ mg l}^{-1}$ , which is explained in a 45.9% by the changes on the EA concentrations after the plume advance 1.

The cell numbers of the supernatant in the high phenolic microcosms were  $\sim 10^6 \text{ cells ml}^{-1}$ . After being in contact with sediments from medium phenolic microcosms cell numbers remain stable after 6 months of total incubation. The cell numbers of the biofilm before the change of conditions reached  $\sim 10^6 \text{ cells per ml}$  of saturated sediments. This value remained stable after the change of conditions.

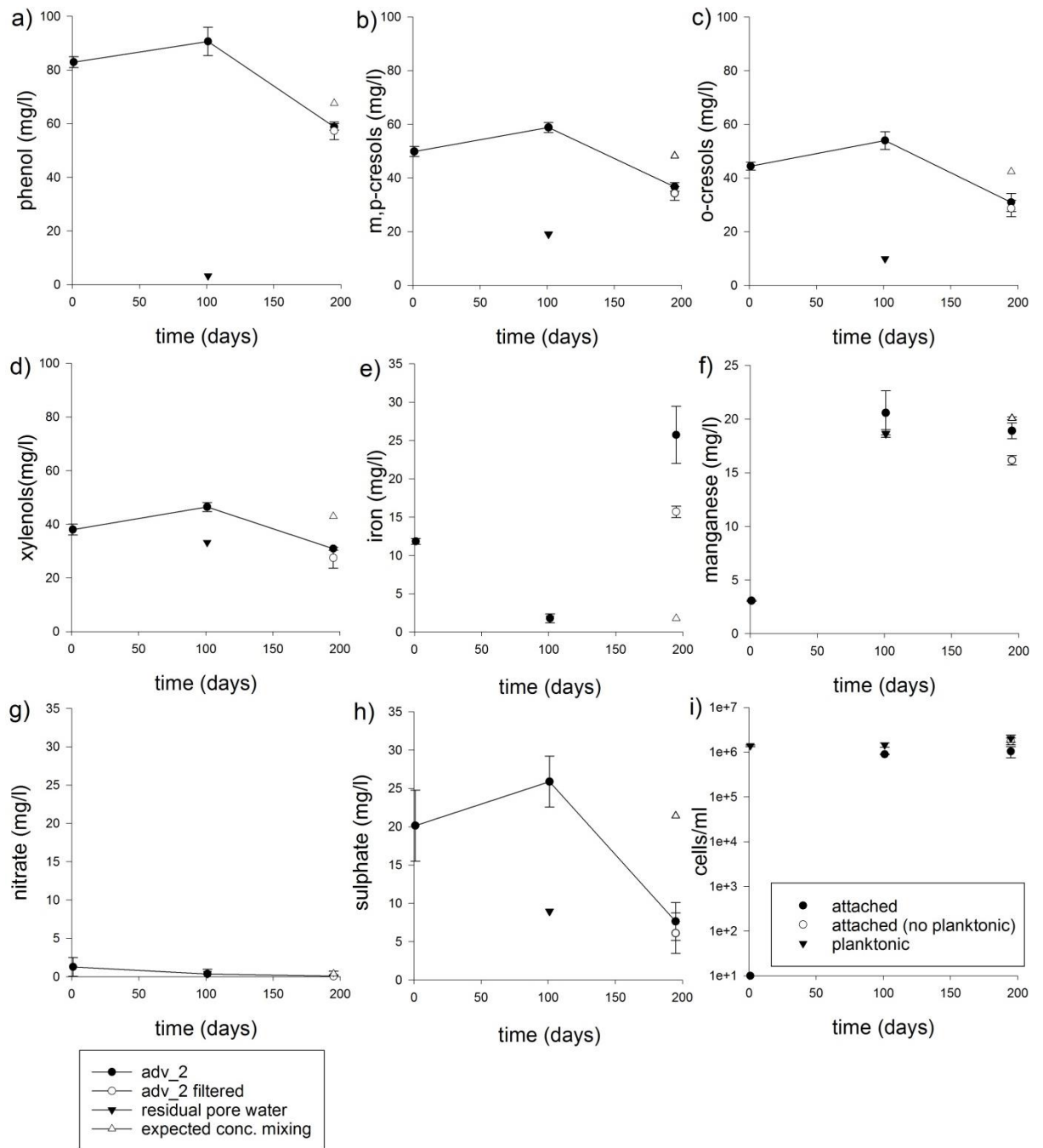


**Figure 3.27.** Monitoring of different chemical species in microcosms recreating the adv\_2. Legend from lower left corner applies for all graphs except for the cell densities in i. Note, adv\_2 was constructed with sediments from medium phenolic microcosms and the supernatant of the high phenolic microcosms. adv\_2 filtered, planktonic community was removed before putting these phases together. Residual pore water was contained in the sediments after the removal of the supernatant. Expected conc. mixing was the predicted concentration as a result of the mixing between the new supernatant (high phenolic) and the residual pore water (medium phenolic).

**Figure 3.28** shows the PCoA weighted analysis of the microbial community. It was possible to observe that attached communities after the change of conditions (adv\_2) were relatively similar to the biofilm communities without any interventions (attached communities from medium phenolic microcosms after 195 days of incubation). The planktonic communities of the adv\_2 treatments, at the end of the experiment shift towards the planktonic communities of the medium and high phenolic microcosms after 195 days of incubation.

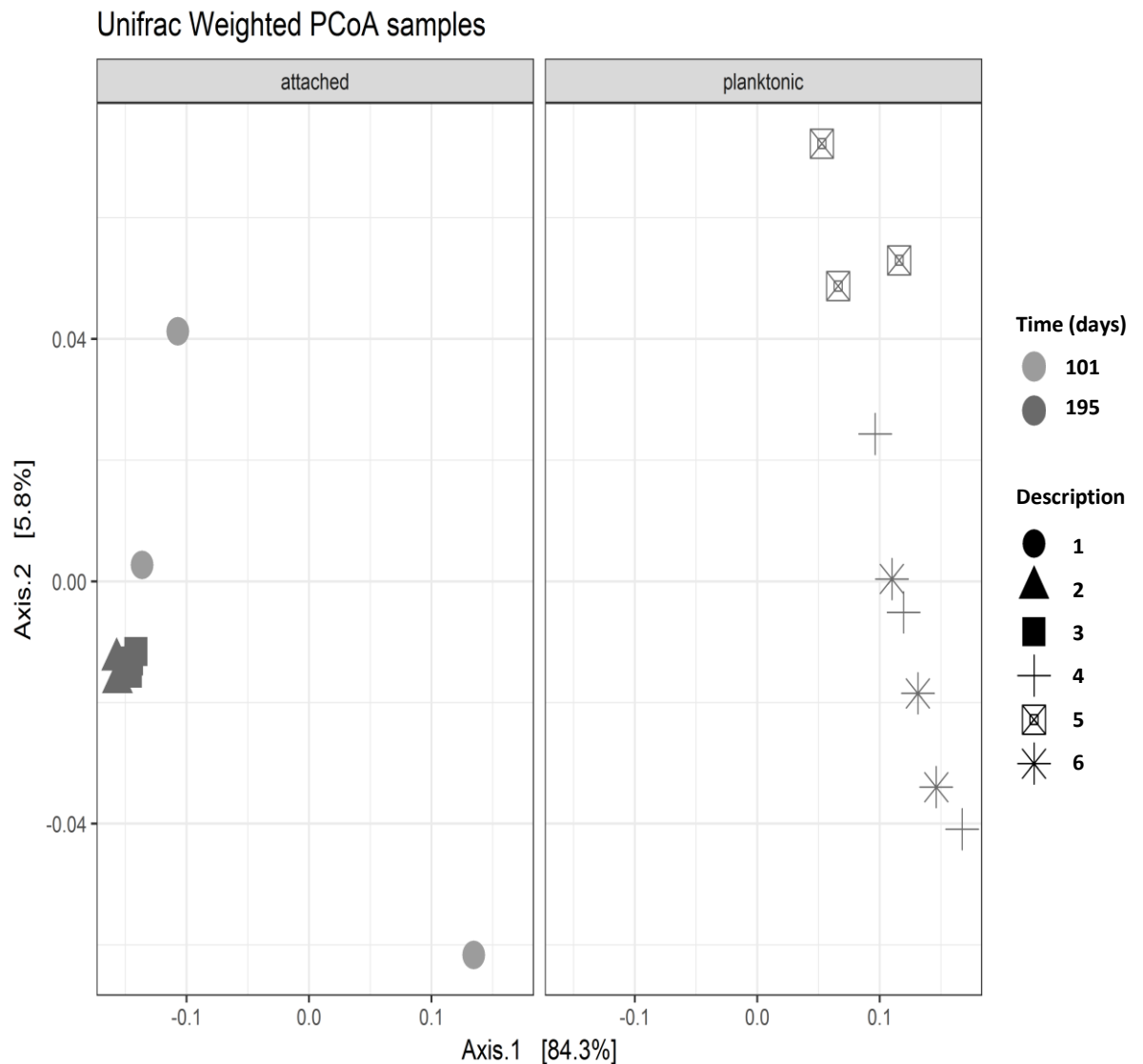


**Figure 3.28.** Unifrac weighted Principal coordinate analysis of attached and planktonic communities harvested from microcosms recreating the adv\_2. Note, 1 and 2 attached communities after 101 and 195 days of incubation in a microcosm inoculated with groundwater from a medium phenolic environment. 3, attached community after 195 days which experimented the change from a medium to a high phenolic environment. 4, planktonic community after 195 days of incubation in medium phenolic microcosms. 5, planktonic communities after 195 days of incubation in a microcosm inoculated with high phenolic content. 6, planktonic community after plume advance 2.

In the sediments previous to the change of conditions there was residual water, which was not possible to be removed, and in this residual groundwater there was a residual planktonic community. The effect of this on the planktonic adv\_2 community was explored through the simulation of a planktonic synthetic community. The simulated community was calculated considering the planktonic communities of the medium and high phenolic microcosms after 195 days of incubation and the volume of each one in the final arrangement (29 and 81 ml, respectively). **Figure 3.29** shows the Unifrac PCoA weighted of planktonic communities. The synthetic communities were located between the original communities. The planktonic community resulting after the change of conditions was distant from this zone. Therefore, there was an influence of the biofilm community on the community structure of the planktonic community.

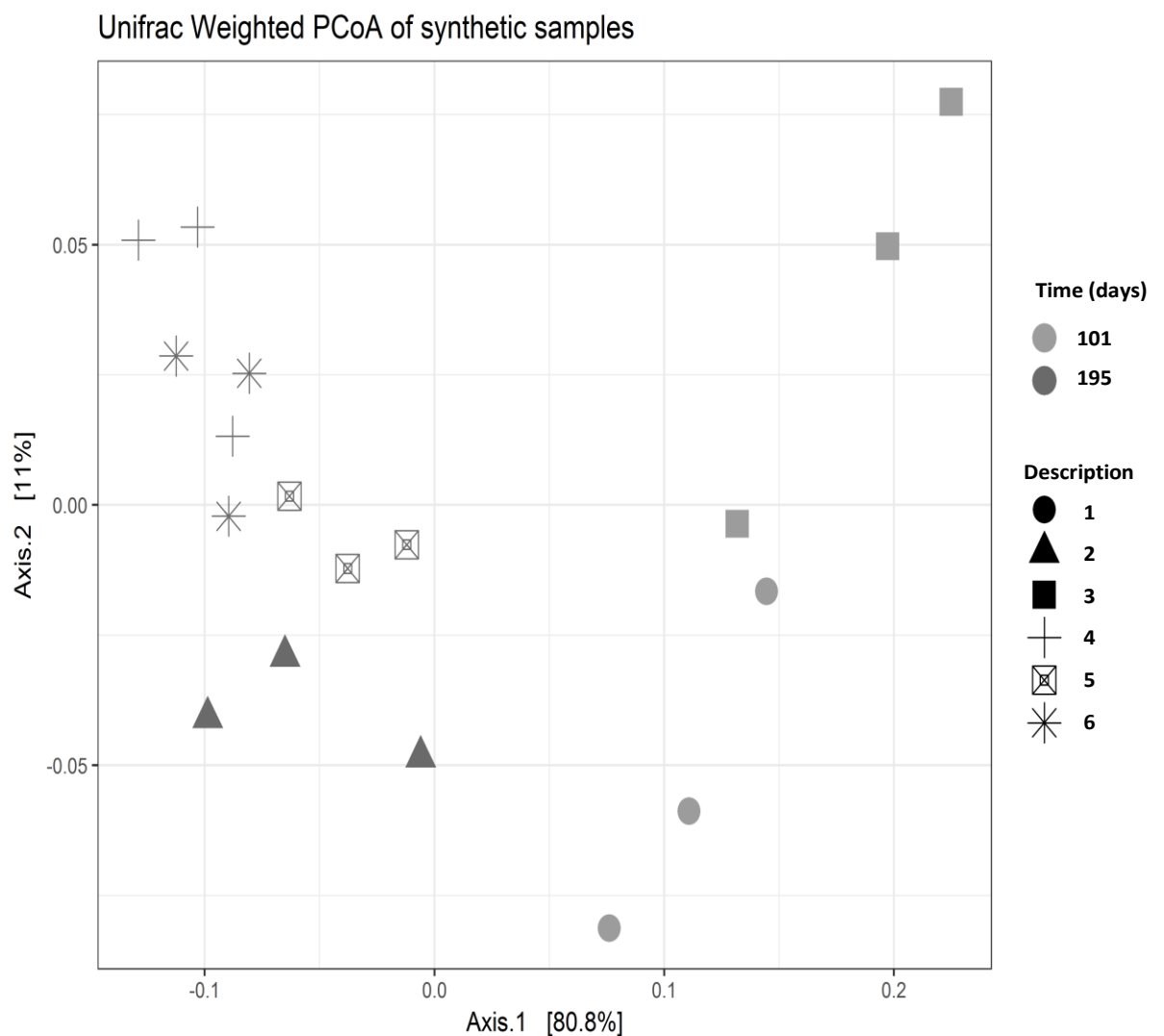


**Figure 3.29.** Unifrac weighted Principal coordinate analysis of planktonic communities related to plume advance 2 treatment. Note 1 and 2, planktonic communities after 101 and 195 days of incubation in a microcosm inoculated with groundwater from a medium phenolic environment. 3 and 4, planktonic communities after 101 and 195 days of incubation in a microcosm inoculated with groundwater from a high phenolic environment. 5, planktonic community after adv\_2. 6, synthetic planktonic community.

PCoA indicated that the biofilm community structures formed after 195 days of incubation with medium phenolic microcosms were similar to the biofilm after the change of conditions. **Figure 3.30** shows a Deseq analysis which contrasted these attached communities considering the impact of a change in conditions. The contrast of these samples indicated significant changes. These differences were related to higher relative abundances of *Corynebacterium* and *Neisseriaceae* in the biofilm formed with groundwater from the medium phenolic environment, and these groups were still present in the biofilm after the change of conditions.

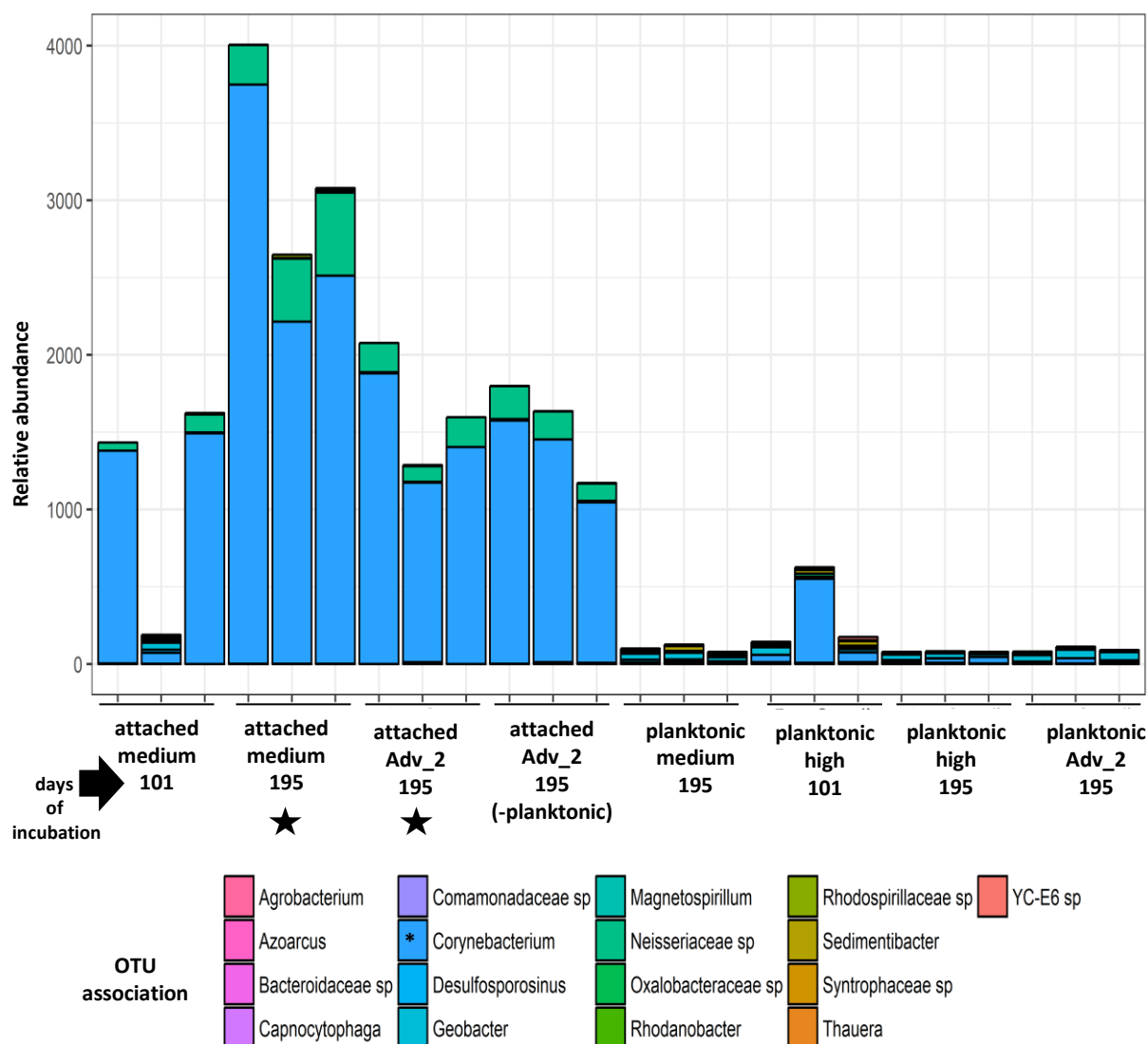


**Figure 3.30.** Deseq analysis between biofilms related to plume advance 2 treatment (\*). OTUs showing statistical differences in the relative abundances between these communities are shown. Note, the relative abundance was normalised to 10,000 counts and (\*) indicates groups which exhibited the larger changes in the relative abundances between these communities.

**Figure 3.31** shows a Deseq analysis which contrasts the attached communities formed after the change of conditions considering the effect of the geochemical environment (through the

removal of the planktonic community). The contrast of these samples indicated a significant change in the relative abundances of different OTUs, but these differences represent less than 1%.

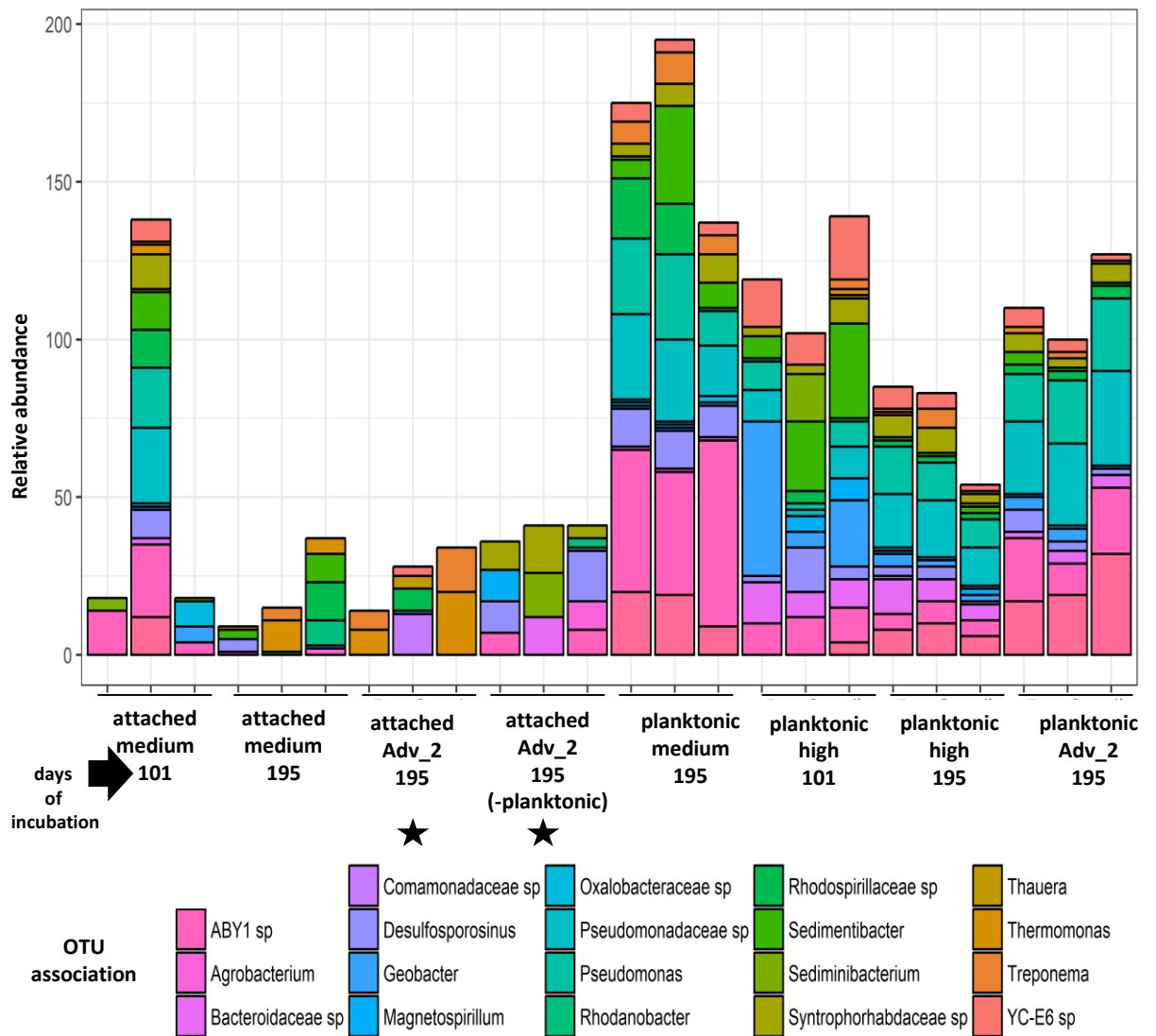


**Figure 3.31.** Deseq analysis between biofilms related to plume advance 2 treatment considering the effect of the geochemical environment, through the removal of the planktonic community (\*). OTUs showing statistical differences in the relative abundances between these communities are shown. Note, the relative abundance was normalised to 10,000 counts.

**Plume refreshing (PR), change from a medium to low phenolic environment, see Figure 3.8 for details.**

The plume refreshing treatments were constructed using sediments from medium phenolic microcosms and the supernatant of the low phenolic microcosms. Both phases were put together after 101 days of independent incubation. Residual pore water was contained in the sediments after the removal of the supernatant and was geochemically related to the supernatant of the medium phenolic treatment. This volume was considered to calculate the expected concentration of different chemical species, as a result of the mixing between the new supernatant (low phenolic) and the residual pore water (medium phenolic). **Figure 4.32** shows different parameters measured in the microcosm recreating this change of condition.

The expected concentration purely by mixing was calculated considering residual pore water (29 ml) plus the supernatant (81 ml). The expected concentrations were,  $\sim 1 \text{ mg l}^{-1}$  phenol,  $6 \text{ mg l}^{-1}$  *m,p,o*-cresols and  $\sim 11 \text{ mg l}^{-1}$  xylenols. Nevertheless, the real pollutant concentrations were lower in both treatments. No statistical differences were found between the filtered and the unfiltered treatments.

An important feature of these treatments was the spiking with a  $\text{NaNO}_3$   $4 \text{ g l}^{-1}$  solution, increased up to  $30 \text{ mg l}^{-1}$  from the change of condition, till the finish of the experiments. Nitrate tends to be consumed immediately after the change of treatment. In the last 50 days of the experiment, nitrate consumption decreases more rapidly after each spiking, reaching depletion levels. Nitrate consumption was higher (lower nitrate content) in the filtered treatment across all the monitoring period.

The total amount of phenol, *m,p,o*-cresols, and xylenols consumed was  $16.52 \text{ mg l}^{-1}$ . The increase of manganese was  $2.31 \text{ mg l}^{-1}$ . This amount could have biodegraded  $0.42 \text{ mg l}^{-1}$  of TPC. The increase of iron was  $2.31 \text{ mg l}^{-1}$ , and this amount could have biodegraded  $0.20 \text{ mg l}^{-1}$  of TPC. The reduction of sulphate related to sulphate reduction was of  $1.29 \text{ mg l}^{-1}$ , and this amount could have biodegraded  $0.93 \text{ mg l}^{-1}$  TPC. The total nitrate consumption after the change of conditions was  $160.62 \text{ mg l}^{-1}$ , this amount could have biodegraded through nitrate reduction and denitrification,  $49.72$  and  $124.29 \text{ mg l}^{-1}$  of TPC respectively. No statistical differences between the filtered and the unfiltered treatments recreating the change of environment were found for sulphate and iron. Nevertheless, there were statistical differences between treatments for nitrate and manganese. In brief, the estimated biodegradation of the TPC was of  $16.52 \text{ mg l}^{-1}$ , which might be explained in 100 % due to nitrate reduction after the plume refreshing treatments were recreated. However, there was still TPC in the supernatant of these treatments at the end of the experiment.



The cell numbers of the supernatant of low phenolic microcosms were  $\sim 10^6$  cells ml<sup>-1</sup>. After being in contact with sediments from medium phenolic microcosm, cell numbers remained stable after 195 days of total incubation. The cell numbers of the biofilm before the change of conditions reached  $\sim 10^6$  cells per ml of saturated sediments. This value remained stable after the change of conditions.

**Figure 3.33** shows the PCoA weighted analysis on the microbial community. It was possible to observe that attached communities after the change of conditions (plume refreshing) were relatively similar to the biofilm communities without any interventions (attached communities from medium phenolic microcosms after 195 days of incubation). At the end of the experiment the planktonic communities of the plume refreshing treatment shift in the opposite direction of the planktonic communities from low phenolic microcosms after 195 days of incubation. This direction is towards the planktonic communities of the medium phenolic microcosms after 195 days of incubation.

In the sediments prior to the change of conditions there was residual water that contained a planktonic community and it was not possible to remove this. The effect of this on the planktonic plume refreshing community was explored through the simulation of a planktonic synthetic community. The simulated community was calculated using the planktonic communities of the low and medium phenolic microcosms after 195 days of incubation and the volume of each microcosm in the final arrangement (81 and 29 ml, respectively). **Figure 3.34** shows the Unifrac weighted PCoA of planktonic communities. The synthetic community was between the original communities. The planktonic community of plume refreshing was distant from this zone. Therefore, there was an influence of the biofilm community on the structure of the planktonic community.

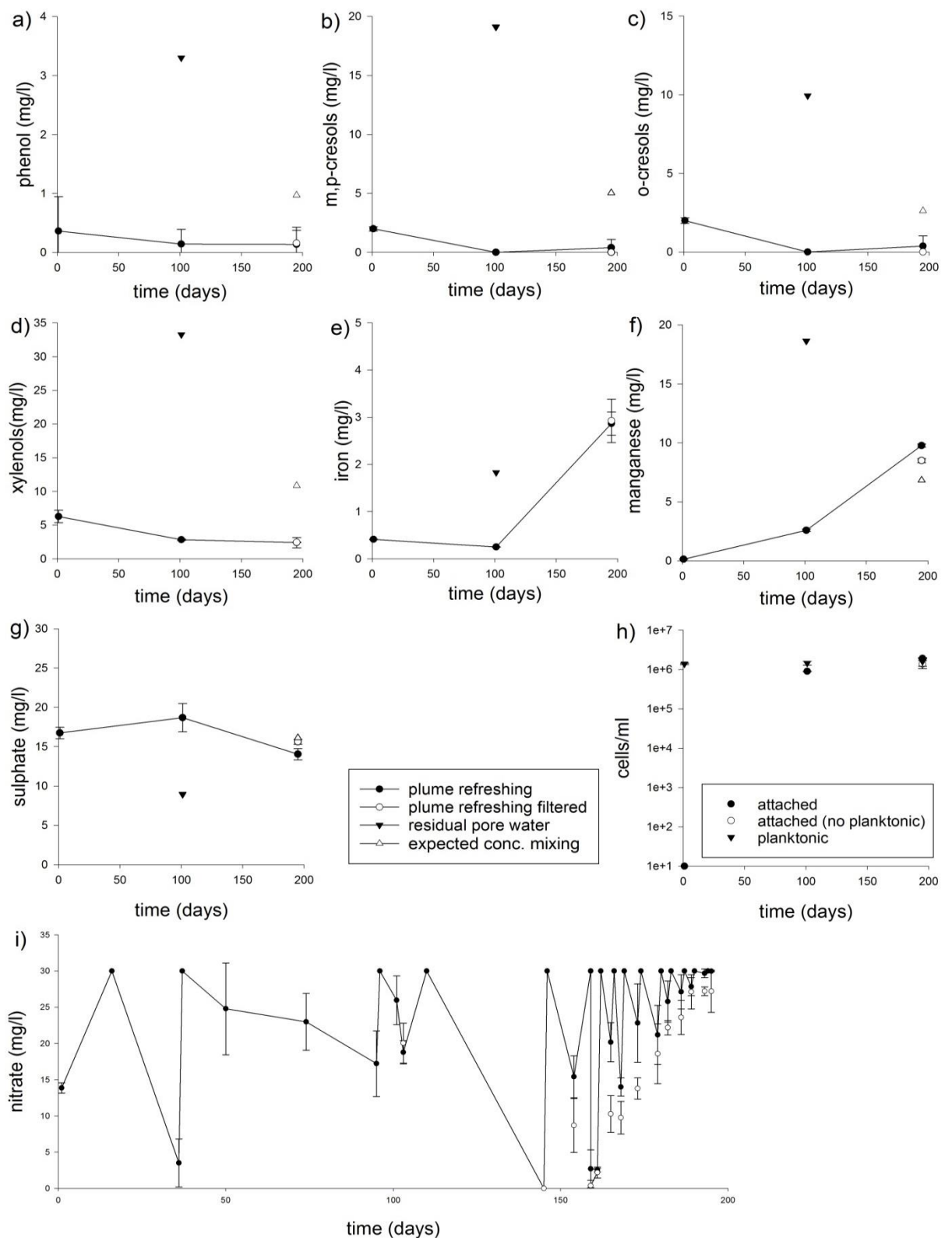


**Figure 3.32.** Monitoring of different chemical species in microcosms recreating the plume refreshing. Legend from the middle applies for all graphs except for the cell densities in h. Note, plume refreshing was constructed with sediments from medium phenolic microcosms and the supernatant of the low phenolic microcosms. Plume refreshing filtered, planktonic community was removed before putting these phases together. Residual pore water, was contained in the sediments after the removal of the supernatant. Expected conc. mixing, was the predicted concentration as a result of the mixing between the new supernatant (low phenolic) and the residual pore water (medium phenolic).

### Unifrac Weighted PCoA samples

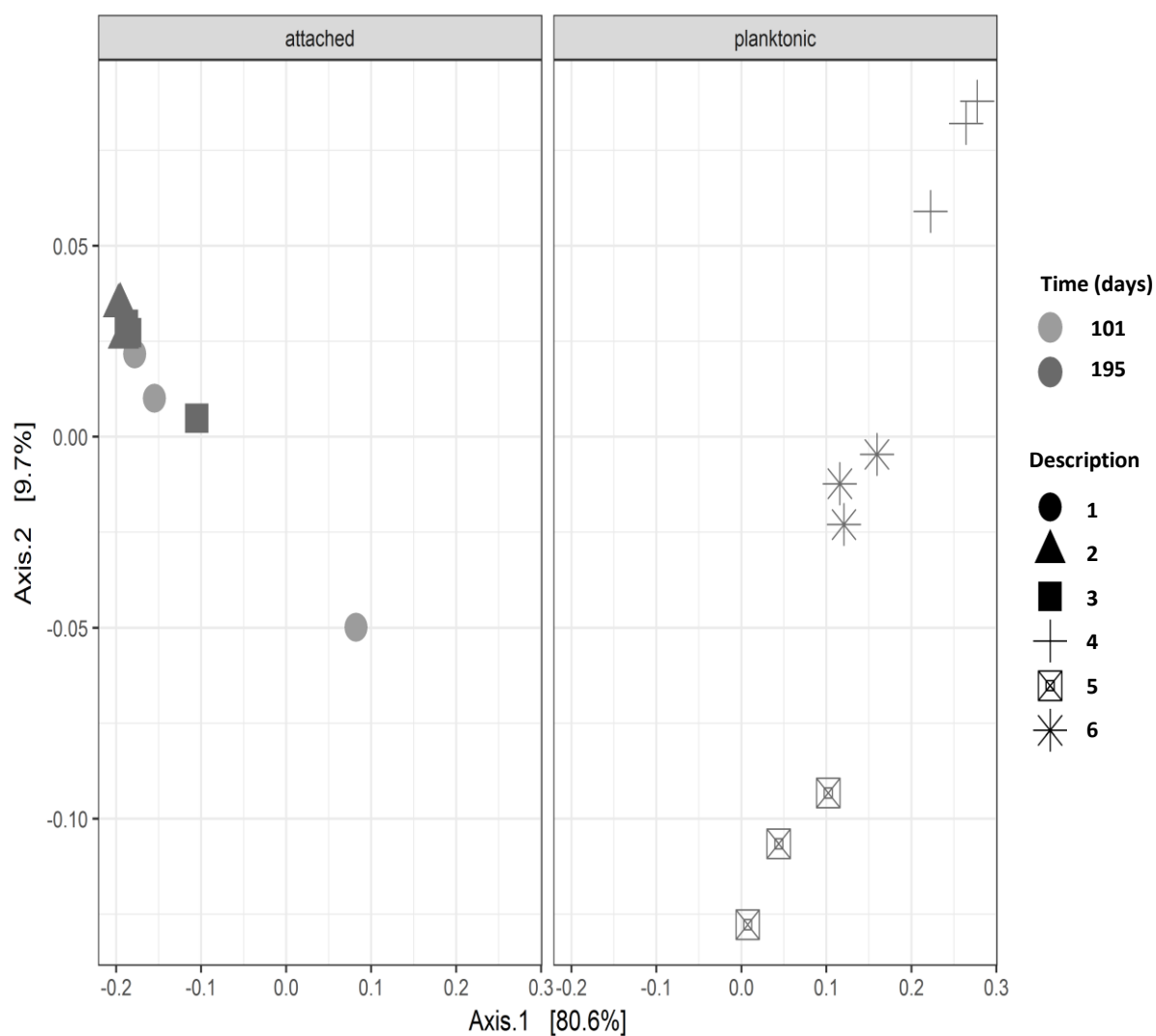


**Figure 3.33.** Unifrac weighted Principal coordinate analysis of attached and planktonic communities harvested from microcosms recreating plume refreshing. Note, 1 and 2 attached communities after 101 and 195 days of incubation in a microcosm inoculated with groundwater from a medium phenolic environment. 3, attached community after 195 days which experimented the change from a medium to a low phenolic environment. 4, planktonic community after 195 days of incubation in low phenolic microcosms. 5, planktonic communities after 195 days of incubation in a microcosm inoculated with medium phenolic content. 6, planktonic community after plume refreshing.

### Unifrac Weighted PCoA of synthetic samples

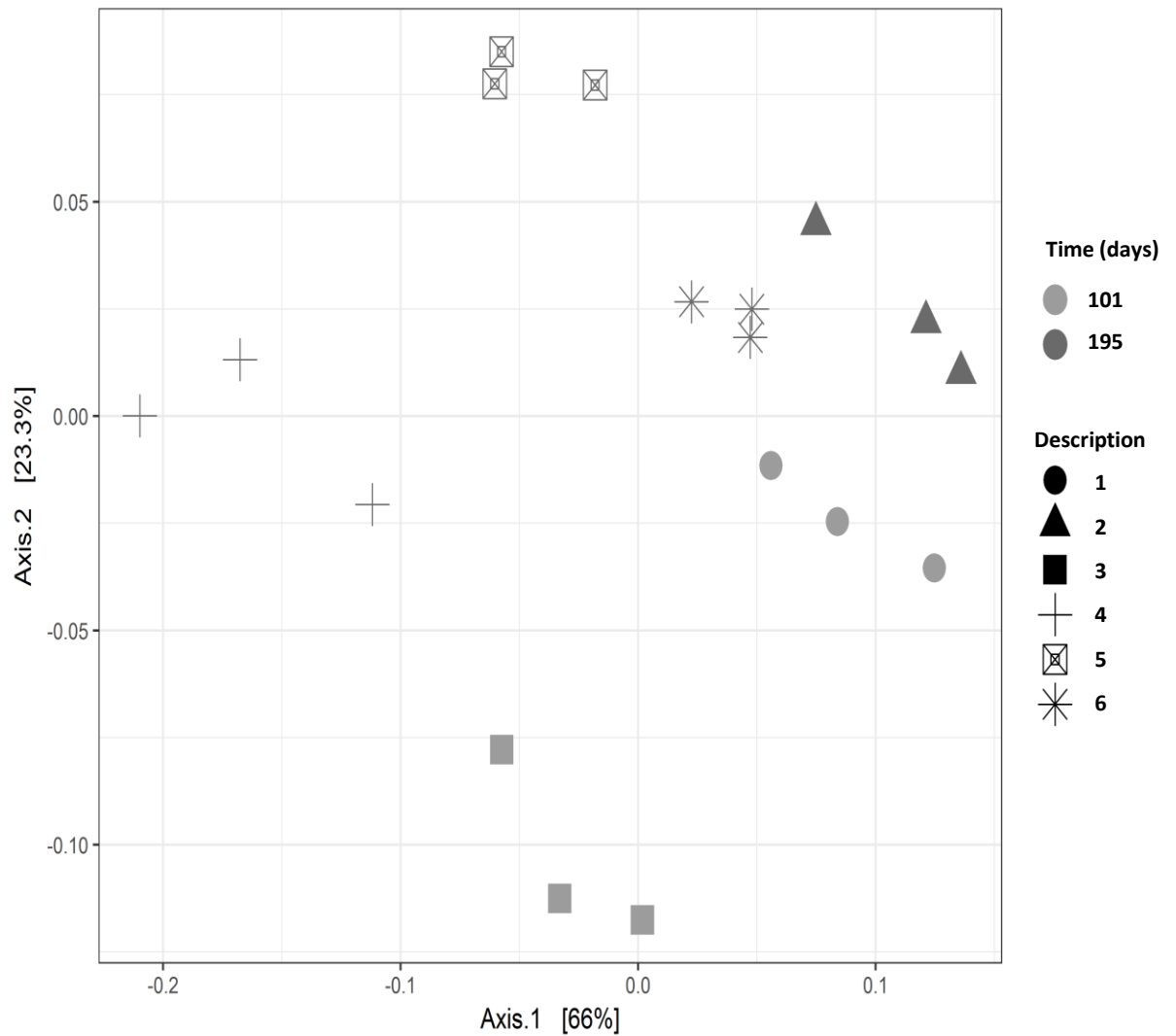


**Figure 3.34.** Unifrac weighted Principal coordinate analysis of planktonic communities related to plume refreshing treatments. Note 1 and 2, planktonic communities after 101 and 195 days of incubation in a microcosm inoculated with groundwater from a low phenolic environment. 3 and 4, planktonic communities after 101 and 195 days of incubation in a microcosm inoculated with groundwater from a medium phenolic environment. 5, planktonic community after plume refreshing. 6, synthetic planktonic community.

PCoA indicated that community structures of the biofilm formed after 195 days of incubation with medium phenolic microcosms, were close to the biofilm after the change of conditions.

**Figure 3.35** shows a Deseq analysis which contrasted these attached communities considering the impact of change of conditions. The contrast of these samples indicated significant changes. These differences were related to higher relative abundances of different OTUs, but these differences represent less than 1%.

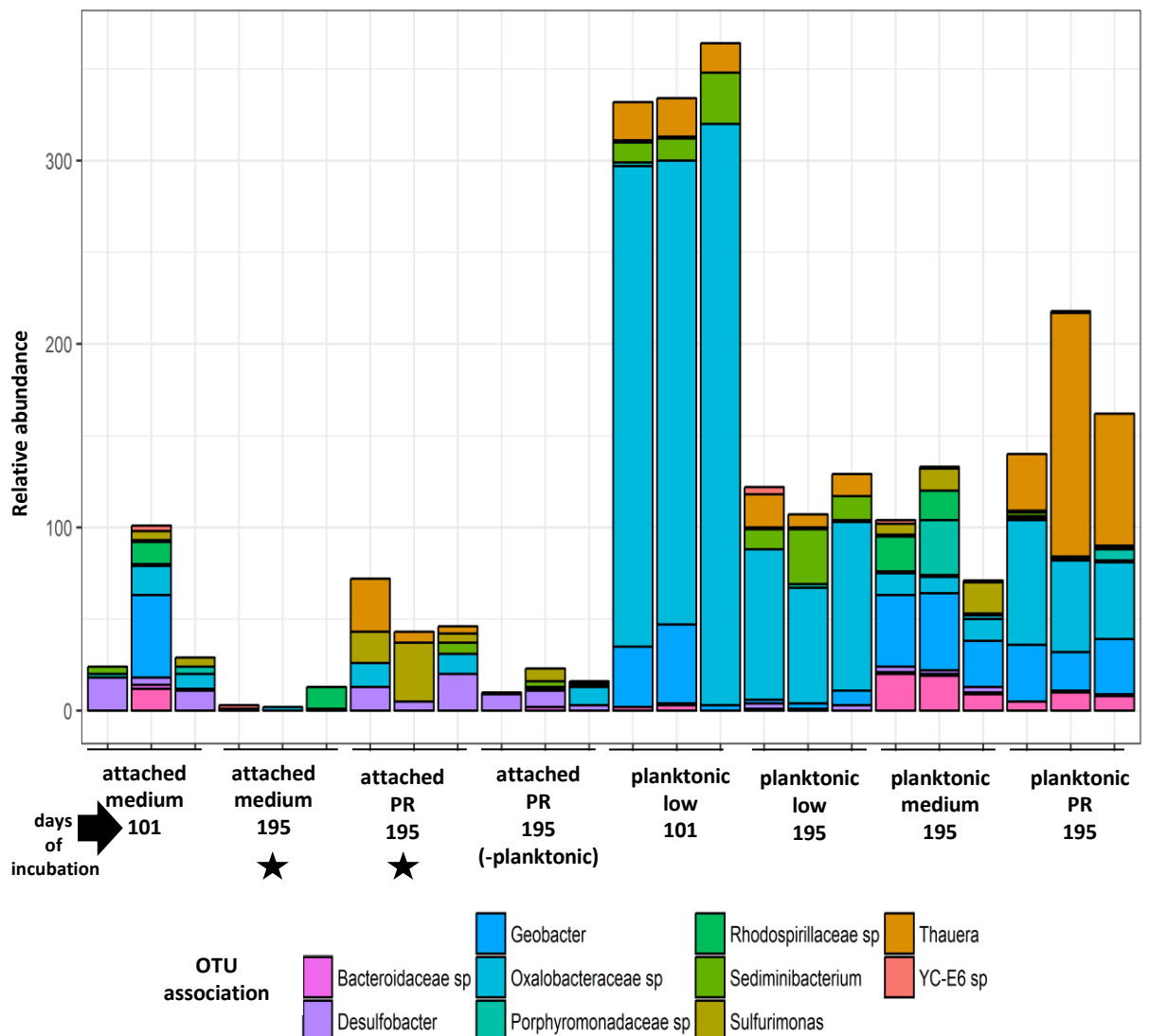


**Figure 3.35.** Deseq analysis between biofilms related to plume refreshing treatment (\*). OTUs showing statistical differences in the relative abundances between these communities are shown. Note, the relative abundance was normalised to 10,000 counts and (\*) indicates groups which exhibited the larger changes in the relative abundances between these communities.

**Figure 3.36** shows a contrast between the attached communities settled after 6 months considering the effect of the geochemical environment (through the removal of the planktonic community). The contrast of these samples indicated a significant change, due to an increase in the relative abundance of *Corynebacterium* in the biofilm recreating the plume refreshing, but only with microbe-free groundwater.

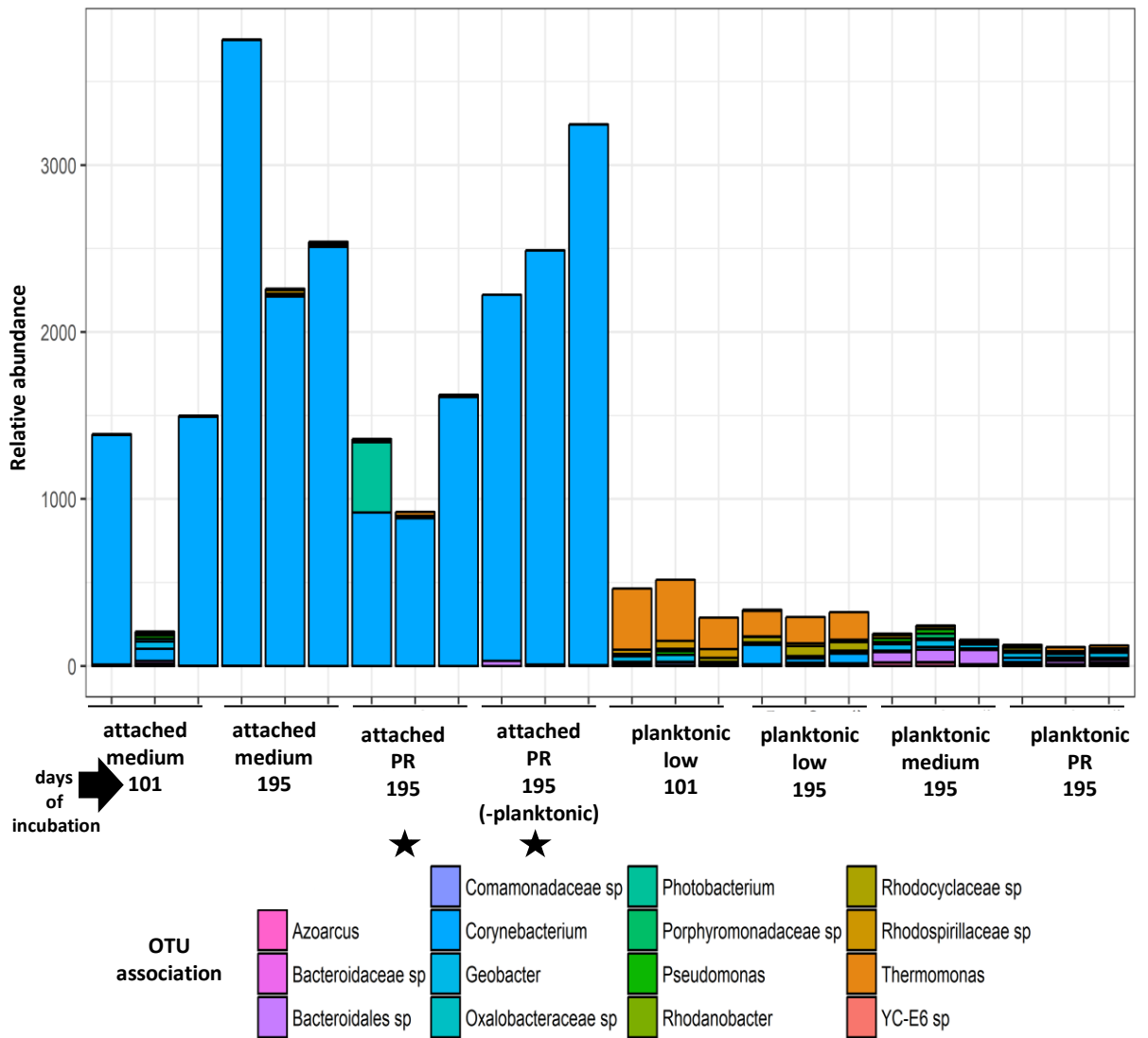


**Figure 3.36.** Deseq analysis between biofilms related to plume refreshing treatment considering the effect of the geochemical environment, through the removal of the planktonic community (\*). OTUs showing statistical differences in the relative abundances between these communities are shown. Note, the relative abundance was normalised to 10,000 counts.

**Source term variation (stv), change from a high to medium phenolic environment, see Figure 3.8 for details.**

The source term variation treatments were constructed using sediments from high phenolic microcosms and the supernatant of the medium phenolic microcosms. Both phases were put together after 101 days of independent incubation. Residual pore water was contained in the sediments after the removal of the supernatant and was geochemically related to the supernatant of the high phenolic treatment. This volume was considered to calculate the expected concentration of different chemical species, as a result of the mixing between the new supernatant (medium phenolic) and the residual pore water (high phenolic). **Figure 3.37** shows different parameters measured in the microcosm recreating this change of condition.

The expected concentration purely by mixing was calculated by considering residual pore water (29 ml) plus the supernatant (81 ml). The expected concentrations were  $\sim 25 \text{ mg l}^{-1}$  phenol,  $45 \text{ mg l}^{-1}$  *m,p,o*-cresols and  $\sim 45 \text{ mg l}^{-1}$  xylenols. Nevertheless, the real pollutant concentrations were lower in both treatments, except for phenol. No statistical differences were found between the filtered and the unfiltered treatments.

The total amount of phenol, *m,p,o*-cresols, and xylenols consumed were of  $41.77 \text{ mg l}^{-1}$ ; and the reduction of sulphate related to sulphate reduction was  $9.49 \text{ mg l}^{-1}$ , this amount could have biodegraded  $6.86 \text{ mg l}^{-1}$  TPC. The increasing of iron was of  $9.80 \text{ mg l}^{-1}$ , and this amount could have biodegraded  $0.88 \text{ mg l}^{-1}$  of TPC. The difference between the expected nitrate content and the real nitrate concentration was  $0.39 \text{ mg l}^{-1}$ , this amount according to the mass balances on the nitrate reduction and denitrification could have biodegraded a total of  $0.12$  and  $0.30 \text{ mg l}^{-1}$  of TPC respectively. No statistical differences between the filtered and the unfiltered treatments recreating the change of environment were found for sulphate and nitrate. In summary, the estimated biodegradation of the TPC was  $41.77 \text{ mg l}^{-1}$ , which is explained in 19.5 % by the changes on the EA concentrations after the source term was recreated.

The cell numbers of the supernatant of medium phenolic microcosms were  $\sim 10^6 \text{ cells ml}^{-1}$ . After being in contact with sediments from high phenolic microcosms cell numbers remain stable after 6 months of total incubation. The cell numbers of the biofilm before the change of conditions reached  $\sim 10^6 \text{ cells ml}^{-1}$  of saturated sediments. This value remained stable after the change of conditions.

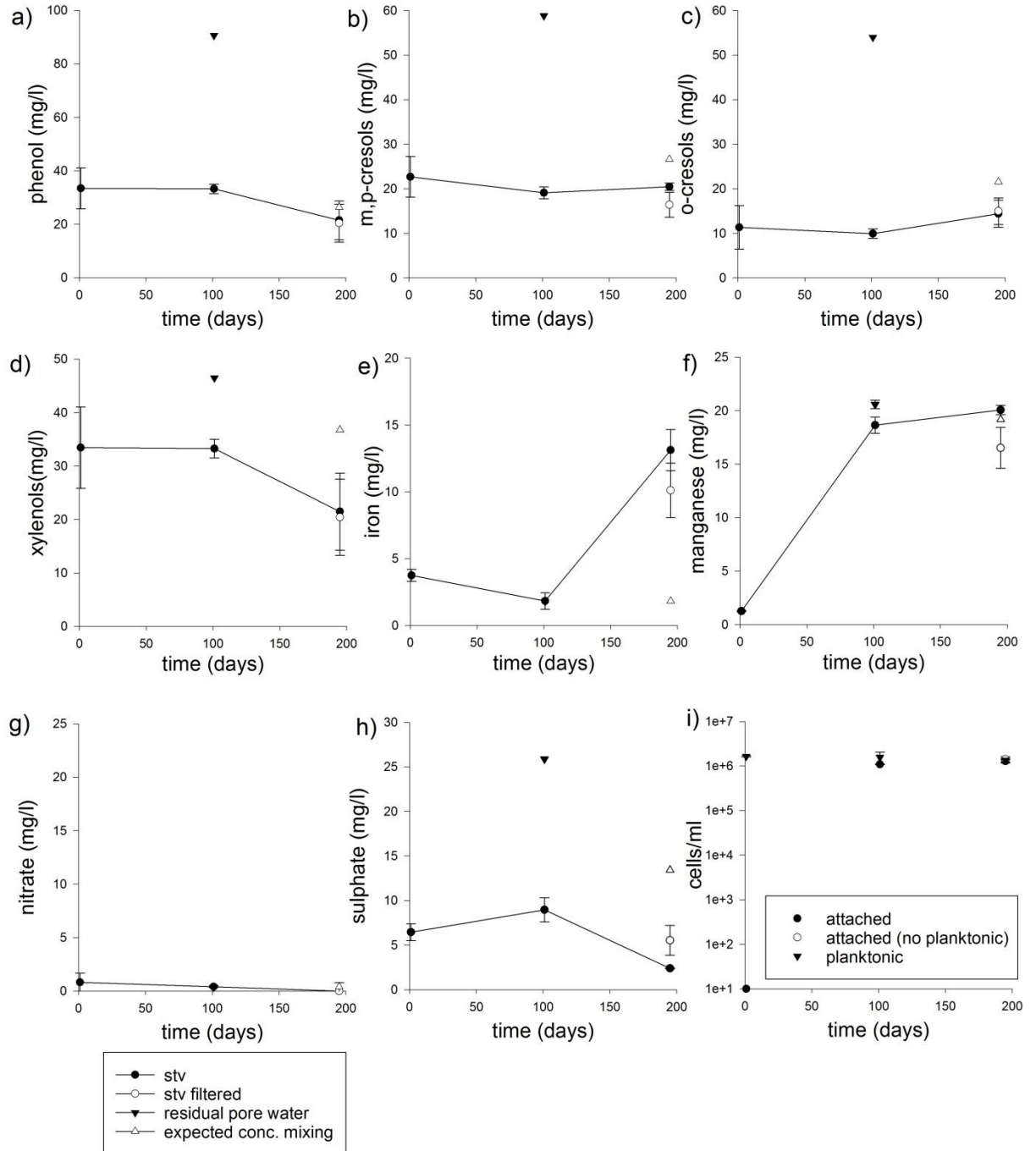


**Figure 3.37.** Monitoring of different chemical species in microcosms recreating the source term variation (stv). Legend from lower left corner applies for all graphs except for the cell densities in i. Note, stv was constructed with sediments from high phenolic microcosms and the supernatant of the medium phenolic microcosms. STV filtered, planktonic community was removed before putting these phases together. Residual pore water was contained in the sediments after the removal of the supernatant. Expected conc. mixing was the predicted concentration as a result of the mixing between the new supernatant (medium phenolic) and the residual pore water (high phenolic).



**Figure 3.38** shows the PCoA weighted analysis on the microbial community. It was possible to observe that after the change of conditions (source term variation, stv) the attached communities were distant to the biofilm communities without any interventions (attached communities from high phenolic microcosms after 195 days of incubation). The planktonic communities subjected to the source term variation shift in a different direction to the planktonic communities without any interventions (planktonic communities from medium and high phenolic microcosms after 195 days of incubation).

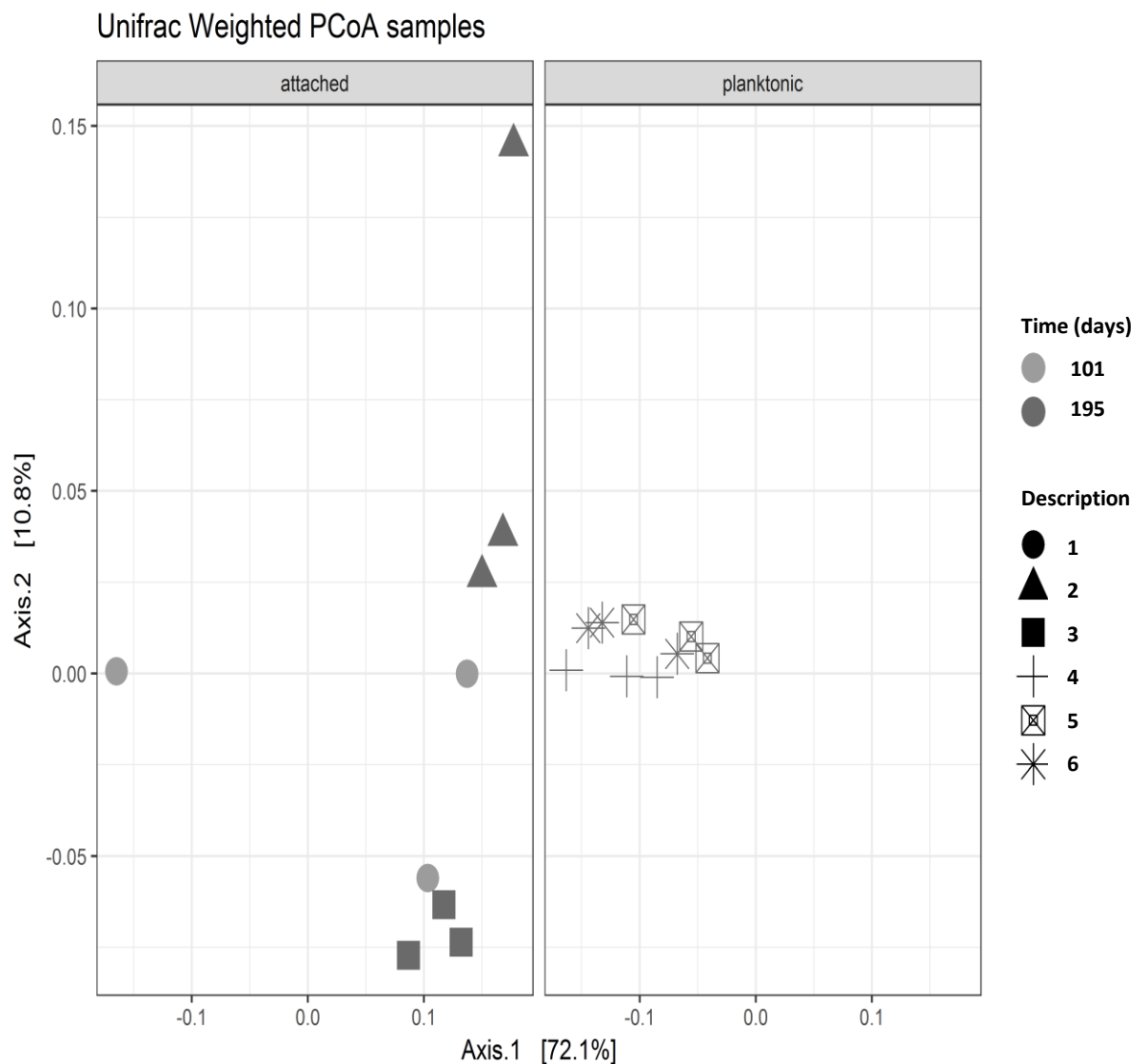


**Figure 3.38.** Unifrac weighted Principal coordinate analysis of attached and planktonic communities harvested from microcosms recreating the source term variation, stv. Note, 1 and 2 attached communities after 101 and 195 days of incubation in a microcosm inoculated with groundwater from a high phenolic environment. 3, attached community after 195 days which experimented the change from a high to a medium phenolic environment. 4, planktonic community after 195 days of incubation in medium phenolic microcosms. 5, planktonic communities after 195 days of incubation in a microcosm inoculated with high phenolic content. 6, planktonic community after stv.

In the sediments previous to the change of conditions there was residual water, which was not possible to be removed, and in this residual groundwater there was a residual planktonic community. The effect on the planktonic source term community was explored through the simulation of a planktonic synthetic community. The simulated community was calculated considering the planktonic communities of the high and medium phenolic microcosms after 195 days of incubation and the volume of each one in the final arrangement (29 and 81 ml, respectively). **Figure 3.39** shows the Unifrac PCoA weighted of planktonic communities. The synthetic community were between the original communities. The synthetic planktonic community of source term variation treatment is not contained in the vector between the two original communities. Therefore, it suggests an influence of the biofilm community on the community structure of the planktonic community.

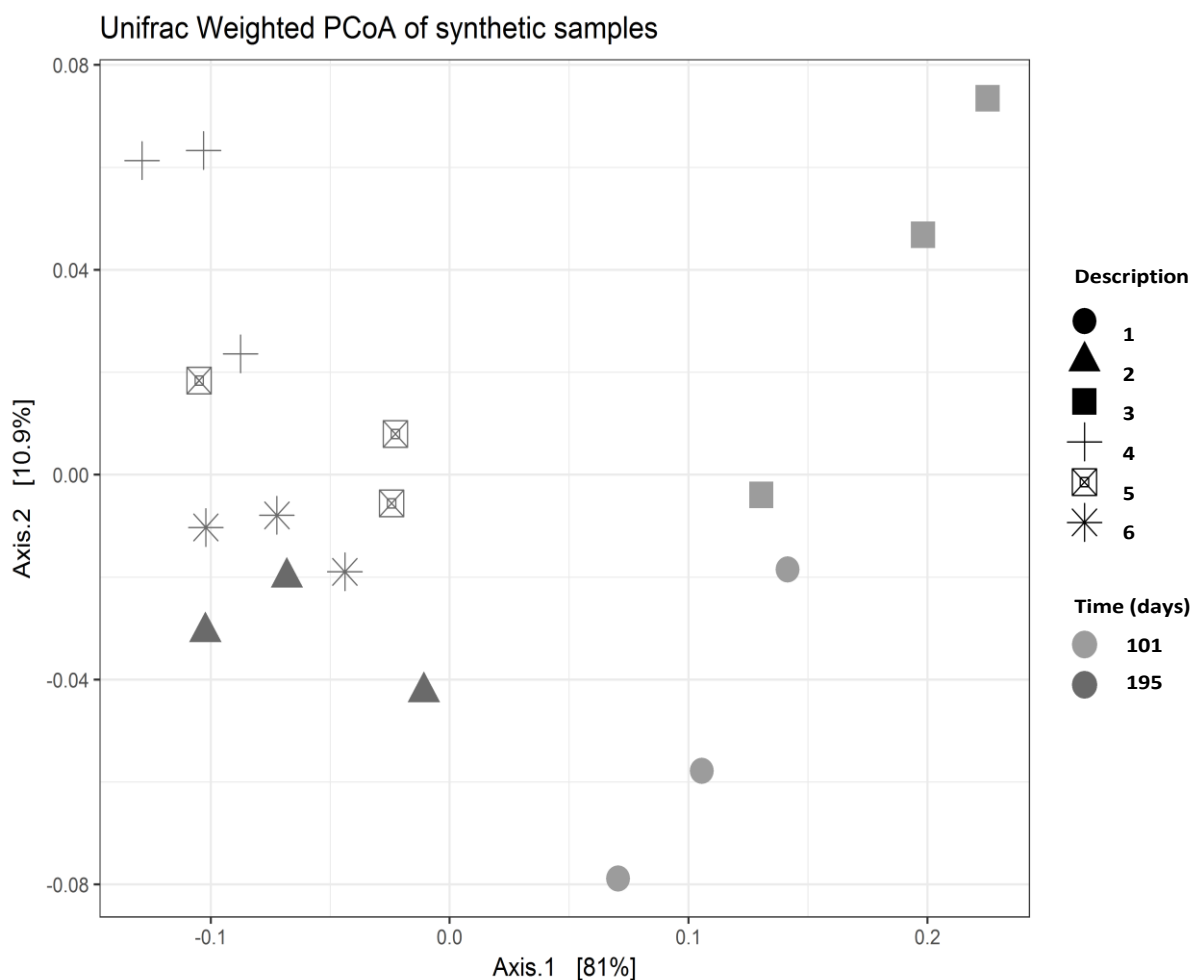


**Figure 3.39.** Unifrac weighted Principal coordinate analysis of planktonic communities related to source term variation treatment. Note 1 and 2, planktonic communities after 101 and 195 days of incubation in a microcosm inoculated with groundwater from a medium phenolic environment. 3 and 4, planktonic communities after 101 and 195 days of incubation in a microcosm inoculated with groundwater from a high phenolic environment. 5, planktonic community after adv\_2. 6, synthetic planktonic community.

PCoA indicated that community structures of samples of the biofilm formed after 195 days of incubation with high phenolic microcosms were distant from the biofilm after the change of conditions. **Figure 3.40** shows a Deseq analysis which contrasted these attached communities considering the impact of change of conditions. The contrast of these samples indicated significant differences; these differences were related to higher relative abundances of *Bradyrhizobiaceae* and *Variovorax* in the biofilm which experience the source term variation.

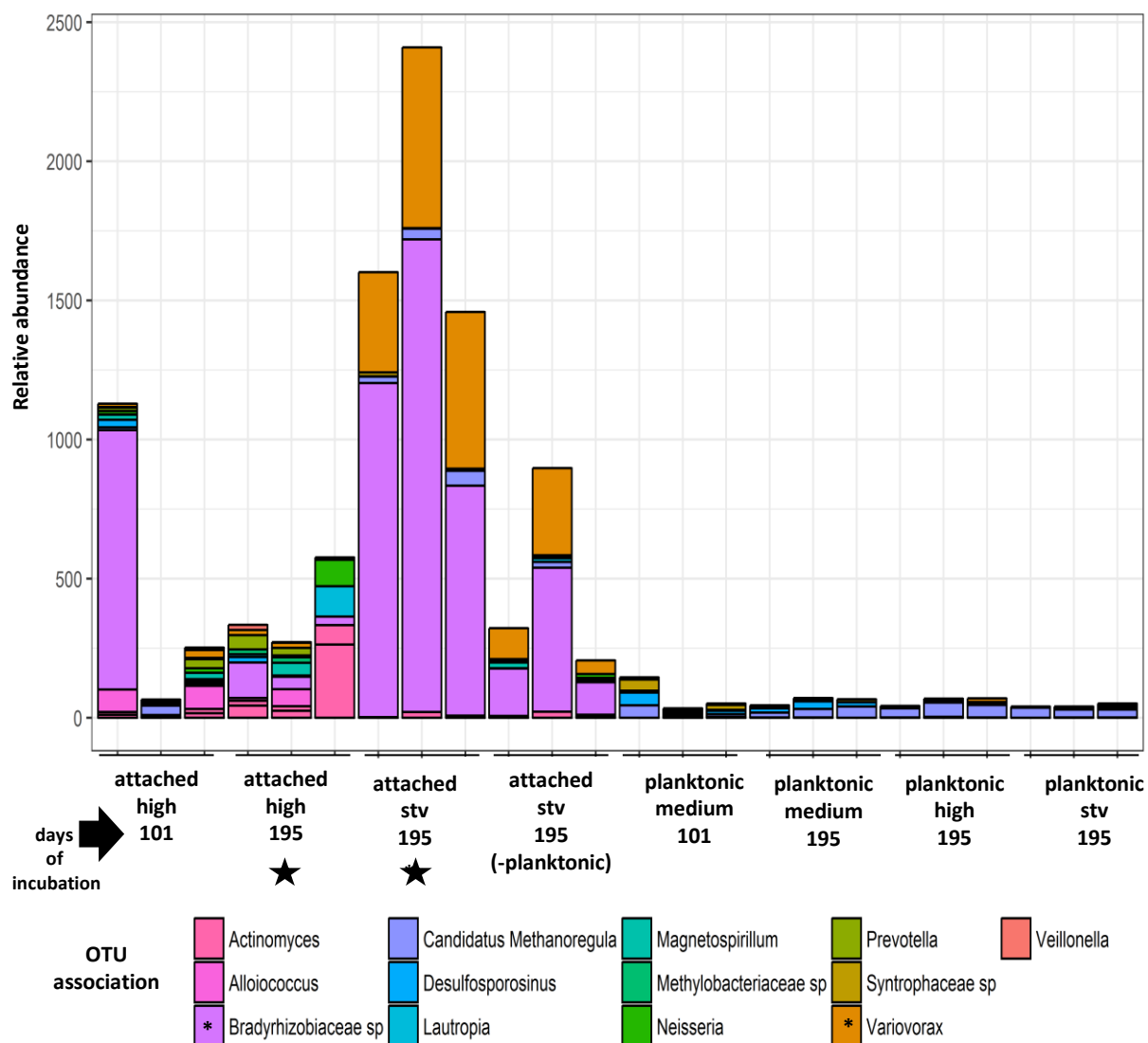


**Figure 3.40.** Deseq analysis between biofilms related to source term variation treatment (\*). OTUs showing statistical differences in the relative abundances between these communities are shown. Note, the relative abundance was normalised to 10,000 counts and (\*) indicates groups which exhibited the larger changes in the relative abundances between these communities.

**Figure 3.41** shows a Deseq analysis which contrasted the attached communities formed after the change of conditions considering the effect of the geochemical environment (through the removal of the planktonic community). The contrast of these samples indicated a significant change in the relative abundances of *Pseudomonas*, with higher presence in the source term variation inoculated with microbe-free groundwater. These changes represent less than 3% of the total relative abundances.

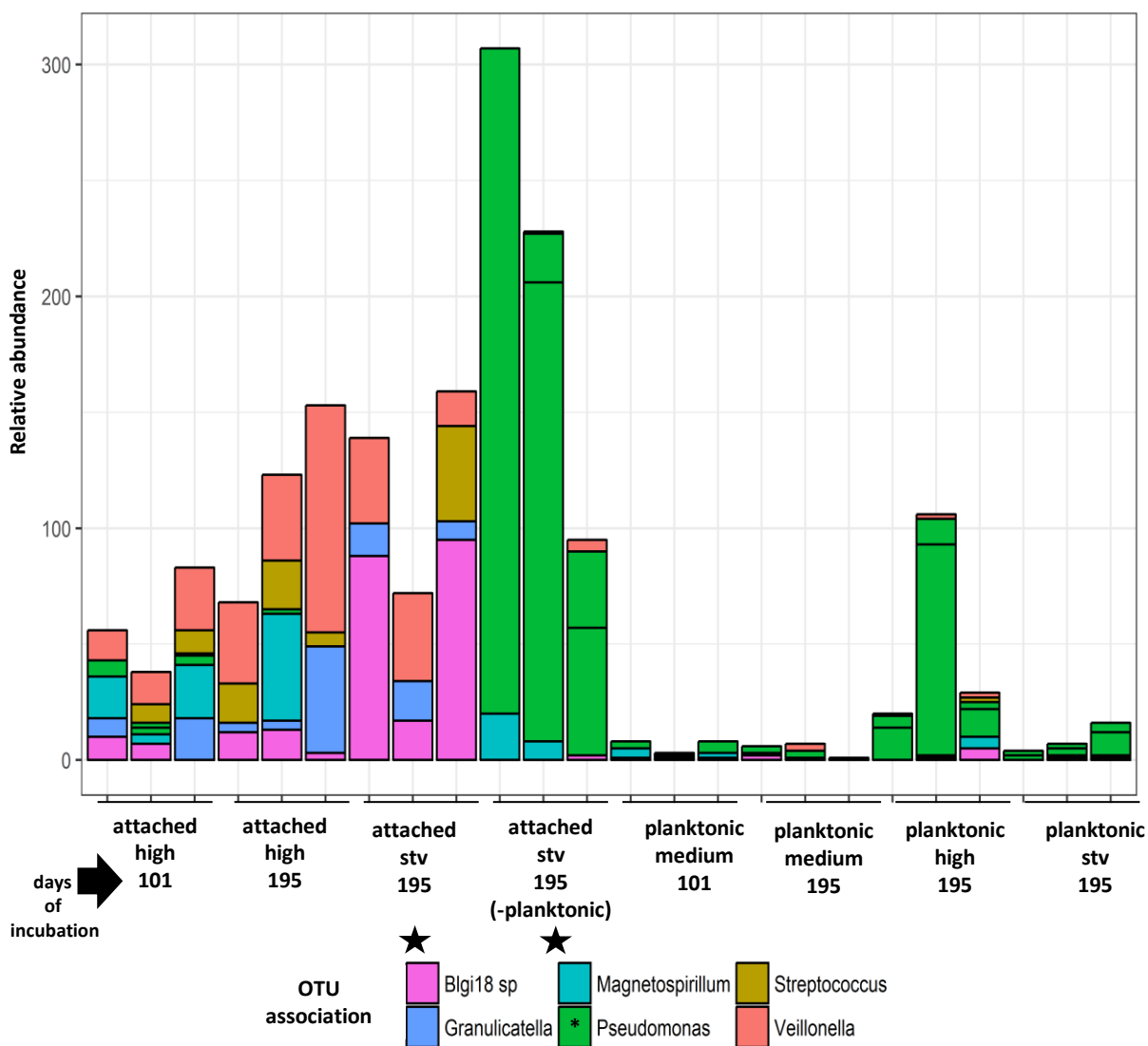


**Figure 3.41.** Deseq analysis between biofilms related to source term variation treatments considering the effect of the geochemical environment, through the removal of the planktonic community (\*). OTUs showing statistical differences in the relative abundances between these communities are shown. Note, the relative abundance was normalised to 10,000 counts.

**Table 3.1** shows a summary with key findings of this chapter.

**Table 3.1** Tabulated key findings for Chapter 4.

Finding	Description	Evidence
1	It was possible to recreate different chemical interfaces environments located in a phenol-contaminated plume	Different Terminal Electron Acceptors Processes (TEAPs) were observed at low, medium and high phenolic microcosms. These processes were associated to the presence of different OTUs.
2	It was possible to recreate different changes of the environments which are experienced by the biofilm communities	Different Terminal Electron Acceptors Processes (TEAPs) were observed during the following change of environment: plume advance, plume refreshing, and source term variation. These processes were associated to the presence of different OTUs.
3	The biofilm or attached communities were able to resist alteration of their chemical environment	The biofilm maintained its cell numbers and community structure after the change of conditions
4	The biofilm community was a response to the geochemical environment	Biofilm supplemented with microbe-free groundwater did not show differences compared to biofilm communities inoculated with the planktonic community

### 3.4 Discussion

Given the complexity of the experimental design, the discussion will be question-guided to cover all the relevant findings derived from the results. Firstly, a set of questions related to the setting-up of different environment, followed by questions related to the change of the chemical environment to different biofilms.

#### ***Do the microcosm treatments recreate the different chemical environments?***

The different inocula taken from the field were able to recreate the geochemical environment likely to be found in chemical interfaces of organic plumes of polluted aquifers. The rationale behind the use of BH-59 and the selection of groundwater of 11, 14 and 21 mbgl was their similarities to the chemical interfaces located in the upper plume fringe and to the plume front. These depths have been consistently characterized as low, medium and high phenolic content by different studies on this site (Lerner *et al.*, 2000; Thornton *et al.*, 2001a; Thornton *et al.*, 2001b) and the pollutant content observed in the different treatments was in tune with these studies.

Once in the microcosm, biodegradation was observed due to reduction of the pollutant content and there were changes in the concentrations of different terminal electron acceptors. These trends are related to microbial communities formed in the different settings. For example, the microcosm formed with groundwater from a low phenolic environment and kept under a nitrate spike regime (**Figure 3.9**), showed a rapid response to the spiking and nitrate was consumed constantly until the depletion of most of the pollutants. This phenomenon is in tune with a community belonging to the upper plume fringe, which has been described to have a high nitrate reduction activity, and relates to the disappearance or reduction in the concentration of this electron acceptor (Williams *et al.*, 2001; Van Breukelen *et al.*, 2004). Similar trends were observed in a set of microcosms constructed with groundwater from a different borehole in the same aquifer, and proved to have nitrate consumption under a spiking regime (Spence *et al.*, 2001).

On the other hand, in the microcosm inoculated with a groundwater inoculum from 14 and 21 mbgl, the medium and high phenolic content was recreated; there was biodegradation of the pollutant, but not complete, a low concentration of nitrate, and a change in the concentration of manganese and sulphate. These treatments aimed to recreate locations in the chemical interface at plume front, which are not available for sampling on this site. Firstly, the low concentrations of nitrate are expected given that nitrate is quickly consumed in the fringes (Thornton *et al.*, 2001a; Watson *et al.*, 2005). Moreover, the increase in manganese is related

to the reductive dissolution of manganese oxides which are present in the coating of the sediments on the site (Lerner *et al.*, 2000; Mayer *et al.*, 2001) and the sediments used in this experiment came from a quarry with similar mineralogy. The sulphate reduction observed in these treatments is related to the bacterial sulphate reduction (BSR), which is active on locations not affected by the toxicity of the pollutants, such as the chemical interfaces to the plume front (Spence *et al.*, 2001; Thornton *et al.*, 2001b)

Another important element to recreate in these different treatments was the microbial community. In term of numbers, the planktonic community showed similar cell densities as in the field, and those values remained stable. The timescale of attachment found in the first experiment was reproducible on these treatments, and the number of cells attached also remained stable after the biofilm was developed. The cell numbers calculated per 1 ml of saturated sand indicated similarities between the planktonic and attached communities, once the biofilm has been established. This similarity increases the importance of the biofilm community in this aquifer, compared to the findings of the first experiment where the planktonic community was more abundant, and could be related to studies in pristine and contaminated aquifers which found higher numbers in the attached phase (Hazen *et al.* 1991; Holm *et al.* 1992; Griebler *et al.*, 2002). The similarity of biomass between the communities determines that any change in the microbial community structures might be linked to external factors and not to the cell number which are constant in the treatments of this experiment.

In brief, the microcosms were able to replicate low, medium and high phenolic environments, representing a good model to study polluted aquifers (Tuxen *et al.*, 2006; Thornton & Rivett, 2008; Elliot *et al.*, 2010a)

***Does the biodegradation observed in the microcosms relate with the presence of OTUs which might be responsible for it?***

The sequencing of the 16S rRNA gene revealed different trends. For example, there was a significant microbial community shift from field samples at 11 mbgl once they were put into a microcosm. In the field, the presence of *Myxococcales sp.*, followed by its disappearance in the planktonic community of the microcosms, is related to most of the members of these groups being strictly aerobic (Treude *et al.*, 2003; Huntley *et al.*, 2011). Once placed in the microcosms, oxygen is rapidly consumed and aerobic groups are overcome by the microbes able to grow in this anoxic environment. Also, in the low phenolic microcosms one group favoured under nitrate spiking conditions was *Pseudomonadaceae*, which increased significantly their abundance. This family of microorganism includes several types of *Pseudomonas spp.*, which have been described as able to biodegrade several types of organic

pollutant in fuel-contaminated or petroleum-contaminated aquifers, and in microcosm derived from these types of sites (Krumme *et al.*, 1993; Mikesell *et al.*, 1993; Stapleton *et al.*, 2000; Aburto *et al.*, 2009). A similar trend was followed by *Enhydrobacter*, a facultative anaerobe able to express the nitrate reductase enzyme in more reduced environments (Staley *et al.*, 1987; León-Zayas *et al.*, 2017). Therefore, the increasing of these groups in a nitrate reducing environment might be sustaining the biodegradation of phenolic compounds.

In the case of the medium and high phenolic microcosms treatments, a shift from the community in the field to the one developed in the supernatant of the microcosms was also observed. This shift is mostly influenced by the significant reduction of *Bacteroidales spp.* This group contains a large diversity of microorganisms, and some of them have been described as part of the natural the intestinal microbiota, associated to different types or protists and some of have been used in groundwater to track faecal pollution (Coyne *et al.*, 2008; Noda *et al.*, 2009; Zhang *et al.*, 2014). In contaminated aquifers, the high concentrations of petroleum hydrocarbons selects for *Bacteroidales spp.*, some of the groups described in these environments are *Magnetobacterium spp.*, *Pseudibacter spp.*, and *Sediminibacterium spp.* (Shi *et al.* 1999; Feris *et al.*, 2004; Rizoulis *et al.*, 2013). The reduction of these groups in the microcosms may be related to the unculturability of microbes belonging to these Genera (Vartoukian *et al.*, 2010). The significant reduction of *Azoarcus sp.* in these treatments represents less than 5% of the total counts, and this reduction could be reflecting the change of environment, from one with low concentrations of nitrate to another more reduced as manganese and sulphate start to be used. *Azoarcus sp.* is a denitrifying bacteria able to biodegrade phenol and different types of xylenols (Rabus *et al.*, 1995; Hess *et al.*, 1997; Winderl *et al.*, 2007; Rizoulis *et al.*, 2013). In absence of this terminal electron acceptor *Azoarcus sp.* will be competitive displaced by the microbes able to use different electron acceptors.

In the medium and high phenolic microcosms there was also a decrease of *Candidatus methanoregula*. This group of methanogenic archaeal microorganisms is able to use hydrogen and carbon dioxide and on some occasions formate during the methanogenesis process (Oren, 2014). This group has been described during the biodegradation of Polyaromatic hydrocarbons and present in hydrocarbon-contaminated aquifers (Berdugo-Clavijo *et al.*, 2012; Shahimin & Siddique, 2017). The ability to identify *archaeal* groups with the primer pair Bact-341F and Bact-805R has been described to be up to 64.6% when one mismatch is allowed (Klindworth *et al.*, 2012). Moreover, similar decrease has been observed for members of the Family *Desulfobacteraceae* and *Desulfosporosinus sp.*, which are microorganisms found in anoxic areas of hydrocarbon-contaminated aquifers, able to use sulphate as an electron acceptor



during the biodegradation of organic pollutants (Robertson *et al.*, 2000; Kleinsteuber *et al.*, 2012; Kümmel *et al.*, 2015). In this sense, the reduction of methanogens and sulphate reducers in these treatments might be associated to the ability of these groups to grow in syntrophy (Plugge *et al.*, 2011; Tischer *et al.*, 2013), and if one is not able to be cultured at lab scale, this unculturability might affect the other syntrophic group. Alternatively, the reduction of these groups in the planktonic community may be associated to these groups becoming colonizers of the attached community, which results in a reduction of their abundances in the microcosms' supernatants.

***Do the biofilm microbial communities developed in these treatments reflect the geochemical environment evolution?***

In the microcosm constructed with groundwater from a low phenolic environment after 101 days of incubation, *Pseudomonadaceae* may have had an important role during the biofilm formation. This is based on their significant increasing in its abundance in the planktonic community from the field, and the following detection of this group in the biofilm. This may be related to preferential attachment events on the sterile sediments by members of this group, as they become more abundant in the planktonic community they are more likely to colonise the available substrates. *Pseudomonas sp.* have been characterized and isolated from hydrocarbon-contaminated sediments showing capability to biodegrade different types organic molecules, such as phenol and mono-chlorophenols (Ringelberg *et al.*, 2001; Farrell and Quilty, 2002; Das & Mukherjee, 2017). Also, *Pseudomonas* in different environment, are precursors of biofilms, showing a large influence in the biofilm architecture when they are present and facilitate the adhesion of other late-colonizer after the synthesis of the biofilm matrix (Allison, 2003; Hall-Stoodley *et al.*, 2004). The presence of phenolic pollutants, a nitrate-reducing environment and the ability to adhere to sediments might explain their presence in the biofilm, and their reduction in the biofilm as other members start to attach to the sediments.

In the low phenolic microcosm, the presence of *Streptophyta sp.* was detected. This is likely to be sequences of the chloroplast 16S rRNA gene, from another source (agricultural activities developed on the site). These sequences have appeared in the characterization of bacterial communities and their presence has been associated to outdoor vegetation material (Hoisington *et al.*, 2016). In the microcosms inoculated with groundwater from a medium and high phenolic environment after 101 days of incubation there was also a presence of *Pseudomonadaceae*, but with lower abundances, which link with the lower nitrate concentrations of the inoculum of these environments.

In the biofilm formed of groundwater with medium and high phenolic environments (and also in the biofilms formed with groundwater from low phenolic environments) the presence of *Geobacter* was observed in the biofilms after 101 days of incubation. *Geobacter* is a group of bacteria relevant in the anaerobic biodegradation of organic pollutants, such as benzene and phenol, which is associated to the reduction of Fe (III) (Ludvigsen *et al.*, 1999; Vanscote & Young, 2000; Watanabe, 2001; Rizoulis *et al.*, 2013). *Geobacter* also has the ability of using Mn(IV) during the biodegradation of different electron donors (Lovley *et al.*, 2011). In the sediments there was an iron and manganese coating which might be used by this group of iron-reducers (Lerner *et al.*, 2000; Mayer *et al.*, 2001). Nevertheless, the increasing of iron in the supernatant was not detected. This might be explained by precipitation as iron sulphide, the latter might become available from the sulphate reduction observed, which is supported by the presence of BSR in the planktonic community of these settings. It is also important to consider that sulphide was not measured in this experiment and could be acting as electron donor, during the re-oxidation process of sulphide, which have been described in the biodegradation process of sediments of organic-contaminated aquifers (Muller *et al.*, 2016).

In the case of manganese, *Geobacter* uses this electron acceptor from manganese oxides which are insoluble in water. As a product of organic oxidation using these oxides as EAs, manganese will be available as Mn(II), which is highly soluble in water (Gounot, 1994). Therefore, the increasing of manganese observed could be related to the manganese reducer activity of *Geobacter*.

Furthermore, in the biofilm constructed with groundwater from the medium and high phenolic environments, a significant increase of *Corynebacterium* and *Staphylococcus* resulted during the biofilm formation. *Corynebacterium* is a Genus of bacteria isolated from different types of environments, and their ability to use manganese as electron acceptor in aquifer sediments has been suggested (Di-Ruggiero and Gounot, 1990; Du *et al.*, 2010). Also, the presence of *Staphylococcus* has been detected in groundwater from contaminated aquifers (Krapac *et al.*, 2002; Ozler and Aydin, 2008; Grisey *et al.*, 2010). The potential ability of these groups to use the iron and manganese oxides might explain their presence in the biofilm.

In this sense, the presence of the groups in the biofilm reflect in part the use of electron acceptors from the supernatant at early stages, and as the biofilm matures the composition might be reflecting the groups able to use the electron acceptor available in the biofilm. Considering all the electron acceptors processes taking place in the microcosm, it seems that they develop simultaneously, instead of occurring in a succession of redox reactions as is

suggested by the plume fringe concept, which is related to the chemical interfaces aimed to recreate with these treatments (Meckenstock *et al.*, 2015).

***Do the changes of environments reflect different Terminal Electron Acceptor Processes (TEAPs) that could take places in dynamic chemical interfaces of polluted aquifers?***

The change of conditions in the settled biofilms showed trends likely to be found in dynamic chemical interfaces. For example, the plume refreshing brought a nitrate reducing environment to the biofilm, which responded quite rapidly to the presence of this electron acceptor (nitrate consumption in both plume refreshing treatments, **Figure 3.32.i**). This rapid response is likely to be responsible of the presence of the Family *Pseudomonadaceae* in these biofilms, since in the filtered supernatant microcosms the planktonic community was removed, and nitrate consumption was still present in these treatments. Moreover, the use of iron and manganese as electron acceptors were processes likely to be active, as the values detected were higher than the expected concentrations purely by mixing (between residual pore water and the new supernatant). Also, the biodegradation of the different phenolic pollutants was active. The ability of the microbial communities in aquifers to respond to changes in their chemical environment has been documented in experiments using pristine aquifer material, which has been exposed to different xenobiotic compounds (Aelion *et al.*, 1987; Swindoll *et al.*, 1988). In the chemical interfaces under the influence of plume refreshing, it seems that different TEAPs occur simultaneously, according to the plume fringe concept, despite the difference in the energy yield obtained through the oxidation of phenol using different electron acceptors (Thornton *et al.*, 2001b; Meckenstock *et al.*, 2015).

The advance of the plume from a low to medium, and medium to high phenolic environment (adv\_1 and adv\_2) are important processes hypothesized to take place at the front of a moving plume. These zones have not been sampled before. These changes were reproduced in the microcosms, with the biodegradation still active after the change of conditions, and coincides with the development of more reduced areas to the core of the plume, during the plume advance in hydrocarbon-contaminated aquifers (Christensen *et al.*, 2000; Bekins *et al.*, 2001). Furthermore, the observed Terminal Electron Acceptor Processes (TEAPs) were related to manganese, iron and sulphate reduction, which again seem to take place simultaneously. The ability of BSR to cope with the increasing pollutant content is related to the inhibitory concentration threshold not been achieved during the change of the chemical environment in these treatments, and these groups are still able to perform biodegradation (Baker *et al.*, 2012; Spence *et al.*, 2001). The use of manganese and iron during the change of condition might be related to members of the biofilm, which might be more dependent on the iron-

manganese dissolution from the metal-oxides contained in the coatings of the sediment (Barbieri *et al.*, 2011; Van Breukelen *et al.*, 2003).

In the source term variation treatments (STV), the temporal-variability of pollutant in the plume was reproduced (Thornton *et al.*, 2001b) and the change of conditions promoted the activity of iron and sulphate reduction. The biodegradation of phenolic compounds through sulphate and iron reduction is related to the processes explained above. Nevertheless, in the biofilm of these treatments the presence of *Variovorax* and *Bradyrhizobiaceae* increased significantly. *Variovorax* has been identified in coal tar-contaminated Sherwood sandstone aquifers, actively degrading benzene, in PAH-contaminated sediments and in the anoxic areas of pristine aquifers (Aburto *et al.*, 2009; Fahy *et al.*, 2005; Ashton, 2012; Ginige *et al.*, 2013; Posman *et al.*, 2017). On the other hand, the Family *Bradyrhizobiaceae* has been described in different environmental environments, with iron reducer activity in contaminated aquifers and also detected in sewage treatment plants (Yu *et al.*, 2010; Marcondes De Souza, 2013; Giatsis *et al.*, 2015). Their increase in the biofilm after the change of conditions, from high to medium pollutant concentration, might be related to their ability to function in anaerobic environments with less concentration of contaminants, which displace the other members of the biofilm.

#### ***How do the planktonic and attached communities respond to changes in their chemical environment?***

The change of treatment implied the mobilization of the planktonic community. In this manner, it was sensible to move the planktonic community together with the geochemical environment, as the planktonic community in the aquifer is entrained in the groundwater flow. Therefore, in the dynamic of chemical interfaces (plume refreshing, plume advance and source term variation) that take place in polluted aquifers, the planktonic community will be present in the different change of environment affecting the biofilm.

In the treatments, it was possible to observe that the planktonic community structure is strongly influenced by the geochemical environment. Despite this, the modelling of synthetic planktonic communities, considering the residual planktonic community and the planktonic community from the new supernatant, revealed that the final stage of the planktonic community was not a result of the interaction between these communities. In this sense, the final planktonic community must have been an influence by the biofilm community, as the latter was able to maintain it after the change of conditions. This might be explained by detachment events from the biofilm towards the planktonic community, given that the detachment process could be due to physical forces during the incorporation of the new supernatant. Similar processes have been described by effect of hydrodynamic turbulence in

the external layer of the biofilms, which promote detachment of cells (Brading *et al.*, 1995; Allison *et al.*, 1998; Donlan, 2002)

On the other hand, the biofilm structure was quite robust to environmental changes. For instance, in the treatments recreating plume refreshing and plume advance scenarios their community structures remain stable. Furthermore, the comparison between the biofilm state after the change of the environmental conditions and the biofilms allowed to develop without changes, indicated significant changes in the abundance of some OTUs, but these differences in general represent less than a 5% of the total community. In this sense, the biofilm remained stable after the change of conditions, since over 90% of the OTUs did not show a response to the change of conditions. This might be a signal of the resistance offered by the biofilm to its members across changes in their chemical environment. It has been described that biofilm organisms tend to be more resilient to biological and physical disturbances, compared when they are in the mobile phase. In some situations, biofilms are able to resist periods of desiccation in aquifers (Weaver *et al.*, 2015; Mitchell *et al.*, 2008; Hancock *et al.*, 2005).

At the beginning of this chapter it was hypothesised that the biofilm exposed to a different chemical environment will change its community structure towards the planktonic community contained in this new environment; and an alternative hypothesis was that the biofilm is more robust and stable and the community structure tends to remain stable. The data from the biofilms exposed to different change of conditions, suggests that settled biofilms located at the chemical interfaces of polluted aquifers are able to remain stable under different types of modifications in their chemical environment.

#### ***How is the biofilm development driven by chemical interfaces in polluted aquifers?***

In this experiment there was an interest to understand how the settled biofilms will respond to inoculation with microbe-free groundwater. The removal of the planktonic community was made through triple-filtering to evaluate the differences on the biofilm structures under this filtered groundwater condition. This process should have been enough to sterilise the supernatant. The filters used have been tested by the manufacturer and are under the active standard ASTM F838 called "Standard Test Method for Determining Bacterial Retention of Membrane Filters Utilized for Liquid Filtration" (ASTM, USA). Despite the presence of potential microbes able to pass through filters, this standard secure the removal up to  $10^7$  cfu  $\text{cm}^{-2}$  of *Brevundimonas diminuta* (McBurnie and Bardo, 2004). The triple filtering reduces the risk of contamination even further. At the beginning of this chapter it was hypothesised that the biofilms are structured due to geochemical conditions and the planktonic microbial community and alternative hypothesis was that the biofilm is structured by the chemical environment. The

data comparison between the biofilm settled with and without microbial community, did not show any differences in the structure of the biofilms. Therefore, the biofilm development in chemical interfaces of polluted aquifers is driven as a response to the geochemical environment.

### **3.5 Conclusions**

This study let us set-up different environments located in the chemical interfaces of polluted aquifers. These settings were able to reproduce the biodegradation processes of microbial communities likely to be found in these locations, which are dominated by different terminal electron acceptor processes. These were the base to recreate different scenarios of chemical modification to biofilms located in chemical interfaces of polluted aquifers. The different change of environments showed different terminal electron acceptor processes, which are in tune with some of the microbial groups identified during the change of conditions. In terms of the planktonic microbial community it was possible to establish the high impact of the history of their chemical environment on the community. The biofilm communities located at chemical interfaces of polluted aquifers proved to be more resistant to modification on their chemical environment, which is the main driver of their development.

# Chapter 4

---

*Microbial community responses to chemical interfaces  
induced by Pump and Treat in a phenolic-contaminated  
aquifer*

---

## 4.1 Introduction

Pump and Treat (PAT) technology is an engineered technique to remediate groundwater pollution based on the introduction of pumping wells into contaminated aquifers and the extraction of pollutants by pumping, following by the *ex-situ* treatment of the contaminants to less harmful species (Keelay, 1989; Palmer *et al.*, 1992). The main objectives of PAT are either the reduction of pollutant concentrations or plume containment, which implies that plume boundaries remain stable in the aquifer (Mackay and Cherry, 1989; Kerr, 1990).

Many factors influence the efficiency of PAT, such as contaminant concentration, depth and extension of the plume, and hydrogeology of the aquifer. These factors are considered to define pumping rates, given that everything extracted must be treated. This also implies that the cleaning-up of pollutants may require the extraction and handling of significant amounts of background groundwater (Langwaldt and Puhakka, 2000). The use of PAT requires constant optimization, which is reached by testing different extraction well locations and variable pumping regimes. These variables are integrated into flow models and then applied on site for the management of pollutant plumes (McKinney and Lin, 1996; Huang and Mayer, 1997; Mattot *et al.*, 2006).

At the study site, the use of Monitored Natural Attenuation (MNA) in the management of a phenolic plume showed that these processes were not enough to cope with the amount of pollutants, and that the plume would spread through the aquifer. Furthermore, the isotope data on this aquifer suggested that Bacterial Sulphate Reduction (BSR) was inhibited when microbial communities were exposed to concentrations above 2000 mg l<sup>-1</sup> total phenolic content (Lerner *et al.*, 2000; Thornton *et al.*, 2001a). At this stage, it was hypothesized that the reduction of phenolic contamination by mass removal using PAT technology would promote the activity of the microbial community (Spence *et al.*, 2001;). **Figure 4.1** shows a schematic representation of the site with the boreholes (59 and 60) and extracting wells (P1 and P2) indicated. PAT showed the expected decrease in pollutant content, and produced the appearance of chemical interfaces likely to be found at the fringes to the core of the plume. The PAT also enhanced the biodegradation by the microbial community (Thornton *et al.*, 2014).



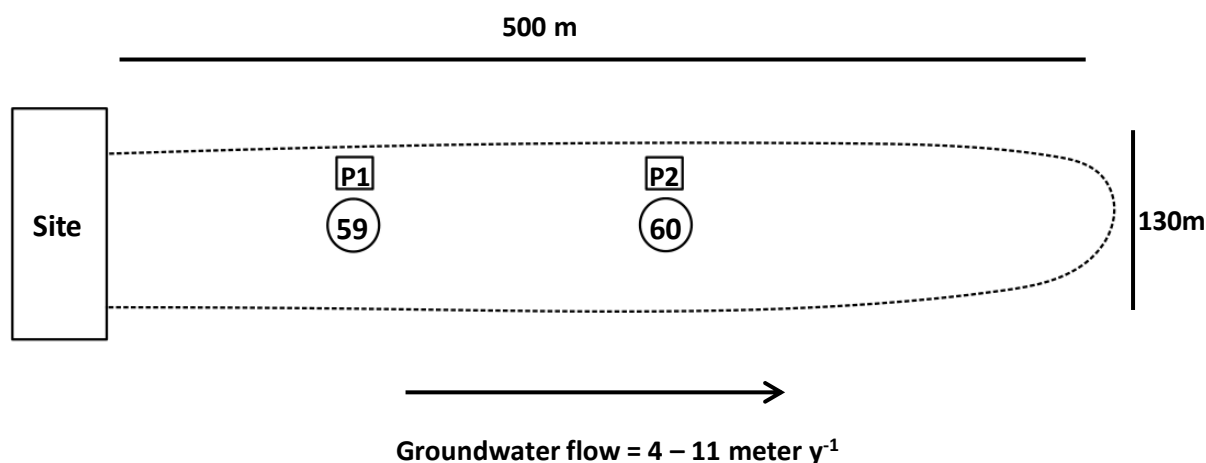


**Figure 4.1.** Plan view of the study site showing location of boreholes (BH) 59 and 60, and extraction wells P1 and P2 used for the operation of the PAT system. The dashed line shows the approximate location of plume boundaries (modified from Thornton *et al.*, 2014).

One of the most relevant features of the study by Thornton *et al.* (2014) was the use of isotopes to determine the activity of the microbial community. In several studies of microbial ecology it has been well established that microbes preferentially use isotopically lighter molecules (Boschker and Middelburg, 2002). For example, the use of preferential electron donor (carbon) creates a fractionation between the  $\delta^{13}\text{C}$  and  $\delta^{12}\text{C}$ -form of the molecules. This has also been observed during the biodegradation of polyaromatic hydrocarbons (Meckenstock *et al.*, 1999). A preference for the lighter form of electron acceptors has also been shown. For instance, the use of lighter form sulphate by bacterial sulphate reducers contributes to an enrichment of the  $\delta^{34}\text{S-SO}_4^{2-}$  pool (Peterson and Fry, 1987; Bottrell *et al.*, 2000). Other types of metabolism such as methanogenesis, which is relevant in anoxic environments, also present a typical isotopic signature resulting in a methane pool with reduced  $\delta^{13}\text{C-CH}_4$  (Botz *et al.*, 1996).

At the discussed study site, after 2 years of operation, one of the extracting wells was stopped (2011). It was not clear how the system (plume) would respond after the cease of operation. Moreover, the response of the microbial community to potential changes in the chemical interfaces induced by PAT was not clear. Thus, in this chapter, the use of molecular biology sequencing technologies and isotope fractionation were used to answer the following research questions.

## **Research questions**

The research questions considered for this chapter are the following:

- How does the switching-off of PAT affect the temporal and spatial distribution of pollutants?
- Does the enhancement of biodegradation persist over time?
- How do the microbial communities respond to the cease of PAT operations?
- How are the microbial communities influenced by an active PAT?
- What chemical gradients explain the variation of the system?

## **Research aim**

The aim of this chapter is to examine the responses of the microbial community to potential changes in the chemical interfaces induced by a PAT system and the influence of an active PAT on these communities. For this, the above mentioned study site was utilised, where PAT was applied in the aquifer to manage a plume composed of a mixture of phenolic compounds. Three annual surveys (2014, 2015 and 2016) were carried out in two multi-level samplers (MLS) close to the extracting wells of a PAT, providing samples for the laboratory experiments.

## **Research Hypothesis**

The following hypotheses were tested:

1. The ceasing of PAT will produce a movement of the chemical interfaces towards pre-implementation conditions. As an alternative hypothesis, it is considered that the PAT effect is sustained over time and the chemical interfaces remain in the position induced by PAT.
2. The termination of PAT will impact the microbial community, which becomes less active after the cease of the operations. As an alternative hypothesis, it is considered that the microbial community will remain active beyond the PAT operations.

## **Research Objectives**

The following objectives were pursued:

1. To determine the evolution of chemical interfaces after PAT operations were stopped in an aquifer polluted with phenolic compounds.
2. To evaluate the differences between the planktonic microbial communities before and after ceasing PAT operations.
3. To compare the effect of an active PAT system on the planktonic microbial community.

## 4.2 Methodology

### Groundwater sampling and chemical analysis

Groundwater samples were collected in July 2014, July 2015 and June 2016, using peristaltic pumps joined to a wellhead sampling tubes connecting to specific depths in two multi-level samplers (BH-59 and BH-60) close to the extraction wells. The methods for groundwater sampling and storage for phenolic, metals and major ions analysis was showed in the Methodology section of Chapter 3. For further details refer to Thornton *et al.* (2001a) and Thornton *et al.* (2014).

### Gas sampling and analysis

For gas sampling, a method comparable to the bubble-strip technique in the study of anoxic groundwater was applied (Lovley *et al.*, 1994; Chapelle *et al.*, 1997). Twenty ml of nitrogen was injected into groundwater-filled striping cells. The cells were linked to the different tubing of the MLS. After 30 minutes of a constant groundwater sample flow, gas was extracted and injected into septum-sealed vials, previously filled with nitrogen. Different blank standards were made in the laboratory and were taken into the field, then measured again in the lab to detect differences in gas content from the field. No changes were detected. In the lab, different standards were made using methane and carbon dioxide (BOC, UK) and analysed using a GC-2014 gas chromatograph containing a Flame Ionizing Detector, FID (Shimadzu, UK). The column used was a GS-Q 30 m x 0.535 mm (Agilent, UK). The mobile phase was nitrogen at a flow rate of 8.0 ml min<sup>-1</sup>. The temperatures of the injection, column and FID were 60, 240 and 240°C respectively. To calculate the final methane concentration, Henry's Law constant for groundwater at 12 °C was applied to the concentration obtained by the GC. **Figure 4.2** shows a picture of the system installed in the field.

### Microbiology sampling and analysis

The methodology for microbiology sample collection for cell counts and DNA extraction were described in the Methodology section of Chapter 3. The library preparation and bioinformatics are also described in Chapter 3.

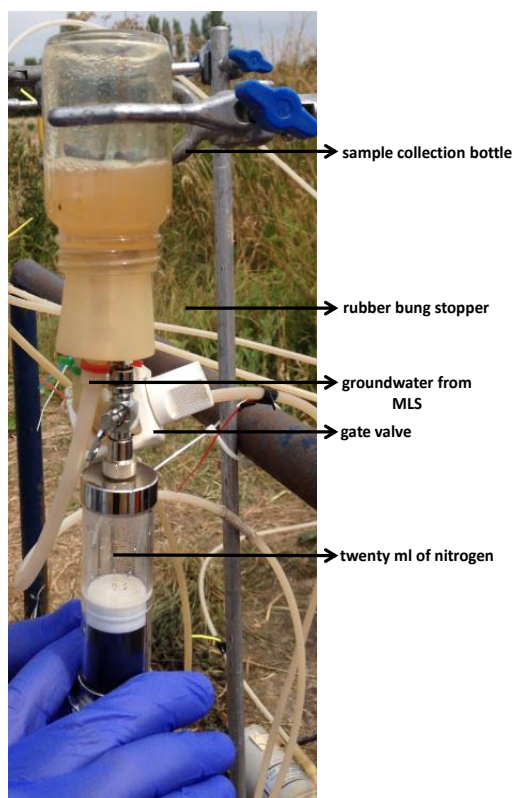


**Figure 4.2.** Gas sampling system used for gas sampling in the field. Groundwater port was connected to an inverted collection bottle. The gate valve was closed and nitrogen was injected into the bottle through the septum of a rubber bung stopper. Then, the gate valve was opened to allow a constant flow of  $\sim 100 \text{ ml min}^{-1}$  into the collection bottle for approximately 30 minutes. After this time, two aliquots of 10 ml of gas were recovered and injected into septum-sealed vials, previously filled with nitrogen.

#### Sample selection for sequencing

For the high throughput sequencing of the field samples a selection was made using their location in the plume and the microbial activity described in Thornton *et al.*, 2014 (**Table 4.1**).

**Table 4.1.** Depth selection for sequencing of field samples harvested during surveys in 2014, 2015 and 2016.

Borehole	Depths (mbgl)	Location	Justification
BH-59	11 and 12	Upper plume fringe	Nitrate reduction in the interface between background groundwater and the plume, due to nitrate reduction activity.
BH-59	13 and 14	Upper plume fringe	Enrichment of the isotopically heavier form of sulphate, due to bacterial sulphate reduction (BSR)
BH-59	24 and 26	Plume core	These depths were related to changes in the abundance of the heavier and lighter forms of

Borehole	Depths (mbgl)	Location	Justification
			sulphate, due to BSR and source-term variation after Pump and Treat (PAT) was switched-off
BH-59	22 and 28	Plume core	These depths were related to changes in the abundance of the heavier and lighter forms of total dissolved inorganic carbon (TDIC), due to beginning and switching-off of PAT
BH-59	29 and 30	Lower plume fringe	Enrichment of the isotopically heavier form of methane due to anaerobic methane oxidation (AMO)
BH-60	18 and 19	Upper plume fringe	Nitrate reduction in the interface between background groundwater and the plume, due to nitrate reduction activity
BH-60	20, 21 and 22 33, 34 and 35	Plume core	These depths were related to changes in the abundance of the heavier and lighter forms of sulphate, TDIC and methane, due to suppression of the inhibitory effect exerted by total phenolic content, increasing in biodegradation due to PAT and AMO, respectively
BH-60	44 and 45	Lower plume fringe	These depths were used to compare lower fringes at these locations

### Statistical analysis

Unifrac Principal Coordinate Analysis (Lozupone *et al.*, 2011) and identification of correlates variable were made using the phyloseq package (McMurdie & Holmes 2013) in R (R Development Core Team, 2011). For the constrained analysis of principal coordinates, all the bulk chemical data of BH-59 and BH-60, showing a significant relationship between the OTU ordination and chemical gradients was used.

```
>anova(cap_ord59)

Permutation test for capscale under reduced model
Permutation: free
Number of permutations: 999

Model: capscale(formula = distance ~ tpc + Fe + Mn + NO3 + SO4 + acetate + CO2
+ CH4 + TDIC + S2, data = data)

          Df SumOfSqs      F Pr(>F)
Model     10 0.062776  2.639  0.001 ***
Residual  19 0.045197
```

The important terms to be analysed for the complete model are shown below.

```
> anova(cap_ord59,by="term", perm.max=199)

Permutation test for capscale under reduced model
Terms added sequentially (first to last)
Permutation: free
Number of permutations: 999

Model: capscale(formula = distance ~ tpc + Fe + Mn + NO3 + SO4 + acetate + CO2
+ CH4 + TDIC + S2, data = data)
      Df SumOfSqs      F Pr(>F)
tpc     1 0.004174  1.7548  0.120
Fe       1 0.005857  2.4623  0.058 .
Mn       1 0.009570  4.0231  0.011 *
NO3      1 0.009174  3.8565  0.013 *
SO4      1 0.003416  1.4361  0.168
acetate  1 0.002090  0.8784  0.422
CO2      1 0.004443  1.8677  0.102
CH4      1 0.008200  3.4470  0.015 *
TDIC     1 0.013840  5.8179  0.001 ***
S2       1 0.002012  0.8458  0.426
Residual 19 0.045197
```

To identify the minimum number of terms to include in the model, a stepwise analysis was performed. This compares the unconstrained model (m0) with constrained models in which terms are added in order of their importance. It is important to note that the addition of a term to the model will generally exclude other terms which are correlated (either positively or negatively) with that term, but does not mean that they are not biologically important.

```
#varespec contains the OTU abundances (normalised for counts)
#varechem contains chemical abundances (normalised by mean and SD)

#The complete model
>m1<-capscale(varespec59[comp59,] ~ .,varechem59sccomplete)

Call: capscale(formula = varespec59[comp59, ] ~ phenol + mpcresols + ocresols
+ xylenols + Fe + Mn + NO3 + SO4 +
acetate + CO2 + CH4 + TDIC + TDIC_d13C + SO4_d34S + CH4_d13C + S2 + tpc, data
= varechem59sccomplete)

              Inertia Proportion Rank
Total          1.504e+06  1.000e+00
Constrained    1.152e+06  7.661e-01  16
Unconstrained  3.518e+05  2.339e-01   8
Inertia is mean squared Euclidean distance
Some constraints were aliased because they were collinear (redundant)

#The unconstrained model
>m0<-capscale(varespec59[comp59,] ~ 1,varechem59sccomplete)
Call: capscale(formula = varespec59[comp59, ] ~ 1, data = varechem59sccomplete
)

              Inertia Rank
Total          1504308
Unconstrained 1504308   24
Inertia is mean squared Euclidean distance

m <- step(m0, scope=formula(m1), test="perm")
```

### Stepwise model addition

```
> m <- step(m0, scope=formula(m1), test="perm")
#Only final step shown
```

```
Step: AIC=352.29
```

```
varespec59[comp59, ] ~ TDIC + CO2 + NO3 + Fe
```

	Df	AIC	F	Pr(>F)
<none>		352.29		
+ Mn	1	352.45	1.4527	0.145
- Fe	1	352.45	1.8072	0.070 .
- CO2	1	352.71	2.0323	0.030 *
+ CH4_d13C	1	352.89	1.0958	0.385
+ TDIC_d13C	1	352.93	1.0645	0.310
- NO3	1	353.01	2.2946	0.015 *
+ CH4	1	353.06	0.9578	0.465
+ S2	1	353.11	0.9193	0.480
+ acetate	1	353.18	0.8595	0.570
+ mpcresols	1	353.47	0.6376	0.775
+ SO4	1	353.57	0.5553	0.870
+ SO4_d34S	1	353.59	0.5382	0.865
+ xylenols	1	353.74	0.4198	0.955
+ tpc	1	353.74	0.4198	0.970
+ ocresols	1	353.79	0.3846	0.970
+ phenol	1	353.79	0.3813	0.985
- TDIC	1	354.52	3.6915	0.005 **

### Isotopes data

Isotopes data was provided by Michael Cook from the University of Leeds, UK.  $\delta^{34}\text{S-SO}_4^{2-}$  was determined by  $\text{BaCl}_2$  precipitation,  $\delta^{13}\text{C-TDIC}$  (Total Dissolved Inorganic Carbon) was calculated through the recovery of  $\text{SrCO}_3$  followed by a reaction with phosphoric acid and  $\delta^{13}\text{C-CH}_4$  was measured by combustion. For details of the method used see Thornton *et al.* (2014).

### 4.3 Results

#### Total phenolic content (TPC)

The PAT system next to BH-59 was switched off in 2011, whereas at BH-60 there was an active PAT. The plume was located between 11 - 30 mbgl and 20 - 45 mbgl for BH-59 and BH-60, respectively. Above the plume, between 5 to 10 mbgl was the background groundwater for BH-59 and, while the background groundwater occupied the depths between 5 to 19 mbgl at BH-60.

**Figure 4.3** shows the concentrations of TPC (phenols, *m,p,o*-cresols and xylenols) at different depths of BH-59 over a three-year sampling period. The highest TPC was registered in 2014 at the plume core (23 to 28 mbgl) with values above 5000 mg l<sup>-1</sup>. Concentrations were much lower within the plume fringes. In 2015, TPC was reduced by approximately half. In 2016, concentrations were reduced further with a peak of only 255 mg l<sup>-1</sup> of TPC (**Figure 4.3.a**). In comparison to BH-59, at BH-60 the TPC content was relatively stable over time. In 2014, the highest concentrations were located at the plume core (28 to 34 mbgl) with values above 4000 mg l<sup>-1</sup>. In 2015, TPC increased up to 6000 mg l<sup>-1</sup>, and in 2016 the range of TPC increased further (~ 6400 mg l<sup>-1</sup>). The effect of the PAT on TPC at BH-60 was stable over time (**Figure 4.3.b**).

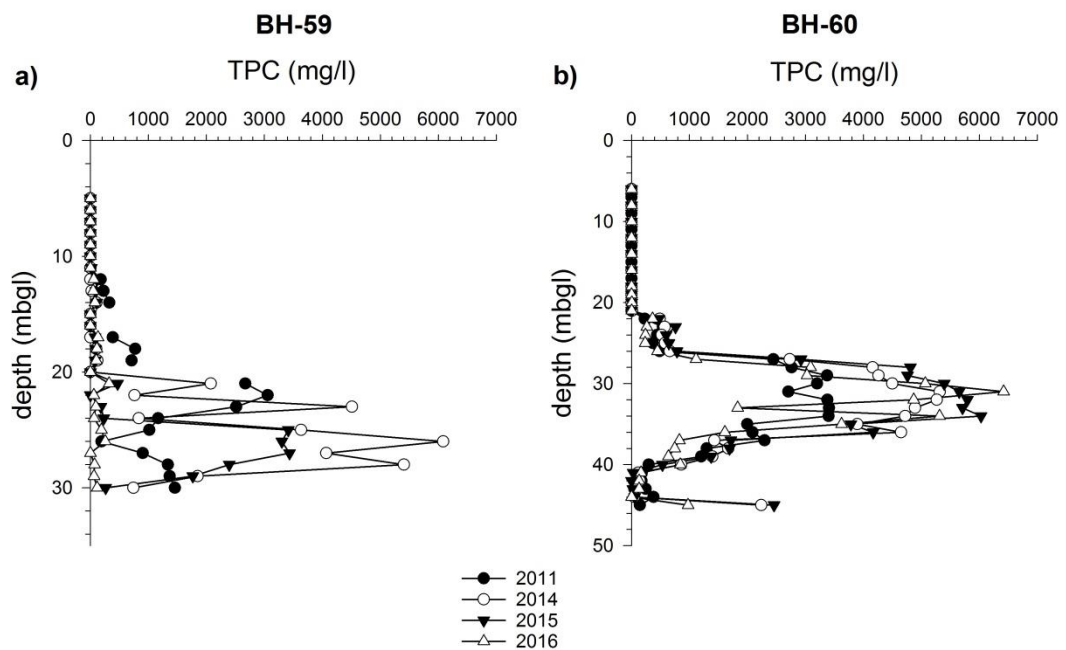


**Figure 4.3.** Depth profiles of TPC in (a) BH-59, close to this BH a PAT was switched-off on 2011 and (b) BH-60, location under the influence of a PAT close to the location (n=1). The water table was located at 5 mbgl approximately.



### ***Indicators of in-situ biodegradation processes***

To assess the temporal and spatial variation in biodegradation, the measurement of different steady-state chemicals and isotopes were carried out. **Figures 5.4, 5.5 and 5.6** show depth profiles at BH-59 and BH-60 of different electron acceptors (nitrate, manganese, iron) and other biodegradation indicators in groundwater.

The nitrate content at BH-59 was higher in the background groundwater ( $\sim 45 \text{ mg l}^{-1}$ ) compared to the plume core during the entire period of monitoring. Nitrate concentration showed a rapid decrease between 11 and 14 mbgl, location occupied by the plume fringe. During 2014, nitrate reached almost depletion levels within the core of the plume, but in 2015 at various locations within the plume core, nitrate was again registered. Nitrate was also detected in 2016, at locations of the plume core close to the lower plume fringe (**Figure 4.4.a**). Similarly, at BH-60, the nitrate content was higher in the background groundwater compared to levels observed within the plume. Here, in the background groundwater the nitrate content increased from  $41 - 105 \text{ mg l}^{-1}$  from 2014 to 2016. The plume fringe at BH-60 was located between 18 and 22 mbgl, where the nitrate concentration decreased sharply. The nitrate content reached depletion levels in the plume core during 2014 and 2016. In 2015 nitrate was detected at the plume core (**Figure 4.4.b**).

At BH-59, manganese content reached depletion levels in the background groundwater during the entire period of monitoring. At the plume fringe, manganese content was still low ( $< 2.5 \text{ mg l}^{-1}$ ) and the plume core manganese concentrations were the highest detected and varied over time. In 2014, the range of manganese concentration in the plume core was between  $6 - 14 \text{ mg l}^{-1}$ . In 2015, manganese content increased ( $7 - 25 \text{ mg l}^{-1}$ ). Finally, in 2016, manganese concentration decreased again ( $6 - 14 \text{ mg l}^{-1}$ ) (**Figure 4.4.c**). At BH-60, manganese concentrations in the background groundwater reached depletion levels similar to BH-59 during different surveys. In the plume fringe, manganese content increased compared to the background groundwater ( $0.01 - 9 \text{ mg l}^{-1}$ ). At the plume core, manganese concentrations were the highest detected. In 2014, the range of manganese concentrations in the plume core was between  $4 - 46 \text{ mg l}^{-1}$ , and in 2015 and 2016, there were no significant changes in the range of manganese concentration observed in the plume core. The effect of the PAT on manganese concentration at BH-60 over time remained stable, and the concentration of this metal at different depths remained relatively unaltered (**Figure 4.4.d**).

At BH-59, iron content reached depletion levels at almost all depths in the background groundwater during the entire period of monitoring, except at 7 mbgl in 2014. In the plume fringe, iron content increased slightly ( $0.3 - 5 \text{ mg l}^{-1}$ ). At the plume core iron concentrations

were the highest levels detected and varied over time. In 2014, the range of iron concentrations in the plume core was between 18 – 33 mg l<sup>-1</sup>. In 2015, iron content increased (4 – 38 mg l<sup>-1</sup>). Finally, in 2016, the range of iron concentrations decreased (0.2 – 33 mg l<sup>-1</sup>). Nevertheless, the range of concentrations did not show considerable variation. Focusing between 20 and 30 mbgl, it was possible to observe a decrease in concentrations from 2014 to 2015, and an increase in the iron content from 2015 to 2016 (**Figure 4.4.e**)

At BH-60, iron concentrations in the background groundwater reached depletion levels during the monitoring period. At the plume fringe, iron content increased compared to the background groundwater (0 – 32 mg l<sup>-1</sup>). At the plume core, iron was at the highest concentration within the depth profile and exhibited different spatial patterns. For instance, between 20 and 27 mbgl iron content was high and stable across the three surveys. After these depths, a dramatic decrease of iron concentrations took place between 27 and 30 mbgl. This trend was stable across the entire period of monitoring. Deeper into the plume the iron concentrations remained low (< 10 mg/L) and stable between 30 and 40 mbgl, followed by a rapid increase to the lower plume fringe. Over the sampling period, these trends remained unaltered by the PAT system close to BH-60 (**Figure 4.4.f**).

At BH-59, sulphate concentrations in the background groundwater were stable during the surveys (~20 mg l<sup>-1</sup>). In the plume fringe, sulphate content decreased compared to the background groundwater, which correlated with an increase in the isotopically heavy form of sulphate ( $\delta^{34}\text{S-SO}_4$ ) between 11 and 14 mbgl. In the plume core, sulphate content showed considerable variations within different depths across the monitoring period. Nevertheless, enrichment in the isotopically heavy form of sulphate was detected between 17 to 22 mbgl, while at deeper levels sulphate became isotopically lighter across the period of study (**Figure 4.5.a**).

At BH-60, sulphate concentrations in the background groundwater were also stable during different surveys (10 – 45 mg l<sup>-1</sup>). In the plume fringe there was an increase in sulphate content (45 – 71 mg l<sup>-1</sup>), which coincided with an enrichment of the isotopically heavy form of sulphate between 18 – 22 mbgl. Deeper into the plume core, between 23 and 35 mbgl, sulphate concentrations increased considerably, reaching approximately 350 mg l<sup>-1</sup> at some depths. At these depths the isotopically lighter form of sulphate became more abundant. A decrease in sulphate concentration was detected from 36 mbgl to the lower plume fringe, which coincided with an enrichment of isotopically heavy form of sulphate. During the different surveys, these trends remained relatively unaltered by the PAT system operating close to BH-60 (**Figure 4.5.b**).

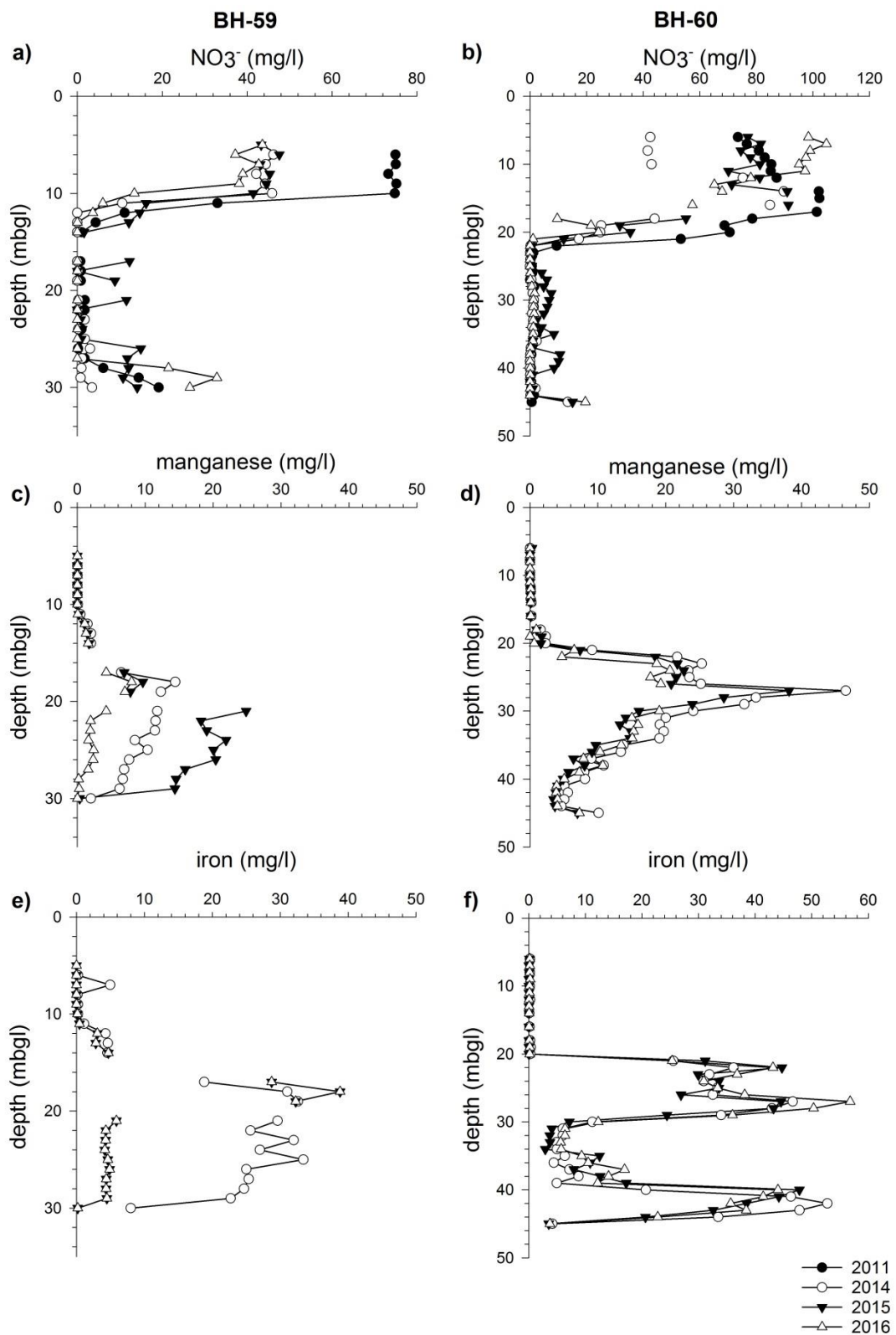


**Figure 4.4.** Depth profiles of different electron acceptors in groundwater at BH59 (left) and BH-60 (right). The water table was located at 5 mbgl approximately (n=1). Manganese and iron were not measured in 2011.

At BH-59, the total dissolved inorganic carbon (TDIC) in the background groundwater was detected to be lower ( $38 - 71 \text{ mg l}^{-1}$ ) than within the plume. The concentration of TDIC

increased rapidly (to 151 – 332 mg l<sup>-1</sup>) in the upper plume fringe, from 2014 to 2015. This increase coincided with an enrichment of the isotopically heavier form of carbon ( $\delta^{13}\text{C-TDIC}$ ). From 2015 to 2016 the carbon in TDIC became isotopically lighter. Towards or within the core of the plume the TDIC increased further, reaching values consistently above 330 mg l<sup>-1</sup> between 19 to 23 mbgl, which correlated with a general trend of enrichment in the lighter form of carbon. TDIC decreased again towards the lower plume fringe, the isotopic enrichment progression following a similar trend observed across the plume fringe (**Figure 4.5.c**).

At BH-60, TDIC was lower in the background groundwater compared to its content in the plume. At the plume fringe TDIC increased dramatically, reaching 450 mg l<sup>-1</sup> approximately. These values remain high down to 25 mbgl. The increase in TDIC coincided with a general trend of enrichment of the isotopically heavy form of carbon. TDIC decreased from 26 to 30 mbgl and these values remained consistently low to 34 mbgl. The decreasing TDIC correlated with an enrichment of the lighter form of carbon. Finally, TDIC increased from 35 mbgl towards the lower plume fringe, which coincided with an enrichment in the heavier form of carbon in the TDIC. Over time, these trends remained unaltered by the PAT system operated at BH-60 (**Figure 4.5.d**).

At BH-59, methane exhibited depletion levels in the background groundwater, while in the plume fringe methane increased rapidly (1 – 19 mg l<sup>-1</sup>). At this chemical interface towards deeper levels in the plume a decrease in the isotopically heavy form of methane ( $\delta^{13}\text{C-CH}_4$ ) was detected. In the plume core, methane content showed considerable variation within different depths across the monitoring period. Nevertheless, enrichment in the isotopically lighter form of methane was detected between 17 to 22 mbgl. On the contrary, between 22 to 24 and 28 to 30 mbgl, an enrichment in the isotopically heavier form of methane was observed (**Figure 4.5.e**).

At BH-60, methane concentrations were depleted in the background groundwater. At the plume fringe there was a slight increase in methane content ( $\sim 0.3$  mg l<sup>-1</sup>). At the plume core methane concentrations increased from 22 to 25 mbgl, and deeper into the plume core, at 26 to 32 mbgl, methane content increased further, reaching approximately 8 mg l<sup>-1</sup> in some depths. In terms of the isotopic signature of methane, two regions could be distinguished. From 18 to 32 mbgl an enrichment of the isotopically heavy form of methane was observed. From 33 to 45 mbgl, in 2014, the isotopically heavy form dominated these depths, while over time methane became isotopically lighter at these locations (**Figure 4.5.f**).

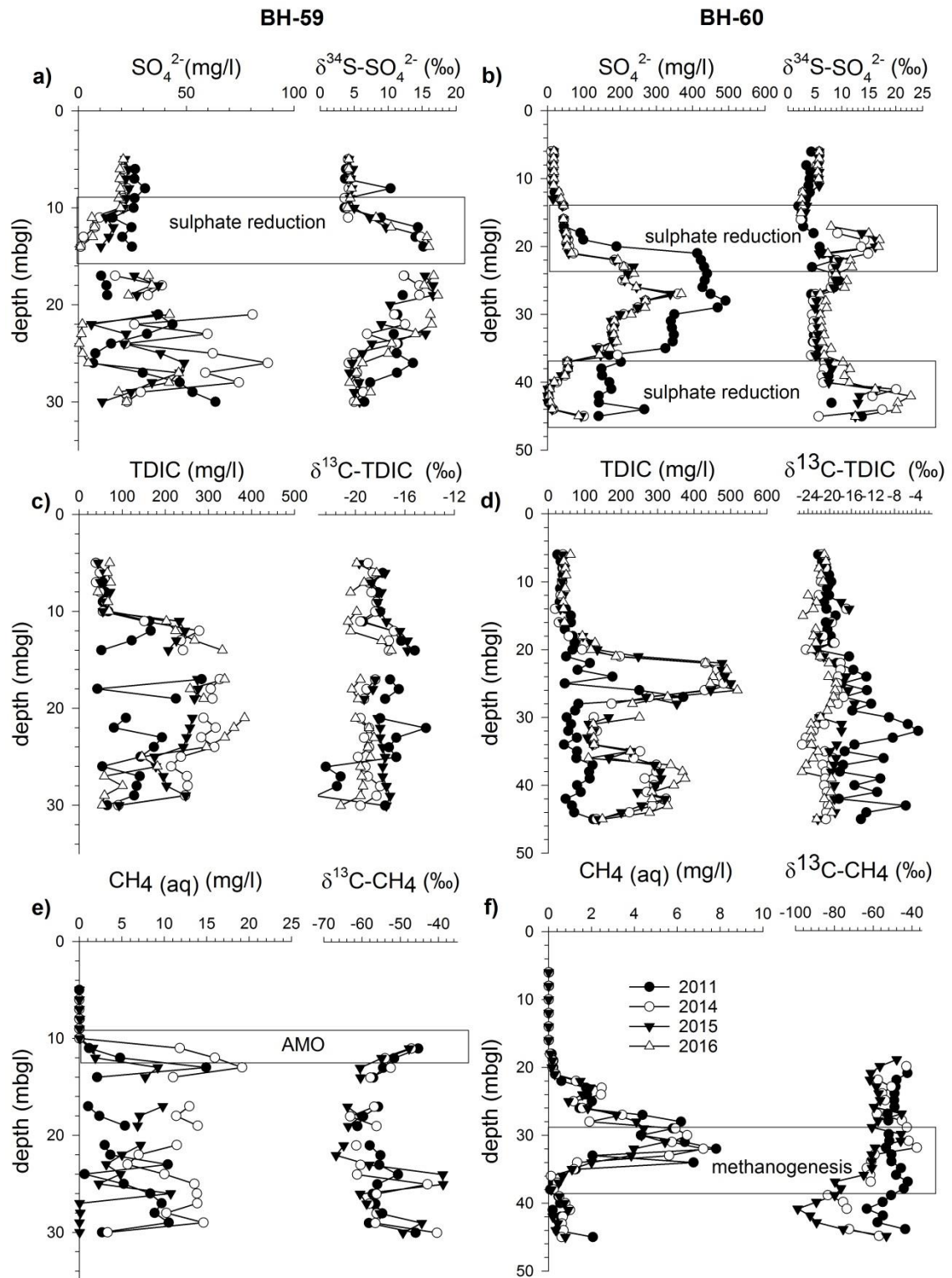


**Figure 4.5.** Depth profiles of different compounds (concentration and isotopic composition) in groundwater at BH-59 (left) and BH-60 (right). The water table was located at 5 mbgl approximately ( $n=1$ ). Potentially dominant processes at specific depth are shown. Methane was not measured in 2011.

At BH-59, acetate was depleted in the background groundwater. In 2014, acetate concentrations reached the highest values of the three surveys. At the upper plume fringe was located the higher acetate content (12 – 91 mg l<sup>-1</sup>), compared to the values to the plume core (23 – 47 mg l<sup>-1</sup>). In the following surveys acetate values decreased considerably. In BH-60, the highest acetate concentrations were detected to the plume core in 2014, reaching values over 100 mg l<sup>-1</sup>. In the following surveys, similarly to the conditions observed at BH-59, acetate values were reduced considerably (Figure 4.6.a-b)

At BH-59, cell numbers of the planktonic community were higher in both the upper and lower plume fringes in 2014. In the following surveys, the cell numbers increased to approximately 10<sup>6</sup> cells ml<sup>-1</sup>, with the higher cell densities located in the upper plume fringe, followed by a few locations within the plume core (17 and 18 mbgl). At BH-60, the general trend was an increase in cell numbers from 2014 to 2016 at the plume core, but across the monitoring period cell densities decreased at different depths of the plume core (Figure 4.6.c-d)

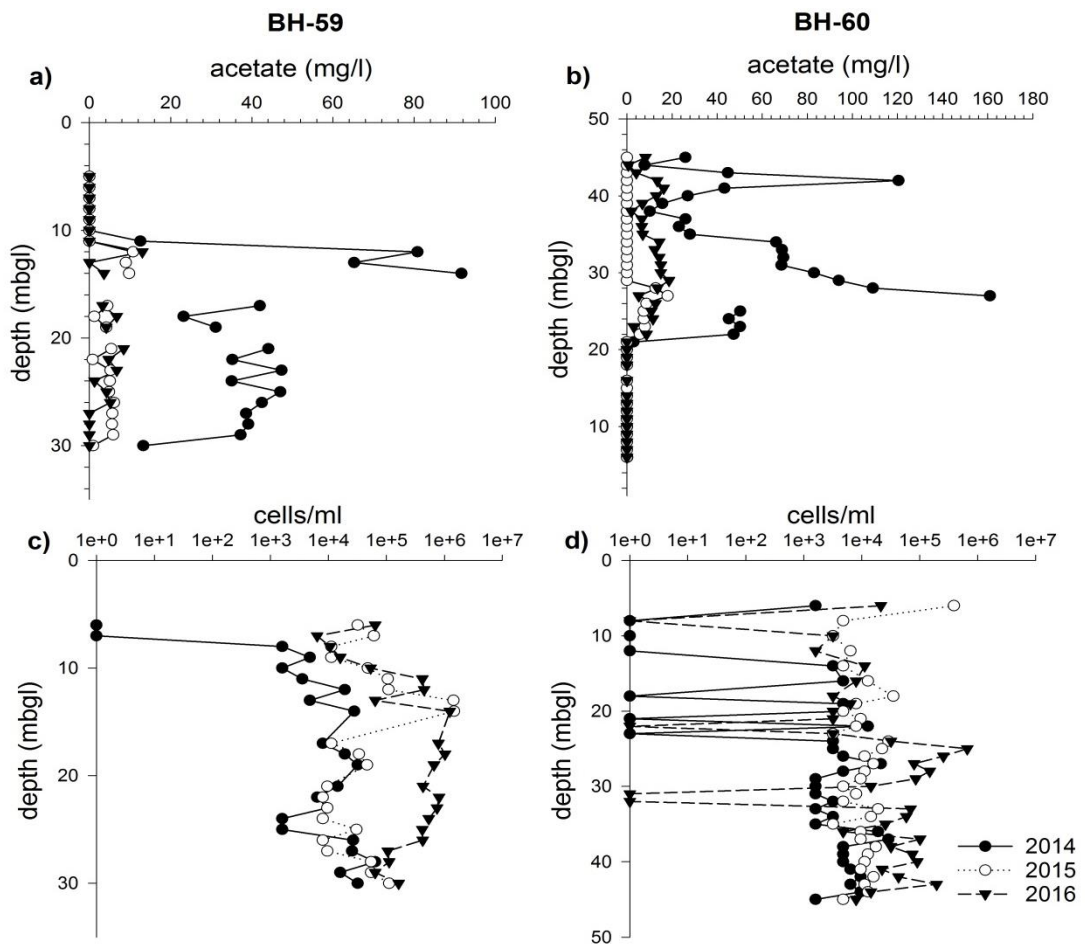


**Figure 4.6.** Depth profiles of acetate concentration and cell densities in groundwater at BH-59 (left) and BH-60 (right). The water table was located at 5 mbgl approximately (n=1). Acetate and cells counts were not measured in 2011.

**Figure 4.7** shows the relative abundances of microbial groups detected at BH-59 and BH-60 over the three-year sampling period. Similar trends can be observed for different microbial groups. For example the Phylum Proteobacteria had high relative abundance at both locations, across different depths and during all the period of the study. One of the main differences were exhibited by the relative abundances of Firmicutes and Bacteroidetes at BH-59 compared to at BH-60.

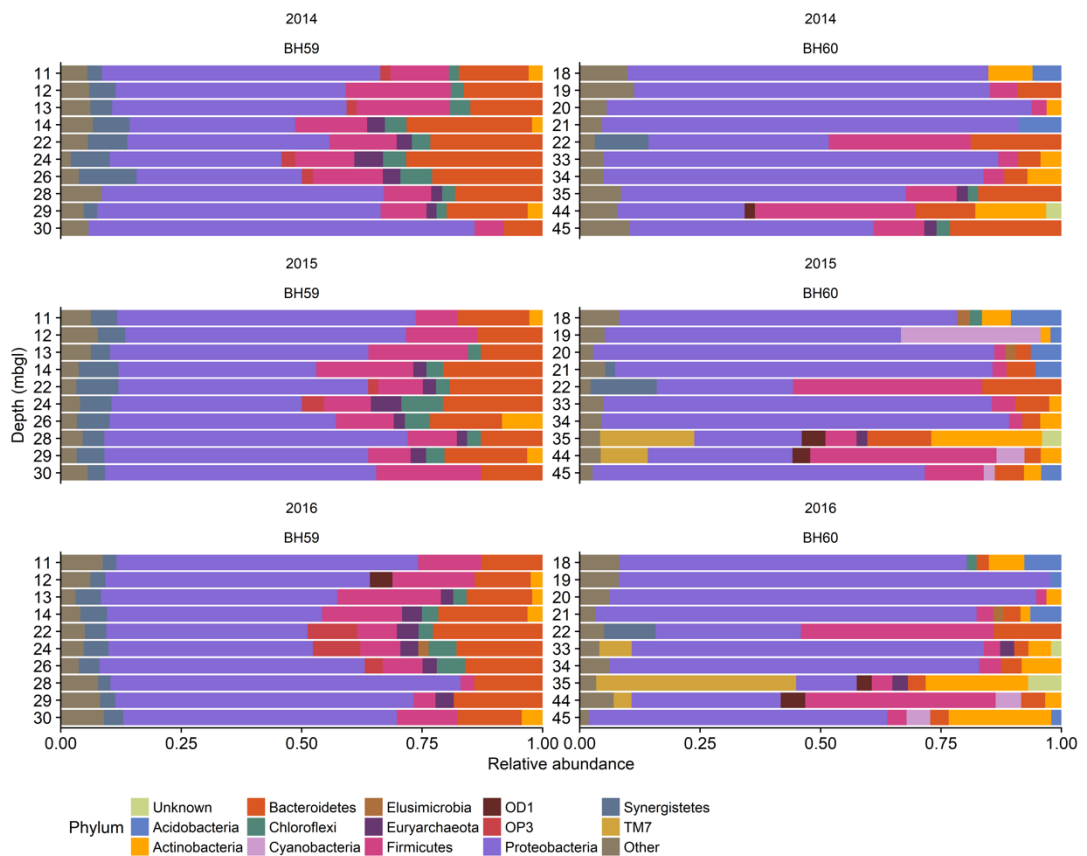


**Figure 4.7.** Relative abundances of different microbial groups at Phylum level at BH-59 (left) and BH-60 (right) over a three year period (2014, 2015 and 2016).

As the *Proteobacteria* were such a large and dominant Phylum the diversity within this taxa was examined. **Figure 4.8** shows the relative abundances of the *alpha*, *beta*, *delta*, and *gamma-Proteobacteria*. *Beta* and *delta-proteobacteria* were the dominant groups in these environments.

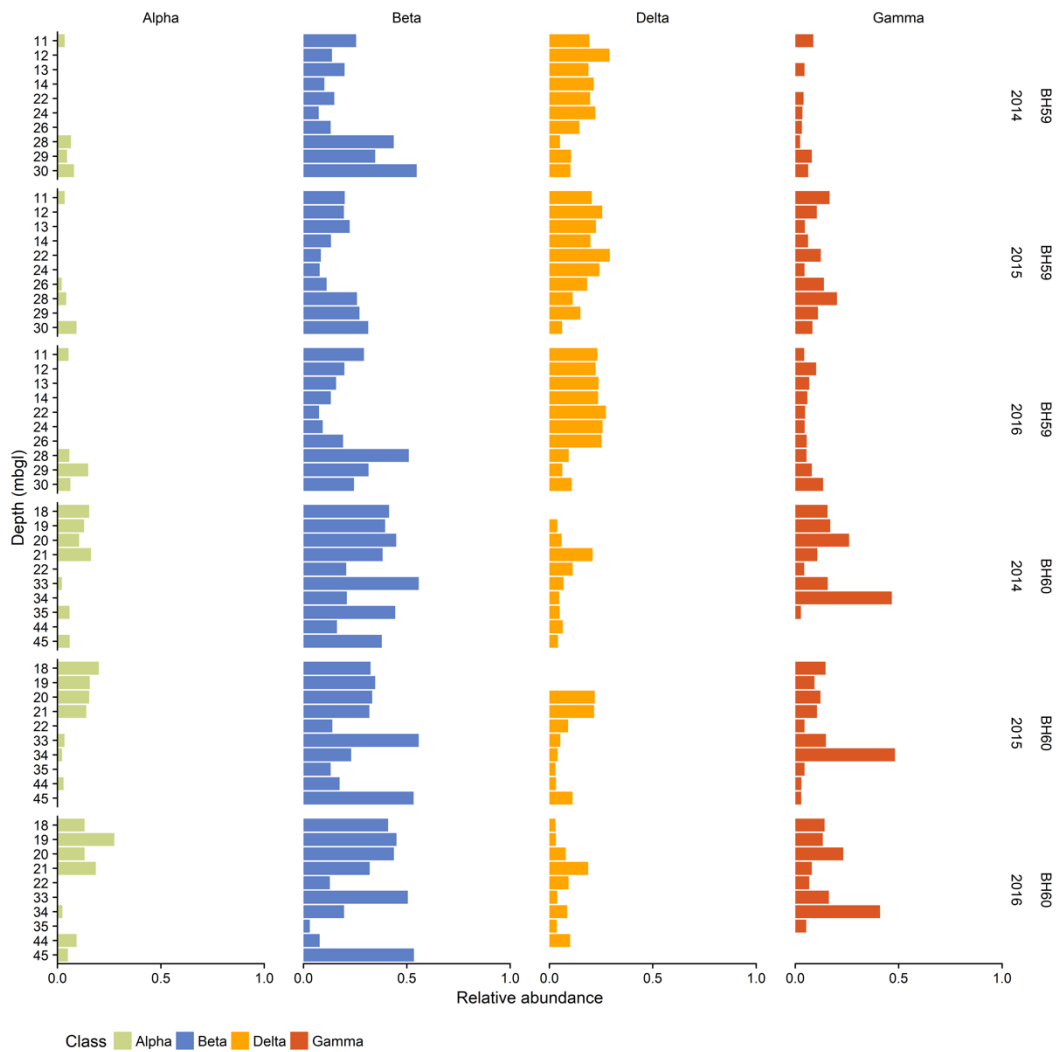


**Figure 4.8** Relative abundances of Proteobacteria Phylum at Class level at BH-59 and BH-60 over a three year period (2014, 2015 and 2016).

Different community structure metrics were considered in the analysis. **Figure 4.9** shows richness, inverse Simpson and Shannon indexes. The different metrics showed variability across depth profiles and over the three years of monitoring at both locations. Analysis of variances (ANOVA) on the richness showed no statistical differences between boreholes ( $F_{1,54}=0.000$ ,  $p=0.991$ ) or years ( $F_{1,54}=2.173$ ,  $p=0.124$ ). Similar analysis on inverse Simpson and Shannon indexes indicated statistical differences between boreholes ( $F_{1,54}=18.646$ ,  $p<0.001$  and  $F_{1,54}=12.851$ ,  $p<0.001$ ). This was an indication that community structures differ between BH-59 and BH-60, as the differences detected on inverse Simpson and Shannon indexes implicate a different OTUs distribution between these two locations.



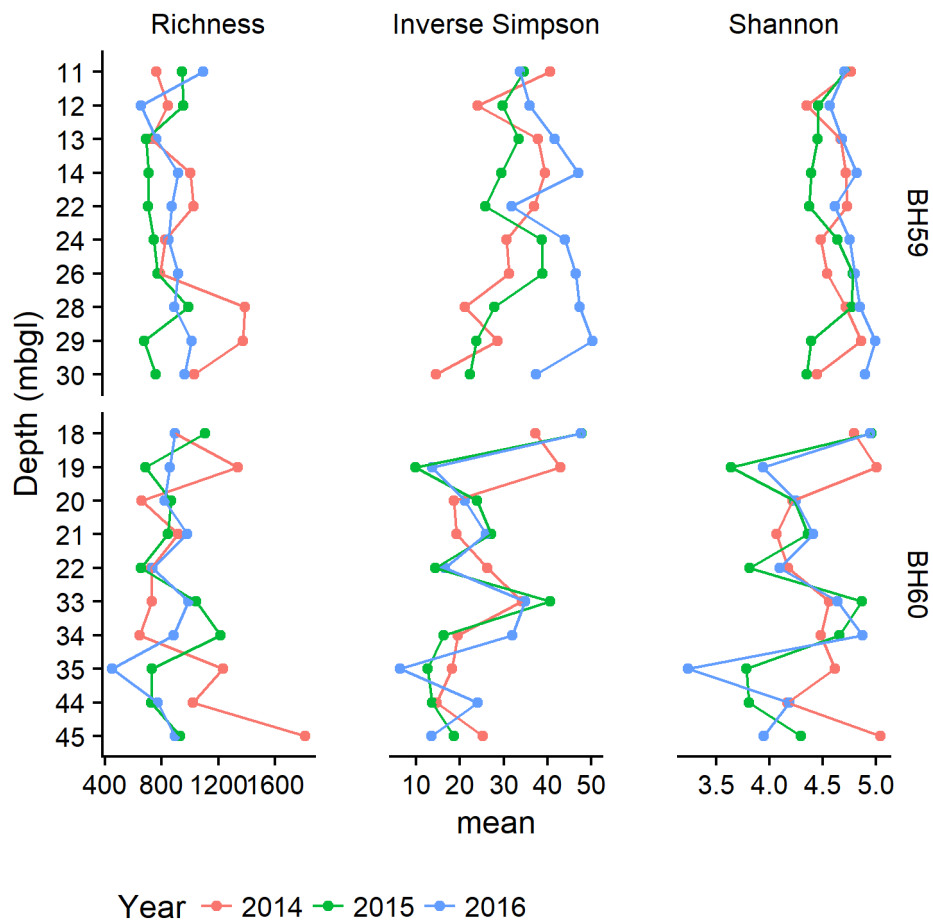


**Figure 4.9.** Community structure metrics of richness, inverse Simpson and Shannon indexes at BH59 and BH-60 over a three year period (2014, 2015 and 2016).

To assess the differences between the microbial communities of each sample in depth, it was necessary to use different ordination methods that take into account the relative abundances, the phylogenetic relationship between different microbial groups, and the geochemical environment.

**Figure 4.10** shows a Principal Coordinate Analysis (PCoA), using weighted Unifrac as the distance measure of OTUs of all samples from both boreholes and years. The PCoA indicated that the borehole had a significant impact on the distribution of the samples within the ordination. The first two axes explained 56% of the variation in the samples (Inspection of the screen plot showed that these were the dominant components). Permutational Multivariate Analysis of Variance using the R package ‘adonis’ showed that the OTU relative abundance between the boreholes differed significantly ( $F_{1,54}=7.884$ ,  $p=0.001$ ) but there was no impact of year of measurement ( $F_{1,54}=7.884$ ,  $0.792$ ,  $p=0.758$ ), nor an interaction between these two

terms ( $F_{1,54}=0.436$ ,  $p=0.834$ ). For the downstream analysis each location was analysed separately.

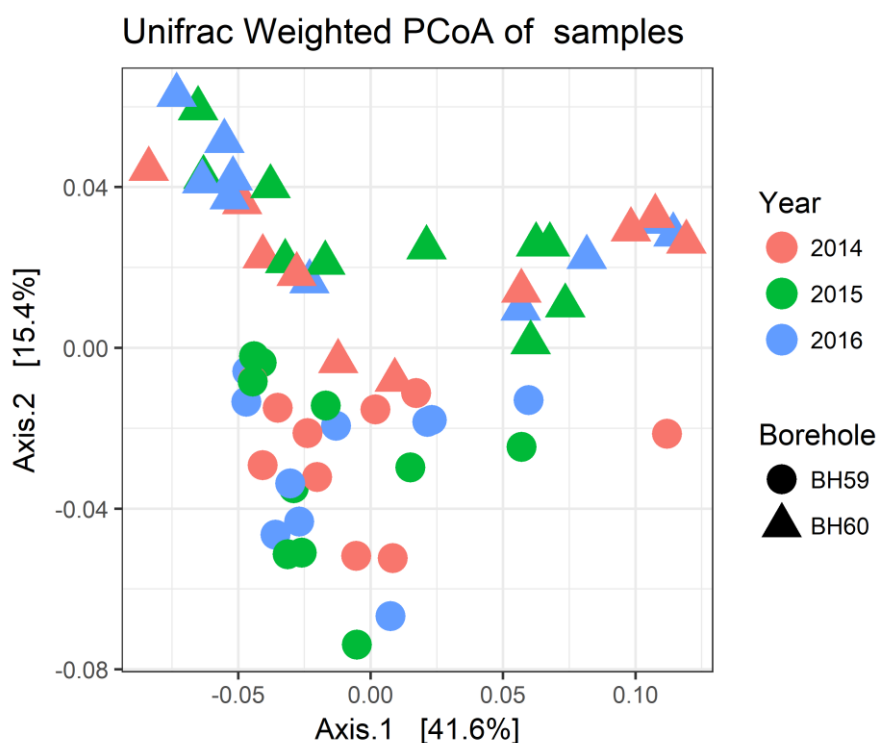


**Figure 4.10.** Unifrac weighted PCoA on the community structures in groundwater at two boreholes in a site polluted with phenolic compounds.

**Figure 4.11** shows PCoAs of BH-59 and BH-60 performed independently and coloured by TPC concentration. These ordinations showed an apparent grouping of high TPC locations. Nevertheless, the grouping based on TPC did not describe entirely the distribution observed. On the other hand, there was not a clear effect of sampling year on the distribution of the samples. Therefore, CAP (Canonical Analysis of Principal Coordinates) was used overlay chemical gradients on the ordination based on the OTU relative abundances.

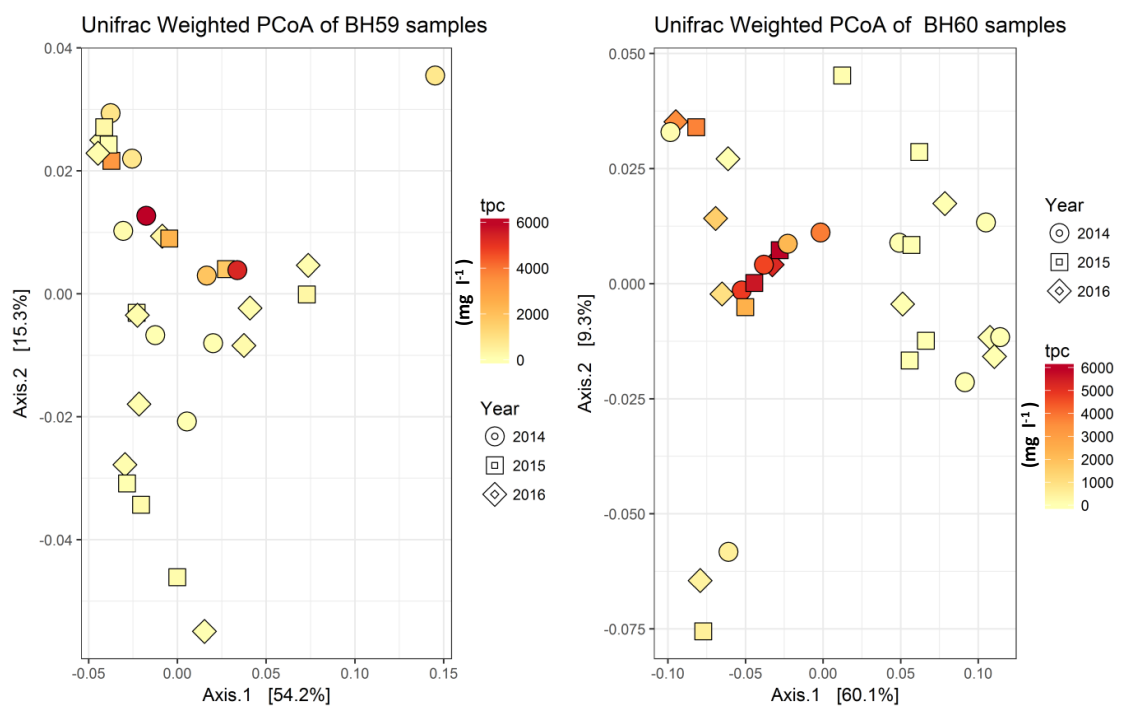


**Figure 4.11.** Unifrac weighted PCoA on the community structures in groundwater at BH-59 (left) and BH-60 (right) of a site polluted with phenolic compounds.

**Figure 4.12** shows CAP for BH-59 and BH-60 using the chemical data (but not the isotopic measurements). In both cases the boreholes showed three major groupings. When the vectors of individual chemical compounds were overlaid onto these ordinations, it was apparent that BH-59 differed to some extent from BH-60. At BH-59, there were strong gradients associated to  $\text{NO}_3^-$ , TDIC and  $\text{CH}_4$  with the other vectors chemicals closely correlated. At BH-60,  $\text{NO}_3^-$  and Fe/TDIC/ $\text{CO}_2$  were important vectors with complex interactions between the other chemicals measured.

This analysis used all the bulk chemical data available but numerous issues need to be considered:

1. These sorts of analyses require complete data sets but the isotopic data were incomplete. Therefore, a subset of the samples was analysed to investigate the relationships between bulk chemicals, isotopes and OTUs.
2. Using all the available data in CAP analysis (and related methods) is inadvisable as factors may be correlated. When determining which factors are important to include in models, only 1 member of a closely correlated group of compounds will be selected but this does not mean that this is the most important member of the correlated group.

Correlations between different variables are shown in **Figure 4.13**. At both boreholes, there were strong, positive correlations between the phenol, *m,p*-cresols, *o*-cresols and xylenols (and the sum, TPC). At BH-59 there were negative correlations between nitrate and TDIC, nitrate and  $\delta^{34}\text{S-SO}_4$ , nitrate and iron; and between sulphate and its heavier isotope. At BH-60,  $\delta^{34}\text{S-SO}_4$  was negatively correlated with all the pollutants, sulphate and manganese.

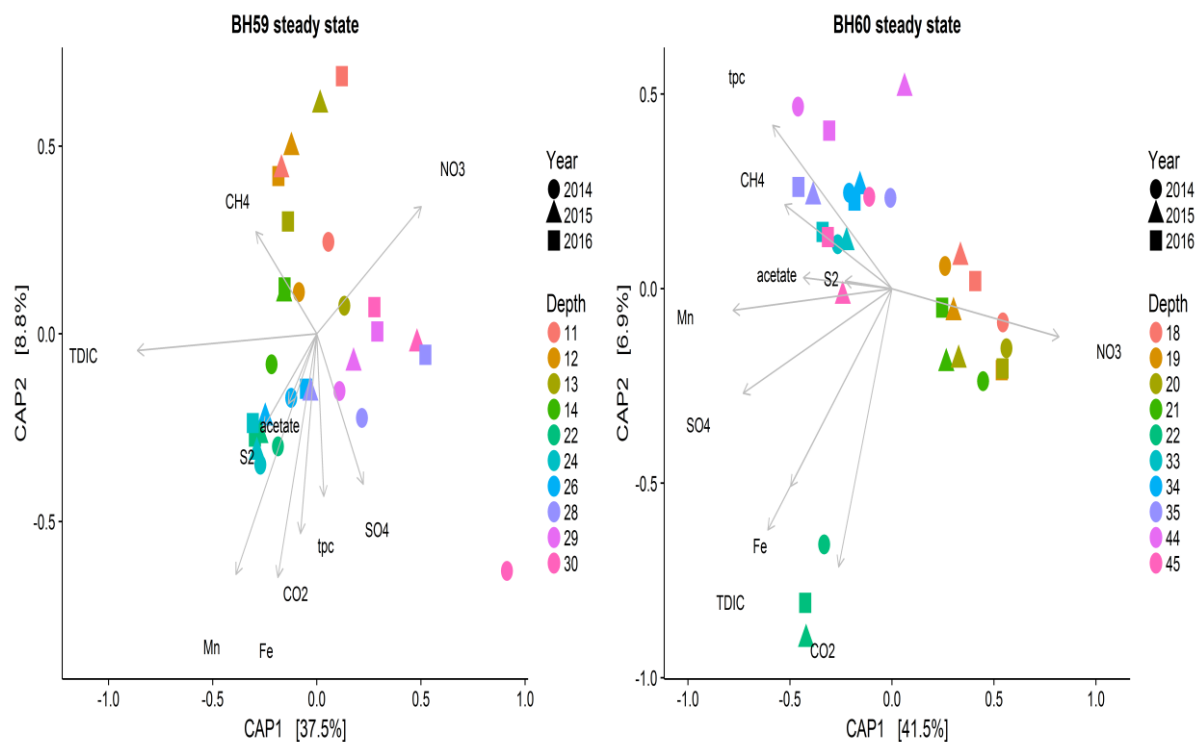


**Figure 4.12.** Canonical Analysis of Principal Coordinates of steady-state data obtained at BH-59 (left) and BH-60 (right) over a 3 years period (2014, 2015 and 2016).

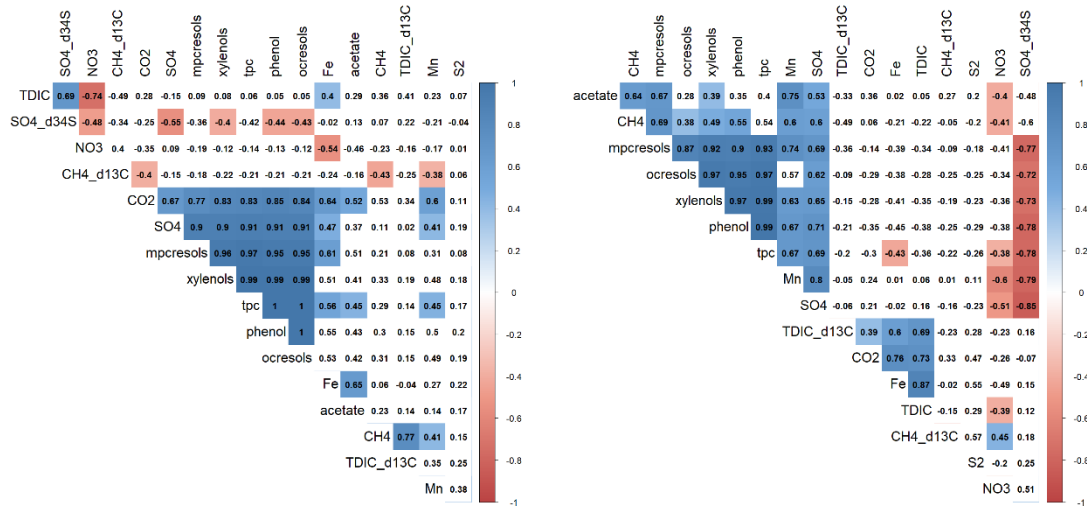


**Figure 4.13.** Correlations between chemical measurements (complete observations only). Coloured squares show significant positive (blue) or negative (red) correlations. BH-59 (left) and BH-60 (right).

The use of a constrained model with all the chemical variables explained a 76 % of the variation at BH-59. Stepwise model selection was used to select which compounds best describe the variation in the borehole data. The model added turns until no improvement was obtained. Note if factors are strongly correlated the model selection will generally identify one factor and not include the others, although all may be equally important.

Stepwise model selection of all parameter at BH-59 identified the following model:

$$M_{BH59} \sim TDIC + CO_2 + NO_3 + Fe$$

The variables identified in the model explains 40 % of the total variation of the site.

**Figure 4.14** shows the constrained ordination (CAP) of samples at BH-59, with chemical gradients of the most relevant parameters overlying. The gradients of concentrations of TDIC, CO<sub>2</sub>, NO<sub>3</sub><sup>-</sup> and Fe could explain to some extent the distribution of different samples in the constrained ordination. For example, at the bottom left corner of the ordination the communities were grouped due to the influence of high TDIC and low concentration of nitrate.

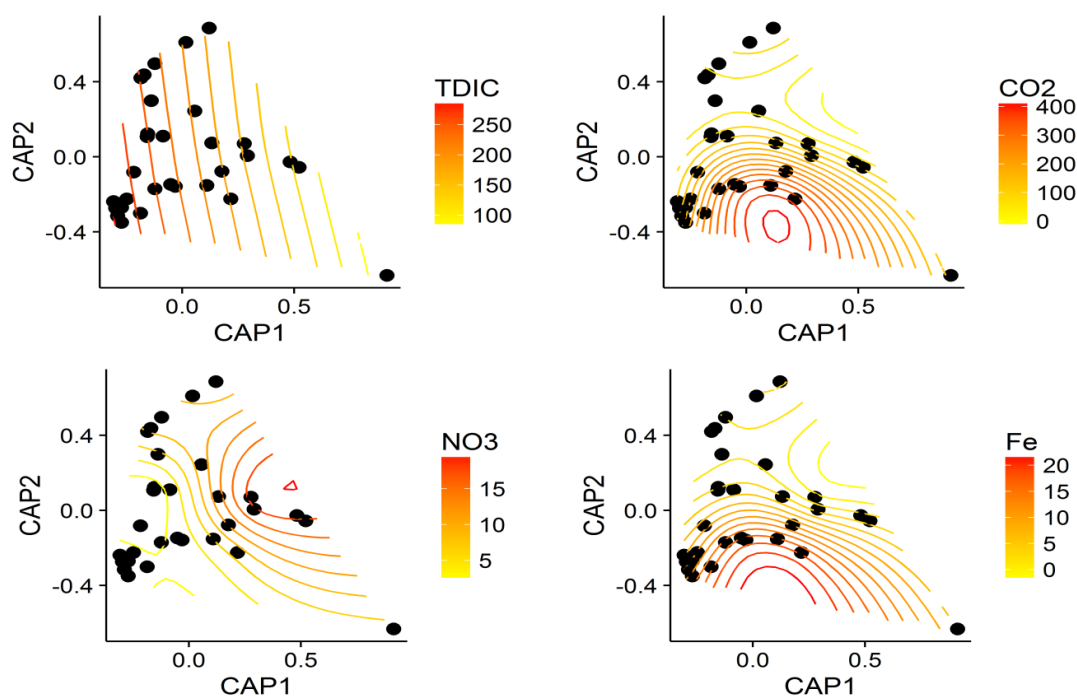


**Figure 4.14.** Constrained ordination based on the chemical gradients of samples at BH-59 over time. Overlying are the chemical gradients of the most relevant compounds explaining the variation of the system.

The constrained model considering all the chemical variables explained a 97 % of the variation BH-60.

The stepwise model selection of all parameter at BH-60 identified the following model:

$$M_{\text{BH60}} \sim \text{phenol} + \text{TDIC} + \text{o-cresols} + \text{xylenols} + \text{SO}_4 + \text{S}_2$$

The variables identified in the model explain 58 % of the total variation of the site.

**Figure 4.15** shows the constrained ordination (CAP) of samples at BH-60, with chemical gradients of the most relevant parameters overlying. The gradients of concentrations of the compounds indicated by the model, could partly explain the distribution of different samples. For instance, to the right in the middle the ordination the communities were grouped due to the influence of high low TPC and high concentration of nitrate.

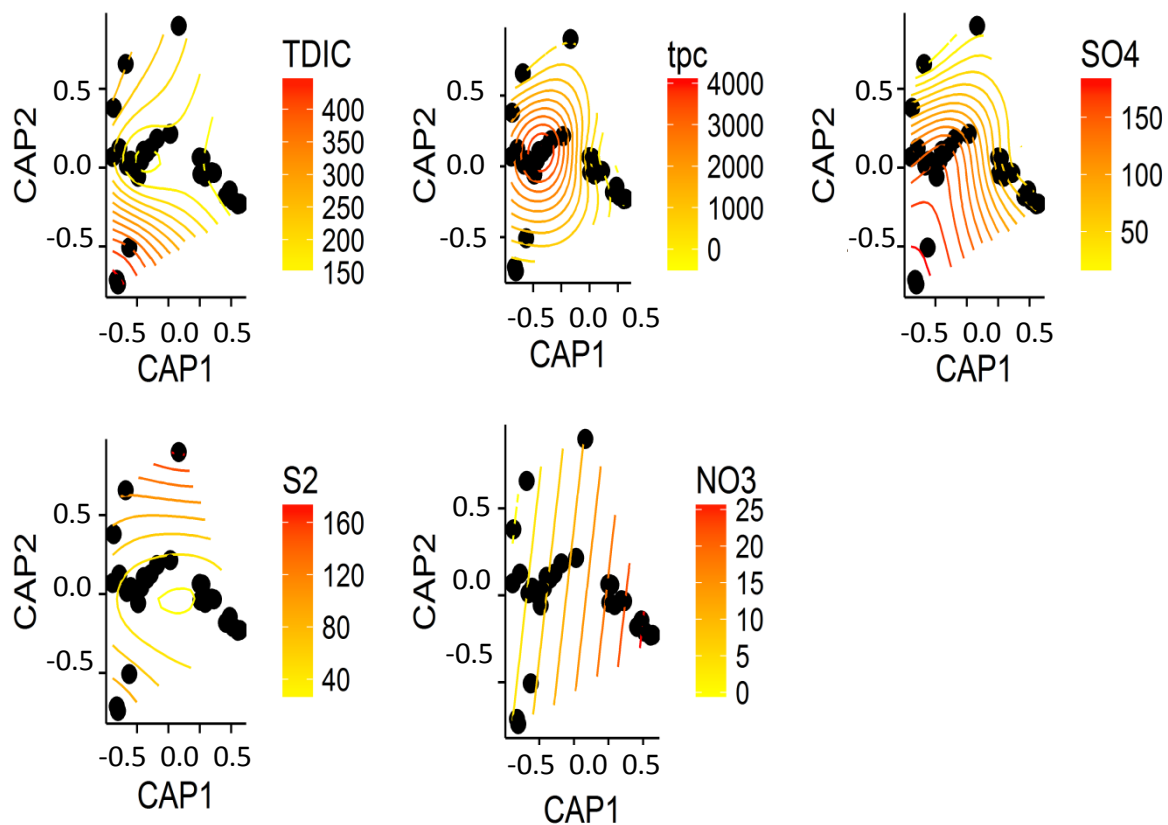


**Figure 4.15.** Constrained ordination based on the chemical gradients of samples at BH-60 over time. Overlying are the chemical gradients of the most relevant compounds explaining the variation of the system.

To relate different OTUs to different chemicals it was necessary to build a model able to construct independent ordinations. These two ordinations are then aligned to determine the presence of correlated vectors between OTUs abundances and different chemical. **Figure 4.16** shows a NMDS ordination based on alignment of two ordinations based on OTUs abundances at class level and chemical compounds. At BH-59 this analysis indicated an anti-correlation between the  $\delta^{13}\text{C-CH}_4$  and *Thermoplasmata* and *Methanomicrobia*. Also, a correlation between  $\delta^{13}\text{C-CH}_4$  and ZB2 and between nitrate and *Saprospirae*. At BH-60 there was a correlation between  $\delta^{34}\text{S-SO}_4$  and *delta-proteobacteria*.

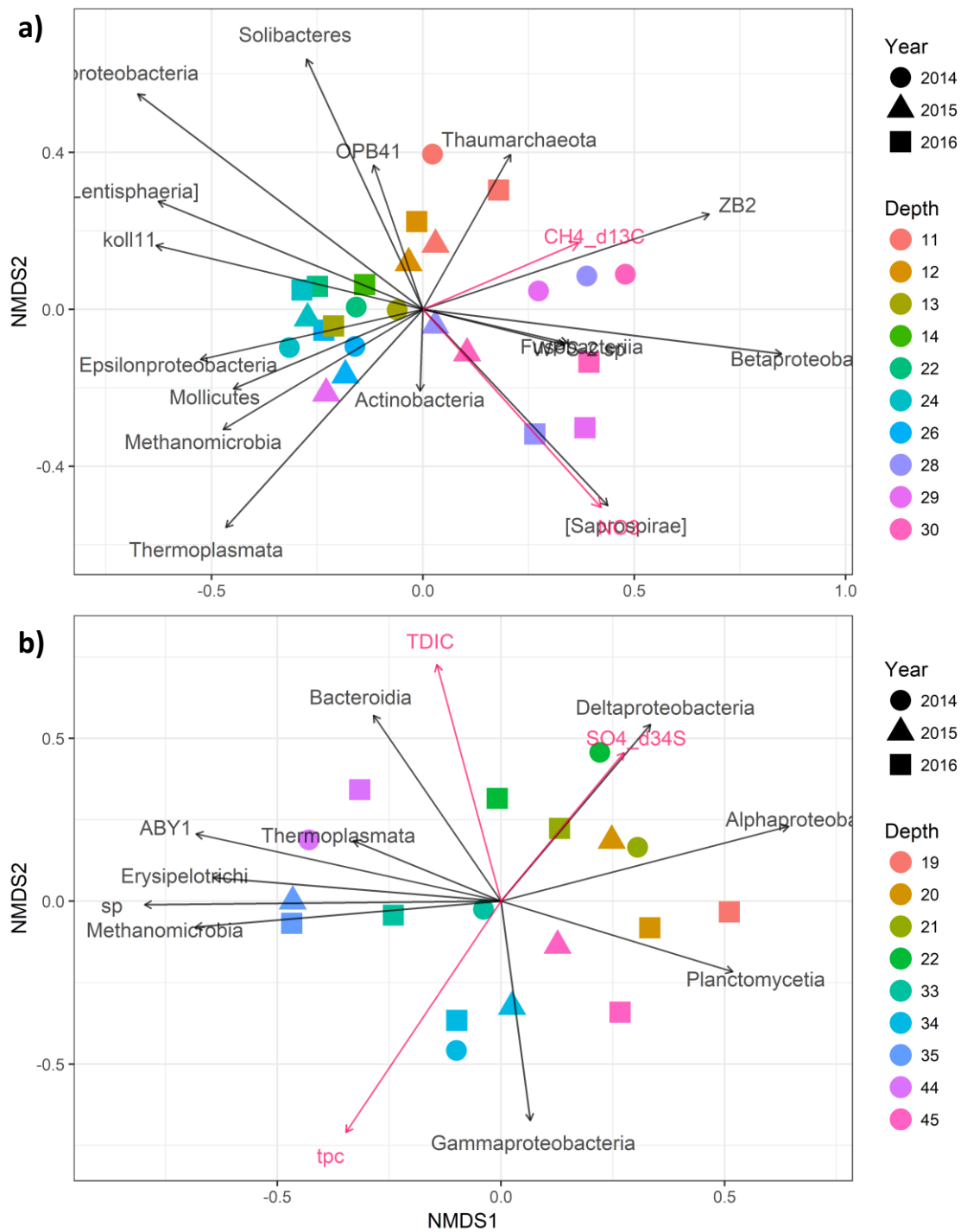


**Figure 4.16.** NMDS of the overlaid ordinations based on OTUs abundances and different chemical species at (a) BH-59 and (b) BH-60.



## 4.4 Discussion

### *How does the switching-off of PAT affect the temporal and spatial distribution of pollutants?*

The cessation of the pumping at BH-59 showed a decrease in TPC pollutant content over the three-year sampling period (2014-2016), started three years after the PAT operations were stopped (2011). The results of this study show that between 2014 and 2016 the total phenolic content was nearly depleted in this part of the plume. This trend contrasts the increasing pollutant concentrations at this borehole registered just one year after the stop of operation, where TPC levels recovered to pre-pumping values (Thornton *et al.*, 2014) and remained consistent until 2014.

The reduction of TPC detected at BH-59 in 2016 may be related to the observation location, probably not situated at the centre of the plume. This location would be strongly influenced by plume narrowing, or plume displacing derived from the PAT activity; both of which phenomena would be derived from the PAT activity. Plume displacement events have been described in the treatment of trichloroethylene (TCE) plumes using PAT (Zhang and Brusseau, 1999). These effects would have been able to decrease the detected contaminant concentrations at BH-59. Alternatively, the decrease may be a response of the source term variation, which has been described as one of the most important factors affecting the plume composition at this site (Thornton *et al.*, 2001a; Baker *et al.*, 2012).

On the other hand, the continuous activity of the PAT close to BH-60 and the stability of TPC across its depth profile were associated to higher pollutant content even in 2016, which generally increases as it becomes more distant from the source area suggested by both Thornton *et al.*, (2001a) and Baker *et al.*, (2012). The persistently high concentrations at BH-60 reflect a complex source history and large amounts of pollution that remain at the site, despite the constant activity of PAT.

The data does support that a cessation of PAT would produce a movement of the chemical interfaces towards pre-implementation conditions at this particular site. This may be the case within 1-3 years of stopping PAT activities, yet in the long term (>3 years) it is the opposite (i.e. further decrease of TPC) is observed. Therefore, the alternative hypothesis that the chemical interfaces would remain in the position induced by PAT cannot be accepted either. The decrease of TPC may be an indicator that the chemical interfaces previously induced were displaced, but there was an insufficient number of observation boreholes to track the direction of this displacement.

### ***Does the enhancement of biodegradation persist over time?***

Previous studies showed that the PAT close to BH-59 after 1 year of operation enhanced the biodegradation of TPC at this location. After cessation of PAT, TDIC levels within the plume remained relatively similar to the enhanced levels (Thornton *et al.*, 2014). Considering that the TPC were reduced over the period of this study, the stability of TDIC implies two processes at this location. Firstly, dilution of pollutants is a major process structuring the chemical environment at this location. Secondly, the enhancing of biodegradation is sustained by the continuous dilution of pollutants. The inhibition of the toxic effect exerted by phenolic compounds on the microbial community was hypothesized to occur with a PAT (Spence *et al.*, 2001) and the data from these surveys suggest that the activity of the microbial community is sustained in a system where dilution becomes a dominant process.

At BH-59, the geochemical steady-state and isotope data suggest the maintenance of different types of microbial metabolisms located at the plume fringe. Bacterial nitrate reduction (BNR) coincided with rapid decrease of nitrate at this chemical interface as was previously also described at this site by Lerner *et al.* (2000) and Thornton *et al.* (2001). Also, there were signals of anaerobic methane oxidation (AMO), whereby microorganisms, able to use lighter form of methane, produced an enrichment in the heavier form of this dissolved gas, as also shown by Whiticar (1999). The biodegradation of phenolic compounds through denitrification processes and AMO may be responsible for the isotopically light signature in the sustained level of TDIC at this plume fringe.

At the plume core, the dominant metabolic processes were bacterial sulphate reduction (BSR), characterized by heavier isotopic signatures of sulphate, which has also been shown by Spence *et al.* (2001) and Baker *et al.* (2012). Moreover, methanogenesis was active at this location, where methanogens produced the typical enrichment of the lighter form of methane (Summonsad *et al.*, 1998)

Therefore, the data from these surveys support the rejection of the null hypothesis that the termination of PAT activities would impact on the microbial community, which would become less active after the cease of the operations. The observed reduction of contaminant mass at this location and the isotope signatures support the alternative hypothesis, which is that the microbial communities will remain active after PAT is stopped.

### ***What is the influence of an active PAT on the microbial communities?***

The ongoing operation of a PAT close to BH-60 has deepened the trends observed at this location (further isotopic enrichment). This may be related to the higher pollutant input still at this location and the continuous operation of the PAT system. The ability of PAT to enhance biodegradation on the site for an extended period was reflected in higher isotopic signals of biodegradation. For instance, the enrichment of the heavier form of sulphate was higher at the fringes of this location where sulphate reduction was taking place. Moreover, at the plume core, the enrichment in the lighter form of carbon of TDIC was also higher, showing active biodegradation processes at the plume core, for the preferential use of lighter contaminant molecules.

### ***How do the microbial communities respond to the cease of PAT operations?***

Microbial communities of polluted aquifers are known to be affected by the introduction of a PAT and its following cessation of operation. Early investigations on the study site of this research revealed that cell numbers tend to be around  $10^6$  cells ml<sup>-1</sup> (Lerner *et al.*, 2000; Pickup *et al.*, 2001). The numbers observed in the 2014 survey are 2 and sometimes 3 orders of magnitude lower. This may be related to the capture zone of the PAT at each borehole being approximately 150 m (Thornton *et al.*, 2014). BH-59 was under the influence of the capture zone, and during the PAT activity, the cell numbers in the planktonic community could have been reduced due to the pumping as well as due to dilution from the background groundwater after stopping the PAT operation. After 3 years, the planktonic community seem to be recovering from these disturbances. The increase in cell numbers in the following surveys (2015-16) relate to the cell numbers registered in early studies. It also needs to be considered that dilution taking place at this location may have promoted better conditions for biodegradation, such as the reduction of the inhibitory effect by phenolic compounds on the microbial community. Also, the appearance of more energetic and favourable electron acceptors, such as nitrate, within the core of the plume kept biodegradation active.

The ongoing operation at BH-60 showed cell numbers equally low due to PAT. In some occasions the microbial community was almost absent. Palmer and Fish (1992) showed that the impact of PAT will be higher in high permeability layers of heterogeneous aquifers, which geological setting is analogous with the study site of this research. Therefore, it is expected that the cell densities will be disturbed.

The PCoA analysis revealed the importance of the borehole effect in the microbial planktonic communities. Yet, it was not possible to determine if the observed differences between these

communities were due to the location of the borehole or the action of the PAT system. The only possibility to determine this would be the sequencing analysis of pre-pumping microbial communities. Nevertheless, at both locations it was possible to observe similarities in communities related to high TPC. These similarities in the communities may be related to similar microbial composition. For instance, at the plume core of BH-60 the communities are likely to have similar members. The isotopic signatures indicated the presence of BSR and methanogenesis. Methanogens activity at these locations is related to the capacity of Archaeal groups to resist highly contaminated environments (De Rosa *et al.*, 1986; Usami *et al.*, 2005) due to the properties of their membranes, which contain a particular ether lipid composition that avoids degradation and is particularly useful in extreme environments (Vossenberg *et al.*, 1998). The ability to identify Archaeal groups with the primer pair Bact-341F and Bact-805R has been described to be up to 64.6 % when one mismatch is allowed (Klindworth *et al.*, 2012). In this chapter, it was possible to link methanogens to the isotope data at class level (Figure 4.15). This is a high taxonomic level which was selected because it gave a better resolution to identify patterns, linking activity to different taxonomic Classes of microorganisms. This decision was made as a strategy to manage an environment which presents different sources of chemical variation. The presence of active BSR communities at the boundaries of the plume core is related to the ability of PAT to reduce TPC to a level, which allows the biodegradation of phenolic compounds, coupled to sulphate reduction (Spence *et al.*, 2001; Thornton *et al.*, 2014)

At this point of the analysis, it was not clear the factors explaining the variation between the microbial communities. Also, the detection of *Cyanobacteria* in some locations over time added an unexpected complexity level to the processes that may be influencing the bacterial communities at different depths. The presence of this group may be related to the recharge events and the influx of background groundwater to the core of the plume due to PAT at BH-60 (Thornton *et al.*, 2014). These factors may be dragging *Cyanobacteria* from shallow depths to an environment where they are not naturally occurring.

Moreover, it was shown that the effect of TPC did not explain the distance between samples with low and medium TPC and the effect of time was not clear.

### ***What chemical gradients explain the variation of the system?***

The use of CAP (Canonical Analysis of Principal Coordinates) with all the steady-state geochemical data is unadvisable for two reasons. Many factors will not be able to constrain the ordination, and correlated variables will not be distinguished, despite they may have equal impact on the ordination (Oksanen, 2012). Nevertheless, this could be controlled with the identification of positive and negative correlated variables. The ordination derived by CAP identified chemical factors related to the variation of the system. The use of CAP as a strategy to reveal relevant patterns in multivariate data sets has been used in the construction of constrained ordination in ecology (Anderson and Willis, 2003), and proved to be useful in our study.

The use of CAP with the identification of correlated variables resulted in the construction of a model with all the data (excluding isotopes), which explained 46 % and 58 % of the total variations at BH-59 and BH-60, respectively.

At both boreholes, the ordinations present a distribution related to concentration gradients of nitrate and TDIC. The samples with high nitrate concentrations belonged to the upper fringe of the plume. In these chemical interface environments, there is a constant supply of nitrate derived from the agricultural activities above the plume (Spence *et al.*, 2001). Mixing between the background groundwater and the plume are driving processes in these environments, promoting conditions for an active microbial community coupled to denitrification processes (Thornton *et al.*, 2001b; Thornton *et al.*, 2014). The samples with higher TDIC levels belong to locations at the plume core. The processes of biodegradation at these locations were related to sulphate reduction and methanogenesis according to the isotope signatures. Nevertheless, the iron and manganese reduction biologically-mediated at these locations may contribute to the TDIC pool. It needs to be considered that isotope content at these locations is correlated to the TDIC. For example, at BH-59,  $\delta^{34}\text{S-SO}_4$  and  $\delta^{13}\text{C-TDIC}$  were positively correlated, whereas  $\delta^{13}\text{C-CH}_4$  was negatively correlated. Therefore, they may be equally important, but they do not appear to explain the variation of the models at each borehole.

The difference between the parameters driving the variation between the boreholes may be related to the pollutant content and the activity level of microbial communities. At BH-60, gradients of TPC, sulphate and sulphide concentrations were indicated as drivers of the variation. The high levels of contaminants at this location are likely to keep the BSR inhibited. Signs of this inhibition are the gradients of sulphate, where locations with high values were not active.

It should be noted that there were an important amount of variations that were not explained by the different models. The model is unable to account for disturbances likely to be found in natural systems. Also, other CAP was performed with the isotopic data included, but there was no change in the ordination nor in the parameters identified as drivers of the variation.

Steady-state measurements are controlled by the geochemical and biological processes, and source term variation. Simple measurements of steady-state variables cannot resolve whether the variation observed was due to a biological process or to source term variation. The isotopic data allowed more confidence in the understanding of biological processes occurring. If the ordination had showed a difference between steady-state data with and without isotopes, it would have implied that the shift was influenced by source term variation. The similarities observed support that the processes detected were due to biological activity.

#### **4.5 Conclusion**

This study let us conclude that reduction of TPC at BH-59 may be a response to the previous activity of PAT. Therefore, the chemical interface was moved by plume displacement or plume narrowing. Also, it was possible to establish that microbial communities at BH-59 remained active after the cessation of PAT, whereas communities at BH-60 maintained the enhancing of biodegradation by PAT, which has deepened the isotopes signatures of sulphate reduction and methanogenesis at the plume core. Moreover, the variation observed at both locations was influenced by concentration gradients of TDIC and  $\text{NO}_3^-$ . At BH-59 the variation was also related to gradients of  $\text{CO}_2$  and Fe, whereas at BH-60 the variation was explained by concentration gradients of TPC,  $\text{SO}_4^{2-}$  and  $\text{S}^{2-}$ . The presence of different groups may be related to the presence of isotopes signatures and other chemical parameters. It needs to be considered that microbial planktonic communities from BH-59 and BH-60 were different across different surveys. Nevertheless, it was not possible to determine if the difference was due to the location or the ongoing PAT system at BH-60.

# Chapter 5

---

## Conclusions

---

The aim of this thesis was to investigate the dynamic responses of microbial communities to different chemical environments that develop in the chemical interfaces of polluted aquifers. The research was structured around different research objectives, which guided the respective field and laboratory experiments and analysis. The findings of these experiments are presented and discussed in the technical chapters 2, 3 and 4. This chapter integrates the results from each chapter and discusses the implications in the context of contaminant plume development and the management of aquifers polluted with organic chemicals.

- ***Time-scales of microbial attachment in plumes are a stable feature at laboratory and field scales***

Chapter 3 addressed simple but fundamental questions regarding the dynamics of microbial communities that may occur at chemical interfaces in a plume of organic chemicals. The time-scales of attachment have not previously been characterised in polluted aquifers. This study showed that it takes approximately 100 days for a planktonic community to establish a stable biofilm in terms of cell numbers. Similar kinetics were observed in sand samples incubated in the field at the fringe of the plume (30 mbgl) and microcosms using groundwater from the same depth as inoculum. This confirms that the laboratory microcosm experiment is a good analogue of the field system and can provide important insight on the dynamics of *in situ* microbial community behaviour. The cells numbers on the attached phase were stable from 101 to 195 days also in microcosms established with groundwater from low, medium and high phenolic content (Chapter 4).

This information is relevant in aquifers where natural attenuation is unable to manage the pollutant inputs. In these scenarios plumes will continue to spread through the aquifer (Lerner *et al.*, 2000; Thornton *et al.*, 2001a; Thornton *et al.*, 2001b). The aquifer ahead of the plume is essentially inoculated by planktonic microorganisms in the contaminated groundwater as the plume advances. The colonizing bacteria will be those present at the plume front. This environment represents a moving chemical interface, the plume fringe, which has been described as being responsible for most of the biodegradation in aquifers polluted with organic compounds (Lerner *et al.*, 2000; Thornton *et al.*, 2001b; Tuxen *et al.*, 2006; Baker *et al.* 2012; Bahr *et al.*, 2015; Meckenstock *et al.*, 2015). The biofilm developed in the location where the plume front has advanced and will be established at this time-scale of around 100 days. This time becomes relevant in groundwater flow models of plumes, which usually assume the presence of a microbial community responsible for the biodegradation on the system (Schäferer *et al.*, 1998; Prommer *et al.*, 2002), but not their intrinsic dynamics such as the time-scale of attachment.



- ***Attached and planktonic communities structures differ over time at chemical interfaces***

The study conducted by Rizoulius *et al.* (2013) illustrated the differences in community structure that can exist between the biofilm and planktonic communities from the same depth in this aquifer, but did not consider any temporal variations. In the current study differences between these communities were evaluated over a two year period. Our study supported the differences between these communities observed earlier at 30 mbgl. This was also observed at lab scale. Moreover, the difference between these two communities was also observed in microcosms established using groundwater from different depths from 11, 14 and 21 mbgl, after 3 and 6 months of incubation (Chapter 4). This means that these communities are likely to develop different structures in different environments.

Nevertheless, an important feature observed in the experiment was that biofilms developed under stable conditions at the laboratory scale, were quite dynamic in terms of the community structure. It was hypothesized that the reduction of evenness at early stages corresponds with some groups becoming dominant in the biofilm development. Subsequently, the evenness increases as other groups start to attach to the aquifer material. These dynamics have been observed in biofilms formed in different systems, such human dental plaque and colon. This reflects the dynamics between early and secondary colonizers (Santegoeds *et al.*, 1998; Jackson, 2001; Jackson, 2003; Rickard *et al.*, 2003; Flint *et al.*, 2007).

The relevance of these findings relates to different community structures having different metabolic abilities. In polluted aquifers different microbial groups are able to biodegrade substrates using different electron acceptors (Lerner *et al.*, 2000; Spence *et al.*, 2001; Thornton *et al.*, 2001a; Tuxen *et al.*, 2006). This biodegradation capacity defines the remediation potential due to biodegradation. In the microcosms established under stable conditions with groundwater from 30 mbgl in the plume, a different pattern of terminal electron acceptors processes (TEAPs) was observed. For instance, nitrate consumption and manganese dissolution. Considering the variability in community structure in the biofilm, it is likely that the changes observed in community structures impact in the biodegradation potential of biofilms located at chemical interfaces.

- ***Biofilm communities are more resilient to changes in their chemical environment***

In chapter 4 the responses of the biofilm to different environmental disturbances was explored. The laboratory scale scenarios were developed based on different processes that are observed in the chemical interfaces of the plume at the study site. For instance, dispersive mixing at the upper and lower plume fringe implies a re-supply of nitrate into the plume from the background groundwater. This terminal electron acceptor consumed by nitrate reducer activity. The plume front advance, plume refreshing and source term variation scenarios were inferred from the temporal and spatial variability observed in the plume at the study site (Thornton *et al.*, 2001a; Thornton *et al.*, 2001b; Spence *et al.*, 2001; Elliot *et al.*, 2010). The microcosm study using groundwater from 11, 14 and 21mbgl recreated different scenarios (chemical interfaces) observed in the plume at the field site. In these experiments the biofilm community was robust and resisted modification of their chemical environment. No significant changes in different groups were observed. The ability of the biofilm to resist environmental disturbances has been described in different systems and is consistent with the observations from this study (Hancock *et al.*, 2005; Mitchell *et al.*, 2008; Weaver *et al.*, 2015).

These findings are relevant in the understanding of polluted aquifers, especially in circumstances where engineered management technologies, such as PAT, are used as an intervention measure. The ability of PAT systems to efficiently remove organic pollutants from high permeability layers (Khan *et al.*, 2015), could affect the densities of the planktonic community at these locations. For instance, at BH-60 (where PAT was still active) at some depths cells numbers were significantly impacted by PAT, with cell densities extremely low. Nevertheless, the enrichment in stable isotope  $\delta^{34}\text{S-SO}_4^{2-}$ ,  $\delta^{13}\text{C-TDIC}$  and  $\delta^{13}\text{C-CH}_4$  indicated activity at these locations, as was previously described at the site (Thornton *et al.*, 2014). Given that the planktonic community was disturbed at these locations, it is likely that biofilms were responsible for the observed enrichment of the isotopes signatures.

Conversely, the experiments showed that the planktonic community is strongly influenced by the geochemical history. This behaviour relates to the fact that this mobile community is entrained in the groundwater flow, and must adapt more rapidly to geochemical changes, which are common in groundwater systems dominated by source term variation.

***Biofilm development is driven by the hydrogeochemical environment***

The effect of removing the planktonic community to assess the possible impact of the geochemical environment in the biofilm was examined in chapter 4. No significant changes in the community members were observed between treatments. This observation supported the

hypothesis that the biofilm is robust and can resist environmental changes. In this case it was a bio-chemical change of conditions (additional removal of planktonic community). The similar community structure in biofilms formed in the absence of a planktonic community, supports the view that the attached phase is developed in response to the geochemical environment.

- ***Microbial communities remain active after cessation of engineered intervention measures***

The effect of chemical interfaces induced by an engineered groundwater remediation measure such as PAT on the planktonic community was explored in chapter 5. First, it was possible to establish a reduction of TPC in the plume (at BH-59). This result contrasts with previous observations of increasing TPC in the plume at this location, after cessation of the PAT (Thornton *et al.*, 2014). The increasing TPC was attributed to source term variation, which was indicated as the main factor responsible for temporal variation in TPC at this site (Thornton *et al.*, 2001a; Thornton *et al.*, 2001b; Thornton *et al.*, 2014). The results from the current study may be related to the observation borehole not being located in the centre of the plume. Any reduction of plume width or plume displacement as a response of the background groundwater entering laterally to the plume, could have produced a reduction of the TPC levels at BH-59. Plume displacement by background groundwater has been described in other PAT systems, with re-injection boreholes in the treatment of TCE contaminant plumes (Parker *et al.*, 2012). Secondly, despite the reduction of pollutant content, the isotopes signatures of  $\delta^{34}\text{S-SO}_4^{2-}$  and  $\delta^{13}\text{C-TDIC}$  at this location indicated that biodegradation processes remain active. Processes such as bacterial sulphate reduction, anaerobic methane oxidation and methanogenesis were indicated by isotopes signatures. This trend has a significant impact regarding the implementation of PAT technologies. Usually these technologies have been criticised for not achieving remedial targets in the short term (Khan *et al.*, 2015). The fact that communities remained active after the cessation of PAT activity of could revalorise the effectiveness of these remediation techniques. Besides reducing contaminant mass and ensuring plume containment (Mackay & Cherry, 1989; Kerr, 1990), PAT could be added the ability to steadily active microbial communities. Given that microbial activity is enhanced in the plume at the study site by the use of PAT to reduce contaminant concentrations, the PAT pumping regime may be modified to optimise the volume of contaminant groundwater, that is treated *ex situ*. This could reduce the cost of *ex situ* treatments and make this remediation measure a more efficient and attractive option.

- ***Different gradients of concentration influence the planktonic bacterial community***

In Chapter 5 it was shown that different gradients in the concentration of geochemical species are related to variation in the composition of the bacterial communities. Some of them were TDIC and nitrate, but the strong correlations to other parameters, may ignore the importance of other equally important variables. In field systems, data analysis with multiple variables has been reported as tremendously complex (Demster, 1971; Das and Nag, 2015; Fatoba *et al.*, 2017). The ordination undertaken attempted to relate different gradients of solute concentration with specific OTUs. This was desirable using the isotopic data, given that studies of polluted groundwater often consider either isotopic distributions of substrates and TEAPs or the sequencing of indigenous microorganisms assumed to be responsible for them, but rarely both. At this point it was possible to relate some OTUs with some geochemical parameters driving the variation among microbial communities. For example, the anti-correlation between the  $\delta^{13}\text{C}\text{-CH}_4$  and *Thermoplasmata* and *Methanomicrobia* at BH-59, may be linking the activity of methanogens to their microbial identity in contaminated aquifers. Nevertheless, further research is required to reach deeper taxonomic levels and linked to the activity indicated by the isotope distributions involved in biodegradation.

- ***Plume fringe concept as a basis to explain the microbial dynamics at chemical interfaces***

The redox zonation concept has for many years been used to explain the spatial and temporal distribution of TEAPs that develop as plumes of organic contaminants evolve in aquifers. In this model redox zones are distributed with reduced zones close to the source area and more oxidized environments to the front and periphery (edge) of the plume. The different redox environments generally vary from methanogenic zones near the source area, followed by sulphate reduction in the plume core, iron and manganese reduction surrounding the core to nitrate and aerobic respiration at the edge of the plume (Bjerg *et al.*, 1995; Lerner *et al.*, 2000; Christensen *et al.*, 2000; Thornton *et al.*, 2001a; McMahon & Chapelle, 2008). This model has been used to explain leachate plumes from landfills and BTEX releases to groundwater, among others (Lyngkilde & Christensen, 1992; Cozarelli *et al.*, 2001). Nevertheless, the concept of redox zonation has been revisited recently because it has been argued that it would not be possible to replenish the aqueous electron acceptors used in the source area to downstream zones. In this sense, the only possible processes in the plume core would be reduction of iron and manganese (manganese and iron reduction) and methanogenesis; nitrate and sulphate reduction would only occur in the plume fringe due to mixing between the contaminants and background groundwater. Therefore, the redox zonation pattern will not develop as expected

(Meckenstock *et al.*, 2015). The results from this study support the plume fringe concept. For example, in Chapter 4 it was shown that microbial communities in microcosms established with groundwater from a more reduced environment in the plume had the ability to use nitrate and sulphate concurrently. In the field system, the presence of nitrate reducers in the upper plume fringe and the isotopes signatures related to sulphate reduction and anaerobic methane oxidation supported the experimental observation, as previously documented (Thornton *et al.*, 2014). In these two examples the TEAPs develop in parallel rather than in temporal succession.

- **Future work**

Further development of the research undertaken in this study should focus on the following topics.

*Define the level of activity of active degraders in microcosms*

Stable isotope probing (SIP) coupled to Raman spectroscopy could be used to address questions related to what proportion of the community is active degrading within the microcosm experiments. For instance, microcosms constructed with groundwater from the site, could be spiked with <sup>13</sup>C-phenol and then the incorporation of these molecules into the cells could be made by Raman spectroscopy. This approach is based on the incorporation of <sup>13</sup>C-labelled molecules, and the detection of the shift of Raman spectrum. It would be suitable to quantify how much of the microbial community is incorporating the labelled molecules and link this with activity. Moreover, the incorporation of <sup>13</sup>C-labelled molecules will generate heavier <sup>13</sup>C-DNA, which could be sequenced, and the activity linked to specific OTUs. This SIP-Raman approach has been used to study different metabolic pathways and to identify phenol degraders from bio sludge (Huang *et al.*, 2004; Huang *et al.*, 2007; Li *et al.*, 2013; Zhang *et al.*, 2015).

The activity in the field system and microcosm experiments could be assessed using quantitative PCR (qPCR) for genes related to nitrate reduction metabolism, *nar* and *nap*, to establish the presence of these microorganisms and how their abundance is related to the groundwater chemistry at different stages of biofilm development and/or at different depths in the field. Moreover, qPCR for *dsr-A* gene related to sulphate reducing bacteria (SRB), could determine effectively if these processes occur in parallel (Moreno-Vivian *et al.*, 1999; Phillipot, 2005; Kondo *et al.*, 2008).

### *Characterise the biofilm architecture at lab scale*

The biofilm development can be investigated using fluorescent-in-situ hybridization (FISH). This technique is based on the use of labelled probes with the ability to hybridise into specific bacterial groups. The identification of OTUs from the experiments provides information on the probes to be used in these systems. Microcosm experiments with a high temporal framework would be useful to understand the architecture of the biofilm (Lee *et al* 1999; Flint *et al.*, 2007; Zhang *et al.*, 2012). As the presence of different Class of Proteobacteria (alpha, beta, gamma and delta) has been determined, these groups could be targeted for identification, as has been done in studies simulating basalt aquifers (Lehman *et al.*, 2001).

### *Finish the molecular biology characterization of pre-pumping scenarios*

To provide a complete history of the effect of the PAT on the microbial community dynamics at in the study site the samples collected pre-pumping and immediately after the system was implemented should be sequenced and analysed through the bioinformatics pipelines developed within this research. In this way, the effect of the PAT could be understood with an extended framework of reference that reflects the original and modified plume interfaces, to compare the direct effect of the PAT on the planktonic microbial community.

### *Deep in the bioinformatics analysis*

The bioinformatics analysis presented in this thesis could be deepened to lower taxonomic levels to understand in more detail the effect of the chemical interfaces on the microbial community. Obtaining a more specific microbial identification could help to understand the microbial dynamics in this environment, and could be associated to different geochemical concentration gradients explaining the variability observed in polluted aquifers.

## References

- Aburto, A., Fahy, A., Coulon, F., Lethbridge, G., Timmis, K. N., Ball, A. S. & McGenity, T. J. (2009), 'Mixed Aerobic and Anaerobic Microbial Communities in Benzene-contaminated Groundwater'. *Journal of Applied Microbiology*, 106(1), 317–328.
- Aelion, C. M. and Bradley, P. M., (1991), 'Aerobic biodegradation potential of subsurface microorganisms from a jet fuel-contaminated aquifer' *Applied and Environmental Microbiology*, 57(1), pp. 57–63.
- Aelion, C. M., Swindoll, C. M. and Pfaender, F. K., (1987), 'Adaptation to and biodegradation of xenobiotic compounds by microbial communities from a pristine aquifer', *Applied and Environmental Microbiology*. 53(9), pp. 2212–2217.
- Allen, D. J., Brewerton, L. J., Coleby, L. M., Gibbs, B. R., Lewis, M. A., MacDonald, A. M., Wagstaff, S. J. & Williams, A. T., (1997), 'The Physical Properties of Major Aquifers in England and Wales' *British Geological Survey Technical Report WD/97/34*, pp. 312.
- Alexander, M., (1994), 'Sorption', *Biodegradation and Bioremediation*, Academic Press, San Diego, California, USA, pp. 114–130.
- Allison D.G., Ruiz B., San Jose C., Jaspe A., Gilbert P., (1998), 'Extracellular products as mediators of the formation and detachment of *Pseudomonas fluorescens* biofilms', *FEMS Microbiology Letters*. 167(2), pp. 179–184.
- Allison, D. G., (2003), 'The biofilm matrix', *Biofouling*. 19(2), pp. 139–150.
- Allouche N., Maanan M., Gontara M., Rollo N., Jmal I., Bouri S., (2017), 'A global risk approach to assessing groundwater vulnerability'. *Environmental Modelling & Software*. 88, pp. 168–182.
- Angles, M. L., Marshall, K. C. & Goodman, A. E., (1993), 'Plasmid Transfer between Marine Bacteria in the Aqueous Phase and Biofilms in Reactor Microcosms'. *Applied and Environmental Microbiology*, 59(3), 843–850.
- Alvarez, P. J. J., Anid, P. J. and Vogel, T. M., (1991), 'Kinetics of aerobic biodegradation of benzene and toluene in sandy aquifer material', *Biodegradation*. 2(1), pp. 43–51.
- Anderson, M. J. and Willis, T. J., (2003), 'Canonical analysis of principal coordinates: a useful method of constrained ordination for ecology', *Ecology*. 84(2), pp. 511–525.
- Anid, P. J., Alvarez, P. J. J. and Vogel, T. M., (1993), 'Biodegradation of monoaromatic hydrocarbons in aquifer columns amended with hydrogen peroxide and nitrate', *Water Research*. 27(4), pp. 685–691.
- Anku, W. W., Mamo, M. A. and Govender, P. P., (2017), 'Phenolic Compounds in Water: Sources, Reactivity, Toxicity and Treatment Methods', in *Phenolic Compounds-Natural Sources, Importance and Applications*. Chapter: 17, Publisher: InTechOpen, Editors: Marcos Soto-Hernandez, Mariana Palma-Tenango and Maria del Rosario Garcia-Mateos, pp.420-443

- Appelo C. A. J., Postma D., (2004), *Introduction to Ground water Geochemistry*. Geochemistry, Groundwater and Pollution (2nd ed.). Balkema Publishers, Leiden.
- Appelo C. A. J. and Rolle, M., (2010), 'PHT3D: A reactive multicomponent transport model for saturated porous media', *Groundwater*. 48(5), pp. 627–632.
- Arias-Estévez M., López-Periago E., Martínez-Carballo E., Simal-Gándara J Mejuto J., Garcia-Rio., (2008), 'The mobility and degradation of pesticides in soils and the pollution of groundwater resources', *Agriculture, Ecosystems & Environment*. 123(4), pp. 247–260.
- Azadpour-Keeley A., Keeley J.W., Russell H.H, Sewell G.W., (2001), 'Monitored natural attenuation of Contaminants in the subsurface: Processes', *Groundwater Monitoring & Remediation*. 21(2), pp. 97–107.
- Bahr A., Fischer A., Vogt C., Bombach P., (2015), 'Evidence of polycyclic aromatic hydrocarbon biodegradation in a contaminated aquifer by combined application of in situ and laboratory microcosms using <sup>13</sup>C-labelled target compounds', *Water Research*. 69, pp. 100–109.
- Baker, K., (2011), 'The geochemical controls on anaerobic microbial ecology in a phenol-contaminated sandstone aquifer'. University of Sheffield, Thesis.
- Barbieri M., Carrera J., Sanchez-Vila X., Ayora C., Cama J., Köck-Schulmeyer M., López de Alda M., Barceló D., Tobella-Brunet J., Hernández-García M., (2011), 'Microcosm experiments to control anaerobic redox conditions when studying the fate of organic micropollutants in aquifer material', *Journal of Contaminant Hydrology*. 126(3), pp. 330–345.
- Barker J. F., Patrick G. C., Lemon L.G., Travis M., (1987), 'Some biases in sampling multilevel piezometers for volatile organics', *Groundwater Monitoring & Remediation*. 7(2), pp. 48–54.
- Bear, J. and Cheng, A. H.-D., (2010), 'Modelling groundwater flow and Contaminant transport'. Science & Business Media.
- Bekins B., Cozzarelli I., Godsy E., Warren E., Essaid H., Tuccillo M.E., (2001), 'Progression of natural attenuation processes at a crude oil spill site: II. Controls on spatial distribution of microbial populations', *Journal of Contaminant Hydrology*. 53(3), pp. 387–406.
- Berdugo-Clavijo C., Dong X., Soh J., Sensen C.W., Gieg L.M., (2012), 'Methanogenic biodegradation of two-ringed polycyclic aromatic hydrocarbons', *FEMS Microbiology Ecology*. 81(1), pp. 124–133.
- Singh, R., Paul, D., Jain, R.K., (2006), 'Biofilms: implications in bioremediation'. *Trends in Microbiology*. 14(9), pp. 389–397.
- Bisaillon J.G., Lépine F., Beaudet R., Sylvestre M., (1991), 'Carboxylation of o-cresol by an anaerobic consortium under methanogenic conditions.', *Applied and Environmental Microbiology*. 57(8), pp. 2131–2134.
- Bjerg PL., Tuxen N., Reitzel L.A., Albrechtsen H.J., Kjeldsen P., (2011), 'Natural attenuation processes in landfill leachate plumes at three Danish sites', *Groundwater*. 49(5), pp. 688–705.



- Bloomfield, J., Goody, D., Bright, M. & Williams, P., (2001), 'Pore-Throat Size Distributions in Permo-Triassic Sandstones from the United Kingdom and Some Implications for Contaminant Hydrogeology'. *Hydrogeology Journal*, 9(3), 219–230.
- Blum P., Sagner A., Tiehm A., Martus P., Wendel T., Grathwohl P., (2011), 'Importance of heterocyclic aromatic compounds in monitored natural attenuation for coal tar contaminated aquifers: A review', *Journal of Contaminant Hydrology*. 126(3), pp. 181–194.
- Böhlke, J. K., (2002), 'Groundwater Recharge and Agricultural Contamination'. *Hydrogeology Journal*, 10(1), 153–179.
- Boll, M. and Fuchs, G., (2005), 'Unusual reactions involved in anaerobic metabolism of phenolic compounds', *Biological Chemistry*, 386(10), pp. 989–997.
- Borden, R.C., Daniel, R.A., LeBrun, L.E., Davis, C.W., (1997), 'Intrinsic biodegradation of MTBE and BTEX in a gasoline-contaminated aquifer', *Water Resources Research*. 33(5), pp. 1105–1115.
- Boschker, H. T. S. and Middelburg, J. J., (2002), 'Stable isotopes and biomarkers in microbial ecology', *FEMS Microbiology Ecology*. 40(2), pp. 85–95.
- Bossert, I. D. and Young, L. Y., (1986), 'Anaerobic oxidation of p-cresol by a denitrifying bacterium.', *Applied and Environmental Microbiology*. 52(5), pp. 1117–1122.
- Bottrell, S. H., Moncaster, S. J., Tellam, J. H., Lloyd, J. W., Fisher, Q. J. & Newton, R. J., (2000), 'Controls on Bacterial Sulphate Reduction in a Dual Porosity Aquifer System: The Lincolnshire Limestone Aquifer, England'. *Chemical Geology*, 169(3–4), 461–470.
- Bottrell, S.H., Parkes, R.J., Cragg, B.A., Raiswell, R., (2000), 'Isotopic evidence for anoxic pyrite oxidation and stimulation of bacterial sulphate reduction in marine sediments', *Journal of the Geological Society*. 157(4), pp. 711–714.
- Botz, R., Pokojski, H.D., Schmitt, M. and Thomm, M., (1996), 'Carbon isotope fractionation during bacterial methanogenesis by CO<sub>2</sub> reduction', *Organic Geochemistry*. 25(3–4), pp. 255–262.
- Brümmer, I. H., Fehr, W. and Wagner-Döbler, I., (2000), 'Biofilm community structure in polluted rivers: abundance of dominant phylogenetic groups over a complete annual cycle.', *Applied and Environmental Microbiology*. 66(7), pp. 3078–82
- Caporaso, J.G., Kuczynski, J., Stombaugh, J., Bittinger, K., Bushman, F.D., Costello, E.K., Fierer, N., Pena, A.G., Goodrich, J.K., Gordon, J.I., Huttley, G.A., (2010), 'QIIME allows analysis of high-throughput community sequencing data', *Nature Methods*. 7(5), pp. 335–336.
- Castelle, C. J., Hug, L. A., Wrighton, K. C., Thomas, B. C., Williams, K. H., Wu, D., Tringe, S. G., Singer, S. W., Eisen, J. A. & Banfield, J. F., (2013), 'Extraordinary Phylogenetic Diversity and Metabolic Versatility in Aquifer Sediment'. *Nature communications*, 4, 2120.
- Carey, M.A., Finnamore, J.R., Morrey, M.J., Marsland, P.A., (2000), 'Guidance on the assessment and monitoring of natural attenuation of Contaminants in groundwater', R. Environment Agency.

Chapelle, F. H., (1996), 'Identifying redox conditions that favor the natural attenuation of chlorinated ethenes in contaminated ground-water systems', in Symposium on Natural Attenuation of Chlorinated Organics in Ground Water, pp. 17–20.

Chapelle, F.H., (2000), Ground-Water Microbiology and Geochemistry, 2<sup>nd</sup> edition. Wiley, New York

Chapelle, F.H., Widdowson, M.A., Brauner, J.S., Mendez, E., Casey, C.C., (2003), 'Methodology for estimating times of remediation associated to monitored natural attenuation', pp. 3–4057.

Chaudhry, G. R. and Chapalamadugu, S., (1991), 'Biodegradation of halogenated organic compounds.', Microbiological Reviews., 55(1), pp. 59–79.

Christensen, T.H., Bjerg, P.L., Banwart, S.A., Jakobsen, R., Heron, G., Albrechtsen, H.J., (2000), 'Characterization of redox conditions in groundwater Contaminant plumes', Journal of Contaminant Hydrology. 45(3), pp. 165–241.

Chistoserdova, L., Kalyuzhnaya, M. G. & Lidstrom, M. E., (2009), 'The Expanding World of Methylophilic Metabolism'. Annual Review of Microbiology, 63, 477–499.

Costerton, J. W., Stewart, P. S. & Greenberg, E. P., (1999), 'Bacterial Biofilms: A Common Cause of Persistent Infections'. Science, 284(5418), 1318–1322.

Council, N. R., (1997), 'Innovations in ground water and soil cleanup: from concept to commercialization'. National Academies Press.

Coyne, M. J. and Comstock, L. E., (2008), 'Niche-specific features of the intestinal *Bacteroidales*', Journal of Bacteriology. 190(2), pp. 736–742.

Crump, B. C., Armbrust, E. V. and Baross, J. A., (1999), 'Phylogenetic analysis of particle-attached and free-living bacterial communities in the Columbia River, its estuary, and the adjacent coastal ocean', Applied and Environmental Microbiology. 65(7), pp. 3192–3204.

Culman, S.W., Gauch, H.G., Blackwood, C.B., Thies, J.E., (2008), 'Analysis of T-RFLP data using analysis of variance and ordination methods: a comparative study', Journal of Microbiological Methods. 75(1), pp. 55–63.

Das, K. and Mukherjee, A. K., (2007), 'Crude petroleum-oil biodegradation efficiency of *Bacillus subtilis* and *Pseudomonas aeruginosa* strains isolated from a petroleum-oil contaminated soil from North-East India', Bioresource Technology. 98(7), pp. 1339–1345.

Das, N. and Chandran, P., (2011), 'Microbial degradation of petroleum hydrocarbon Contaminants: an overview', Biotechnology Research International.

Danese, P. N., Pratt, L. A. & Kolter, R., (2000), 'Exopolysaccharide Production Is Required for Development of Escherichia Coli K-12 Biofilm Architecture'. Journal of bacteriology, 182(12), 3593–3596.

Declerck, P., (2010), 'Biofilms: the Environmental playground of *Legionella pneumophila*', Environmental Microbiology. pp. 557–566.

Delleur, J. W., (2006), The handbook of groundwater engineering. CRC press.

- DeLong, E. F., Franks, D. G. and Alldredge, A. L., (1993), 'Phylogenetic diversity of aggregate-attached vs. free-living marine bacterial assemblages', *Limnology and Oceanography*. 38(5), pp. 924–934.
- DeSantis, T.Z., Hugenholtz, P., Larsen, N., Rojas, M., Brodie, E.L., Keller, K., Huber, T., Dalevi, D., Hu, P. and Andersen, G.L., (2006), 'Greengenes, a chimera-checked 16S rRNA gene database and workbench compatible with ARB', *Applied and Environmental Microbiology*. 72(7), pp. 5069–5072.
- De Giglio, O., Barbuti, G., Trerotoli, P., Brigida, S., Calabrese, A., Di Vittorio, G., Lovero, G., Caggiano, G., Uricchio, V. F. & Montagna, M. T., (2016), 'Microbiological and Hydrogeological Assessment of Groundwater in Southern Italy'. *Environmental Monitoring and Assessment*, 188(11), 638.
- Di-Ruggiero, J. and Gounot, A. M., (1990), 'Microbial manganese reduction mediated by bacterial strains isolated from aquifer sediments', *Microbial Ecology*. 20(1), pp. 53–63.
- Donlan, R. M., (2002), 'Biofilms: microbial life on surfaces', *Emerging Infectious Diseases*. 8(9), p. 881.
- Du, Z.J., Jordan, E.M., Rooney, A.P., Chen, G.J., Austin, B., (2010), '*Corynebacterium marinum* sp. nov. isolated from coastal sediment', *International Journal of Systematic and Evolutionary Microbiology*. 60(8), pp. 1944–1947.
- Edgar, R. C., (2010), 'Search and clustering orders of magnitude faster than BLAST', *Bioinformatics*. 26(19), pp. 2460–2461.
- Edmunds, W. M. and Shand, P., (2008), 'Natural Groundwater Quality-Summary and Significance for Water Resources Management', *Natural Groundwater Quality*. pp. 441–462.
- Edwards, E.A., Wills, L.E., Reinhard, M. and Grbić-Galić, D., (1992), 'Anaerobic degradation of toluene and xylene by aquifer microorganisms under sulfate-reducing conditions', *Applied and Environmental Microbiology*. 58(3), pp. 794–800.
- Edwards, E. A. and Grbić-Galić, D., (1992), 'Complete mineralization of benzene by aquifer microorganisms under strictly anaerobic conditions.', *Applied and Environmental Microbiology* 58(8), pp. 2663–2666.
- Eisentraeger, A., Klag, P., Vansbotter, B., Heymann, E. & Dott, W., (2001), 'Denitrification of Groundwater with Methane as Sole Hydrogen Donor'. *Water research*, 35(9), 2261–2267.
- Elliott, D.R., Scholes, J.D., Thornton, S.F., Rizoulis, A., Banwart, S.A., Rolfe, S.A., (2009), 'Dynamic changes in microbial community structure and function in phenol-degrading microcosms inoculated with cells from a contaminated aquifer', *FEMS Microbiology Ecology*. 71(2), pp. 247–259.
- Farrell, A. and Quilty, B., (2002), 'Substrate-dependent autoaggregation of *Pseudomonas putida* CP1 during the degradation of mono-chlorophenols and phenol', *Journal of Industrial Microbiology and Biotechnology*. 28(6), pp. 316–324.

- Fahy, A., Lethbridge, G., Earle, R., Ball, A. S., Timmis, K. N. & McGenity, T. J., (2005), 'Effects of Long-term Benzene Pollution on Bacterial Diversity and Community Structure in Groundwater'. *Environmental Microbiology*, 7(8), 1192–1199.
- Fahy, A., McGenity, T.J., Timmis, K.N. & Ball, A.S., (2006), 'Heterogeneous aerobic benzene-degrading communities in oxygen-depleted groundwaters'. *FEMS Microbiology Ecology*, 58, 260–270.
- Fahy, A., Ball, A.S., Lethbridge, G., McGenity, T.J. & Timmis, K.N., (2008), 'High benzene concentrations can favour Gram-positive bacteria in groundwaters from a contaminated aquifer'. *FEMS Microbiology Ecology*, 65, 526–533
- Felske, A. and Osborn, A. M., (2005), 'DNA fingerprinting of microbial communities', *Molecular Microbial Ecology*. pp. 65–90.
- Feris, K. P., Hristova, K., Gebreyesus, B., Mackay, D. & Scow, K. M., (2004) 'A Shallow BTEX and MTBE Contaminated Aquifer Supports a Diverse Microbial Community. *Microbial ecology*'. 48(4), 589–600.
- Fitts, C. R., (2002), *Groundwater science*. Academic press.
- Finlay, B. J., Maberly, S. C. & Cooper, J. I., (1997), 'Microbial Diversity and Ecosystem Function'. *Oikos*, 209–213.
- Flint, H.J., Duncan, S.H., Scott, K.P., Louis, P., (2007), 'Interactions and competition within the microbial community of the human colon: links between diet and health', *Environmental Microbiology*. 9(5), pp. 1101–1111.
- Flynn, T. M., Sanford, R. A., Ryu, H., Bethke, C. M., Levine, A. D., Ashbolt, N. J. & Santo Domingo, J. W., (2013), 'Functional Microbial Diversity Explains Groundwater Chemistry in a Pristine Aquifer'. *BMC Microbiology*, 13(1), 146.
- Folwell, B. D., McGenity, T. J. & Whitby, C., (2016), 'Biofilm and Planktonic Bacterial and Fungal Communities Transforming High-Molecular-Weight Polycyclic Aromatic Hydrocarbons'. *Applied and environmental microbiology*, 82(8), 2288–2299.
- Fritsche, W. and Hofrichter, M., (2008), 'Aerobic degradation by microorganisms', *Biotechnology Set, Second Edition*. pp. 144–167.
- Frohlich, R.K., Urish, D.W., Fuller, J., O'Reilly, M., (1994), 'Use of geoelectrical methods in groundwater pollution surveys in a coastal environment', *Journal of Applied Geophysics*. 32(2–3), pp. 139–154.
- Fuchs, G., Boll, M. and Heider, J., (2011), 'Microbial degradation of aromatic compounds—from one strategy to four', *Nature Reviews Microbiology*. 9(11), pp. 803–816.
- Garrett, T. R., Bhakoo, M. and Zhang, Z., (2008), 'Bacterial adhesion and biofilms on surfaces', *Progress in Natural Science*. 18(9), pp. 1049–1056.

- Gao, Z., Tseng, C., Pei, Z. & Blaser, M. J., (2007), 'Molecular Analysis of Human Forearm Superficial Skin Bacterial Biota'. *Proceedings of the National Academy of Sciences*, 104(8), 2927–2932.
- Giatsis, C., Sijkema, D., Smidt, H., Heilig, H., Benvenuti, G., Verreth, J., Verdegem, M., (2015), 'The impact of rearing environment on the development of gut microbiota in tilapia larvae', *Scientific Reports*, 5. p.
- Gillham, R.W., Sudicky, E.A., Cherry, J.A., Frind, E.O., (1984), 'An advection-diffusion concept for solute transport in heterogeneous unconsolidated geological deposits', *Water Resources Research*. 20(3), pp. 369–378.
- Ginige, M.P., Kaksonen, A.H., Morris, C., Shackelton, M., Patterson, B.M., (2013), 'Bacterial community and groundwater quality changes in an anaerobic aquifer during groundwater recharge with aerobic recycled water', *FEMS Microbiology Ecology*. 85(3), pp. 553–567.
- Gleick, P. H., (1993), 'Water in crisis: a guide to the worlds fresh water resources.' New York Oxford University Press 1993.
- Gonzalez, P.J., Correia, C., Moura, I., Brondino, C.D., Moura, J.J.G., (2006), 'Bacterial nitrate reductases: molecular and biological aspects of nitrate reduction', *Journal of Inorganic Biochemistry*. 100(5), pp. 1015–1023.
- Godsy, E. M., Goerlitz, D. F., Grbic-Galic, D. (1992), 'Methanogenic Biodegradation of Creosote Contaminants in Natural and Simulated Ground-water Ecosystems'. *Groundwater*, 30(2), 232–242.
- Goody, D. C., Hughes, A. G., Williams, A. T., Armstrong, A. C., Nicholson, R. J. & Williams, J. R., (2001), 'Field and Modelling Studies to Assess the Risk to UK Groundwater from Earth-based Stores for Livestock Manure'. *Soil Use and Management*, 17(2), 128–137.
- Gounot, A.M, (1994), 'Microbial Oxidation and Reduction of Manganese: Consequences in Groundwater and Applications'. *FEMS Microbiology Reviews*, 14(4), 339–349.
- Gregory, S. P., Maurice, L. D., West, J. M. & Goody, D. C., (2014), 'Microbial Communities in UK Aquifers: Current Understanding and Future Research Needs' Geological Society of London.
- Griebler, C., Mindl, B., Slezak, D. & Geiger-Kaiser, M., (2002), 'Distribution Patterns of Attached and Suspended Bacteria in Pristine and Contaminated Shallow Aquifers Studied with an in Situ Sediment Exposure Microcosm'. *Aquatic Microbial Ecology*, 28(2), 117–129.
- Grisey, E., Belle, E., Dat, J., Mudry, J. & Aleya, L., (2010), 'Survival of Pathogenic and Indicator Organisms in Groundwater and Landfill Leachate through Coupling Bacterial Enumeration with Tracer Tests'. *Desalination*, 261(1–2), 162–168.
- Hall-Stoodley, L., Costerton, J. W. and Stoodley, P., (2004), 'Bacterial biofilms: from the natural environment to infectious diseases', *Nature Reviews Microbiology*. 2(2), pp. 95–108.
- Hancock, P. J., Boulton, A. J. and Humphreys, W. F., (2005), 'Aquifers and hyporheic zones: towards an ecological understanding of groundwater', *Hydrogeology Journal*. 13(1), pp. 98–111.

- Hausner, M. & Wuertz, S., (1999), 'High Rates of Conjugation in Bacterial Biofilms as Determined by Quantitative in Situ Analysis'. *Applied and Environmental Microbiology*, 65(8), 3710–3713.
- Hazen, T.C., Jiménez, L., de Victoria, G.L., Fliermans, C.B., (1991), 'Comparison of bacteria from deep subsurface sediment and adjacent groundwater', *Microbial Ecology*. 22(1), pp. 293–304.
- Hedbavna, P., Rolfe, S.A., Huang, W.E., Thornton, S.F., (2016), 'Biodegradation of phenolic compounds and their metabolites in contaminated groundwater using microbial fuel cells', *Bioresource Technology*. 200, pp. 426–434.
- Hernandez, M. E. & Newman, D. K., (2001), 'Extracellular Electron Transfer. Cellular and Molecular Life Sciences' *CMLS*, 58(11), 1562–1571.
- Hess, A., Zarda, B., Hahn, D., Häner, A.N.D.R.E.A.S., Stax, D., Höhener, P., Zeyer, J., (1997), 'In situ analysis of denitrifying toluene- and m-xylene-degrading bacteria in a diesel fuel-contaminated laboratory aquifer column', *Applied and Environmental Microbiology*. *Am Soc Microbiol*, 63(6), pp. 2136–2141.
- Hiscock, K. M., (2009), *Hydrogeology: principles and practice*. John Wiley & Sons.
- Holm, P.E., Nielsen, P.H., Albrechtsen, H.J., Christensen, T.H., (1992), 'Importance of unattached bacteria and bacteria attached to sediment in determining potentials for degradation of xenobiotic organic Contaminants in an aerobic aquifer', *Applied and Environmental Microbiology*. 58(9), pp. 3020–3026.
- Hoisington, A., Maestre, J. P., Kinney, K. A. & Siegel, J. A., (2016), 'Characterizing the Bacterial Communities in Retail Stores in the United States'. *Indoor Air*, 26(6), 857–868.
- Huang, C. and Mayer, A. S., (1997), 'Pump-and-treat optimization using well locations and pumping rates as decision variables', *Water Resources Research*. 33(5), pp. 1001–1012.
- Huang, W.E., Oswald, S.E., Lerner, D.N., Smith, C.C., Zheng, C., (2003), 'Dissolved oxygen imaging in a porous medium to investigate biodegradation in a plume with limited electron acceptor supply', *Environmental Science & Technology*. 37(9), pp. 1905–1911.
- Hutchins, S. R., (1991), 'Biodegradation of monoaromatic hydrocarbons by aquifer microorganisms using oxygen, nitrate, or nitrous oxide as the terminal electron acceptor'. *Applied and Environmental Microbiology*. 57(8), pp. 2403–2407.
- Ihrmark, K., Bödeker, I., Cruz-Martinez, K., Friberg, H., Kubartova, A., Schenck, J., Strid, Y., Stenlid, J., Brandström-Durling, M., Clemmensen, K.E., Lindahl, B.D., (2012), 'New primers to amplify the fungal ITS2 region—evaluation by 454-sequencing of artificial and natural communities', *FEMS Microbiology ecology*. 82(3), pp. 666–677.
- Jackson, C. R. (2003) 'Changes in community properties during microbial succession', *Oikos*. 101(2), pp. 444–448.
- Jackson, C. R., Churchill, P. F. and Roden, E. E., (2001), 'Successional changes in bacterial assemblage structure during epilithic biofilm development', *Ecology*. 82(2), pp. 555–566.

- Jefferson, K. K., (2004), 'What Drives Bacteria to Produce a Biofilm?' FEMS microbiology letters, 236(2), 163–173.
- Johnson, A. C., White, C. & Bhardwaj, C. L., (2000), 'Potential for Isoproturon, Atrazine and Mecoprop to Be Degraded within a Chalk Aquifer System'. Journal of Contaminant Hydrology, 44(1), 1–18.
- Johnson, A., Llewellyn, N., Smith, J., van der Gast, C., Lilley, A., Singer, A. & Thompson, I., (2004), 'The Role of Microbial Community Composition and Groundwater Chemistry in Determining Isoproturon Degradation Potential in UK Aquifers'. FEMS microbiology ecology, 49(1), 71–82.
- Joutey, N.T., Bahafid, W., Sayel, H., El Ghachtouli, N., (2013), 'Biodegradation: involved microorganisms and genetically engineered microorganisms', in Biodegradation-Life of Science.
- Keely, J. F. and Boulding, J. R. (1989) 'Performance evaluations of pump-and-treat remediations'. United States Environmental Protection Agency US EPA.
- Kemper, K. E., (2004,) 'Groundwater—from development to management', Hydrogeology Journal., 12(1), pp. 3–5.
- Khan, F. I. and Husain, T., (2001), 'Risk-based monitored natural attenuation—a case study', Journal of hazardous materials. 85(3), pp. 243–272.
- Keuper B., Wealthall G., Smith J., Leharne S., Lerner D., (2003), 'An Illustrated Handbook of DNAPL Transport and Fate in the Subsurface' Environment Agency, available at [https://clu-in.org/conf/itrc/dnaplpa/dnapl\\_handbook\\_binal.pdf](https://clu-in.org/conf/itrc/dnaplpa/dnapl_handbook_binal.pdf)
- Kleinsteuber, S., Schleinitz, K. M. and Vogt, C., (2012), 'Key players and team play: anaerobic microbial communities in hydrocarbon-contaminated aquifers', Applied Microbiology and Biotechnology. 94(4), pp. 851–873.
- Klindworth, A., Pruesse, E., Schweer, T., Peplies, J., Quast, C., Horn, M., Glöckner, F.O., (2013), 'Evaluation of general 16S ribosomal RNA gene PCR primers for classical and next-generation sequencing-based diversity studies'. Nucleic acids research. 41(1), pp. e1–e1.
- Kolter, R., Siegele, D. A. and Tormo, A., (1993), 'The stationary phase of the bacterial life cycle', Annual Reviews in Microbiology. 47(1), pp. 855–874.
- Konopka, A. and Turco, R., (1991), 'Biodegradation of organic compounds in vadose zone and aquifer sediments.', Applied and Environmental Microbiology. 57(8), pp. 2260–2268.
- Krapac, I. G., Dey, W. S., Roy, W. R., Smyth, C. A., Storment, E., Sargent, S. L. & Steele, J. D., (2002), 'Impacts of Swine Manure Pits on Groundwater Quality'. Environmental Pollution, 120(2), 475–492.
- Krumme, M. L., Timmis, K. N. and Dwyer, D. F., (1993), 'Degradation of trichloroethylene by *Pseudomonas cepacia* G4 and the constitutive mutant strain G4 5223 PR1 in aquifer microcosms.', Applied and Environmental Microbiology. 59(8), pp. 2746–2749.

- Kümmel, S., Herbst, F.A., Bahr, A., Duarte, M., Pieper, D.H., Jehmlich, N., Seifert, J., von Bergen, M., Bombach, P., Richnow, H.H., Vogt, C., (2015), 'Anaerobic naphthalene degradation by sulfate-reducing *Desulfobacteraceae* from various anoxic aquifers'. *FEMS Microbiology ecology*. 91(3), p. fiv006.
- Ladino-Orjuela, G., Gomes, E., da Silva, R., Salt, C., Parsons, J.R., (2016), 'Metabolic pathways for degradation of aromatic hydrocarbons by bacteria', in *Reviews of Environmental Contamination and Toxicology Volume 237*. pp. 105–121.
- Langille, M. G. I., Zaneveld, J., Caporaso, J. G., McDonald, D., Knights, D., Reyes, J. A., Clemente, J. C., Burkepile, D. E., Thurber, R. L. V. & Knight, R., (2013), 'Predictive Functional Profiling of Microbial Communities Using 16S rRNA Marker Gene Sequences'. *Nature biotechnology*, 31(9), 814.
- Langwaldt, J. H. and Puhakka, J. A., (2000), 'On-site biological remediation of contaminated groundwater: a review', *Environmental Pollution*. 107(2), pp. 187–197.
- Lapworth, D.J., Baran, N., Stuart, M.E., Ward, R.S., (2012), 'Emerging organic Contaminants in groundwater: a review of sources, fate and occurrence', *Environmental Pollution*. 163, pp. 287–303.
- Lehman, R. M., Colwell, F. S. & Bala, G. A., (2001), 'Attached and Unattached Microbial Communities in a Simulated Basalt Aquifer under Fracture-and Porous-Flow Conditions'. *Applied and Environmental Microbiology*, 67(6), 2799–2809.
- Lehman, R. M., Roberto, F. F., Earley, D., Bruhn, D. F., Brink, S. E., O'Connell, S. P., Delwiche, M. E. & Colwell, F. S., (2001), 'Attached and Unattached Bacterial Communities in a 120-Meter Corehole in an Acidic, Crystalline Rock Aquifer'. *Applied and Environmental Microbiology*, 67(5), 2095–2106.
- León-Zayas, R., Peoples, L., Biddle, J.F., Podell, S., Novotny, M., Cameron, J., Lasken, R.S., Bartlett, D.H., (2017), 'The metabolic potential of the single cell genomes obtained from the Challenger Deep, Mariana Trench within the candidate *superphylum Parcubacteria* (OD1)', *Environmental Microbiology*. 19(7), pp. 2769–2784.
- Lerner, D.N., Thornton, S.F., Spence, M.J., Banwart, S.A., Bottrell, S.H., Higgo, J.J., Mallinson, H.E., Pickup, R.W., Williams, G.M., (2000), 'Ineffective Natural Attenuation of Degradable Organic Compounds in a Phenol-Contaminated Aquifer', *Groundwater*. 38(6), pp. 922–928.
- Lerner, D. N. and Harris, B., (2009), 'The relationship between land use and groundwater resources and quality', *Land use policy*. 26, pp. S265–S273.
- Lewis, W. J., Foster, S. S. D. and Drasar, B. S., (1982), 'Risk of groundwater pollution by on-site sanitation in developing countries; a literature review', *International Reference Centre for Wastes*.
- Lindsay, D., Brözel, V. S., Mostert, J. F. & Von Holy, A., (2002), 'Differential Efficacy of a Chlorine Dioxide-containing Sanitizer against Single Species and Binary Biofilms of a Dairy-associated *Bacillus Cereus* and a *Pseudomonas Fluorescens* Isolate'. *Journal of Applied Microbiology*, 92(2), 352–361.



- List, B., Lerner, R. A. and Barbas, C. F., (2000), 'Proline-catalyzed direct asymmetric aldol reactions', *Journal of the American Chemical Society*. 122(10), pp. 2395–2396.
- Logue, J. B., Findlay, S. E. G. and Comte, J., (2015), 'Microbial responses to Environmental changes', *Frontiers in Microbiology*. Frontiers Media SA, 6.
- Lovley, D. R., Chapelle, F. H. and Woodward, J. C., (1994), 'Use of dissolved H<sub>2</sub> concentrations to determine distribution of microbially catalyzed redox reactions in anoxic groundwater', *Environmental science & technology*. 28(7), pp. 1205–1210.
- Lovley, D. R., Ueki, T., Zhang, T., Malvankar, N. S., Shrestha, P. M., Flanagan, K. A., Aklujkar, M., Butler, J. E., Giloteaux, L. & Rotaru, A.E., (2011), *Geobacter: 'The Microbe Electric's Physiology, Ecology, and Practical Applications'* *Advances in microbial Physiology*, (pp. 1–100).
- Lovley, D. R., Holmes, D. E. and Nevin, K. P., (2004), 'Dissimilatory Fe (iii) and Mn (iv) reduction', *Advances in Microbial Physiology*. 49, pp. 219–286.
- Lovley, D. R. and Phillips, E. J. P., (1988), 'Novel mode of microbial energy metabolism: organic carbon oxidation coupled to dissimilatory reduction of iron or manganese', *Applied and Environmental Microbiology*. 54(6), pp. 1472–1480.
- Lu, X., Zhang, T., Fang, H.H.P., Leung, K.M., Zhang, G. (2011), 'Biodegradation of naphthalene by enriched marine denitrifying bacteria', *International Biodeterioration & Biodegradation*. 65(1), pp. 204–211.
- Ludvigsen, L., Albrechtsen, H.J., Ringelberg, D.B., Ekelund, F., Christensen, T.H., (1999), 'Distribution and composition of microbial populations in a landfill leachate contaminated aquifer (Grindsted, Denmark)', *Microbial Ecology*. 37(3), pp. 197–207.
- Lyngkilde, J. and Christensen, T. H., (1992), 'Fate of organic Contaminants in the redox zones of a landfill leachate pollution plume (Vejen, Denmark)', *Journal of Contaminant Hydrology*. 10(4), pp. 291–307.
- MacIntyre, W.G., Boggs, M., Antworth, C.P., Stauffer, T.B., (1993), 'Degradation kinetics of aromatic organic solutes introduced into a heterogeneous aquifer', *Water Resources Research*. 29(12), pp. 4045–4051.
- Mackay, D. M. and Cherry, J. A., (1989), 'Groundwater contamination: Pump-and-treat remediation', *Environmental Science & Technology*. 23(6), pp. 630–636.
- Madsen, E. L., (2015), *Environmental Microbiology: from genomes to biogeochemistry*. John Wiley & Sons.
- Madsen, E. L., Sinclair, J. L. and Ghiorse, W. C., (1991), 'In situ biodegradation: microbiological patterns in a contaminated aquifer.', *Science*. pp. 830–833.
- Madsen, J.S., Burmølle, M., Hansen, L.H., Sørensen, S.J., (2012), 'The interconnection between biofilm formation and horizontal gene transfer', *FEMS Immunology & Medical Microbiology*. pp. 183–195.

- Martiny, A.C., Jørgensen, T.M., Albrechtsen, H.J., Arvin, E., Molin, S., (2003), 'Long-term succession of structure and diversity of a biofilm formed in a model drinking water distribution system', *Applied and Environmental Microbiology*. 69(11), pp. 6899–6907.
- Matott, L. S., Rabideau, A. J. and Craig, J. R., (2006), 'Pump-and-treat optimization using analytic element method flow models', *Advances in Water Resources*. 29(5), pp. 760–775.
- Mayer, K.U., Benner, S.G., Frind, E.O., Thornton, S.F., Lerner, D.N., (2001), 'Reactive transport modeling of processes controlling the distribution and natural attenuation of phenolic compounds in a deep sandstone aquifer', *Journal of Contaminant Hydrology*. 53(3), pp. 341–368.
- McBain, A.J., Bartolo, R.G., Catrenich, C.E., Charbonneau, D., Ledder, R.G., Rickard, A.H., Symmons, S.A., Gilbert, P., (2003), 'Microbial characterization of biofilms in domestic drains and the establishment of stable biofilm microcosms', *Applied and Environmental Microbiology*. 69(1), pp. 177–185.
- McBurnie, L. & Bardo, B., (2004), 'Validation of Sterile Filtration'. *Pharmaceutical Technology*. 24, S13.
- McDonald, D., Price, M.N., Goodrich, J., Nawrocki, E.P., DeSantis, T.Z., Probst, A., Andersen, G.L., Knight, R., Hugenholtz, P., (2012), 'An improved Greengenes taxonomy with explicit ranks for ecological and evolutionary analyses of bacteria and archaea'. *The ISME journal*. 6(3), pp. 610–618.
- McKinney, D. C. and Lin, M.D., (1996), 'Pump-and-treat ground-water remediation system optimization', *Journal of Water Resources Planning and Management*. 122(2), pp. 128–136.
- McMurdie, P. J. and Holmes, S., (2013), 'phyloseq: an R package for reproducible interactive analysis and graphics of microbiome census data', *PloS one*. 8(4), p. e61217.
- Meckenstock, R.U., Morasch, B., Warthmann, R., Schink, B., Annweiler, E., Michaelis, W., Richnow, H.H., (1999), '<sup>13</sup>C/<sup>12</sup>C isotope fractionation of aromatic hydrocarbons during microbial degradation', *Environmental Microbiology*. 1(5), pp. 409–414.
- Meckenstock, R.U., Elsner, M., Griebler, C., Lueders, T., Stumpp, C., Aamand, J., Agathos, S.N., Albrechtsen, H.J., Bastiaens, L., Bjerg, P.L., Boon, N., (2015), 'Biodegradation: updating the concepts of control for microbial cleanup in contaminated aquifers'. *ACS*.
- Megharaj, M., Ramakrishnan, B., Venkateswarlu, K., Sethunathan, N., Naidu, R., (2011), 'Bioremediation approaches for organic pollutants: a critical perspective', *Environment International*. 37(8), pp. 1362–1375.
- Mercer, J. W., Skipp, D. C. and Giffin, D., (1990), *Basics of pump-and-treat ground-water remediation technology*. Robert S. Kerr Environmental Research Laboratory, Office of Research and Development, US Environmental Protection Agency.
- Michałowicz, J. and Duda, W., (2007), 'Phenols--Sources and Toxicity.', *Polish Journal of Environmental Studies*, 16(3).

- Mikesell, M. D., Kukor, J. J. and Olsen, R. H., (1993), 'Metabolic diversity of aromatic hydrocarbon-degrading bacteria from a petroleum-contaminated aquifer', *Biodegradation*. 4(4), pp. 249–259.
- Mitchell, A.C., Phillips, A.J., Hamilton, M.A., Gerlach, R., Hollis, W.K., Kaszuba, J.P., Cunningham, A.B., (2008), 'Resilience of planktonic and biofilm cultures to supercritical CO<sub>2</sub>', *The Journal of Supercritical Fluids*. 47(2), pp. 318–325.
- Morris, B.L., Lawrence, A.R., Chilton, P.J.C., Adams, B., Calow, R.C., Klinck, B.A., (2003), 'Groundwater and its susceptibility to degradation: a global assessment of the problem and options for management'. United Nations Environment Programme.
- Müller, H., Bosch, J., Griebler, C., Damgaard, L. R., Nielsen, L. P., Lueders, T. & Meckenstock, R. U., (2016), Long-Distance Electron Transfer by Cable Bacteria in Aquifer Sediments. *The ISME journal*, 10(8), 2010.
- Naik, M. G. and Duraphe, M. D., (2012), 'Review paper on–parameters affecting bioremediation', *International Journal of Life Science and Pharma Research*, 2(3), pp. L77–L80.
- Nicolella, C., Van Loosdrecht, M. C. M. & Heijnen, J. J., (2000), 'Wastewater Treatment with Particulate Biofilm Reactors'. *Journal of Biotechnology*, 80(1), 1–33.
- Nicolella, C., van Loosdrecht, M. C. M. & Heijnen, S. J., (2000), 'Particle-Based Biofilm Reactor Technology'. *Trends in Biotechnology*, 18(7), 312–320.
- Nielsen, P.H., Bjerg, P.L., Nielsen, P., Smith, P., Christensen, T.H., (1995), 'In situ and laboratory determined first-order degradation rate constants of specific organic compounds in an aerobic aquifer', *Environmental science & Technology*. 30(1), pp. 31–37.
- Noda, S., Hongoh, Y., Sato, T., Ohkuma, M., (2009), 'Complex coevolutionary history of symbiotic *Bacteroidales* bacteria of various protists in the gut of termites', *BMC evolutionary biology*. 9(1), p. 158.
- O'Dwyer, J., Dowling, A. & Adley, C. C., (2014), 'Microbiological Assessment of Private Groundwater-Derived Potable Water Supplies in the Mid-West Region of Ireland'. *Journal of Water and Health*, 12(2), 310–317.
- O'toole, G. A. & Kolter, R., (1998), 'Initiation of Biofilm Formation in *Pseudomonas Fluorescens* WCS365 Proceeds via Multiple, Convergent Signalling Pathways: A Genetic Analysis'. *Molecular Microbiology*, 28(3), 449–461.
- O'Toole, G., Kaplan, H. B. and Kolter, R., (2000), 'Biofilm formation as microbial development', *Annual Reviews in Microbiology*. 54(1), pp. 49–79.
- Oksanen, J., (2012), 'Constrained Ordination: Tutorial with R and vegan'. R tutorial available on the web: <http://cc.oulu.fi/~jarioksa/opetus/metodi/sessio2.pdf>
- Oren, A., (2014), 'The Prokaryotes-Other Major Lineages of Bacteria and the Archaea'. Springer-Verlag, New York.

- Osborn, A. M., Moore, E. R. B. and Timmis, K. N., (2000), 'An evaluation of terminal-restriction fragment length polymorphism (T-RFLP) analysis for the study of microbial community structure and dynamics', *Environmental Microbiology*. 2(1), pp. 39–50.
- Özler, H. M. & Aydın, A., (2008), 'Hydrochemical and Microbiological Quality of Groundwater in West Thrace Region of Turkey'. *Environmental Geology*, 54(2), 355–363.
- Palmer, C. D. and Fish, W., (1992), Chemical enhancements to pump-and-treat remediation. Superfund Technology Support Center for Ground Water, Robert S. Kerr Environmental Research Laboratory.
- Peterson, B. J. and Fry, B., (1987), 'Stable isotopes in ecosystem studies', *Annual Review of Ecology and Systematics*. pp. 293–320.
- Pickup, R.W., Rhodes, G., Alamillo, M.L., Mallinson, H.E.H., Thornton, S.F., Lerner, D.N., (2001), 'Microbiological analysis of multi-level borehole samples from a contaminated groundwater system', *Journal of Contaminant Hydrology*. 53(3), pp. 269–284.
- Pinheiro, J., Bates, D., DebRoy, S., Sarkar, D., R., (2011), 'R Development Core Team. 2010. nlme: linear and nonlinear mixed effects models. R package version 3.1-97', R Foundation for Statistical Computing, Vienna.
- Plugge, C.M., Zhang, W., Scholten, J., Stams, A.J., (2011), 'Metabolic flexibility of sulfate-reducing bacteria', *Frontiers in Microbiology*.
- Posman, K. M., DeRito, C. M. and Madsen, E. L., (2017), 'Benzene Degradation by a *Variovorax* Species within a Coal Tar-Contaminated Groundwater Microbial Community', *Applied and Environmental Microbiology*. 83(4), pp.
- Price, P. B. & Sowers, T., (2004), 'Temperature Dependence of Metabolic Rates for Microbial Growth, Maintenance, and Survival'. *Proceedings of the National Academy of Sciences of the United States of America*, 101(13), 4631–4636.
- Proestos, C. and Komaitis, M., (2013), 'Analysis of naturally occurring phenolic compounds in aromatic plants by RP-HPLC coupled to diode array detector (DAD) and GC-MS after silylation', *Foods*, 2(1), pp. 90–99.
- Qiu, J., (2010), 'China faces up to groundwater crisis'. *Nature*.
- Qureshi, N., Annous, B. A., Ezeji, T. C., Karcher, P. & Maddox, I. S., (2005), 'Biofilm Reactors for Industrial Bioconversion Processes: Employing Potential of Enhanced Reaction Rates'. *Microbial Cell Factories*, 4(1), 24.
- Rabus, R. and Widdel, F., (1995), 'Anaerobic degradation of ethylbenzene and other aromatic hydrocarbons by new denitrifying bacteria', *Archives of Microbiology*. 163(2), pp. 96–103.
- Rees, H.C., Oswald, S.E., Banwart, S.A., Pickup, R.W., Lerner, D.N., (2007), 'Biodegradation processes in a laboratory-scale groundwater Contaminant plume assessed by fluorescence imaging and microbial analysis', *Applied and Environmental Microbiology*. 73(12), pp. 3865–3876.

Rickard, A.H., Gilbert, P., High, N.J., Kolenbrander, P.E., Handley, P.S., (2003), 'Bacterial coaggregation: an integral process in the development of multi-species biofilms', *Trends in Microbiology*. 11(2), pp. 94–100.

Ringelberg, D.B., Talley, J.W., Perkins, E.J., Tucker, S.G., Luthy, R.G., Bouwer, E.J., Fredrickson, H.L., (2001), 'Succession of phenotypic, genotypic, and metabolic community characteristics during in vitro bioslurry treatment of polycyclic aromatic hydrocarbon-contaminated sediments', *Applied and Environmental Microbiology*. 67(4), pp. 1542–1550.

Rivett M., Tomlinson D., Thornton S., Thomas A., Leharne S., Wealthall G., (2014), 'An Illustrated Handbook of LNAPL Transport and Fate in the Subsurface' CLAIRE, available at [www.claire.co.uk/LNAPL](http://www.claire.co.uk/LNAPL)

Rivett, M.O., Buss, S.R., Morgan, P., Smith, J.W., Bemment, C.D., (2008), 'Nitrate attenuation in groundwater: A review of biogeochemical controlling processes', *Water Research*. 42(16), pp. 4215–4232.

Rivett, M. O., Feenstra, S. and Cherry, J. A., (2001), 'A controlled field experiment on groundwater contamination by a multicomponent DNAPL: creation of the emplaced-source and overview of dissolved plume development', *Journal of Contaminant Hydrology*. 49(1), pp. 111–149.

Rivett, M. O. and Thornton, S. F., (2008), 'Monitored natural attenuation of organic Contaminants in groundwater: principles and application', in *Proceedings of the Institution of Civil Engineers-Water Management*. pp. 381–392.

Rizoulis, A., Elliott, D.R., Rolfe, S.A., Thornton, S.F., Banwart, S.A., Pickup, R.W., Scholes, J.D., (2013), 'Diversity of planktonic and attached bacterial communities in a phenol-contaminated sandstone aquifer', *Microbial ecology*. 66(1), pp. 84–95.

Robertson, W. J., Franzmann, P. D. and Mee, B. J., (2000), 'Spore-forming, Desulfosporosinus-like sulphate-reducing bacteria from a shallow aquifer contaminated with gasoline', *Journal of Applied Microbiology*. 88(2), pp. 248–259.

Rooney-Varga, J.N., Anderson, R.T., Fraga, J.L., Ringelberg, D., Lovley, D.R., (1999), 'Microbial communities associated to anaerobic benzene degradation in a petroleum-contaminated aquifer', *Applied and Environmental Microbiology*. 65(7), pp. 3056–3063.

Rowan, A. K., Snape, J. R., Fearnside, D., Barer, M. R., Curtis, T. P. & Head, I. M., (2003), 'Composition and Diversity of Ammonia-Oxidising Bacterial Communities in Wastewater Treatment Reactors of Different Design Treating Identical Wastewater'. *FEMS Microbiology Ecology*, 43(2), 195–206.

De Rosa, M., Gambacorta, A. and Gliozzi, A., (1986), 'Structure, biosynthesis, and physicochemical properties of archaebacterial lipids.', *Microbiological Reviews*. 50(1), p. 70.

Rügner, H., Finkel, M., Kaschl, A. and Bittens, M., (2006), 'Application of monitored natural attenuation in contaminated land management—a review and recommended approach for Europe', *Environmental science & Policy*. 9(6), pp. 568–576.

- Santegoeds, C.M., Ferdelman, T.G., Muyzer, G., de Beer, D., (1998), 'Structural and functional dynamics of sulfate-reducing populations in bacterial biofilms', *Applied and Environmental Microbiology*. 64(10), pp. 3731–3739.
- Sauer, K., Camper, A. K., Ehrlich, G. D., Costerton, J. W. & Davies, D. G., (2002), '*Pseudomonas Aeruginosa* Displays Multiple Phenotypes during Development as a Biofilm'. *Journal of bacteriology*, 184(4), 1140–1154.
- van Schie, P. M. and Young, L. Y., (2000), 'Biodegradation of phenol: mechanisms and applications', *Bioremediation Journal*. 4(1), pp. 1–18.
- Schrader, C., Schielke, A., Ellerbroek, L., Johne, R., (2012), 'PCR inhibitors—occurrence, properties and removal', *Journal of applied Microbiology*. 113(5), pp. 1014–1026.
- Scherr, K. E., Backes, D., Scarlett, A. G., Lantschbauer, W. & Nahold, M., (2016), 'Biogeochemical Gradients above a Coal Tar DNAPL'. *Science of the Total Environment*, 563, 741–754.
- Schwartz, F. W., (1977), 'Macroscopic dispersion in porous media: The controlling factors', *Water Resources Research*. 13(4), pp. 743–752.
- Schwarzenbach, R.P., Egli, T., Hofstetter, T.B., Von Gunten, U., Wehrli, B., (2010), 'Global water pollution and human health', *Annual Review of Environment and Resources*. 35, pp. 109–136.
- Shahimin, M. F. M. and Siddique, T., (2017), 'Sequential biodegradation of complex naphtha hydrocarbons under methanogenic conditions in two different oil sands tailings', *Environmental Pollution*. 221, pp. 398–406.
- Shi, Y., Zwolinski, M. D., Schreiber, M. E., Bahr, J. M., Sewell, G. W. & Hickey, W. J., (1999), 'Molecular Analysis of Microbial Community Structures in Pristine and Contaminated Aquifers: Field and Laboratory Microcosm Experiments'. *Applied and Environmental Microbiology*, 65(5), 2143–2150.
- Sihag, S., Pathak, H. and Jaroli, D. P., (2014), 'Factors Affecting the Rate of Biodegradation of Polyaromatic Hydrocarbons ' *International Journal of Pure & Applied Biosciences* 2(3), pp. 185–202.
- Smith, C.J., Danilowicz, B.S., Clear, A.K., Costello, F.J., Wilson, B., Meijer, W.G., (2005), 'T-Align, a web-based tool for comparison of multiple terminal restriction fragment length polymorphism profiles', *FEMS Microbiology Ecology*. 54(3), pp. 375–380.
- Solomon, S., Kachiprath, B., Jayanath, G., Sajeevan, T.P., Singh, I.B., Philip, R., (2016), 'High-quality metagenomic DNA from marine sediment samples for genomic studies through a preprocessing approach', *3 Biotech*. 6(2), p. 160.
- de Souza, J.A.M., Alves, L.M.C., de Mello Varani, A. and de Macedo Lemos, E.G., (2014), 'The Family Bradyrhizobiaceae', in *The Prokaryotes*, pp. 135–154.
- Spence, M.J., Bottrell, S.H., Higgo, J.J.W., Harrison, I., Fallick, A.E., (2001), 'Denitrification and phenol degradation in a contaminated aquifer', *Journal of Contaminant Hydrology*. 53(3), pp. 305–318.

- Spence, M.J., Bottrell, S.H., Thornton, S.F., Lerner, D.N., (2001), 'Isotopic modelling of the significance of bacterial sulphate reduction for phenol attenuation in a contaminated aquifer', *Journal of Contaminant Hydrology*. 53(3), pp. 285–304.
- Srivastava, J., Kalra, S. J. S. and Naraian, R., (2014), 'Environmental perspectives of *Phragmites australis* (Cav.) Trin. Ex. Steudel', *Applied Water Science*. 4(3), pp. 193–202.
- Staley, J. T., Irgens, R. L. and Brenner, D. J., (1987), 'Enhydrobacter aerosaccus gen. nov., sp. nov., a gas-vacuolated, facultatively anaerobic, heterotrophic rod', *International Journal of Systematic and Evolutionary Microbiology*. 37(3), pp. 289–291.
- Stapleton, R. D., Bright, N. G. and Sayler, G. S., (2000), 'Catabolic and Genetic Diversity of Degradative Bacteria from Fuel-Hydrocarbon Contaminated Aquifers.', *Microbial ecology*. 39(3).
- Steinberger, R. E. & Holden, P. A., (2005), 'Extracellular DNA in Single-and Multiple-Species Unsaturated Biofilms'. *Applied and environmental microbiology*, 71(9), 5404–5410.
- Stewart, P. S. & Franklin, M. J., (2008), 'Physiological Heterogeneity in Biofilms'. *Nature Reviews Microbiology*, 6(3), 199.
- Stoodley, P., Sauer, K., Davies, D. G. & Costerton, J. W., (2002), 'Biofilms as Complex Differentiated Communities'. *Annual Reviews in Microbiology*, 56(1), 187–209.
- Suarez, M. P. and Rifai, H. S., (1999), 'Biodegradation rates for fuel hydrocarbons and chlorinated solvents in groundwater', *Bioremediation Journal*. 3(4), pp. 337–362.
- Summons, R. E., Franzmann, P. D. and Nichols, P. D., (1998), 'Carbon isotopic fractionation associated to methylotrophic methanogenesis', *Organic Geochemistry*. 28(7), pp. 465–475.
- Swindoll, C. M., Aelion, C. M. and Pfaender, F. K., (1988), 'Influence of inorganic and organic nutrients on aerobic biodegradation and on the adaptation response of subsurface microbial communities.', *Applied and Environmental Microbiology*. 54(1), pp. 212–217.
- Thornton, S.F., Quigley, S., Spence, M.J., Banwart, S.A., Bottrell, S., Lerner, D.N., (2001a), 'Processes controlling the distribution and natural attenuation of dissolved phenolic compounds in a deep sandstone aquifer', *Journal of Contaminant Hydrology*. 53(3), pp. 233–267.
- Thornton, S. F., Lerner, D. N. and Banwart, S. A., (2001b), 'Assessing the natural attenuation of organic Contaminants in aquifers using plume-scale electron and carbon balances: model development with analysis of uncertainty and parameter sensitivity', *Journal of Contaminant Hydrology*. 53(3), pp. 199–232.
- Thornton, S.F., Baker, K.M., Bottrell, S.H., Rolfe, S.A., McNamee, P., Forrest, F., Duffield, P., Wilson, R.D., Fairburn, A.W., Cieslak, L.A., (2014), 'Enhancement of in situ biodegradation of organic compounds in groundwater by targeted pump and treat intervention', *Applied geochemistry*. 48, pp. 28–40.
- Thornton, S. F., Morgan, P. and Rolfe, S. A., (2017), 'Bioremediation of Hydrocarbons and Chlorinated Solvents in Groundwater: Characterisation, Design and Performance Assessment',

Hydrocarbon and Lipid Microbiology Protocols: Pollution Mitigation and Waste Treatment Applications. pp. 11–64.

Tischer, K., Kleinstaub, S., Schleinitz, K.M., Fetzer, I., Spott, O., Stange, F., Lohse, U., Franz, J., Neumann, F., Gerling, S., Schmidt, C., (2013), 'Microbial communities along biogeochemical gradients in a hydrocarbon-contaminated aquifer', *Environmental Microbiology*. 15(9), pp. 2603–2615.

Tolba, M. K., (2001), 'Our Fragile World: Challenges and Opportunities for Sustainable Development'-Volume II. EOLSS Publications.

Treude, N., Rosencrantz, D., Liesack, W., Schnell, S., (2003), 'Strain FAC12, a dissimilatory iron-reducing member of the Anaeromyxobacter subgroup of *Myxococcales*', *FEMS Microbiology ecology*. 44(2), pp. 261–269.

Tuxen, N., Albrechtsen, H.-J. and Bjerg, P. L., (2006), 'Identification of a reactive degradation zone at a landfill leachate plume fringe using high resolution sampling and incubation techniques', *Journal of Contaminant Hydrology*. 85(3), pp. 179–194.

Unesco, (2002), 'Groundwater Contamination Inventory: A Methodological Guide', IHP-VI, Series on groundwater'

Usami, R., Fukushima, T., Mizuki, T., Yoshida, Y., Inoue, A., Horikoshi, K., (2005), 'Organic solvent tolerance of halophilic archaea, *Haloarcula* strains: effects of NaCl concentration on the tolerance and polar lipid composition', *Journal of bioscience and bioengineering*. Elsevier, 99(2), pp. 169–174.

Vartoukian, S. R., Palmer, R. M. and Wade, W. G., (2010), 'Strategies for culture of "unculturable" bacteria', *FEMS Microbiology letters*. 309(1), pp. 1–7.

Van Breukelen, B.M., Röling, W.F., Groen, J., Griffioen, J., van Verseveld, H.W., (2003), 'Biogeochemistry and isotope geochemistry of a landfill leachate plume', *Journal of Contaminant Hydrology*. 65(3), pp. 245–268.

Van Breukelen, B. M. and Griffioen, J., (2004), 'Biogeochemical processes at the fringe of a landfill leachate pollution plume: potential for dissolved organic carbon, Fe (II), Mn (II), NH<sub>4</sub>, and CH<sub>4</sub> oxidation', *Journal of Contaminant Hydrology*. 73(1), pp. 181–205.

Van de Vossenberg, J. L. C. M., Driessen, A. J. M. and Konings, W. N., (1998), 'The essence of being extremophilic: the role of the unique archaeal membrane lipids', *Extremophiles*. 2(3), pp. 163–170.

Wang, H., Liu, S. and Du, S., (2013), 'The investigation and assessment on groundwater organic pollution', in *Organic Pollutants-Monitoring, Risk and Treatment*..

Wang, L., Fan, D., Chen, W., Terentjev, E.M., (2015), 'Bacterial growth, detachment and cell size control on polyethylene terephthalate surfaces', *Scientific Reports*. Nature

Wang, Q., Garrity, G.M., Tiedje, J.M., Cole, J.R., (2007), 'Naive Bayesian classifier for rapid assignment of rRNA sequences into the new bacterial taxonomy', *Applied and Environmental Microbiology*, 73(16), pp. 5261–5267.



- Watanabe, K., (2001), 'Microorganisms relevant to bioremediation', *Current opinion in biotechnology*. 12(3), pp. 237–241.
- Watnick, P. & Kolter, R., (2000), 'Biofilm, City of Microbes'. *Journal of bacteriology*, 182(10), 2675–2679.
- Watson, I.A., Oswald, S.E., Banwart, S.A., Crouch, R.S., Thornton, S.F., (2005), 'Modeling the dynamics of fermentation and respiratory processes in a groundwater plume of phenolic Contaminant s interpreted from laboratory-to field-scale', *Environmental Science & Technology*. 39(22), pp. 8829–8839.
- Weaver, L., Webber, J.B., Hickson, A.C., Abraham, P.M., Close, M.E., (2015), 'Biofilm resilience to desiccation in groundwater aquifers: a laboratory and field study', *Science of the Total Environment*. 514, pp. 281–289.
- Weber, K. A., Achenbach, L. A. and Coates, J. D., (2006), 'Microorganisms pumping iron: anaerobic microbial iron oxidation and reduction', *Nature Reviews Microbiology*. 4(10), pp. 752–764.
- Weber Jr, W. J., McGinley, P. M. and Katz, L. E., (1992), 'A distributed reactivity model for sorption by soils and sediments. 1. Conceptual basis and equilibrium assessments', *Environmental Science & Technology*. 26(10), pp. 1955–1962.
- West, J. M. & Chilton, P. J., (1997), 'Aquifers as Environments for Microbiological Activity'. *Quarterly Journal of Engineering Geology and Hydrogeology*, 30(2), 147–154.
- Whiticar, M. J., (1999), 'Carbon and hydrogen isotope systematics of bacterial formation and oxidation of methane', *Chemical Geology*. 161(1), pp. 291–314.
- Williams, G.M., Pickup, R.W., Thornton, S.F., Lerner, D.N., Mallinson, H.E.H., Moore, Y., White, C., (2001), 'Biogeochemical characterisation of a coal tar distillate plume', *Journal of Contaminant Hydrology*. 53(3), pp. 175–197.
- Williamson, W.M., Close, M.E., Leonard, M.M., Webber, J.B., Lin, S., (2012), 'Groundwater biofilm dynamics grown in situ along a nutrient gradient', *Groundwater*. 50(5), pp. 690–703.
- Wilson, R. D., Thornton, S. F. and Mackay, D. M., (2004), 'Challenges in monitoring the natural attenuation of spatially variable plumes', *Biodegradation*. 15(6), pp. 359–369.
- Winderl, C., Schaefer, S. and Lueders, T., (2007), 'Detection of anaerobic toluene and hydrocarbon degraders in contaminated aquifers using benzylsuccinate synthase (bssA) genes as a functional marker', *Environmental Microbiology*. 9(4), pp. 1035–1046.
- Wingender, J., Neu, T. R. & Flemming, H.C., (1999), 'What Are Bacterial Extracellular Polymeric Substances? Microbial Extracellular Polymeric substances, (pp. 1–19). Springer.
- Wright, J., Kirchner, V., Bernard, W., Ulrich, N., McLimans, C., Campa, M. F., Hazen, T., Macbeth, T., Marabello, D. & McDermott, J., (2017), 'Bacterial Community Dynamics in Dichloromethane-Contaminated Groundwater Undergoing Natural Attenuation'. *Frontiers in Microbiology*, 8.

Yu, R., Gan, P., MacKay, A.A., Zhang, S., Smets, B.F., (2009), 'Presence, distribution, and diversity of iron-oxidizing bacteria at a landfill leachate-impacted groundwater surface water interface', *FEMS Microbiology ecology*. 71(2), pp. 260–271.

Yoshida-Takashima, Y., Nunoura, T., Kazama, H., Noguchi, T., Inoue, K., Akashi, H., Yamanaka, T., Toki, T., Yamamoto, M. & Furushima, Y., (2012), 'Spatial Distribution of Viruses Associated to Planktonic and Attached Microbial Communities in Hydrothermal Environments'. *Applied and Environmental Microbiology*, 78(5), 1311–1320.

Yu, Z. and Morrison, M., (2004), 'Comparisons of different hypervariable regions of *rrs* genes for use in fingerprinting of microbial communities by PCR-denaturing gradient gel electrophoresis', *Applied and Environmental Microbiology*. 70(8), pp. 4800–4806.

Zhang, W., Wang, C.-B. and Lien, H.L., (1998), 'Treatment of chlorinated organic Contaminant s with nanoscale bimetallic particles', *Catalysis today*. 40(4), pp. 387–395.

Zhang, Y., Kelly, W.R., Panno, S.V., Liu, W.T., (2014), 'Tracing fecal pollution sources in karst groundwater by Bacteroidales genetic biomarkers, bacterial indicators, and Environmental variables', *Science of The Total Environment*. 490, pp. 1082–1090.

Zhang, Z. and Brusseau, M. L., (1999), 'Nonideal transport of reactive solutes in heterogeneous porous media: 5. Simulating regional-scale behavior of a trichloroethene plume during pump-and-treat remediation', *Water Resources Research*, 35(10), pp. 2921–2935.

# Appendix

### Chapter 3

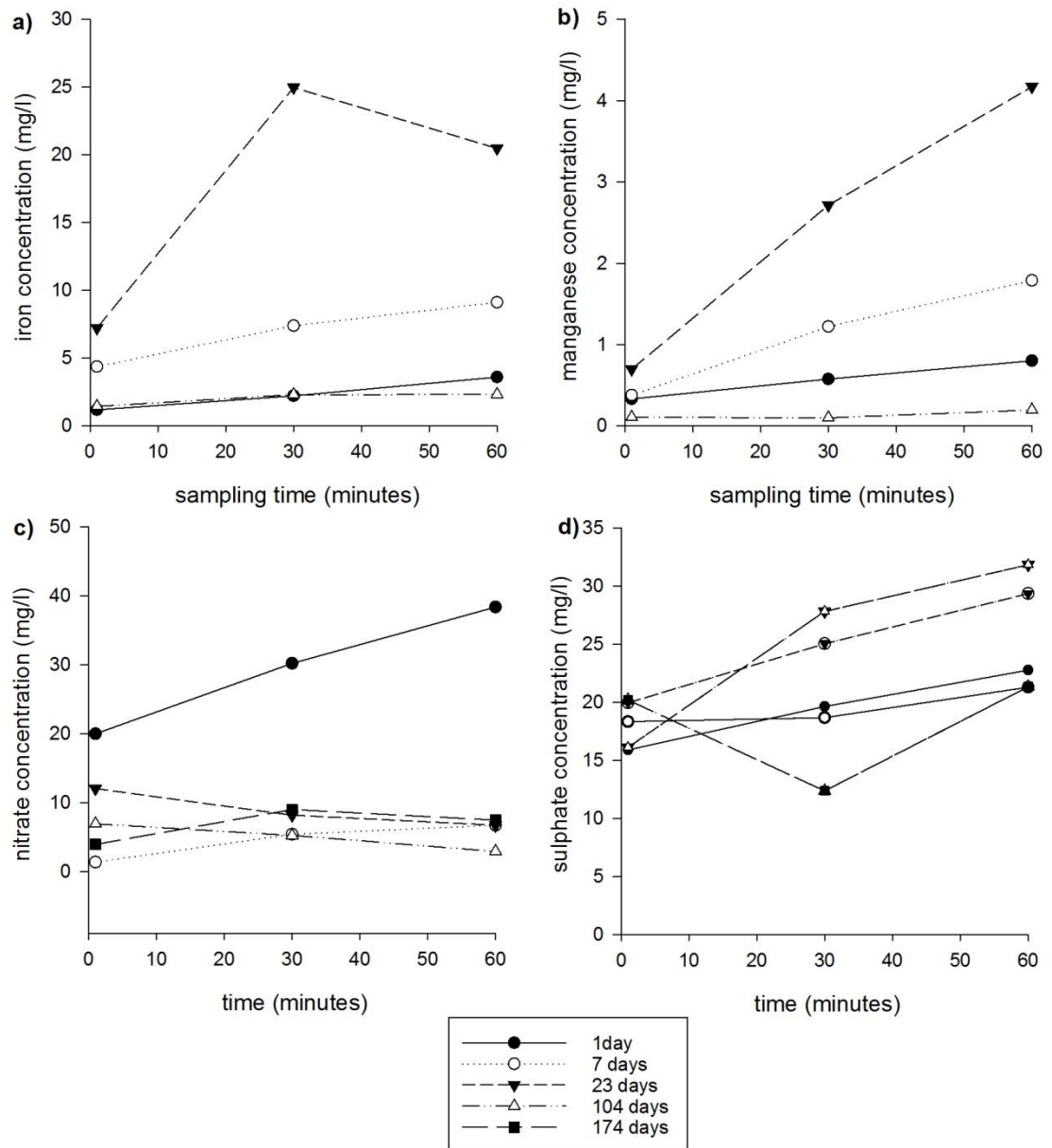


**Figure 6.1.** Concentration change of chemical species within 60 minutes of sampling of groundwater from 30 mbgl at BH-59.

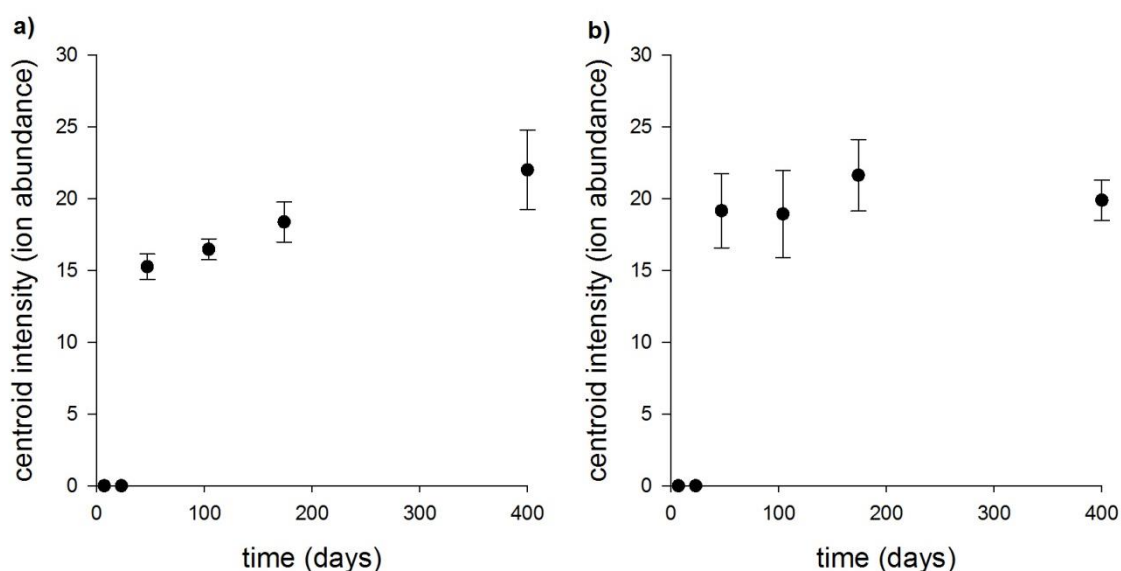


**Figure 6.2** Metabolites detection in the microcosm. (a) 4-hydroxybenzoic acid, (b) 4-hydroxy-3-methyl benzoic acid. Results were the average of 3 independent microcosms +/- standard deviation sampled destructively at each time point.

#### **t-TFLP preparation and preliminary results**

The first step in this analysis was to secure a good lysis method and a successful extraction of DNA. Different lysis methods were tested, Vortex Mobio adapter and mixer, and good quantities of DNA were observed from samples from the field site. The first method of lysis was selected to perform the DNA extraction from the samples (**Figure 6.3**). The next step was to evaluate the feasibility of the use of labelled primers, to amplify the 16S rRNA gene through Polymerase Chain Reaction (PCR), on DNA samples from the site. PCR amplification on 16S rRNA gene using two different primers FAM-63F and HEX-805R, and a combination of both primers, result in the expected production of an amplicon of approximately 800 base pairs (bp) (**Figure 6.4**). No differences in the bands produced were observed considering the lysis method or the labelled-primer used.

The suitability of labelled-primer for samples from the site let explore the PCR amplification of 16S rRNA on samples collected from the experiment. The PCR amplification using the supernatant from microcosm samples generated a similar amplicon (800 bp) with the use of FAM-63F and HEX-805R, and a combination of both primers (**Figure 6.5**). No differences in the bands produced were observed considering the labelled-primer used.

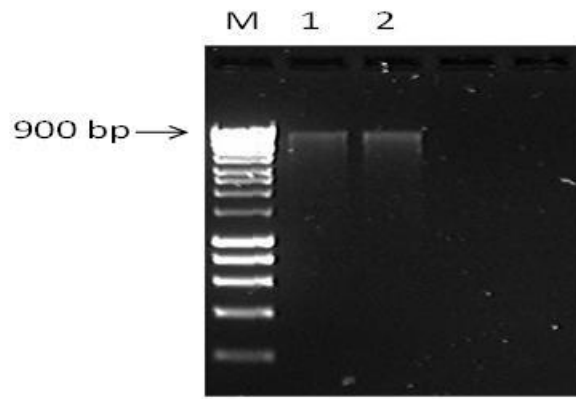


**Figure 6.3.** DNA extraction of groundwater from the study site using two different method of mechanic lysis. (1) Vortex Mobio adapter and (2) mixer M: Ladder IV

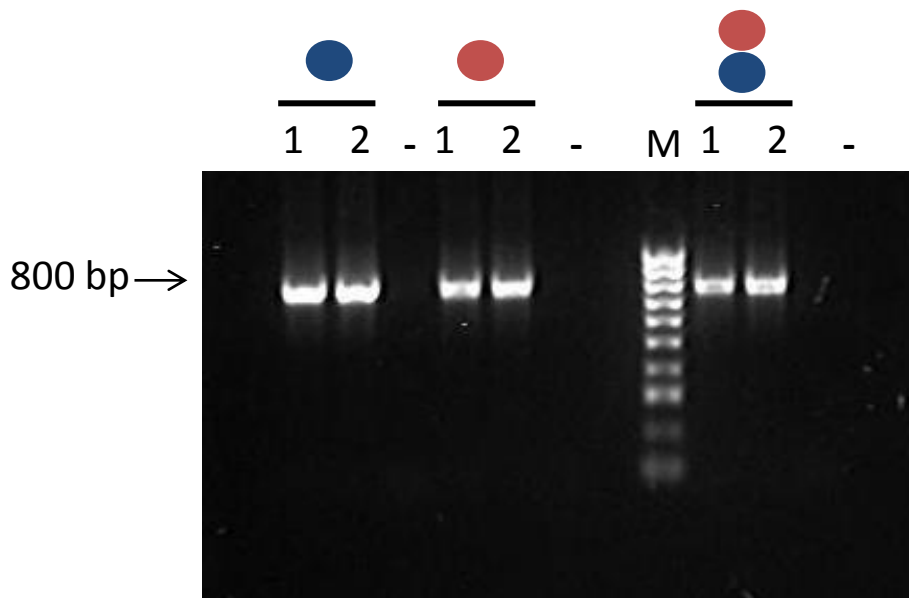


**Figure 6.4.** PCR Amplification of 16S rRNA gene of DNA from the study site using different method of lysis. Amplification was made using 63F and 806R primers labelled with FAM (blue), HEX (red) or both. M: Ladder IV, (1) Vortex Mobio adapter, (2) mixer (-) Negative control.

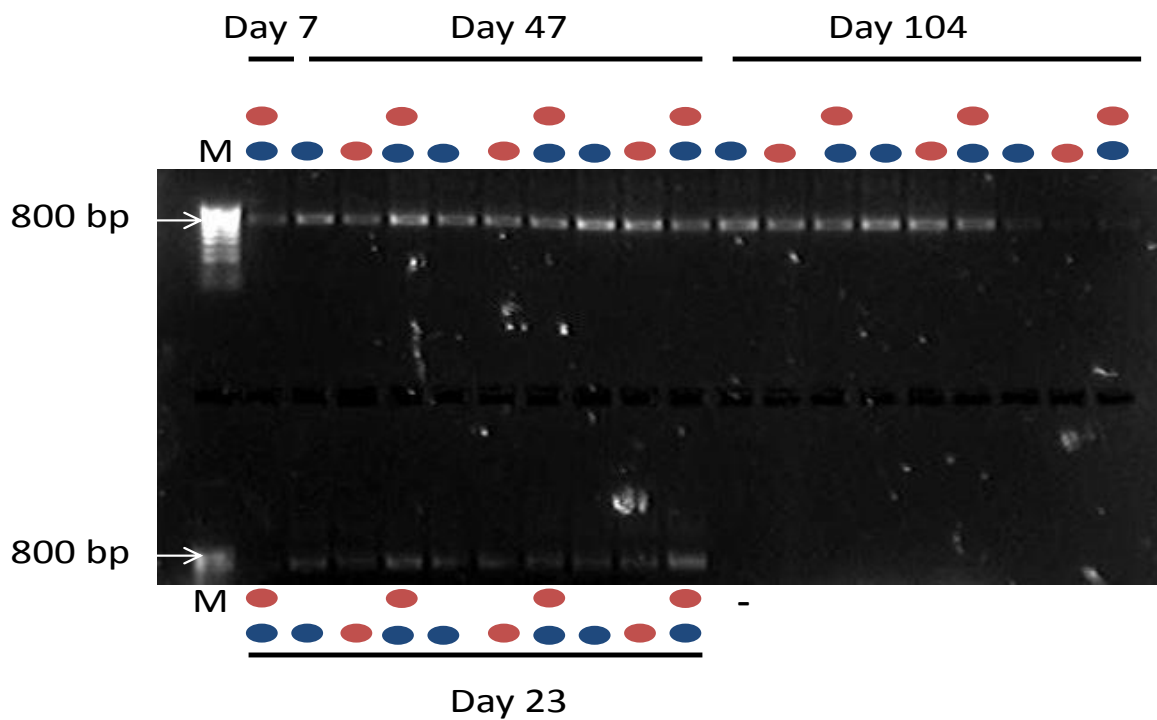


**Figure 6.5.** PCR Amplification of 16S rRNA gene of groundwater harvested from microcosm at different intervals after the inoculation. Amplification was made using 63F and 806R primers labelled with FAM (blue), HEX (red) or both. M: Ladder IV (+) Positive control (-) Negative control.

One of the main features of t-RFLP is the use of restriction enzymes. These enzymes cut the amplicon in different sizes, according to the presence of restriction enzyme sites in the amplicon. The presence of labelled ends let identify the size of this fragment and its abundance in the samples. The size and intensities of the fragments are usually read as peaks with different software. These two properties are related to the presence of Operational Taxa Units (OTUs) and its abundances. This information is useful to analysis the community fingerprint in a sample. On this regard, is necessary to use restriction enzymes which let produce different end-labelled sizes.

Two different enzymes (AluI and CfoI) were used to digest the amplicons produced with the amplification of 16S rRNA using FAM-63F and HEX-805R primers on the supernatant samples from microcosms. Both enzymes were able to generate different end-labelled fragments (**Figure 6.6.**). The peaks generated with both enzymes could be related to different OTUs, which change their abundances as the experiment progressed. For example, using AluI, the OTU of peak size of 208 bp approximately, reduced its abundance from day 7 to day 47, and then increased 104 days after the inoculation. On the contrary, OTU of peak size of 215 bp approximately, increased their abundances across the experiment (**Figure 6.6.**). The numbers of

peak generated with different enzymes on FAM-labelled amplicons, determined that AluI caused more peaks compared to CfoI enzyme. AluI was chosen to the t-RFLP analysis because its ability to create a richer community fingerprints (number of OTUs).

The confirmation of DNA extraction and PCR amplifications, allowed the use of downstream applications to obtain the community fingerprint from the samples of this experiment. Nevertheless, some considerations were taken before proceeding with the community profile. *In silico* analysis of the amplification of 16S rRNA gene (Cotton, 2014), using 63F and 806R primers, suggested that this primer pair have low rates of amplification for bacterial groups. The use of the Bakt341F and Bakt805R primer pair was predicted to amplify most of the bacterial groups, including some archaeal group, also relevant on these polluted groundwater systems. This consideration guided the change of the first primer pair to FAM-Bakt341F and Bakt805R. Also, based on the enzyme restriction analysis AluI was applied for the amplification of the amplicons generated with the new primer pair.



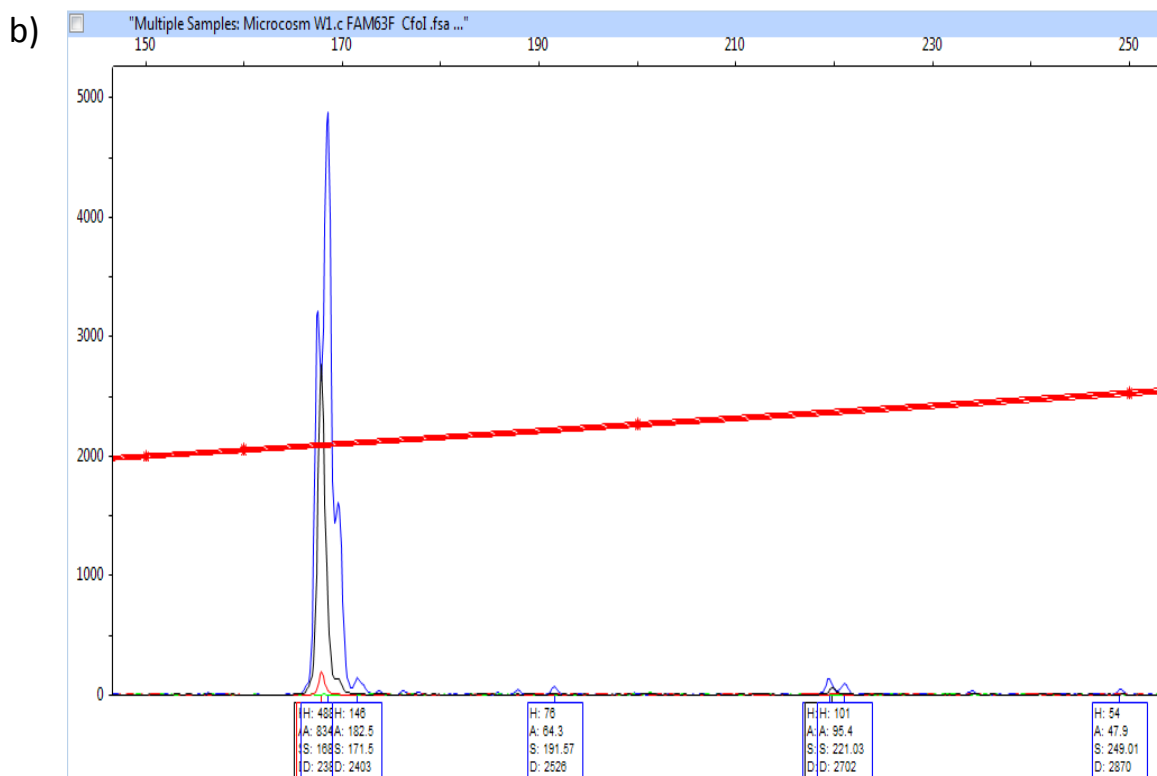
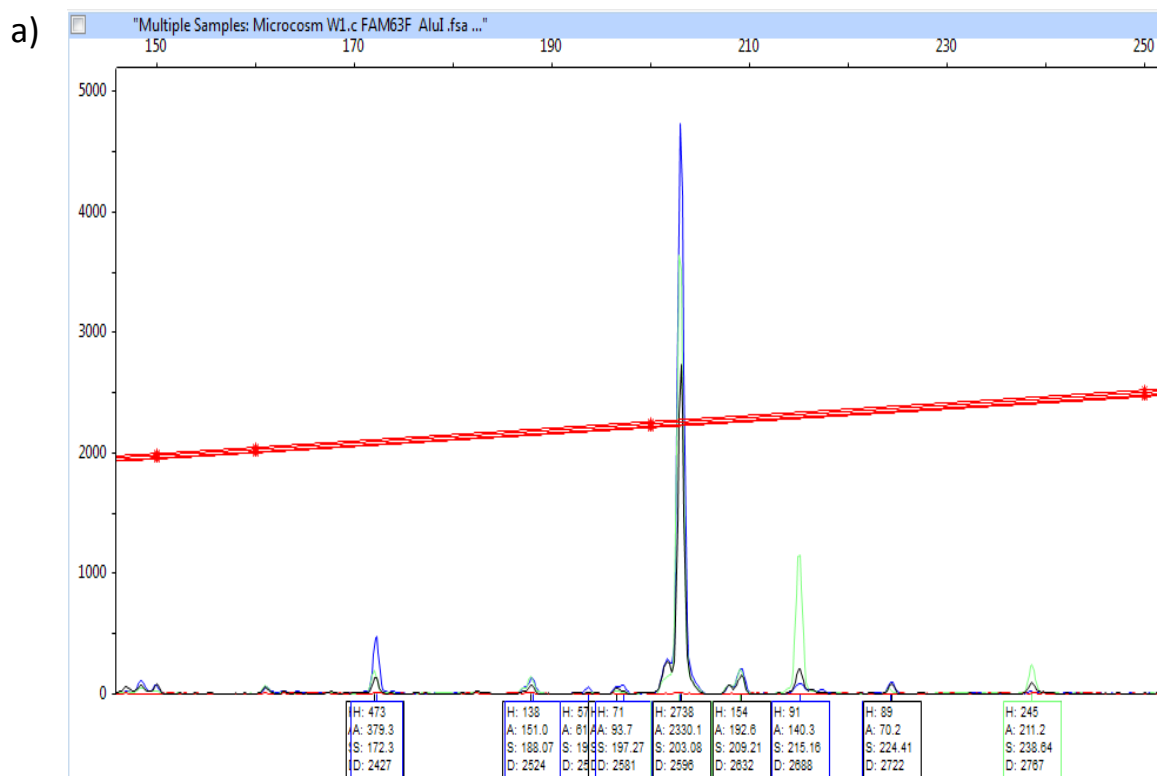


**Figure 6.6.** t-RFLP peaks of FAM labelled amplicons of 16S rRNA gene. These peaks were obtained after digestion with different restriction enzymes (a) AluI and (b) CfoI. The samples were harvested from the supernatant of microcosms at different intervals: 7 (blue), 23 (red), 47 (black) and 104 (green) days after the inoculation.

The amplification of 16S rRNA gene using FAM-Bakt341F and Bakt805R primers on the sediments samples from the sand bags collected from the field and microcosms generated an amplicon of approximately 500 bp. The band intensities of the amplicons were too low to proceed with downstream applications (**Figure 6.7**). The amount of DNA, as template, was doubled in the PCR reactions for sediments, but the bands were to still faint (**Figure 6.8**). The amount of DNA pre-enzyme digestion required to be of mid-high intensity. In order to produce the desired band, 6 aliquots of sediment samples were took it and finally concentrated using a 11 mM NaCl according to the manufacturer's troubleshooting guide instructions. The concentrated samples were then subjected to PCR amplification and the amplicons band intensity increased to the desired levels. The amplicons from the microcosm and field augmented their intensity as long as the incubation of the sediments progressed in both settings; this is related to the early increase in cell number on the biofilm during the rapid phase of attachment observed during the first stages of the experiment (**Figure 6.9**).

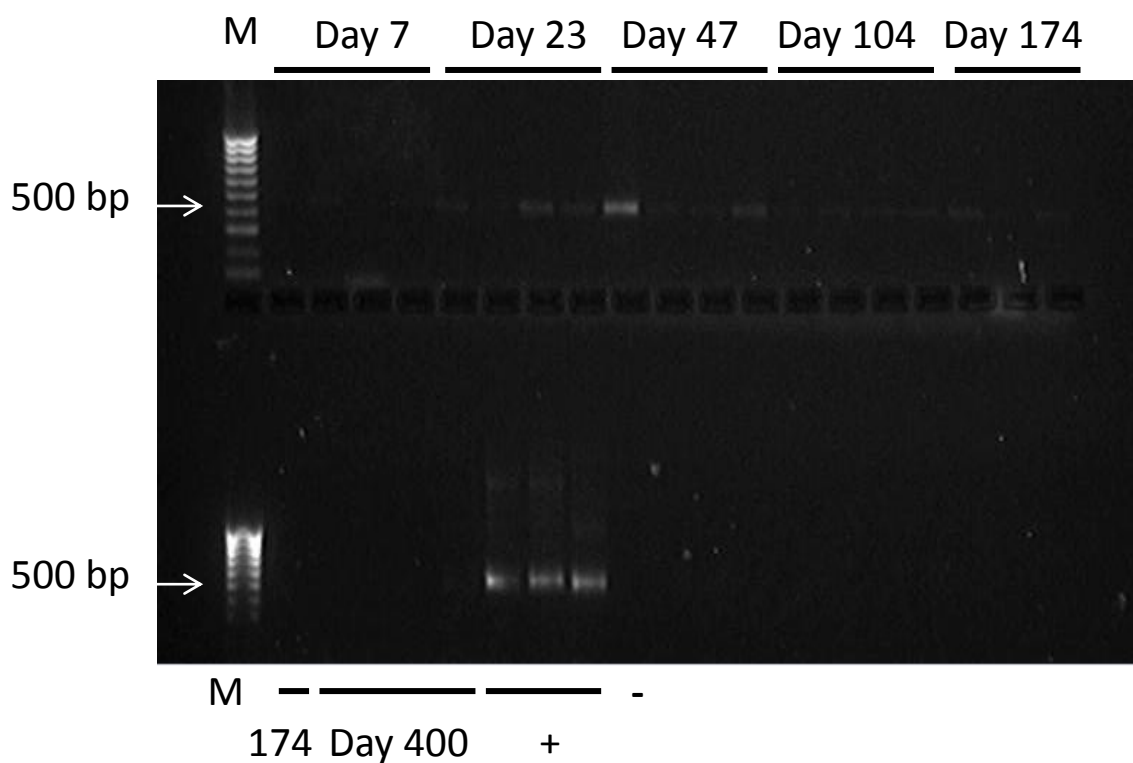


**Figure 6.7.** PCR Amplification of 16S rRNA gene of sediments harvested from microcosm at different intervals after the inoculation. Amplification was made using FAM labelled 341F and 805R primers M: Ladder IV (+) Positive control (-) Negative control

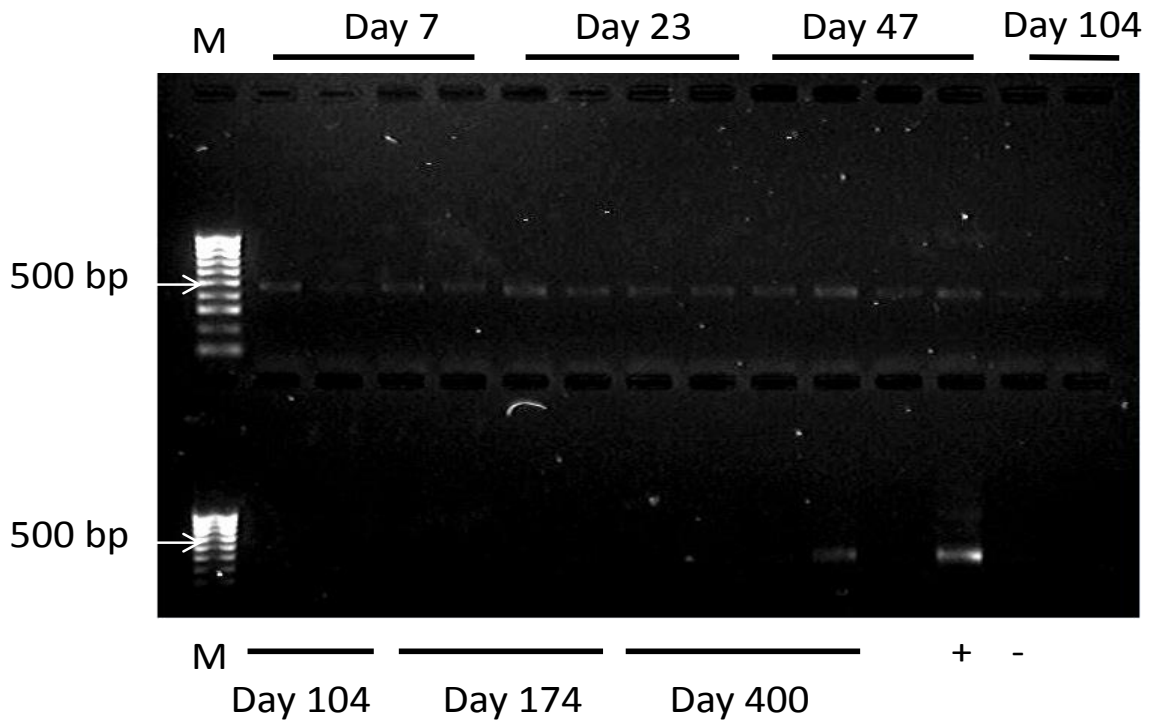


**Figure 6.8.** PCR Amplification of 16S rRNA gene of sediments harvested from microcosm at different intervals after the inoculation. The amount of DNA was doubled. Amplification was made using FAM labelled 341F and 805R primers M: Ladder IV (+) Positive control (-) Negative control.

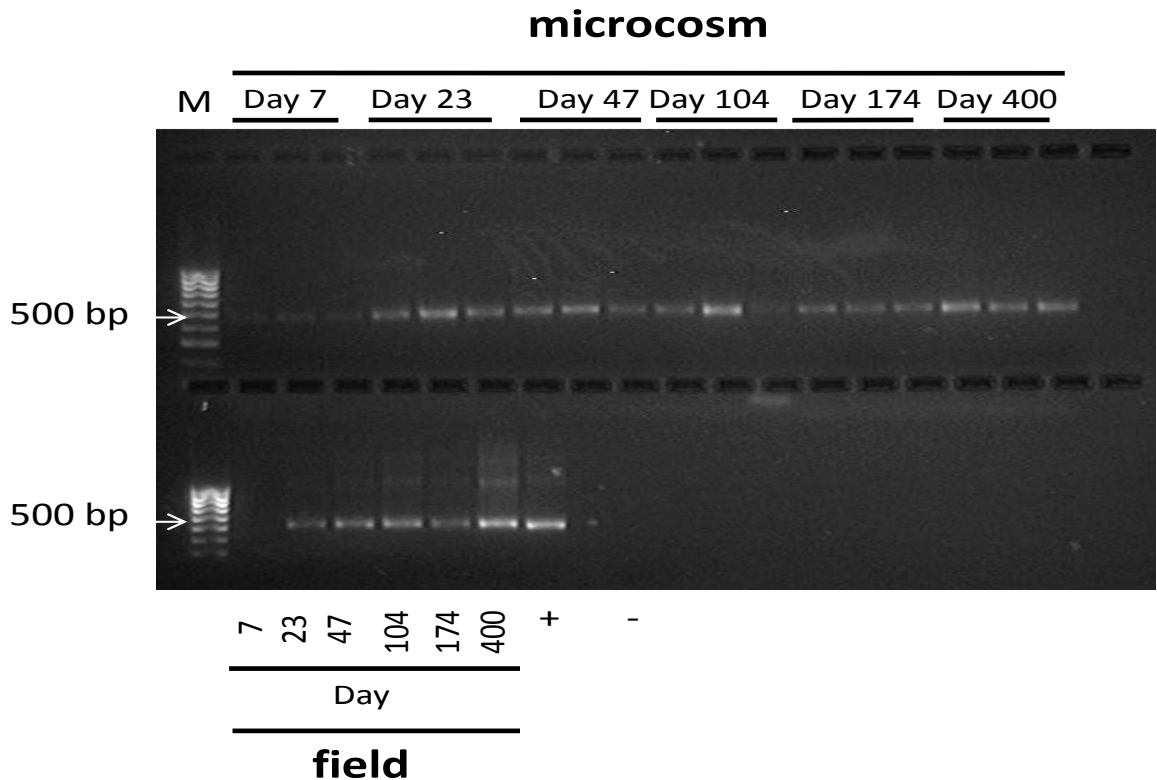


**Figure 6.9.** PCR Amplification of 16S rRNA gene of sediments harvested from microcosm and field at different intervals after the inoculation. DNA template was a result of DNA concentration of 6 aliquots. Amplification was made using FAM labelled 341F and 805R primers M: Ladder IV (+) Positive control (-) Negative control

The amplification of 16S rRNA using FAM-Bakt341F and Bakt805R primers on the groundwater samples and supernatant from microcosms generated an amplicon of approximately 500 bp. The band intensities for this mobile phase were the desire to proceed with the t-RFLP. The amplicons from the supernatants from the microcosm increased their intensity, as long as the number of the planktonic community recovers from the drop observed during the first stage of the experiment; on the other hand the high number registered in the field reflected in stable band intensities during the sampling of the open scree of BH-59 (**Figure 6.10**).

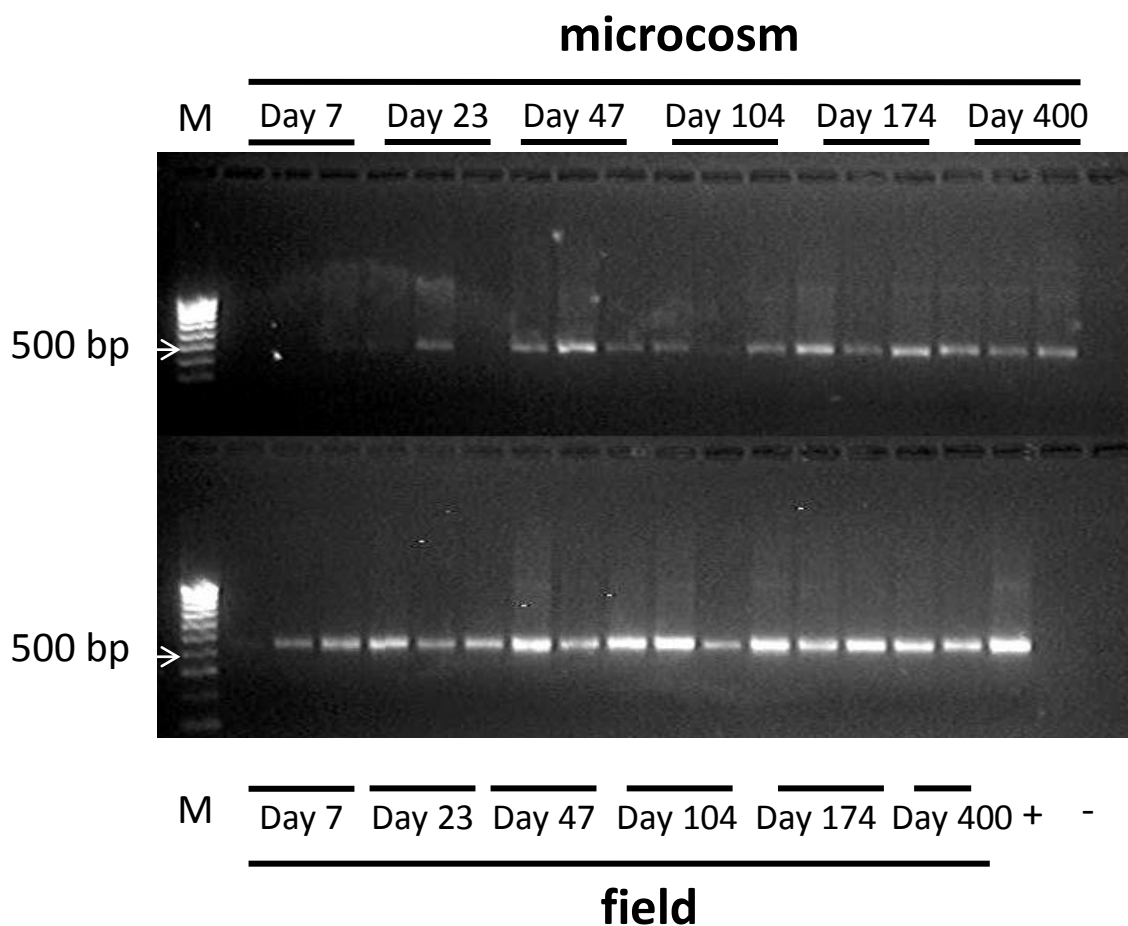


**Figure 6.10.** PCR Amplification of 16S rRNA gene of groundwater harvested from microcosm and field at different intervals after the inoculation. Amplification was made using FAM labelled 341F and 805R primers M: Ladder IV (+) Positive control (-) Negative control

The amplicons generated using FAM-Bakt341F and Bakt805R primers on DNA samples from supernatant, groundwater and sediments were subjected to AluI digestion. The digested samples were analysed using an electrophoresis. Peak scanner version 2.1 was used to determine the size, height and area of each one of the peaks among the entire data set. The

final product of this analysis was a table .txt file containing the peak name, sample, size, height, area and data point. This .txt file was used in the T-REX software. Part of the data processing on this software involved the selection of working the peak to nearest integer length size. After this, an Additive Main Effects and Multiplicative Interaction (AMMI) model was analysed for 3 sources of data: presence of absence of the peak, peak size and peak area.

The AMMI model used an ANOVA (Analysis of Variances) to fraction the sources of variation (t-RFs, Environments, Interaction) in the data set, t-RFs were related to OTUs and the environments were the replicates of each treatment. The Model after the variation fractioning applied a PCA (Principal Component Analysis) into this interaction. A low interaction value indicates similarity between the communities, whereas high interaction differences between them.

The analysis on the binary data, unweighted analysis, considered the presence and absence of different OTUs among the data set. In the microcosms, the comparison between the planktonic and attached communities revealed high interaction values (51.73 %). The comparisons between each community indicated for the planktonic community an interaction of 28.46 % and for the attached community of 48.91 %. The analysis of the peak height and area (weighted analysis) between planktonic and attached communities in the microcosm were the highest values (44.37 and 44.54 % respectively). The comparison within the planktonic community showed values of 22.43 and 25.27 % and within the attached community in the microcosm interaction values for peak high and area of 40.8 and 36.59 % respectively (**Table 6.1**). The IPCA of binary data reflected the differences between the planktonic and attached communities, with samples from the planktonic community separate from the attached community. Moreover, this IPCA represents the highest similarity within the planktonic community with all of samples clustering together, whereas the attached community samples were separate from each other (**Figure 6.11.a**). The IPCAs of the peak height and area, showed the trend of grouping of different communities according similarity, but this trend was not clear and could have been drawn with different orientation and the differences could became less clear (**Figure 6.11.b-c**)

In the field, the comparison between the planktonic and attached communities revealed high interaction values (63.17 %). The comparisons between each community indicated for the planktonic community an interaction value of 55.31 % and for the attached community the highest value in this setting was registered with 66.47 %. The analysis of the peak height and area between planktonic and attached communities in the field were of 48.45 and 50.05 % respectively. The comparison within the planktonic community showed values of 21.63 and 24.66 % and within the attached community in the microcosm interaction values for peak high

and area of 62.1 and 61.58 % respectively (**Table 6.1**).The IPCA of binary data, reflected partially the differences from the AMMI model between the planktonic and attached communities in the field. There was a trend of grouping of different communities together, but this trend was not clear and could have been drawn with different orientation and the differences could become less clear (**Figure 6.12.a**). Furthermore the interaction values of peak size and area, within each community, were not showed a particular grouping (**Figure 6.12.b-c**).

The global comparison, considering planktonic and attached microbial communities from the microcosm and the field, showed interaction values for binary data, peak height and area of 60.04, 57.01 and 57.99 % respectively. The IPCAs for the three types of data did not show a clear grouping (**Table 6.1; Figure 6.a-c**).

**Table 6.1** Percent of variation in T-RFLP data set from analysis of variance. Three type of data was considered in every comparison.

Comparison	Main effects	T-RFs	Environments	Interaction effects	Signal	Noise	Total
	%						
<b>(planktonic + attached communities) (microcosm)</b>							
binary	48.28	42.11	6.17	51.73	26.39	25.34	100
height	56.63	56.63	0	43.37	27.42	15.95	100
area	55.46	55.46	0	44.54	26.79	17.75	100
<b>(planktonic community) (microcosm)</b>							
binary	71.54	61.81	9.73	28.46	0.07	28.39	100
height	77.57	77.57	0	22.43	3.88	18.55	100
area	74.72	74.72	0	25.27	5.57	19.7	100
<b>(attached community) (microcosm)</b>							
binary	51.09	46.31	4.78	48.91	24.46	24.45	100
height	59.2	59.2	0	40.8	29.2	11.6	100
area	63.41	63.41	0	36.59	22.66	13.93	100
<b>(planktonic + attached communities) (field)</b>							
binary	36.84	32.65	4.19	63.17	48.37	14.8	100
height	54.54	54.54	0	48.45	42.79	5.66	100
area	49.95	49.95	0	50.05	43.48	6.57	100
<b>(planktonic community) (field)</b>							
binary	44.69	43.5	1.19	55.31	35.54	19.77	100
height	78.37	78.37	0	21.63	14.72	6.91	100
area	75.34	75.34	0	24.66	16.59	8.07	100
<b>(attached community) (field)</b>							
binary	33.52	23.34	10.18	66.47	N/A	N/A	100
height	37.9	37.9	0	62.1	N/A	N/A	100
area	38.42	38.42	0	61.58	N/A	N/A	100
<b>(planktonic + attached communities) (microcosm + field)</b>							
binary	39.58	35.59	3.99	60.4	38.3	22.1	100
height	42.99	42.99	0	57.01	45.77	11.24	100
area	42.01	42.01	0	57.99	45.74	12.25	100

The preliminary results using TREX software suggested the presence of differences between the planktonic and attached communities from the microcosm; based on binary data (presence/absence) of different T-RFs. A similar trend was also observed using the peak height and area. In the field, only binary data suggested differences between the planktonic and attached communities.

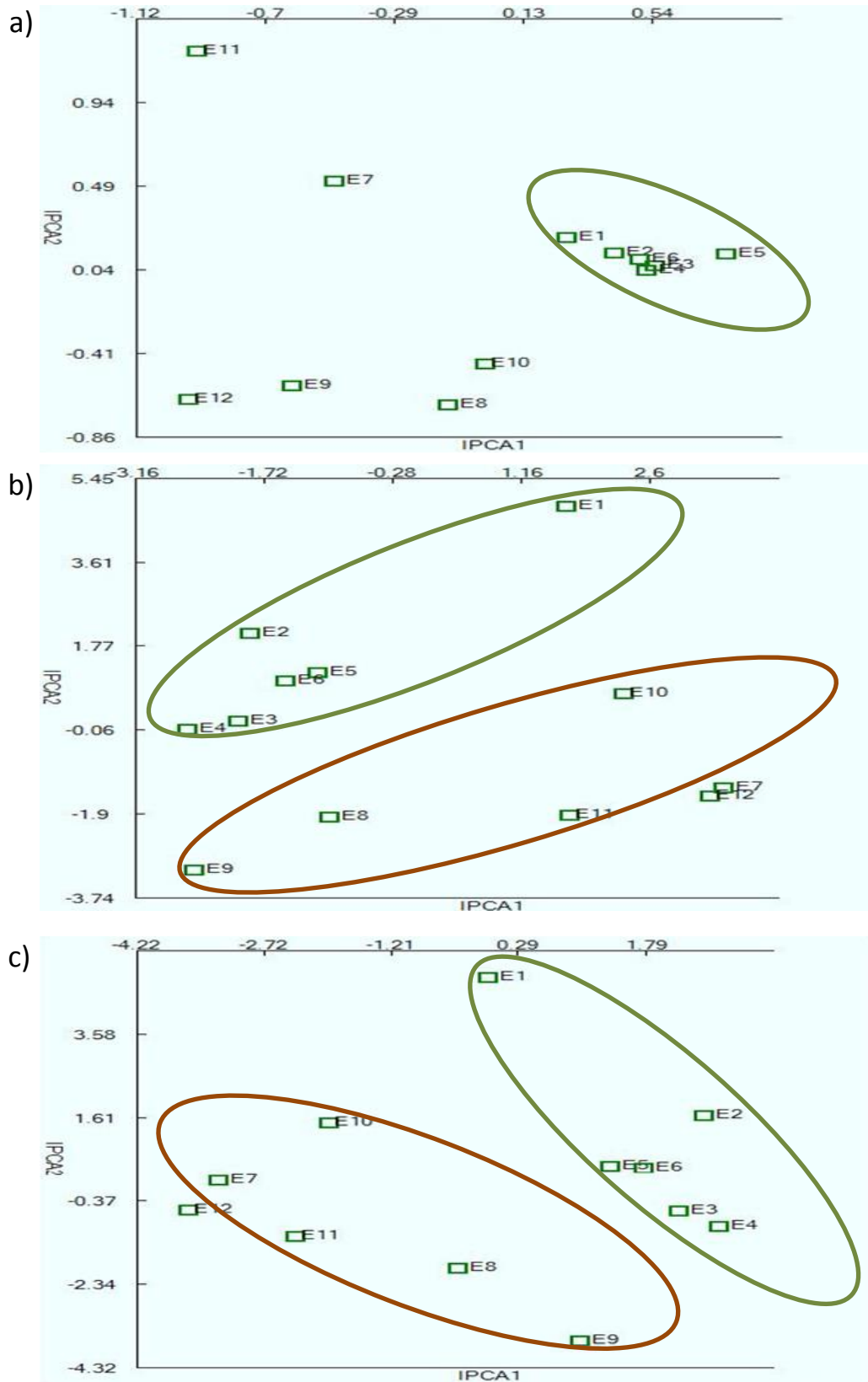


**Figure 6.11.** Additive Main Effects and Multiplicative Interaction (AMMI) of planktonic and attached communities in the microcosms. The data considered was (a) binary data, (b) peak height and (c) peak area. E1 to E6 represents planktonic community (green oval) and E7 to E12 attached community (brown oval) at different intervals.

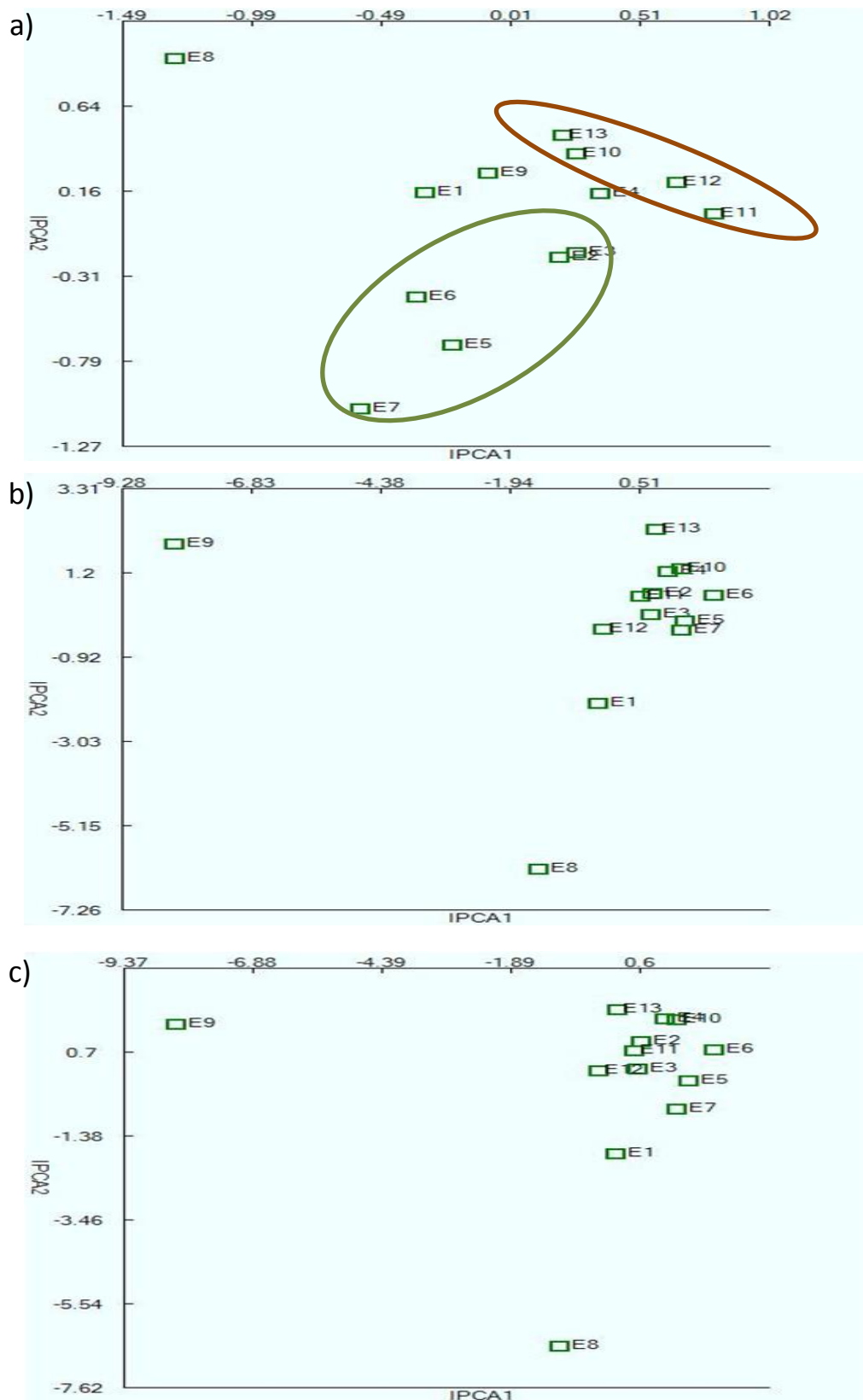


**Figure 6.12.** Additive Main Effects and Multiplicative Interaction (AMMI) of planktonic and attached communities in the field. The data considered was (a) binary data, (b) peak height and (c) peak area. E1 to E7 represents planktonic community (green oval) and E8 to E13 attached community (brown oval) at different intervals.



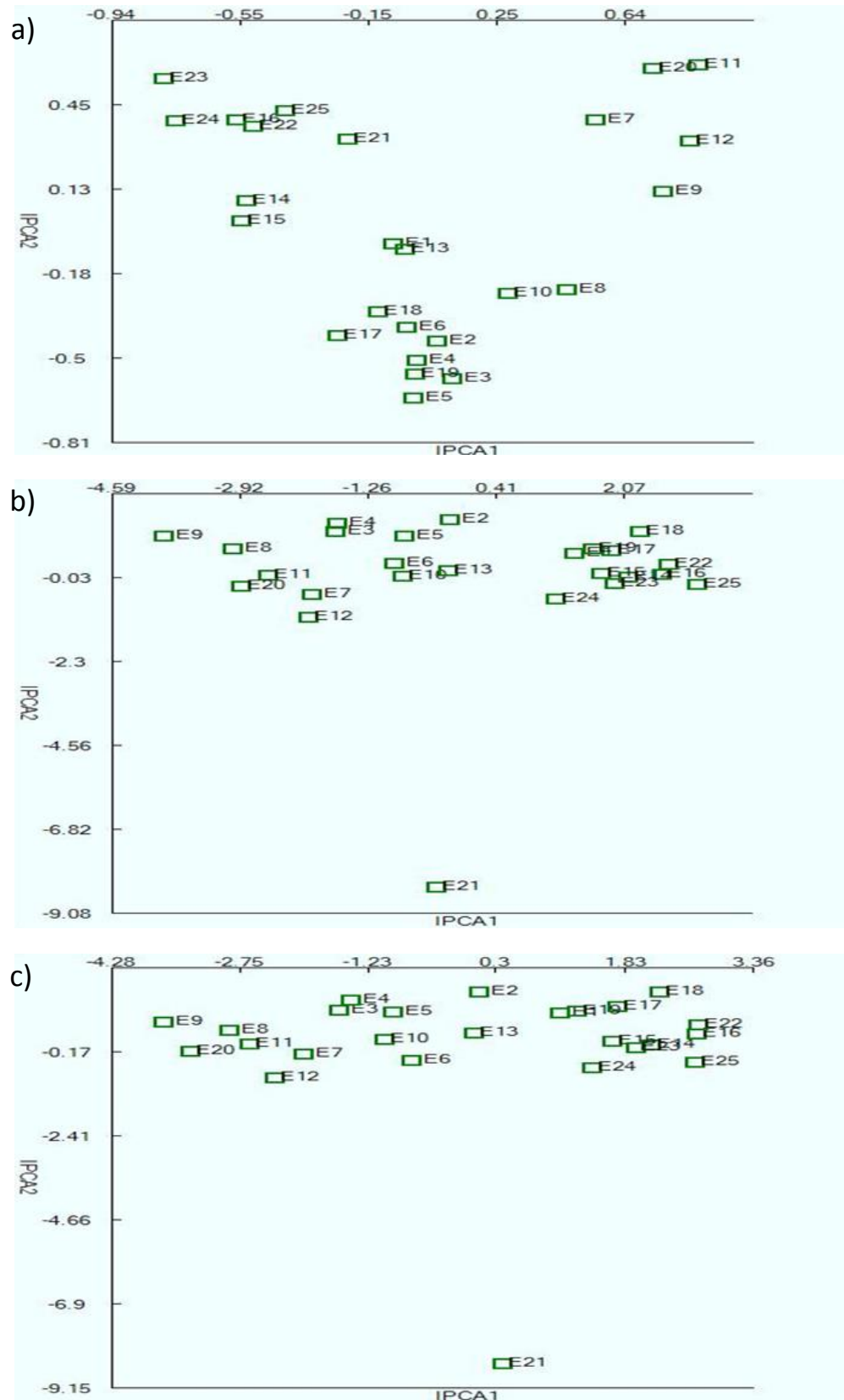


**Figure 6.13.** Additive Main Effects and Multiplicative Interaction (AMMI) of planktonic and attached communities in microcosm and the field. The data considered was (a) binary data, (b) peak height and (c) peak area. E1 to E6 represents planktonic microcosm community, E7 to E12 sediment microcosm community, E13 to E19 field planktonic community and E20 to E25 attached field community at different intervals.

### Sequencing library preparation

The PCR amplifications of the previous trials were made using MyTaq<sup>R</sup> polymerase, to test the performance of different polymerases; another polymerase (KAPA) was used to evaluate the difference in the amplification and to resolve the null amplification of sediments. The PCR amplification using the MyTaq<sup>R</sup> and KAPA polymerases on groundwater samples did not generate different band intensities. The sediment amplifications were not possible using the enzymes and with protocol modification made at that stage (**Figure 6.14**).

Considering that sediments were original from a polluted site, made to suspect the potential presence of inhibitors in the DNA extracted from the sediments. These inhibitors might have been responsible for the suppressing of the PCR.

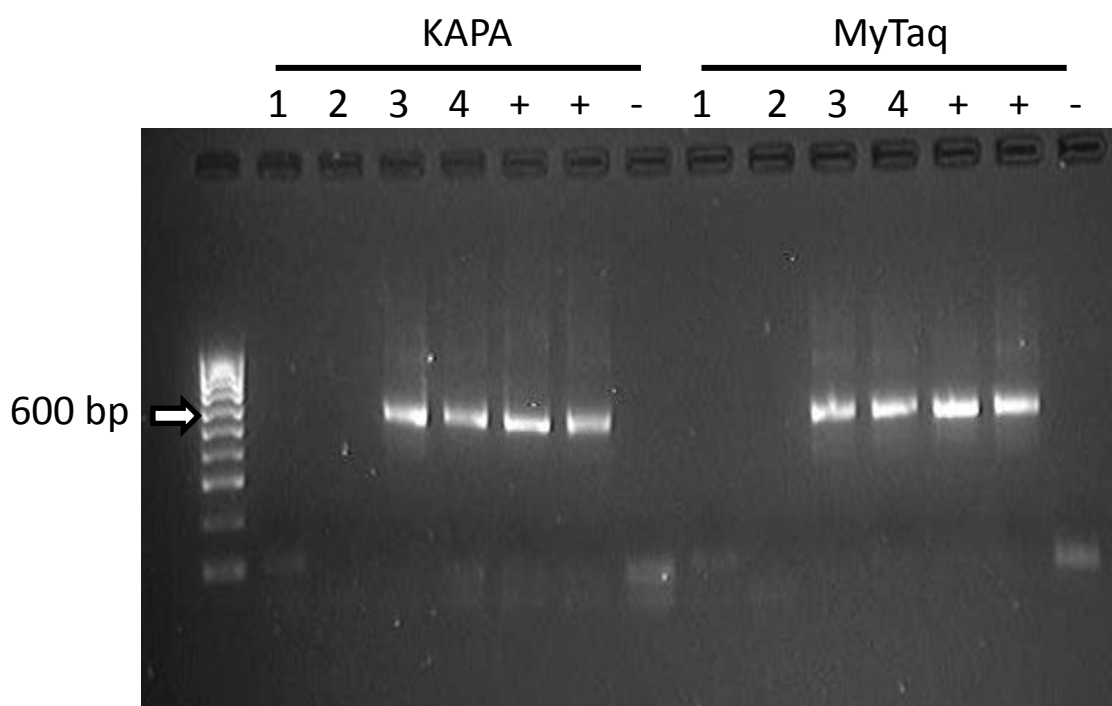


**Figure 6.14.** PCR Amplification of 16S rRNA gene of supernatant and sediments harvested from microcosm at different intervals after the inoculation. The amplification was made using Illumina 341 and 805 primers and two different polymerases. M: Ladder IV (1-2) sediments, (3-4) planktonic, (+) Positive control and (-) Negative control.

To determine the presence of soluble inhibitors in the DNA from sediments the following approach was taken. A positive control was used to check the amplification of the PCR reaction, another PCR reaction was made only with half of the volume as template and a mixture of the positive control with DNA from sediments from the field. As a result of this PCR, the expected bands of 600 bp were observed in the positive controls, with similar intensity

when half of the volume of the positive control was applied in the PCR as input. The mixtures of the positive controls with DNA from the sediments, results in no amplification (**Figure 6.15**). This PCR suggested the presence of soluble PCR inhibitors in the sediments samples, and the reason behind of the null amplification observed in the previous trials.

In order to proceed with the Illumina 16S rRNA sequencing library preparation, it was necessary follow a strategy to clean the DNA of these soluble inhibitors, without compromising the sediments DNA samples. Different DNA cleaning-up methods were explored, using small pore size membranes (0.025 $\mu$ m) to perform dialysis and standardized methods, such as Microcon DNA Fast Flow PCR Grade with Ultracel membrane, dual cycle EtOH treated.

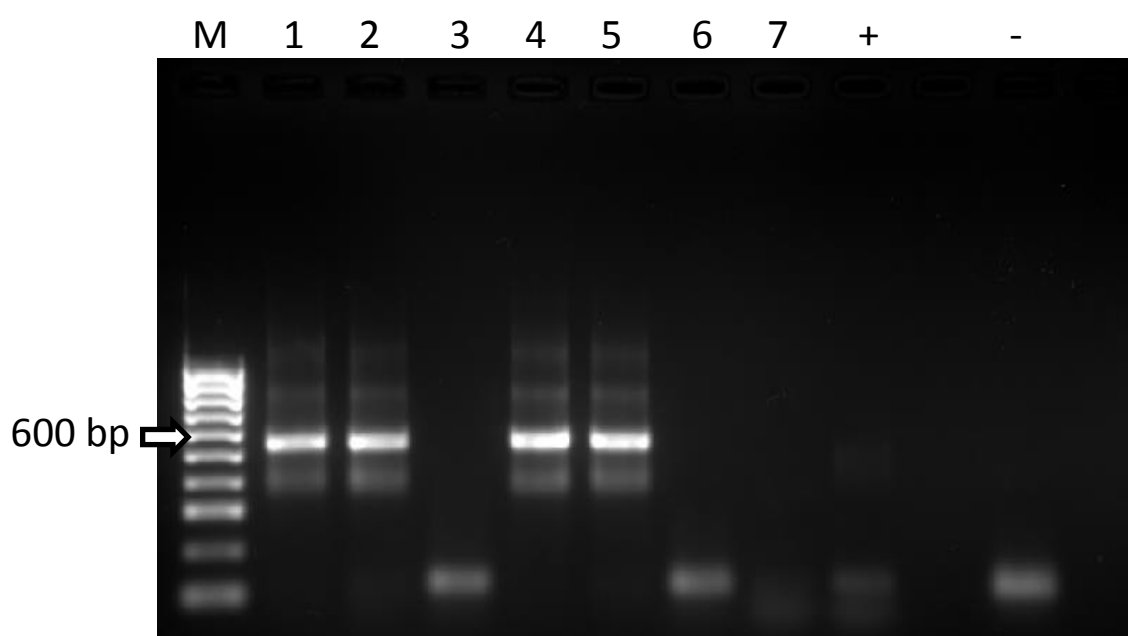


**Figure 6.15.** PCR Amplification of 16S rRNA gene to DNA extracted from sediments to demonstrate the presence of soluble inhibitors. The amplification was made using Illumina 341 and 805 primers. (M) Ladder IV, (1 and 4) positive controls, (2 and 5) half of the input template of the positive controls, (3, 6 and 7) mix of sediment samples and positive controls, (+) Positive control and (-) Negative control.

The first DNA cleaning trial was made through dialysis with a pore size membrane of 0.025 $\mu$ m in an adapted device. Firstly, using a dye into the device the ability of dialysis was confirmed DNA samples were subjected to 6 hours of dialysis, and the dialysed DNA was recovered and subjected to PCR amplification using the Illumina-Bakt341F and Illumina-Bakt805R primer pair. No amplification was observed (**Figure 6.16**) and this method for cleaning DNA from sediments was discarded.

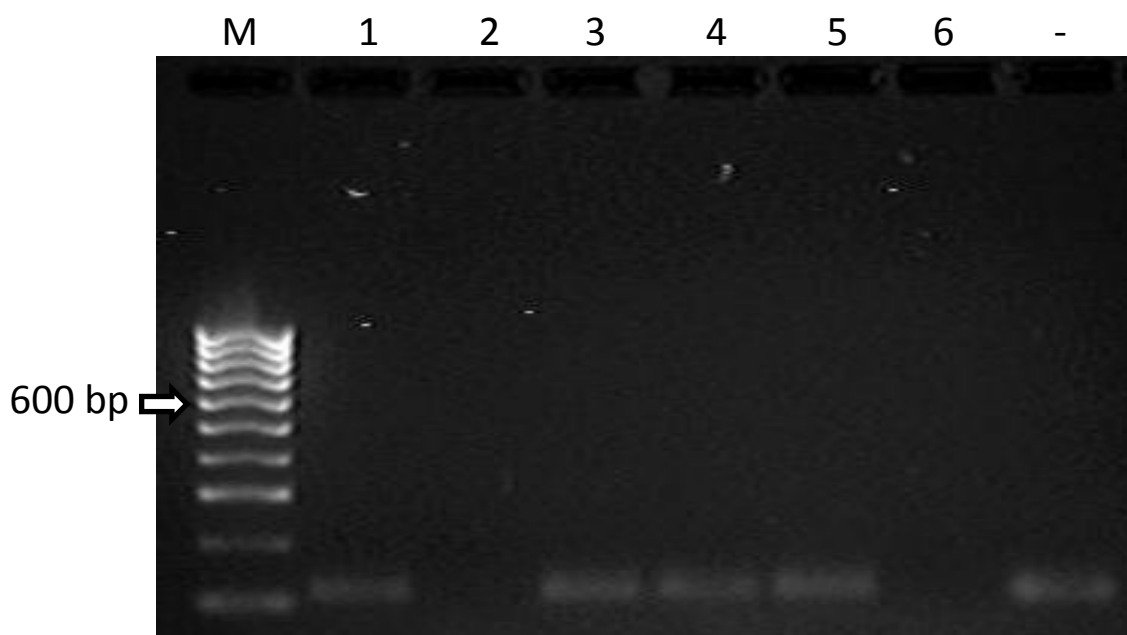


**Figure 6.16.** PCR Amplification of 16S rRNA gene of DNA extracted from sediments and treated with dialysis. The amplification was made using Illumina 341 and 805 primers. (M) Ladder IV, sediments after (1) 7, (2) 23, (3) 47, (4) 104, (5) 174 and (6) 400 days after the inoculation.

The second DNA cleaning trial was made through drop-dialysis (Saraswat *et al.*, 2013) for 6 hours using a pore size membrane of 0.025  $\mu\text{m}$ , floating in UHQ water inside of a petri dish. The drop from several samples were recovered and amplified through PCR. It was possible to observe the expected 600 bp band in some of the DNA samples from sediments (**Figure 6.17**). There was amplification but this method was discarded, because it was not consistent across all the samples and was not reproducible enough to secure amplification.

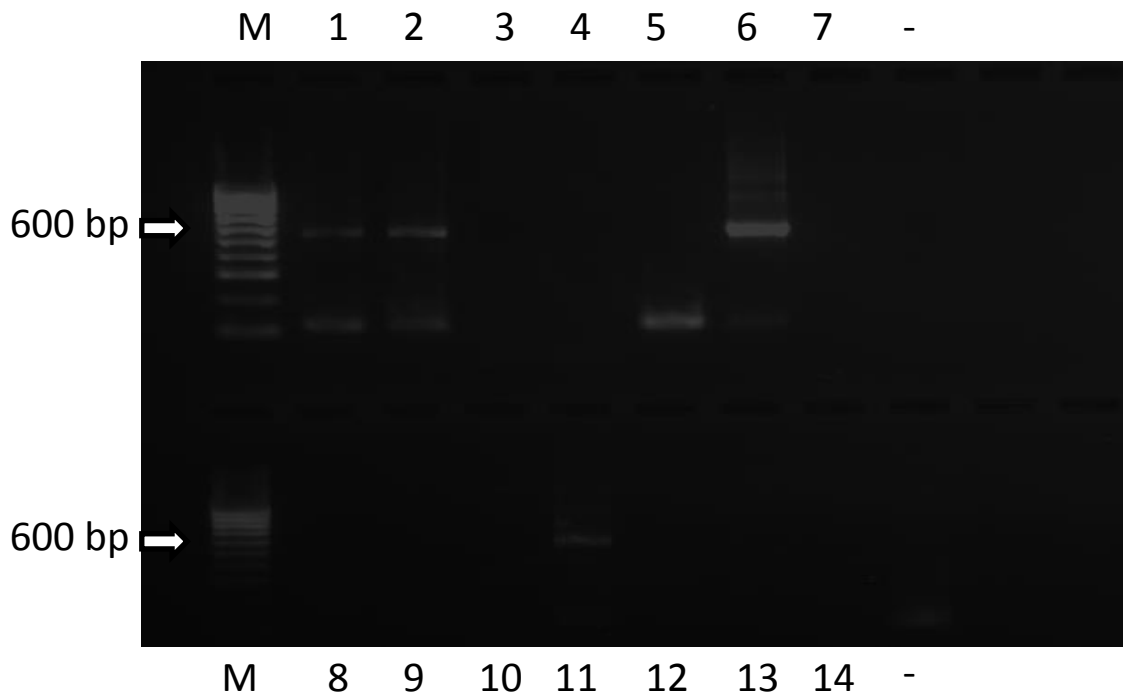


**Figure 6.17.** PCR Amplification of 16S rRNA gene of DNA extracted from sediments and treated with drop-dialysis. The amplification was made using Illumina 341 and 805 primers. (M) Ladder IV, sediments after (1 and 8) 7, (2 and 9) 23, (3 and 10) 47, (4 and 11) 104, (5 and 12) 174 and (6, 7, 13 and 14) 400 days after the inoculation.

The third method for cleaning DNA from these sediments was the use of Microcon DNA Fast Flow PCR Grade with Ultracel membrane, dual cycle EtOH treated. The trial was made with DNA from sediment obtained 780 days after the incubation, to avoid loss of valuable samples that were intensively used in the previously attempts. After following the manufacturer's instructions no amplification was observed in the samples, only in 1 reaction which contained a final volume of 50 ul, which was higher compared to the 20 ul used the Illumina protocol, presented the expected band of 600 bp (**Figure 6.16.a**). Finally, using the troubleshooting guide, and adding UHQ water to facilitate the removal of the potential inhibitors into the microcon device, it was possible to obtain a high intensity band from PCR from the cleaned samples (**Figure 6.16.b**).

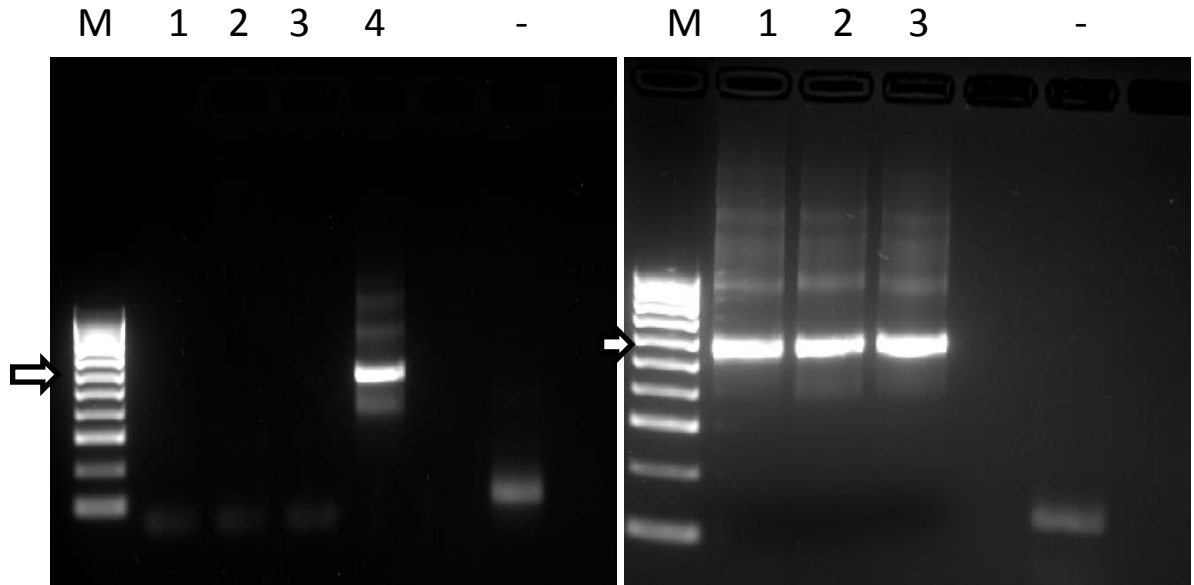


**Figure 6.18.** PCR Amplification of 16S rRNA gene of DNA extracted from sediments and treated (a) microcon according to manufacture instructions and (b) extra desalting steps. The amplification was made using Illumina 341 and 805 primers. (M) Ladder IV, (1-3) Sediments after 780 days of inoculation, (4) sediments final volume reaction of 50 ul. Note arrow indicates approximately 600 bp.

The final protocol modifications were chosen for the cleaning of DNA from the sediments. The use of microcon in the entire sample set, covering sediments samples after 7 to 780 days of inoculation, and final amplification of the 16S rRNA was consistent and proved to be effective in the removal of inhibitors and allowed PCR (**Figure 6.19.a**)

In the amplification of these sediments it was possible to observe the appearance of primers, primers dimers and unspecific band products. To perform the sequencing on these samples, it was necessary to remove the presence of these unwanted products. For the cleaning of the PCR products several kit were considered. The use of AMPure XP PCR purification beads, involving the use of a magnetic plate and different washing steps with ethanol 80% showed to be successful to clean the PCR product (**Figure 6.19.b**).

After the null amplification of sediments was resolved, with a suitable and consistent cleaning method for DNA and a purification of PCR products demonstrated to be effective, it was possible to continue with the library preparation of the entire sample set.

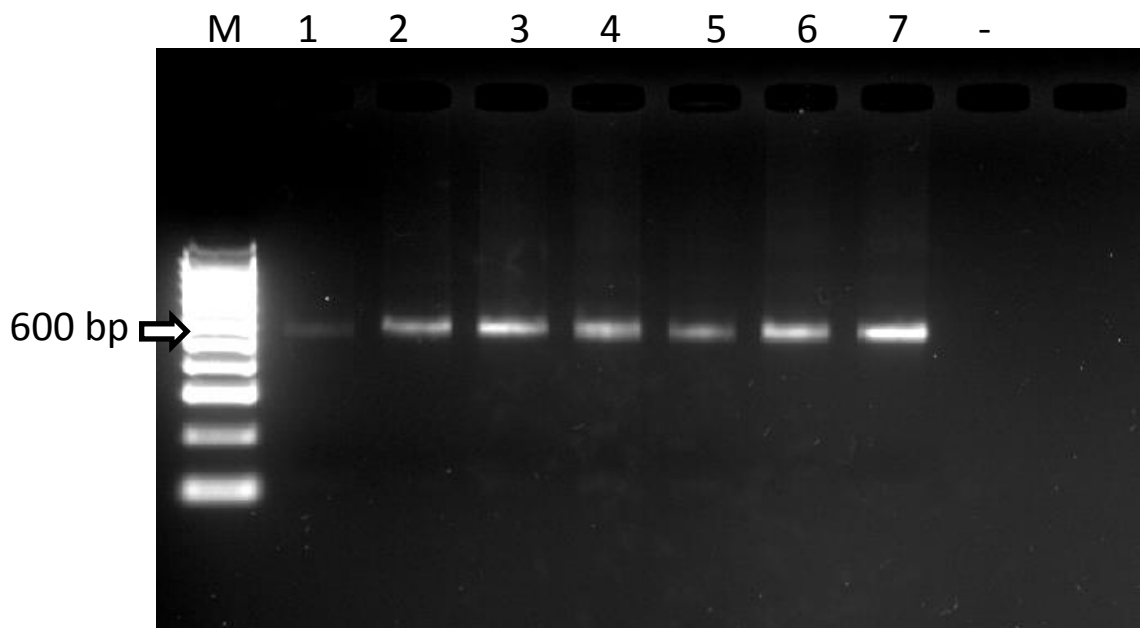
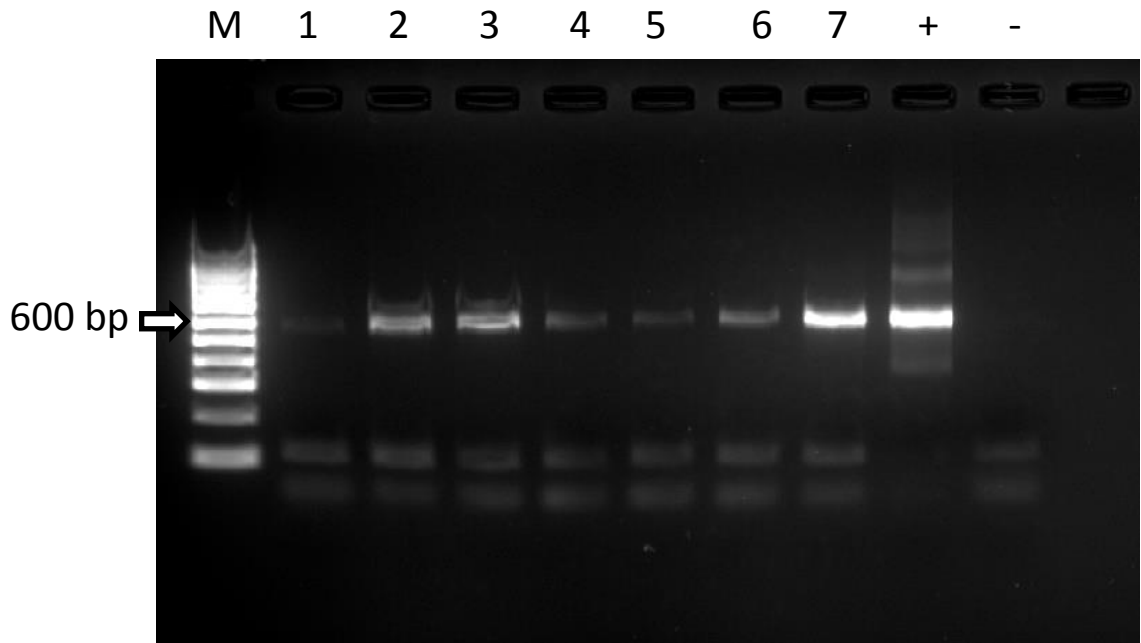


**Figure 6.19.** PCR Amplification of 16S rRNA gene of DNA extracted from sediments and treated with microcon plus extra desalting steps. (a) The amplification was made using Illumina 341 and 805 primers. (M) Ladder IV, sediments after (1) 7, (2) 23, (3) 47, (4) 104, (5) 174, (6) 400 and (7) 780 days the inoculation. (b) previous samples treated with AM pure beads.

The amplification of 16S rRNA using Illumina-Bakt341F and Illumina-Bakt805R primers on the sediments samples from the sand bags collected from the field and microcosms generated an amplicon of approximately 600 bp. The samples were previously treated using microcon devices to clean the sediments from soluble inhibitors.

One of the challenges at this stage of the sequencing library preparation, was to obtain a low and medium band intensities, considering also an index-PCR on the PCR products, to tag them and were be pooled together as one sample.

In the case of the sediments PCR products, in the microcosm and the field band intensities were mid-low, with low intensities located at early stages of the experiment, this is related to low cell numbers observed at this period, afterwards the intensity increased as long as the biofilm developed on the grains. (Figure 6.20 and 6.21)

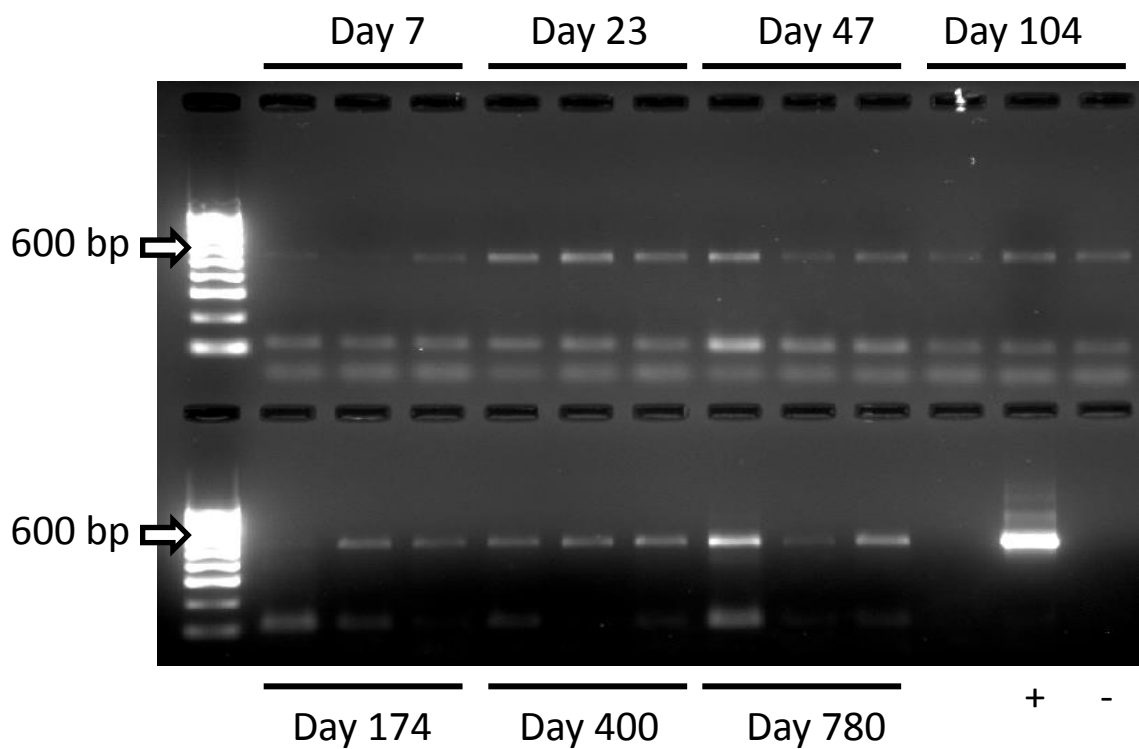


**Figure 6.20.** PCR Amplification of 16S rRNA gene of sediments harvested from microcosm at different intervals after the inoculation. DNA was treated with microcon to eliminate soluble inhibitors. Amplification was made using FAM labelled 341F and 805R primers M: Ladder IV (+) Positive control (-) Negative control



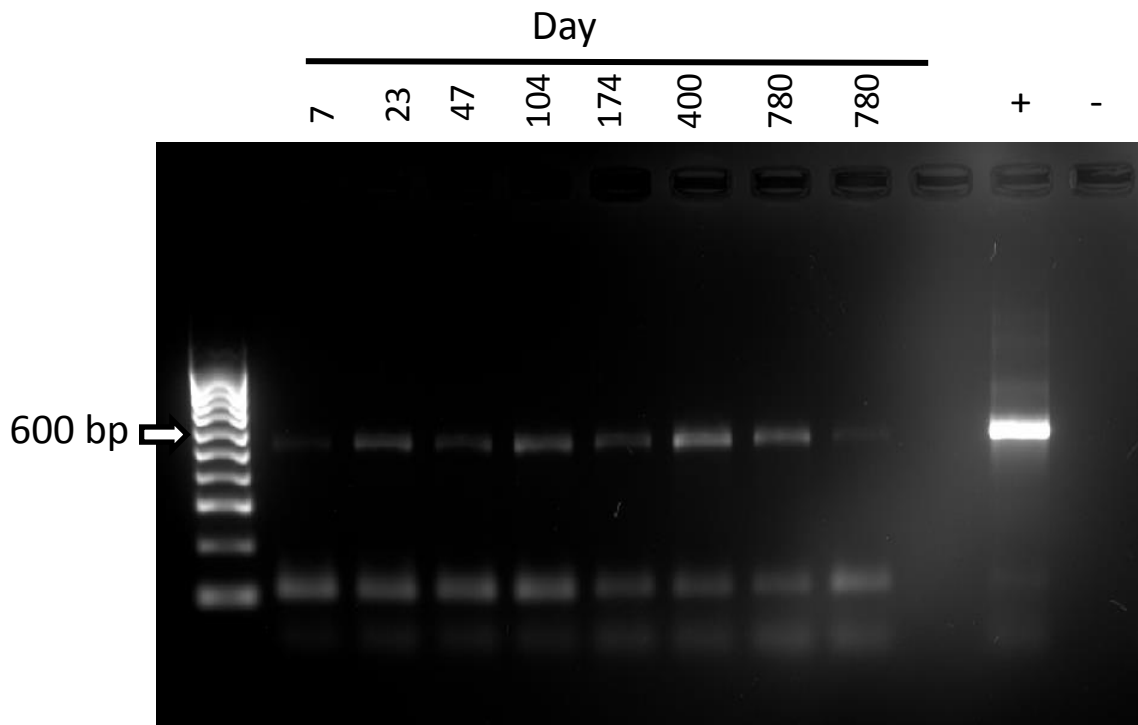


**Figure 6.21.** PCR Amplification of 16S rRNA gene of sediments harvested from field at different intervals after the inoculation. DNA was treated with microcon to eliminate soluble inhibitors. Amplification was made using FAM labelled 341F and 805R primers M: Ladder IV (+) Positive control (-) Negative control

In the case of the planktonic community, a consistent band of approximately 600 bp appeared in all the samples from the microcosm and the field. The planktonic samples from the supernatant of the microcosm and from the groundwater, did not have inhibitors and cell numbers were higher compared to the cell numbers in the biofilm (**Figure 6.22.a-b**). These two features make that band intensities in the planktonic community were extremely high. In order to obtain low-mid band intensities, several dilution were applied into the DNA template and different PCR trials were made till bring the intensity of the bands to the desired levels (**Figure 6.22 and 6.23**).

After the PCR amplification of all the samples, the purification step tried previously was applied, followed by the Index-PCR and another purification step. Finally samples were quantified, diluted and pooled together and sent to sequencing

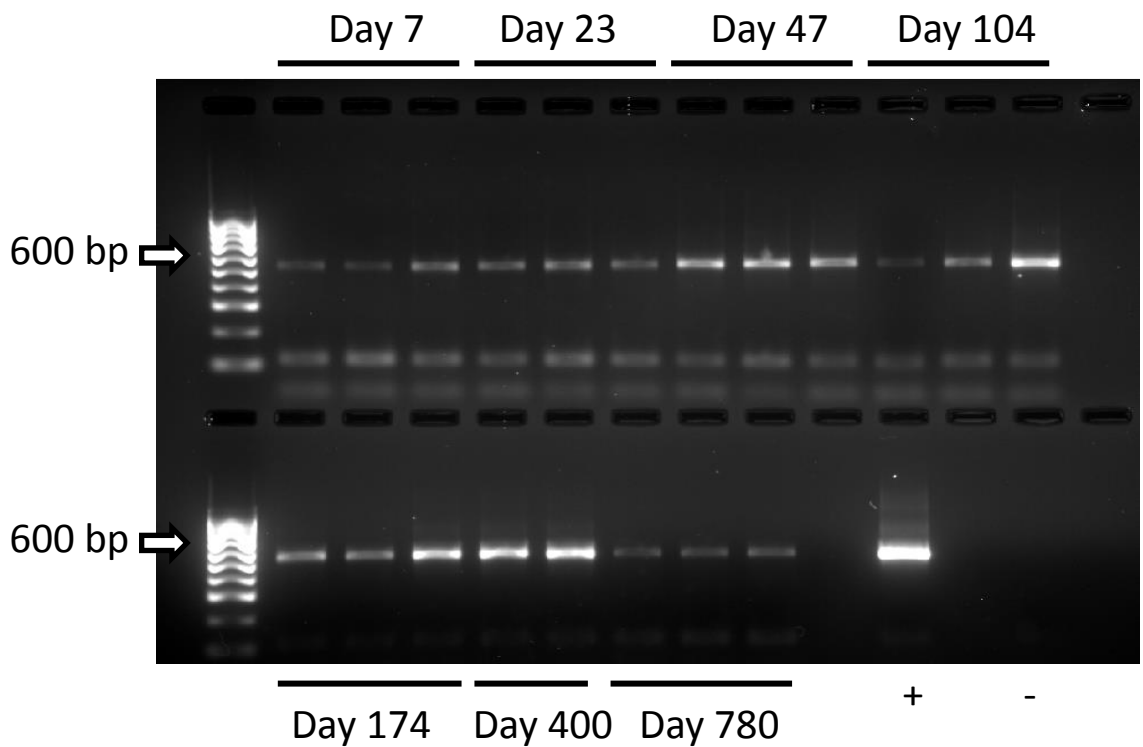


**Figure 6.22.** PCR Amplification of 16S rRNA gene of supernatant harvested from microcosm at different intervals after the inoculation. Amplification was made using FAM labelled 341F and 805R primers M: Ladder IV (+) Positive control (-) Negative control

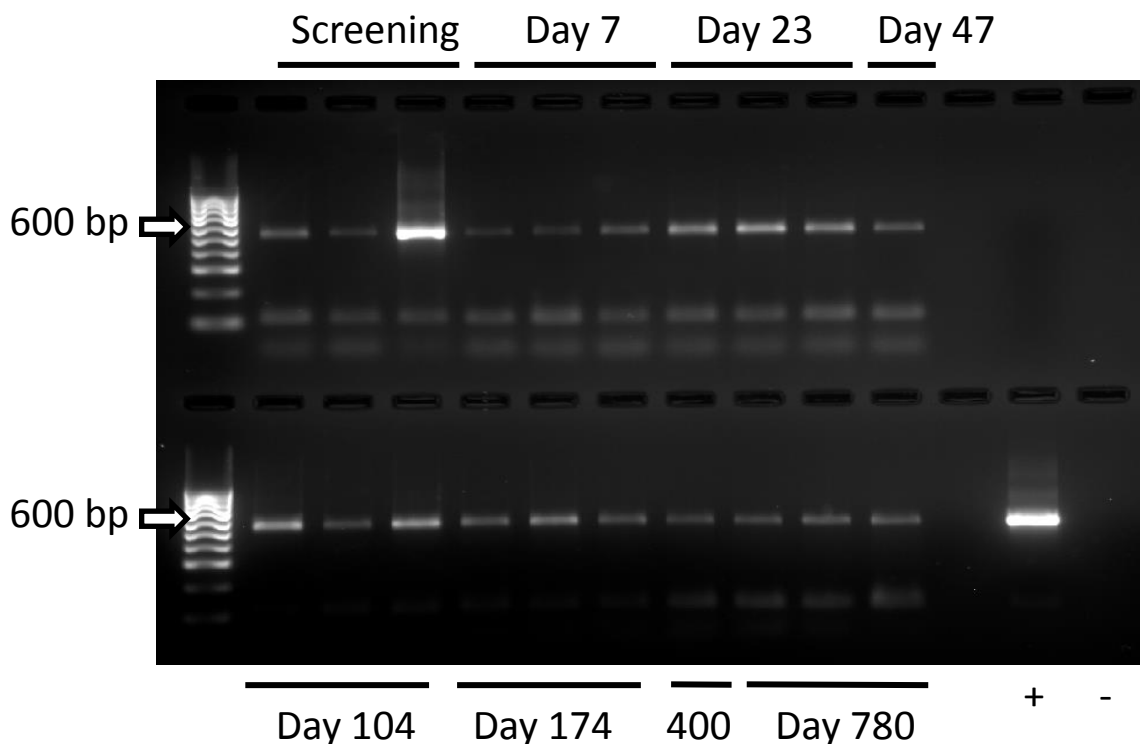


**Figure 6.23.** PCR Amplification of 16S rRNA gene of groundwater harvested from field at different intervals after the inoculation. Amplification was made using FAM labelled 341F and 805R primers M: Ladder IV (+) Positive control (-) Negative control. Note Screening represents samples previous to the beginning of the experiment

Chapter 5.

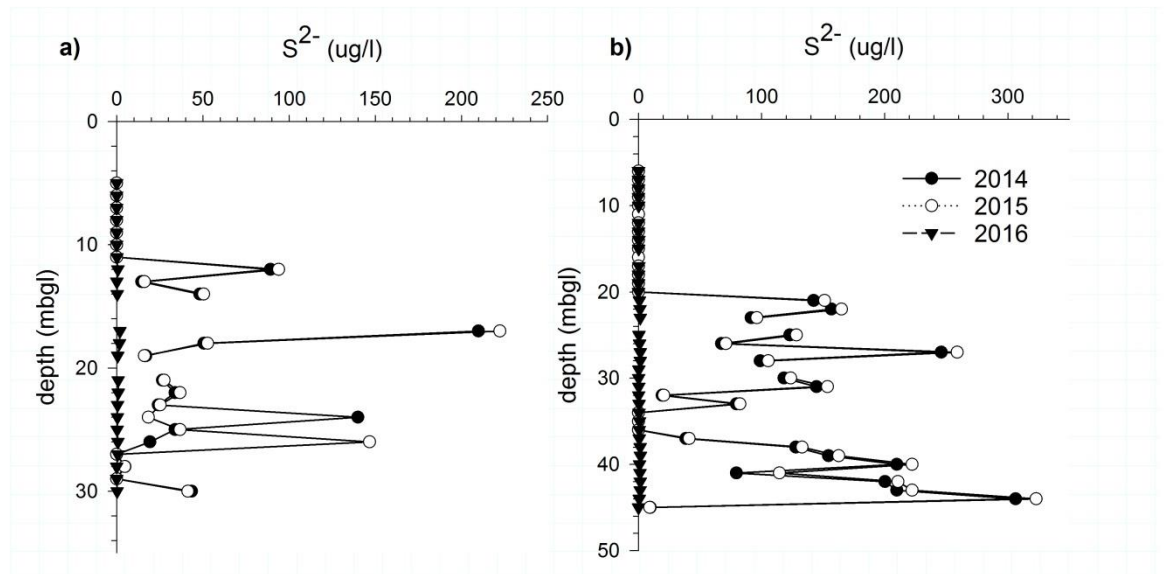


Figure 6.24. Depth profiles of sulfide in groundwater at BH59 (left) and BH-60 (right). The water table was located at 5 mbgl approximately (n=1).